THE ROLE OF ASTROCYTES IN FRAGILE X NEUROBIOLOGY

THE ROLE OF ASTROCYTES IN FRAGILE X NEUROBIOLOGY

BY

SHELLEY JACOBS, B.Sc. (Hons)

A Thesis

Submitted to the School of Graduate Studies

in Partial Fulfillment of the Requirements

for the Degree

Doctor of Philosophy

McMaster University

DOCTOR OF PHILOSOPHY (2009) McMaster University
(Medical Sciences) Hamilton, Ontario

TITLE: The Role of Astrocytes in Fragile X Neurobiology
AUTHOR: Shelley Jacobs, B.Sc. (Hons.) (McMaster University)
SUPERVISOR: Dr. L.C. Doering
NUMBER OF PAGES: xvii , 308

Abstract

Fragile X Syndrome (FXS) is the most common inherited disease of mental impairment, typically caused by a mutation in the *Fragile X mental retardation 1* (*FMR1*) gene. The clinical features are thought to result from abnormal neurobiology due to a lack of the Fragile X mental retardation protein (FMRP). Previously, it was thought that FMRP was confined exclusively to neurons; however, our laboratory recently discovered that astrocytes also express FMRP. Consequently, it is possible that astrocytes also suffer abnormalities as a result of a lack of FMRP. Astrocytes play integral roles in the development and maintenance of communication in the central nervous system. Therefore, it is now important to determine the contribution of astrocytes to the abnormal neuronal phenotype seen in FXS. In these experiments, neurons and astrocytes were independently isolated from wild type (WT) or *FMR1* null mice and grown in a co-culture. Neurons were evaluated using immunocytochemistry in combination with computer-aided morphometric and synaptic protein analyses. The findings presented here provide convincing evidence that Fragile X astrocytes contribute to the abnormal neurobiology seen in FXS. Fragile X astrocytes alter the dendrite morphology and excitatory synaptic protein expression of WT neurons in culture; and, importantly, when Fragile X neurons are grown with WT astrocytes these changes are prevented. Interestingly, the Fragile X astrocytes appear to act by causing a delay in development; even WT neurons grown in the presence of Fragile X astrocytes, that displayed an abnormal phenotype at 7 days in culture, exhibited nearly normal dendrite morphology and expression of excitatory synapses at 21 days. Furthermore, the results suggest that the dendritic abnormalities induced by the Fragile X astrocytes specifically target neurons with a spiny stellate morphology. This research establishes a role for astrocytes in the development of the abnormal neurobiology seen in FXS, and as such, the results presented here have significant implications for Fragile X research. The novel prospect that astrocytes are key contributing components in the development of FXS provides an exciting new direction for investigations into the mechanisms underlying FXS, with many unexplored avenues for potential treatment strategies.

Preface

This doctoral dissertation is presented as a *sandwich thesis* and is comprised of author-generated versions of four manuscripts prepared for publication. At the time of writing, one manuscript was published and three were submitted for publication. The author performed the experiments reported in these manuscripts during the author's PhD programme. Due to the common focus of the manuscripts the reader will encounter a significant degree of overlap, specifically in the literature review and introduction/discussion sections of each article.

Following a review of the relevant literature (Chapter 1), the hypotheses and specific aims of the thesis will be stated (Chapter 2). Then, each manuscript will be presented as an individual chapter (Chapters 3-6). Each of these chapters will begin with a brief note detailing the author's contribution to the work therein, and outlining the background and rationale for the manuscript. Following the presentation of the four manuscripts, a concluding chapter will summarize the major findings from each article, and the contribution of each to the thesis as a whole (Chapter 7). The thesis will conclude with a presentation significant advances of knowledge gained from the work presented herein and suggestions for future research directions (Chapter 7).

Literature citations are included in the style required by the journal to which each manuscript was submitted, and refer only to the reference list within that paper. Elsewhere, the references will adhere to the formatting guidelines described by the American Psychological Association (5th Edition), with a list of citations appearing in a separate references section at the end of the dissertation.

Details regarding common materials and methods not elsewhere described will appear in Appendix I.

Any permissions regarding the use of copyright material, not otherwise addressed are included in Appendix II.

Acknowledgements

I would like to say thank you…

To my supervisor, Dr. L.C. Doering for all of his guidance and support throughout my studies. Thank you for caring when I didn't care. For believing in me, when I didn't believe. For having faith in me, no matter how many times I tested your faith.

To my committee – Drs. Foster, Mishra and Niles – thank you for keeping me focused. I think I can finally say, "Yes, that's a fabulous idea/experiment. However, I think I'll let someone else have a go at that one."

To the National Science and Engineering Research Council – thank you for supporting my studies.

To the members (and honorary members) of the Ball and West-Mayes Labs – especially to "the boys" (present and past) Jay, Joe, Joe, Jon, Jeff, Karlo, and Mike, for making lunches, well, interesting.

To Jackie, for your friendship and support. Tell Dennis I am sorry for all of those times I kept you late in the lab discussing 'our experiments'.

To Laura, a special thanks. Thank you for finding the astrocyte FMRP! Without you, none of this would have been possible (and I would still be watching mice run in circles – sorry, Jackie).

To Meera, for a coffee mug that has seen me through the writing of this dissertation, for your companionship through seemingly never-ending ICC sessions, and for your unwavering determination to excel in the lab. You did it! And thanks to you, I *only* had to characterize 1400 neurons!

To Momal, for your friendship and enthusiasm that kept me excited when I was ready to give in, for making my job as a TA so enjoyable (it is students like you who make teachers love to teach), and for your initiative to volunteer in a lab … and then your perseverance to stay in the lab after being subjected to yet *another* set of cells to count.

To my family, and my friends: AP, JB, JH, JR, KN, MW, SW. I know many of you threatened I couldn't quit after all *we* had been through. Well – *we* did it! I couldn't have done it without you. Thank you for understanding when I couldn't be around, the last-minute cancelations, the birthdays I missed, and the Holidays I wasn't present at when I decided my mice were better company.

To my mum, for her unconditional support regardless of what I decided. Thank you for listening to my endless complaints, and for continual reassurance each of the many times

I was ready to quit.

To my sister Lindsay, for always asking how "it" was going.

To my Dad, for all of the scientific advice. Now there will be two Drs. Stead…err, I mean one Dr. Stead and one Dr. Jacobs in the family.

To my mother and father in law, Mr and Mrs Jacobs, for watching Raedon and for trying to understand how I could be "working" when I was sitting at home in my pajamas.

Most importantly, I would like to say thank-you to my husband and son.

Raedon, you were too young to remember any of this – thank goodness. So many times I said I couldn't play, because "Mommy was working". Well, Mommy is done working! Know that I love you, and that I wish I hadn't missed so many memories. But also know, that I needed to finish that which I had started and continue to devote myself to my studies so that I was/am/will be a role model you can be proud of. For the moments you sacrificed, I thank-you.

And perhaps if you, by some miracle, have learned something from this, you will have learned that some things are worth working hard for – but, sometimes, no matter how hard you work, you can't do everything and you can't always be everything for everybody; and that does not make you less of a person, it makes you human…sometimes the dusting needs to be left for another day (or week).

Stephen, my most accommodating and supportive husband, I thank you for everything you have given from the bottom of my heart. Thank you for supporting me through the exciting discoveries and the discouraging set-backs, for being an ear that patiently listed to my ideas (and complaints), and for being a shoulder that I could cry on – when "I don't know" why.

And I thank you, as I thanked Raedon, for giving me time. For being a single parent this past couple of weeks (or should I say months or years?), for the evenings of that first year I returned to work after Raedon was born, and for the time taken and the lost memories. I will make it up to you. I promise. Next summer really will be better!

Table of Contents

List of Figures & Tables

Chapter 1

Chapter 3

Chapter 4

Chapter 5

Chapter 6

List of Abbreviations

α-CaMKII	alpha subunit of calcium/calmodulin-dependent protein kinase II
AMPA	α-amino-3-hydroxyl-5-methyl-4-isoazole-propionate
AMPAR	AMPA receptor
ANOVA	analysis of variance
AP-1	adaptor protein 1
AP-2a	activator protein (transcription factor) 2a
AraC	cytosine arabinoside
BDNF	brain derived neurotrophic factor
bFGF	basic fibroblast growth factor
BRAG1	brain related apoptosis gene 1
BSA	bovine serum albumin
CA	*Cornu Ammonis* (Ammon's horn)
CA1	region 1 of Ammon's horn
CA2	region 2 of Ammon's horn
CA3	region 3 of Ammon's horn
CA4	region 4 of Ammon's horn
cAMP	cyclic adenosine monophosphate
CaMKII	calcium/calmodulin-dependent kinase II
Celsr2/3	cadherin EGF LAG seven-pass G-type receptor 2 or 3
CKO	conditional knockout
CMF	calcium magnesium free
Cpg15	candidate plasticity gene 15
CNS	central nervous system
comm	commissural fibers
da	dendritic arborization
dFMR1	*drosophila FMR1*
DAPI	4',6-diamidino-2-phenylindole
DG	dentate gyrus

DHPG	(S)3,5-dihydroxyphenylglycine
dH2O	distilled water
DiI	1,1',di-octadecyl-3,3,3'3'-tetramethylindocarbocyanine perchlorate
DiO	3,3'-dioladecyloxacarbocyanine perchlorate
DIV	days *in vitro*
Dscam	Down's syndrome-related cell adhesion molecule
E1	embryonic day 1
E17	embryonic day 17
E19	embryonic day 19
EDTA	ethylenediaminetetraacetic acid
E/I	excitatory/inhibitory
EM	electron microscopy
Eph	ephrin
EtOH	ethanol
F-actin	filamentous actin
FMR1	*Fragile X Mental Retardation 1* gene
FMRP	Fragile X Mental Retardation Protein
FXR1	Fragile X mental retardation Related protein 1
FXR2	Fragile X mental retardation Related protein 2
FXS	Fragile X Syndrome
FXTAS	Fragile X Tremor Ataxia Syndrome
GABA	γ-Aminobutyric acid
GFAP	glial fibrillary acidic protein
GLT1	glutamate transporter 1
Gly	glycine
GM	glial media
HBSS	hanks buffered saline solution
IIPMF	intra- and infrapyramidal mossy fiber
IR	immunoreactive

IRES	internal ribosome entry site
KCl	potassium chloride
KH	hnRNP-K-protein homology
KO	knockout
LGN	lateral geniculate nucleus
LTD	long-term depression
LTP	long-term potentiation
MAGUK	membrane-associated guanylate kinase
MAP	microtubule associated protein
MAP1B	microtubule associated protein 1B
MAP2	microtubule associated protein 2
MeCP	methyl-CpG-binging protein
MEM	minimal essential media
mf	mossy fibers
mGluR	metabotropic glutamate receptor
MPEP	2-methyl-6-(phenylethynyl)-pyridine
MRI	magnetic resonance imaging
mRNA	messenger RNA (ribonucleic acid)
mRNP	messenger ribonucleoprotein
MS	multiple sclerosis
NaCl	sodium chloride
NCAMs	neural cell adhesion molecules
NES	nuclear export signal
NGF	neural growth factor
Ngn2	Neurogenin 2
NLS	nuclear localization signal
NMDA	N-methyl-D-aspartic acid
NMDAR	NMDA receptor
NMM	neural maintenance media

NT	neurotrophin
P6	post-natal day 6
P9	post-natal day 9
P12	post-natal day 12
P15	post-natal day 15
PBS	phosphate buffered saline
PLL	poly-L-lysine
PND	post-natal day
pp	perforant pathway
PSD	post-synaptic density
PSD-95	post-synaptic density protein 95
RGG	arginine-glycine-glycine
RGS5	regulator of G-protein signaling protein 5
RNAi	RNA interference
SAP90	synapse associated protein 90kDa
SAPAP3	SAP90/PSD95-associated protein 3
Sch	Schaffer collaterals
s.e.m.	standard error of the mean
SER	smooth endoplasmic reticulum
siRNA	small interfering RNA
SNARE	SNAP (soluble NSF [N-ethylmaleimide-sensitive factor] attachment protein) receptors
Str.lac.	*Stratum lacunosum*
Str.mol.	*Stratum moleculare*
SynGAP	synaptic Ras-GTPase activating protein
Syp/p38	synaptophysin
TF	transcription factors
TrkB	neurotrophic tyrosine kinase receptor, type 2
USF1/2	upstream stimulatory factors 1 and 2

UTR	untranslated region
VAMP2	synaptobrevin
V-ATPase	V-type adenosine triphosphatase
WT	wild type

CHAPTER 1:
LITERATURE REVIEW

1. Chapter 1: Literature review

1.1 Fragile X Syndrome

1.1.1 Clinical Presentation

Fragile X Syndrome (FXS) is the most common cause of inherited mental retardation, most recently documented as having a prevalence of approximately 1 in 2500 (including both males and females affected with the full-mutation) (Hagerman, 2008). Being an X-linked disorder, more males than female are affected with FXS. Symptoms of the disease in affected males include mild to moderate mental retardation, learning and memory deficits, hyperactivity, attention deficits, social withdrawal, increased susceptibility to seizures, motor disorders and autistic like behaviours (Beckel-Mitchener & Greenough, 2004; O'Donnell & Warren, 2002). Additionally, individuals with FXS present with a number of physical characteristics such as a long narrow face, protruding jaw and ears, hyper-extensible joints and enlarged testicles (Beckel-Mitchener & Greenough, 2004; O'Donnell & Warren, 2002). In general, affected females display a less severe phenotype, with the severity of the impairments correlated to the degree of inactivation of the abnormal X-chromosome (Sobesky, et al., 1996).

1.1.1.1 Gross neuroanatomical correlates

The gross neuroanatomical features of individuals with FXS are less well characterized, due to contradictory findings. A number of studies have shown a lack of significant neruoanatomical abnormalities in males with Fragile X at autopsy (as reviewed in, O'Donnell & Warren, 2002). Other studies comparing MRI images from Fragile X patients with those of controls found that there is an increased ventricular volume (Lee, et al., 2007; Reiss, Abrams, Greenlaw, Freund, & Denckla, 1995), a decrease in the volume of the posterior vermis of the cerebellum (Mostofsky, et al., 1998), an increase in the volume of the superior temporal gyrus (Reiss, Lee, & Freund,

1994), and an increase in the volume of the caudate nucleus (Hessl, Rivera, & Reiss, 2004; Reiss, Freund, Baumgardner, Abrams, & Denckla, 1995). Furthermore, these alterations correlated with the level of cognitive functioning and the expression of the gene responsible for FXS (Mostofsky, et al., 1998; Reiss, Freund, et al., 1995). Alteration of the amygdala volume was also correlated with degree of cognitive functioning in twins with Fragile X (Reiss, Abrams, et al., 1995). Reiss (1994) also found enlargements of the hippocampus in children and young adults with FXS, and this was supported by similar findings of Kates and colleagues (1997). Although, a study by Jäkälä and others (1997) did not reproduce this finding, they did observe atypical hippocampal morphologies on MRI. Most recently, Haas and colleagues (2009) found that male children with FXS had altered white-matter anatomy in their ventral frontostriatal pathways. The anatomical regions listed above control a number of cognitive and behavioural processes, such as the processing of complex auditory stimuli and emotion, learning, memory and the execution and regulation of motor behaviours. Many of those cognitive and behavioural processes are found altered in individuals with FXS, and therefore it is tempting to speculate that these gross neuroanatomical abnormalities are at the root of the cognitive deficiencies seen in individuals with FXS. However, this theory should be balanced with caution as it is not yet known whether these alterations are *the cause* of the impairments seen in individuals with FXS, or whether they are *caused by* the deficits.

1.1.1.2 Cellular neurobiological correlates

Microscopic evaluations of the brain tissue from autopsy specimens of individuals with FXS revealed that the number of neurons is not altered compared to controls. However, evaluation of the dendrites of Golgi-impregnated neurons showed that the neurons of the parietal-occipital cortex in individuals with Fragile X exhibit unusually long, spindly, tortuous, seemingly immature dendritic spines (Rudelli, et al., 1985). This observation was later confirmed in five other Fragile X patients (Hinton, Brown, Wisniewski, & Rudelli, 1991; Irwin, et al., 2001). Irwin and colleagues (2001) found that

individuals with FXS have a significant increase in the immature dendritic spines in both the temporal and visual cortices. However, the number of patient samples evaluated is small, and therefore more similar studies are warranted to reduce the possibility of confounding factors that could provide alternate explanations for the abnormal dendritic spine morphologies.

1.1.1.3 Genetics of Fragile X Syndrome

1.1.1.3.1 *The* FMR1 *gene*

In 1991, the gene responsible for FXS was identified by positional cloning, and was named the *Fragile X Mental Retardation 1* (*FMR1*) gene (Verkerk, et al., 1991). In 2001, Oostra and Chiurazzi reviewed the properties of the *FMR1* gene and its function. The *FMR1* gene is located at Xq27.3, spans 38 kb (from base pair 146,801,200 to base pair 146,840,302) and consists of 17 exons (Eichler, Richards, Gibbs, & Nelson, 1993)(**Fig.1**). The *FMR1* gene is highly conserved between species, with significant homology between humans, mice, chicken, *Xenopus leavis*, monkey and *Drosophila*. Transcription of the *FMR1* gene results in up to 20 different transcripts via alternative splicing; however, only 4-5 of these *FMR1* mRNAs are actually detected in various tissues. The full length mRNA is 4.4kb and encodes a protein with maximal length of 632 amino acids.

1.1.1.3.2 FXS is a trinucleotide repeat disorder

Named for the cytogenetic "fragile" site visible at the tip of the long arm of the X chromosome, FXS is typically the result of an expansion of a (CGG)n repeat within the 5' untranslated region (UTR) of the *FMR1* gene (Kremer, et al., 1991)(**Fig.1.1c, Fig.1.2a**). In the normal population, this repeat generally occurs between 5 and 55 times (Brouwer, Willemsen, & Oostra, 2008; Oostra & Willemsen, 2009).

Figure 1.1: The *FMR1* gene

(a) Images of the X Chromosome depicting the Fragile X site on the long arm of the X Chromosome. Light microscope image (left) and scanning electron microscope image (right) revealing the chromatid gap on the X Chromosome from an individual with FXS (Images obtained from (Raffa, 2009)). (b) The location of the *FMR1* gene on the X Chromosome. The *FMR1* gene is located on the long arm of the X Chromosome at position 27.3; specifically from base pair 146, 801, 200 to base pair 146, 840, 302.
(Image available from the NIH, ghr.nlm.nih.gov/gene=fmr1) (c) The 17 exons of the *FMR1* gene. The horizontal grey line represents the entire gene, orange segments are the coding regions, blue segments are non-translated regions. (Image adapted from http://commons.wikimedia.org/wiki/File:FMR1-Struktur1.png)

a

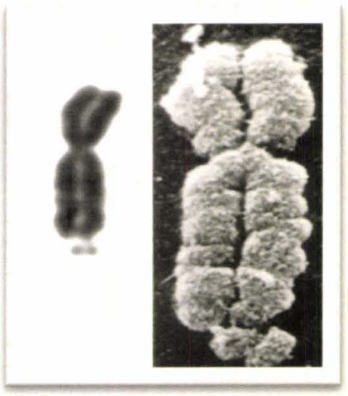

b

c

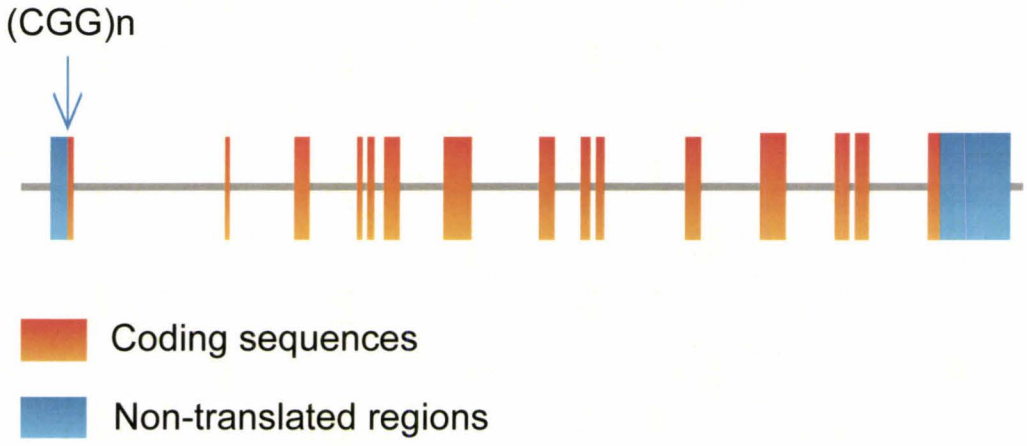

Figure 1.1

Figure 1.2: FXS is a trinucleotide repeat disorder

In normal individuals, there are between 5-55 CGG repeats (green segment) upstream of the *FMR1* gene (red). In individuals with the premutation expansion (55-200 repeats), the gene produces excess mRNA but low levels of FMRP thought to result in FXTAS. In individuals with the full mutation of greater than 200 repeats, the gene promoter region is methylated (purple ovals), silencing the *FMR1* gene and resulting in little or no mRNA/protein. Therefore no FMRP is available for proper brain development, and the absence of FMRP is responsible for FXS.

(Image adapted from the Hagerman Lab website, http://wizard1.ucdavis.edu/html/anatomy_of_a_gene.cfm).

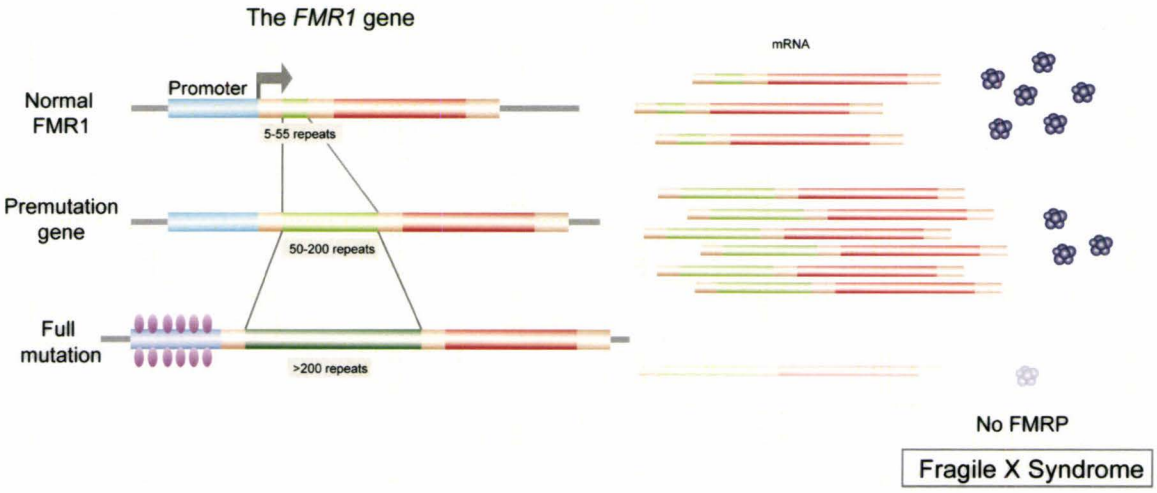
The *FMR1* gene
Normal FMR1
Promoter
5-55 repeats
Premutation gene
50-200 repeats
Full mutation
>200 repeats
mRNA
No FMRP
Fragile X Syndrome

Figure 1.2

Figure 1.3: The structure of FMRP

The structure of FMRP depicting the location of the key conserved regions identified. N, C, represent the N and C terminals of the protein, respectively, NLS, nuclear localization signal, NES, nuclear export signal, KH, hnRNP-K-protein homology domains, RGG box, arginine-glycine-glycine rich box.

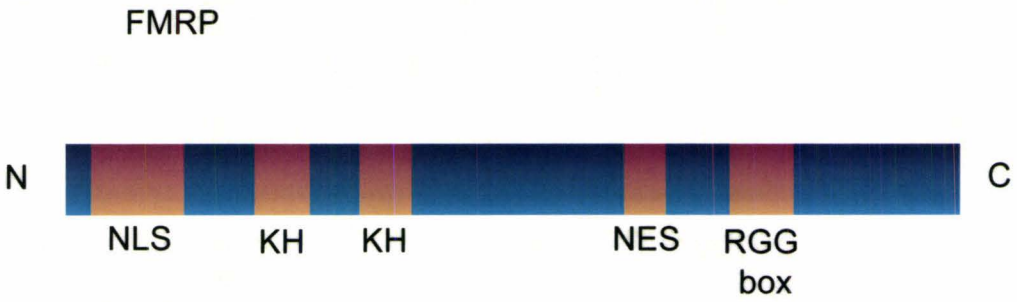

Figure 1.3

Individuals with between 55-200 repeats are considered to have the premutation allele, which tends to expand when transmitted (Brouwer, et al., 2008; Oostra & Willemsen, 2009). In the Canadian population, the prevalence of the premutation is 1 in 259 females and 1 in 813 males (Hagerman & Hagerman, 2004a). Premutation carriers show elevated levels of *FMR1* mRNA with normal protein levels and generally have only mild, if any, typical symptoms of FXS (Hagerman & Hagerman, 2004a). However, these individuals do exhibit characteristics that are not consistent with the spectrum of abnormalities in FXS, and that appear to be unique to the premutation. For example, males with the premutation are at increased risk for developing Fragile X Tremor/Ataxia Syndrome (FXTAS), a Parkinson-like disorder (Brouwer, et al., 2008; Hagerman & Hagerman, 2004b; Hagerman, et al., 2001; Oostra & Willemsen, 2009). Additionally, females with the premutation exhibit an increased risk for premature ovarian failure (Hagerman & Hagerman, 2004b; Murray, Webb, Grimley, Conway, & Jacobs, 1998; Oostra & Willemsen, 2009).

When passed to offspring, the premutation allele can either undergo a relatively small expansion that is still within the premutation range, or it can go through a massive expansion to 200 or more repeats resulting in the full mutation. The expansion of the repeat causes the hypermethylation of the *FMR1* promoter region, and *FMR1* expression is silenced, preventing the production of the Fragile X Mental Retardation Protein (FMRP) (Sutcliffe, et al., 1992). The end result is a complete lack of the gene product, FMRP, leading to FXS (**Fig.1.2**).

1.1.2 FMRP

1.1.2.1 Structure of FMRP

FMRP is a 70-80kDa protein (predominantly 71kDa) that is one of three paralogous proteins (with the FXR1 and FXR2 proteins) in mammals. It contains several highly conserved regions including: an internal ribosome entry site (IRES), a nuclear localization signal (NLS), a nuclear export signal (NES), two hnRNP-K-protein

homology (KH) domains and an arginine-glycine-glycine (RGG) box (**Fig.1.3**). The IRES, a sequence that is commonly found in regulatory proteins, is encoded just upstream of the CGG repeat in the untranslated region and is thought to facilitate the FMRP-mediated translation of mRNAs in the dendrites (Chiang, Carpenter, & Hagerman, 2001; Dobson, Kube, Timmerman, & Krushel, 2008). The NLS and NES are encoded at base pairs 111-154 and 408-418, respectively and aid in the translocation of the FMRP in and out of the nucleus (Eberhart, Malter, Feng, & Warren, 1996). The best-characterized motifs in FMRP are the two KH and the RGG domains, located in exons 8, 10 and 15 respectively. These are common to RNA binding proteins and permit the interaction of FMRP with its target mRNAs (Ashley, Wilkinson, Reines, & Warren, 1993). More specifically, the first KH domain binds to mRNA (Adinolfi, et al., 1999), the second KH domain is required for the association of FMRP with ribosomes (Feng, Absher, et al., 1997), and the RGG box permits FMRP binding with mRNAs containing an intramolecular G quartet structure (Darnell, et al., 2001).

1.1.2.2 FMRP Expression

FMRP expression is widespread throughout the body in humans, mice and rats, with the highest levels in the brain and testes (Bakker, et al., 2000; Devys, Lutz, Rouyer, Bellocq, & Mandel, 1993; Feng, Gutekunst, et al., 1997; Hinds, et al., 1993). Within the brain, the highest expression of FMRP is found in the hippocampus, cerebellum and cortex (Bakker, et al., 2000; Devys, et al., 1993; Feng, Gutekunst, et al., 1997; Hinds, et al., 1993). In neurons, FMRP resides largely in the cytoplasm, with less than 5% existing in the nucleus (Feng, Gutekunst, et al., 1997). Within the cytoplasm, high concentrations of FMRP are found in regions rich with ribosomes (>85%, Khandjian, Corbin, Woerly, & Rousseau, 1996), at the bases of dendrites and within dendritic spines (Antar, Afroz, Dictenberg, Carroll, & Bassell, 2004; Feng, Gutekunst, et al., 1997).

FMRP was originally thought to reside solely in neurons (Bakker, et al., 2000; Devys, et al., 1993; Feng, Gutekunst, et al., 1997; Hinds, et al., 1993); however, in 2004, Wang and colleagues provided evidence of a possible role for FMRP in oligodendrocytes

in development. Most recently, our lab provided evidence for FMRP in cells of the early glial lineage (Pacey & Doering, 2007).

FMRP expression is altered by a number of factors such as: age, sex, stage of development, experience and synaptic activity. Expression peaks in early development (Lu, et al., 2004; Pacey & Doering, 2007; Wang, et al., 2004) and gradually declines with age (Singh, Gaur, & Prasad, 2007; Singh & Prasad, 2008). Furthermore, FMRP expression is up-regulated in critical periods for learning (Winograd, Clayton, & Ceman, 2008). The expression of FMRP can also be altered with experience. For example, FMRP expression is up-regulated in the visual cortex of rats following light exposure (Gabel, et al., 2004), in the rat hippocampus after exposure to a complex environment (Irwin, et al., 2005), and in the rat somatosensory cortex after whisker stimulation (Todd, Malter, & Mack, 2003). FMRP expression is also altered in response to neuron activation. *In vitro*, FMRP and *FMR1* mRNA expression was rapidly increased following KCl depolarization of hippocampal neurons (Antar, et al., 2004), and in response to metabotropic glutamate receptor (mGluR) activation in culture (Todd, Mack, & Malter, 2003; Weiler, et al., 1997).

These alterations are mediated at the molecular level by a number of biological signals that regulate the expression of FMRP, some of which are known. The expression of *FMR1* mRNA can be regulated through a number of mechanisms including epigenetic modifications, RNAi-mediated methylation, and regulation by transcription factors (e.g., AP-2a and USF1/2) (reviewed in Lim, Booker, & Fallon, 2005). One specific example of *FMR1* mRNA regulation has been shown to occur in the mouse hippocampus, where brain derived neurotrophic factor (BDNF), via TrkB signaling, down-regulates the expression of *FMR1* mRNA (Castren, et al., 2002). Furthermore, FMRP contains a number of motifs that could lead to its phosphorylation, amidation, N-myristoylation, N-glycosylation or methylation (Denman, Dolzhanskaya, & Sung, 2004). Modification of these sites would provide a number of avenues for regulating FMRP through a variety of second-messenger pathways.

1.1.2.3 Function of FMRP

In humans and other species, FMRP has been suggested to be instrumental in behaviours such as learning (Smit, et al., 2008; Winograd, et al., 2008), memory (Dockendorff, et al., 2002; Gatto & Broadie, 2009), social behaviours (Spencer, Alekseyenko, Serysheva, Yuva-Paylor, & Paylor, 2005; Spencer, Graham, Yuva-Paylor, Nelson, & Paylor, 2008), and the regulation of circadian rhythms (Dockendorff, et al., 2002; Gatto & Broadie, 2009; Zhang, et al., 2008). Furthermore, at the cellular level FMRP plays a role in neuron development (Gatto & Broadie, 2008; Lu, et al., 2004; Pan, Zhang, Woodruff, & Broadie, 2004; Reeve, et al., 2005; Zhang, et al., 2001), synaptic plasticity (Bureau, Shepherd, & Svoboda, 2008; Huber, Gallagher, Warren, & Bear, 2002; Li, Pelletier, Perez Velazquez, & Carlen, 2002; Muddashetty, Kelic, Gross, Xu, & Bassell, 2007; Pfeiffer & Huber, 2007; Schuett, Falley, Richter, Kreienkamp, & Kindler, 2009; Todd, Mack, et al., 2003; Zalfa, et al., 2007), and the formation of neural networks (Bureau, 2009; Bureau, et al., 2008; Tessier & Broadie, 2008).

The means by which FMRP exerts action in the mammalian brain are not entirely understood, although a number of possible mechanisms have been postulated that include the regulation of mRNA translation (Castets, et al., 2005; Laggerbauer, Ostareck, Keidel, Ostareck-Lederer, & Fischer, 2001), the transporting of mRNAs or mRNA localization (Dictenberg, Swanger, Antar, Singer, & Bassell, 2008), and the post-transcriptional control or degradation of mRNAs (i.e., mRNA stability)(Zalfa, et al., 2007).

In accordance with its proposed role as an mRNA transporter, FMRP bears a nuclear localization signal (NLS) and a nuclear export signal (NES), suggesting that the Fragile X protein shuttles between the nucleus and cytoplasm (Eberhart, et al., 1996). One theory suggests that FMRP is involved in the transport of synaptic mRNAs from the cell body to the synaptic regions, where they are then situated for activity dependent translation (Antar, et al., 2004). Accordingly, FMRP is localized to the base of dendritic spines where it is thought to play a role in local synaptic protein translation (Weiler &

Greenough, 1999; Weiler, et al., 1997).

FMRP has been shown to be part of mRNA-containing ribonucleoprotein particles (mRNPs) (Eberhart, et al., 1996; Feng, Absher, et al., 1997; Khandjian, et al., 2004), transporting stalled mRNAs to (and holding them at) their target location. Additionally, FMRP is found associated with actively translating polyribosomes (Corbin, et al., 1997; Feng, Gutekunst, et al., 1997; Khandjian, et al., 2004; Stefani, Fraser, Darnell, & Darnell, 2004), in an mRNA dependent manner (Eberhart, et al., 1996). Recently, Dictenberg and colleagues (2008), provided evidence in support of the role of FMRP in dendritic mRNA localization, and correlated this with dendritic spine morphology. They found that in hippocampal neurons from *FMR1* null mice, dendritic mRNAs were not localized to dendritic spines, and when FMRP was acutely suppressed in wild type (WT) neurons, the neurons exhibited the characteristic long immature filopodia, providing evidence for FMRP in stimulus induced dendritic mRNA localization (Dictenberg, et al., 2008).

Initially it was thought that FMRP acted solely as a negative regulator of translation (Laggerbauer, et al., 2001; Li, et al., 2001; Sung, et al., 2003); however, more recently it has been demonstrated that the levels of some proteins are decreased in the absence of FMRP (Brown, et al., 2001; Liao, Park, Xu, Vanderklish, & Yates, 2008; Todd, Mack, et al., 2003), suggesting a more complex regulatory role for FMRP. Most recently, FMRP was shown to positively regulate the translation of *Superoxide Dismutase 1* (*Sod1*) mRNA (Bechara, et al., 2009). Whether FMRP is acting as a enhancer or repressor of translation, its action is reversed upon synaptic activation, and it is thought that the phosphorylation state of FMRP may determine the nature of its regulatory role under the two conditions (Ceman, et al., 2003).

FMRP associates with three major classes of mRNAs: mRNAs harboring a G-quartet, poly (U) stretches, or a kissing complex motif (Chen, Yun, Seto, Liu, & Toth, 2003; Darnell, Fraser, et al., 2005; Darnell, et al., 2001; Jin, Alisch, & Warren, 2004; Schaeffer, Beaulande, Ehresmann, Ehresmann, & Moine, 2003). Furthermore, it appears

that FMRP may be able to associate with non-coding RNAs, such as BC1 RNA, enabling the indirect association of FMRP with mRNAs (Zalfa, et al., 2003). However, recent studies failed to verify the results represented by Zalfa and colleagues (Iacoangeli, et al., 2008a), creating some controversy (Bagni, 2008; Iacoangeli, et al., 2008b).

Whether via direct or indirect interactions, a number of target mRNAs for FMRP have been suggested (Brown, et al., 2001; Darnell, Mostovetsky, & Darnell, 2005; Miyashiro, et al., 2003; Sung, Conti, Currie, Brown, & Denman, 2000; Zou, et al., 2008). In fact, up to 4% of brain mRNA transcripts are possible targets for FMRP (Brown, et al., 2001), and many of those encode proteins that are involved in neuron growth and development, specifically in the appropriate extension and development of neurites and maturation of synapses. For example, microtubule associated protein 1B (MAP1B), which is important for microtubule stability and neurite development (Bittel, Kibiryeva, & Butler, 2007; Lu, et al., 2004; Zhang, et al., 2001) and post-synaptic density protein 95 (PSD-95), which is a key player in synaptic plasticity (Muddashetty, et al., 2007; Todd, Mack, et al., 2003; Zalfa, et al., 2007). Furthermore, FMRP has been shown to bind to its own mRNA (Schaeffer, et al., 2001).

1.1.2.4 FMRP and synaptic plasticity

Synaptic plasticity, the ability of neurons to change the strength of synaptic transmission, is important in learning and the formation of new memories. Furthermore, synaptic plasticity is crucial for the building of neural networks via its role in the formation, maturation, and elimination of synapses. There are two major forms of long-term synaptic plasticity associated with learning and memory: long-term potentiation (LTP) and long-term depression (LTD). For a more in depth discussion of synaptic plasticity see **Section 1.3.2.2.1**.

It has been suggested that FMRP may be involved in the process underlying a specific type of LTD in the hippocampus. Stimulation of group 1 metabotropic glutamate receptors (i.e., mGluR1 and mGluR5) results in local protein synthesis and a protein-dependent internalization of N-methyl-D-aspartic acid (NMDA) and α-amino-3-

hydroxyl-5-methyl-4-isoazole-propionate (AMPA) receptors – a series of events representing a form of synaptic plasticity appropriately named mGluR-dependent LTD (Snyder, et al., 2001). Since LTD has been associated with learning and memory, a role for FMRP may help explain some of the learning and memory impairments associated with FXS.

The localization of FMRP and *FMR1* mRNA to dendritic spines, the major site of synaptic plasticity in cortical neurons, and its association with polyribosomes and dendritic mRNAs, suggest that FMRP plays a role in spine development and synaptic plasticity. Numerous studies have demonstrated that FMRP might bind to and regulate a subset of dendritic mRNAs such as: *MAP1b* (Antar, Dictenberg, Plociniak, Afroz, & Bassell, 2005); the post-synaptic scaffolding protein, *SAPAP3* (Brown, et al., 2001; Kindler, Rehbein, Classen, Richter, & Bockers, 2004); the mRNA encoding regulator of G-protein signaling, *RGS5* (Miyashiro, et al., 2003); the alpha subunit of calcium/calmodulin-dependent protein kinase II, *α-CaMKII* (Bramham & Wells, 2007; Zalfa, et al., 2003); the activity-regulated cytoskeletal associated protein, *Arc/Arg3.1* (Bramham & Wells, 2007; Zalfa, et al., 2003); and *PSD-95* (Muddashetty, et al., 2007; Zalfa, et al., 2007). Under basal conditions FMRP acts as a translational repressor of these proteins, and thereby the levels of its target proteins is decreased *in vitro* (Laggerbauer, et al., 2001; Li, et al., 2001). However, in the absence of FMRP *in vivo*, the expression of these proteins is increased (Lu, et al., 2004; Muddashetty, et al., 2007; Zalfa, et al., 2003).

Not only does a lack of FMRP alter the basal expression levels of synaptic proteins, but also there is a dysregulation of activity-dependent translation. In fact, Muddashetty and colleagues (2007) demonstrated that synaptoneurosomes from *FMR1* null mice were characterized by an excess of mRNA translation under baseline conditions and a loss of stimulus induced translation. In experiments designed to promote synaptic plasticity, FMRP levels have been shown to increase in cortical areas following environmental stimulation of the sensory, visual and motor systems (Gabel, et al., 2004; Irwin, et al., 2005; Todd, Malter, et al., 2003). In addition, the synthesis of FMRP can be

altered by the manipulation of molecules that are known to function as regulators of synaptic plasticity. Weiler and colleagues (1997) demonstrated that the levels of *FMR1* mRNA and FMRP that could be detected in rat cortical synaptoneurosomes significantly increased when these preparations were stimulated with mGluR1 specific agonists. Moreover, synaptic protein levels are increased in response to synaptic activity (Snyder, et al., 2001), and FMRP is necessary for stimulus-induced synaptic protein synthesis (Weiler, et al., 2004). In further support of a role for FMRP in synaptic plasticity, Li and colleagues (2002) showed that cortical synaptic plasticity was reduced in *FMR1* null mice.

Since FMRP was found to be one of the proteins elevated following stimulation of group 1 mGluRs, and was important for the activity-dependent alterations in expression of other dendritic proteins, it was implicated as having a role in mGluR-dependent LTD. This concept prompted Huber and colleagues to investigate the involvement of FMRP in hippocampal LTD – the idea being that if mGluR-dependent LTD coincided with an increase in FMRP, a lack of FMRP should somehow disrupt the mechanisms of mGluR-dependent LTD. Surprisingly however, rather than a deficit, LTD was found to be selectively enhanced in cultured hippocampal neurons from mice lacking FMRP compared to their WT counterparts (Huber, et al., 2002).

1.1.2.5 FMRP, mGluR-dependent LTD & the mGluR theory of Fragile X

As mentioned above, stimulation of mGluRs results in a specific form of synaptic plasticity – mGluR-dependent LTD. This form of LTD requires local translation of proteins, the regulation of which is mediated by FMRP (reviewed in Willemsen, Oostra, Bassell, & Dictenberg, 2004). In this scenario, under normal conditions FMRP would bind to and inhibit the translation of a subset of mRNAs (including its own); and FMRP is important for regulating the mGluR activation dependent synthesis of proteins seen in LTD (Bear, Huber, & Warren, 2004) (**Fig.1.4a**). In the absence of FMRP, there would be no attenuation of the mGluR-dependent protein synthesis – over-activity of group 1 mGluR signaling would ensue, as would the up-regulated translation of this subset of

mRNAs, resulting in altered synaptic protein dynamics (Bear, et al., 2004) (**Fig.1.4b**). The enhanced mGluR-dependent LTD, and the abnormal synaptic protein dynamics that would exist in the absence of FMRP could be fundamental to the development of the many variable symptoms of FXS, including the abnormal morphology of synapses and dendritic spines. Or in other words, as the 'mGluR theory' of FXS suggests: the neurological and physiological symptoms of FXS, including changes in synaptic plasticity and synapse maturation, can all be attributed to the over-activity of group 1 mGluRs (Bear, et al., 2004; Huber, et al., 2002).

1.1.3 Treatments for Fragile X Syndrome

Currently there is no cure for FXS, and as such, treatments of the disorder are used to mediate the symptoms and maximize functioning of the individuals with FXS. Behavioural therapy and specialized learning programs are implemented in an attempt to minimize cognitive disabilities, and pharmaceuticals, such as anticonvulsants are used to alleviate seizures.

New potential treatments are being investigated as potential means to address the underlying neural defect resulting from the absence of FMRP. One such intervention is based on the mGluR theory of FXS.

1.1.3.1 The mGluR theory & treatment for FXS

The mGluR theory suggests that the underlying neurobiological abnormalities of FXS are a result of enhanced mGluR-dependent LTD and/or exaggerated mGluR function. From this, it follows that drugs that target the mGluR pathway, specifically group 1 mGluR antagonists, may be potential treatments for FXS.

There is solid evidence in support of this theory. The administration of 2-methyl-6-(phenylethynyl)-pyridine (MPEP), an mGluR5 antagonist, to neurons *in vitro* corrects the abnormal excessive internalization of AMPA receptors (AMPAR) (Nakamoto, et al., 2007). MPEP also reduces excess protein synthesis in hippocampal slices from *FMR1* null mice, towards normal levels (Dolen, et al., 2007). Furthermore, the excess immature

Figure 1.4: The mGluR theory of FXS

FMRP regulates protein translation in response to activation of the group 1 mGluRs. (a) Under normal conditions FMRP acts as a negative regulator of translation of a number of synaptic proteins involved in LTD. In response to group 1 mGluR activation, the synthesis of a number of proteins involved in synaptic plasticity ensues. The translation of FMRP is also up-regulated in response to group 1 mGluR activation. As a negative regulator of translation, FMRP regulates mGluR activation dependent protein synthesis. (c) In the absence of FMRP, as in *FMR1* null mice, group 1 mGluR dependent protein synthesis is dysregulated. The resultant increase in protein synthesis has been implicated in the formation of the altered dendritic spine morphology and abnormal synaptic plasticity seen in FXS.

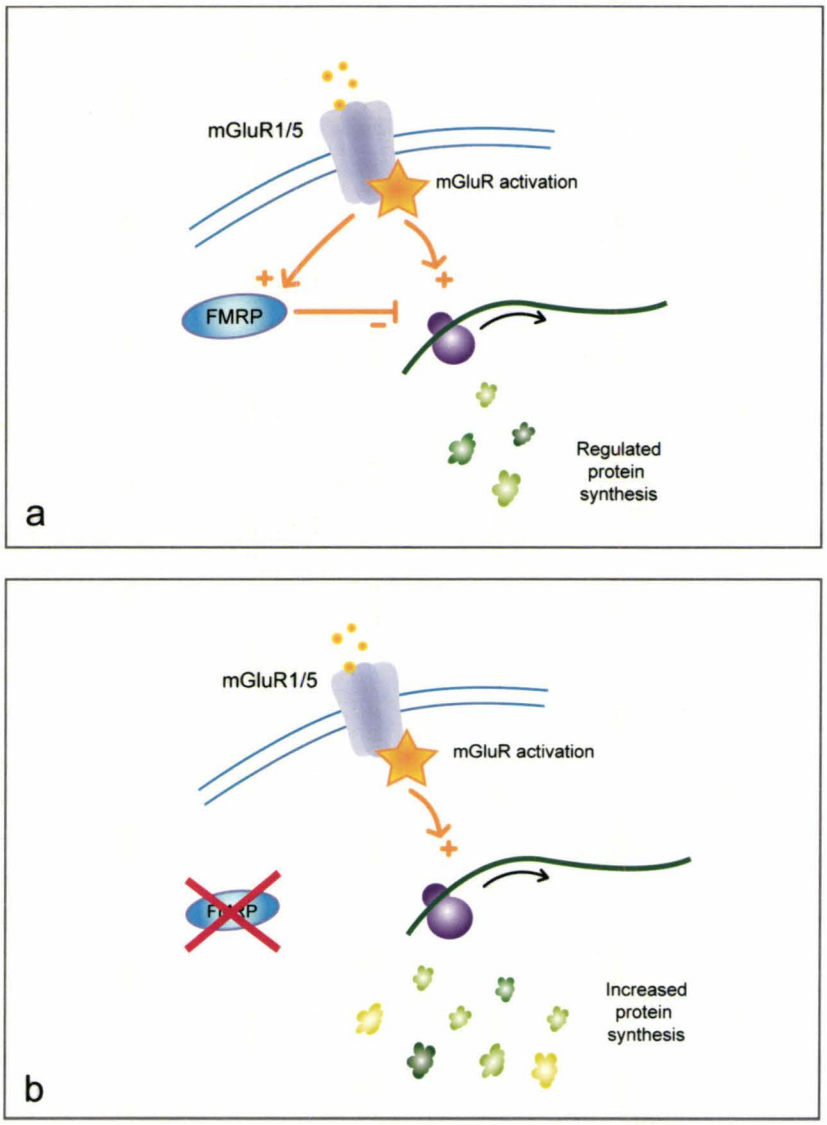
mGluR1/5
mGluR activation
FMRP
Regulated protein synthesis
a
mGluR1/5
mGluR activation
Increased protein synthesis
b

Figure 1.4

dendritic spines observed in *FMR1* null hippocampal neurons *in vitro*, can be corrected by exposure to MPEP (de Vrij, et al., 2008). *In vivo*, the administration of MPEP has corrected morphological, physical, and behavioural impairments in animal models of FXS (Bassell & Gross, 2008; McBride, et al., 2005; Yan, Rammal, Tranfaglia, & Bauchwitz, 2005). Additionally, a genetic reduction in mGluR5 has yielded similar promising results (Bassell & Gross, 2008; Dolen, et al., 2007).

1.1.4 The *FMR1* knock-out mouse model of Fragile X Syndrome

In order to study the underlying neurobiology, and investigate the potential treatments for FXS, an appropriate animal model is necessary. The *FMR1* knockout (KO, null) mouse was developed in 1994, to address such a requirement (Bakker, et al., 1994). The mouse *FMR1* gene has 97% amino acid homology with the human gene (Ashley, et al., 1993). Furthermore, the FMRP expression shows similar tissue and cell specific patterns in both humans and mice (Hinds, et al., 1993).

The *FMR1* KO mouse was created by the transfection of a neomycin cassette into exon 5 of the *FMR1* gene in embryonic stem cells, and homologous recombination (Bakker, et al., 1994). FMRP is absent in the resulting homozygous KO mice (Comery, et al., 1997), and although the mouse model results from a knock out, whereas the human condition results from an expansion, the result is the same – no FMRP. As a result, both humans and *FMR1* null mice exhibit the following characteristics: learning and memory impairments (Bakker, et al., 1994; Brennan, Albeck, & Paylor, 2006; Dobkin, et al., 2000), hyperactivity (Bakker, et al., 1994; Qin, Kang, & Smith, 2002), susceptibility to seizures (Chen & Toth, 2001; Musumeci, et al., 2007), characteristics associated with attention deficits (Nielsen, Derber, McClellan, & Crnic, 2002), predictors of autistic behaviours (Frankland, et al., 2004), and abnormal neuronal dendritic spine development (Comery, et al., 1997; Galvez, Gopal, & Greenough, 2003; Grossman, Elisseou, McKinney, & Greenough, 2006; Irwin, et al., 2002; Nimchinsky, Oberlander, & Svoboda, 2001). Given the behavioural and neuroanatomical similarities of the *FMR1* null mouse compared to the human Fragile X counterpart, this model is an important tool

in the investigation into the effects due to a loss of FMRP.

Recently, Mientjes and colleagues (2006) developed a conditional *FMR1* knockout mouse and a conditional *FMR1* restoration mouse, which will lead to further advances in Fragile X research. These new models will permit the investigation of the consequences of removing (or adding) FMRP from (to) specific brain regions, or specific cell types, in isolation.

1.2 The hippocampus

The hippocampus is one of a group of structures collectively referred to as the hippocampal formation: the hippocampus, dentate gyrus, subiculum and the entorhinal cortex. However, for simplicity, in the following the term 'hippocampus' will refer to both the hippocampus proper and the dentate gyrus.

The majority of work studying synaptic plasticity has been accomplished using *in vitro* preparations, whether in the form of slice cultures or cultured primary neurons, of the hippocampus. Slice cultures of the hippocampus allow the study of signaling and plasticity within hippocampal neural networks due to the maintenance of the anatomical organization that this preparation affords. Hippocampal neurons in culture provide a relatively clean population of primary neurons, whose *in vitro* properties have been well characterized. One of the morphological features of hippocampal pyramidal cells that enhances their usefulness as a tool to study synaptic plasticity is the presence of dendritic spines, which are maintained in culture.

The structure, function and signaling capabilities of the cells of the hippocampus are often a focus of Fragile X research (discussed below). Gross anatomical observations of patients with FXS have revealed abnormalities in hippocampal volume (Kates, et al., 1997) and morphology (Jakala, et al., 1997), and the hippocampus is one of the brain regions in which FMRP is most highly expressed (Bakker, et al., 2000; Devys, et al., 1993; Feng, Gutekunst, et al., 1997; Hinds, et al., 1993; Pacey & Doering, 2007), and in which the characteristic abnormalities of dendritic spines are found (Antar, Li, Zhang, Carroll, & Bassell, 2006; Braun & Segal, 2000; de Vrij, et al., 2008; Dictenberg, et al.,

2008; Grossman, et al., 2006; Segal, Kreher, Greenberger, & Braun, 2003). For these reasons, and others mentioned below, the author chose to use primary mouse hippocampal neurons in her experiments, and as such this structure (with a focus on the rodent hippocampus) warrants a brief discussion here.

1.2.1 The structure of the hippocampus

1.2.1.1 Gross neuroanatomy

The hippocampus is a bilateral limbic structure, which in the human is a relatively small structure located deep within the temporal lobes (**Fig.1.5a**). In the rodent, the hippocampus actually forms a relatively large part of the entire brain (Paxinos & Watson, 2007). Each half of the rodent hippocampus resembles a "C", running rostrally from the septum (septal pole) to curve around down into the lateral temporal lobes where it ends at its temporal pole (**Fig.1.5b**). The hippocampus is situated so that it forms the medial and part of the inferior wall of the lateral ventricles.

The internal structure of the hippocampus is the same along its length, consisting of an infolded convolution of the older and more simple allocortex (i.e., archicortex or paleocortex), with its principal neurons aligned in a single layer. A cross-section taken perpendicular to the long axis (septal-temporal) of the hippocampus will reveal that the internal structure is made up of two interlocking "Cs" (**Fig.1.6**). One "C" is Ammon's horn (i.e., the hippocampus proper), and the other is the dentate gyrus. Ammon's horn (*Cornu Ammonis*; CA), is divided into four morphologically and functionally distinct regions: CA1, CA2, CA3 and CA4 (Lombroso & Ogren, 2009). CA1 is located in front of the dorsal hippocampus, and CA4 is located at the boundary of the dentate gyrus (DG) (Lombroso & Ogren, 2009) (**Fig.1.6**). In fact, CA4 is commonly considered the hilar region of the dentate gyrus.

Figure 1.5: The hippocampus

A comparison of the hippocampus in the human (a) and rodent (b) brains. In each image, the hippocampus is coloured blue.

a

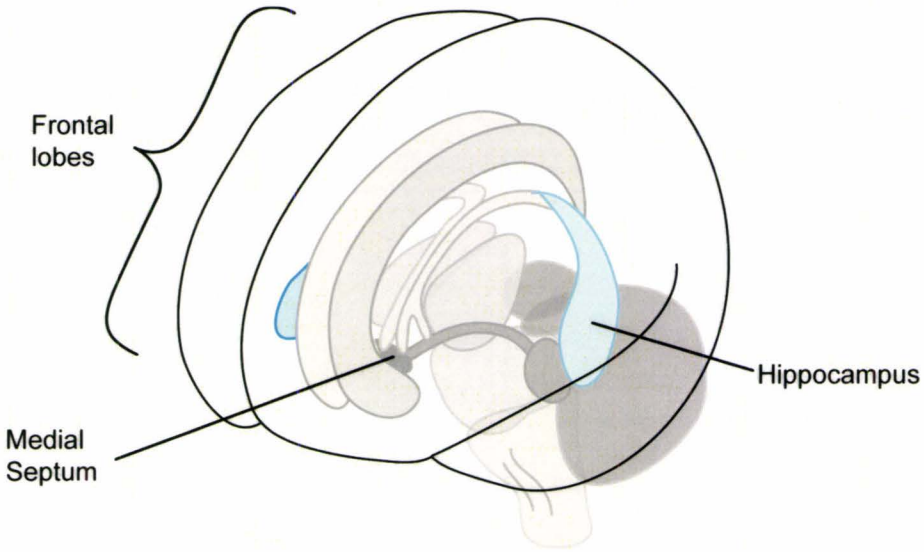
Frontal
lobes
Hippocampus
Medial
Septum

b

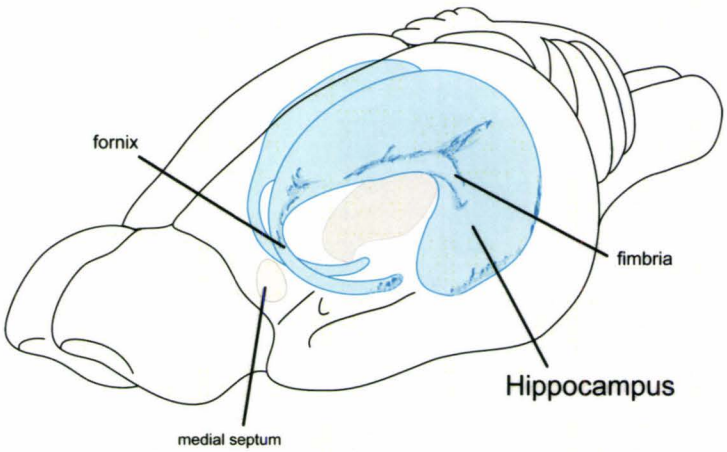
fornix
fimbria
Hippocampus
medial septum

Figure 1.5

Figure 1.6: The trisynaptic circuit

Schematic of the rodent hippocampus in cross section illustrating the regions of Ammon's horn (CA1, CA2, CA3, CA4) and the dentate gyrus (DG), the principle cell layer in each of Ammon's horn (i.e., pyramidal, triangles) and the dentate gyrus (i.e., dentate granule cells, circles), and the major excitatory pathways of the hippocampus that form the tri-synaptic circuit. Fibers enter the hippocampus from cortical regions via the perforant pathway (pp) and synapse on the granule cells in the DG. The granule cells of the DG then send projections via the mossy fibers (mf) to the pyramidal neurons in CA3. CA3 pyramidal neurons signal to CA1 pyramidal neurons via the Schaffer collaterals (Sch). The CA1 neurons project out of the hippocampus to extracortical regions, completing the circuit. In addition, the commissural connections (comm) support signaling between the two hippocampi.

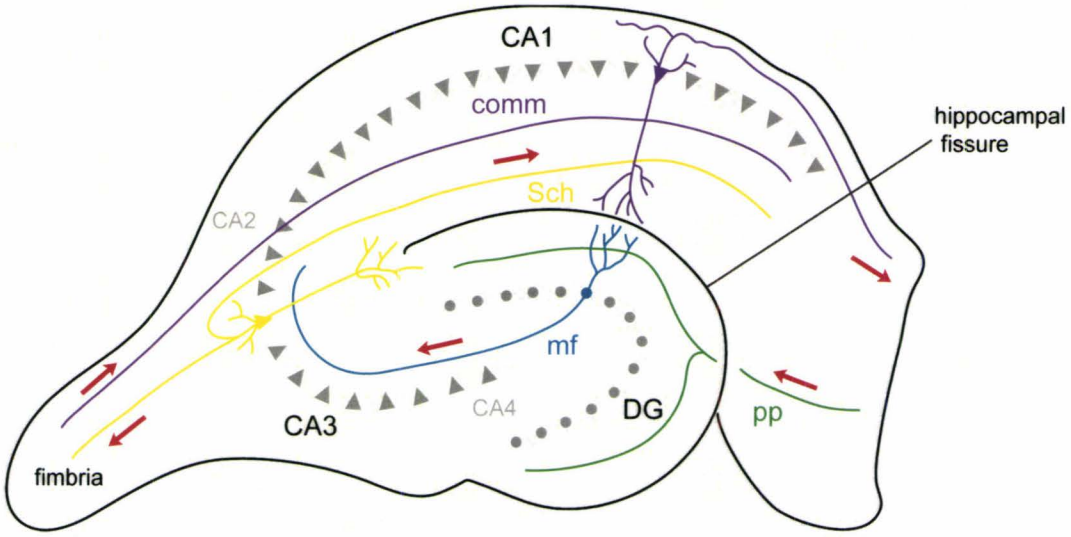
CA1
comm
hippocampal
fissure
Sch
CA2
mf
CA4
DG
CA3
pp
fimbria

Figure 1.6

1.2.1.2 Cytoarchitecural features

There are two principal cell types of the hippocampus: the dentate granule cell of the dentate gyrus, and the pyramidal cell of Ammon's horn (Traub & Miles, 1991). Both of these cell types are excitatory and use glutamate as their neurotransmitter. In addition, there are a number of inhibitory interneurons in the hippocampus, such as: dentate gyrus basket cells (Ribak & Seress, 1983), pyramidal basket cells (Seress & Ribak, 1990), chandelier cells (axo-axonic cells) (Somogyi, Nunzi, Gorio, & Smith, 1983), and mossy cells (Ribak, Seress, & Amaral, 1985). The majority (but not all), of the non-pyramidal cells in the hippocampus proper are presumed to be inhibitory (Traub & Miles, 1991).

1.2.1.2.1 The dentate gyrus

The dentate granule cells of the dentate gyrus exist in a single layer, the *stratum granulosum* or granule cell layer, which is divided into the suprapyramidal layer and the infrapyramidal layer based on the location of the dentate gyrus compared to the pyramidal layer of the hippocampus. Adjacent to the granule cell layer there are two other layers; one on either side. The polymorphic layer is the most superficial layer, and contains the interneurons and axons of the dentate granule cells. Deep to the granule cell layer is the molecular layer or *stratum moleculare* (*str. mol.*), which is divided into the inner third and external two thirds. The *str. mol.* 1/3 contains the commissural fibers and the inputs from the medial septum, both of which terminate on the proximal dendrites of the granule cells. The *str. mol.* 2/3 is the deepest of the layers, lying just superficial to the hippocampal fissure and across from the *str. mol* of the CA fields. This layer contains the fibers of the perforant path, terminating in excitatory synapses on distal apical dendrites of the dentate granule cells.

1.2.1.2.2 The hippocampus proper (*Cornu Ammonis*)

Ammon's horn is also organized in layers, with the *stratum pyramidale* (or the pyramidal cell layer) as the principle cell layer. The layers, from deep to superficial are: *stratum moleculare*, *stratum lacunosum*, *stratum radiatum*, *stratum lucidum* and then the

stratum pyamidale, *stratum oriens*, and the *alveus*. The *alveus* contains the axons of the pyramidal cells as they pass to the fimbria/fornix. The *stratum oriens* consists of the bodies of the inhibitory basket cells, and the horizontal trilaminar cells. Within this layer also exist the basal dendrites of the pyramidal neurons and the septal and commissural fibers. The *stratum pyramidale*, as mentioned, contains the pyramidal neuron cell bodies. Also, in this layer are a variety of interneurons such as axo-axonic cells, bistratified cells and radial trilaminar cells. *Stratum lucidum* is one of the thinnest layers, containing the mossy fibres from the dentate granule cells. The septal, commissural and Schaffer collaterals lie within the next layer, the stratum radiatum. Also within this layer are various interneurons including the basket cells, and the bistratified radial trilaminar cells. The *stratum lacunosum* (*str. lac.*) is a thin layer that consists of the Schaffer collaterals and the perforant path fibers. Due to its small size the *str. lac.* is often grouped with the next more deep layer, the *stratum moleculare*, into a single stratum lacunosum-moleculare. The deepest layer is the *stratum moleculare*. It contains the perforant path synapses on the distal apical dendrites of the pyramidal cells.

1.2.2 The neuronal circuitry of the hippocampus

Via extra-hippocampal connections, the hippocampus interacts most closely with the temporal cortex and the septum (Lombroso & Ogren, 2009). The major inputs to the hippocampus originate from cortical sources including the opposite and same hippocampus, the dentate gyrus and the entorhinal cortex; and from non-cortical sources such as the septum, hypothalamus, brainstem raphe nuclei and locus coeruleus (Traub & Miles, 1991). In turn, the hippocampus sends outputs via pyramidal cells to cortical targets such as the hippocampus, subiculum, entorhinal cortex, and cingulated gyrus; and via both pyramidal and non-pyramidal outputs, to non-cortical areas including the septum (Traub & Miles, 1991). With the exception of the γ-Aminobutyric acid (GABA) fibers from the septum (Freund & Antal, 1988), and the dentate hilar cell commissural projections (Ribak, et al., 1986), most inputs and outputs to the hippocampus are excitatory (Traub & Miles, 1991).

The hippocampus itself consists of three major excitatory pathways that use glutamate as their neurotransmitter, and are the components of the tri-synaptic circuit of the hippocampus (Lombroso & Ogren, 2009; Traub & Miles, 1991) (Fig.1.4). The first is the perforant pathway entering the hippocampus from the entorhinal cortex that synapses on the granule cells of the dentate gyrus. Second, the mossy fiber pathway consists of axons from dentate granule cells and projects to the dendritic fields of CA3 pyramidal neurons. Third, the axons of the CA3 neurons project to CA1 pyramidal neurons via the Schaffer collateral pathway. In addition, there are also commissural connections, recurrent excitatory connections within CA1 and CA3, and inhibitory circuitry (Traub & Miles, 1991).

1.2.3 Function of the hippocampus

The hippocampus is a cortical structure that is required for the formation of new memories. The critical functions of the hippocampus were first discovered in 1953, when a 27-year-old patient, H.M., underwent a bilateral temporal lobectomy to manage his seizures (Lombroso & Ogren, 2008). The seizures were better controlled, however H.M. lost his ability to form new memories (Lombroso & Ogren, 2008). Since then, much research has been completed to investigate the structure, cellular function and circuitry of the hippocampus and has provided a more in depth understanding of the function of the hippocampus in health and disease.

In general, the hippocampus plays a role in the formation of memories. In 2004, Eichenbaum reviewed the functions of the hippocampus. In that paper, he describes the function of the hippocampus as three memory-related cognitive processes: associative representation, sequential organization and the consolidation of memories (Eichenbaum, 2004). These functions are all a part of declarative memory processing, for which the hippocampus is perhaps best known. In addition, in rodents, the hippocampus contains special types of cells that respond to spatial location cues, called place cells (Traub & Miles, 1991).

1.2.4 The hippocampus in disease

Abnormal hippocampal cellular structure, function and connectivity play a role in the development of a number of diseases. For example, the hippocampus is one of the first brain regions affected in Alzheimer's disease (deToledo-Morrell, Stoub, & Wang, 2007), participates in the generation of seizures in some forms of epilepsy (Bertram, 2009), and has been implicated in the neuropathology associated with psychosis (Lisman, et al., 2008), depression (McKinnon, Yucel, Nazarov, & MacQueen, 2009) and some forms of mental retardation (Hessl, et al., 2004; Pulsifer, 1996).

1.2.4.1 The hippocampus and Fragile X Syndrome

As mentioned earlier, the hippocampus is one of the regions of the CNS in which FMRP is most highly expressed (Bakker, et al., 2000; Devys, et al., 1993; Feng, Gutekunst, et al., 1997; Hinds, et al., 1993). As such, it is not surprising that abnormalities of hippocampal structure, at both the gross neuroanatomical and the microscopic levels, are seen in individuals with FXS (Jäkälä, et al., 1997; Kates, et al., 1997; Reiss, et al., 1994). Furthermore, some of the key behavioural features associated with individuals with FXS, such as impairments of learning and memory, are related to the structural changes in the hippocampus (Beckel-Mitchener & Greenough, 2004; O'Donnell & Warren, 2002).

Therefore, as would be expected, both clinical and basic science research in FXS are often focused on understanding the neurophysiological alterations associated with a lack of FMRP in the hippocampus. Numerous studies, both *in vivo* and *in vitro* of hippocampal neurons of the *FMR1* knockout mouse have provided evidence for altered hippocampal neuron structure and function in the absence of FMRP. For example, Braun and Segal (2000) demonstrated that FMRP-deficient neurons in culture, from the newborn hippocampus, develop more slowly than neurons from the normal mouse. *In vitro* studies have consistently revealed a decrease in the number of dendritic spines (Antar, et al., 2006; Braun & Segal, 2000). Furthermore, *in vivo* the hippocampal neurons of the *FMR1* null mouse exhibit an immature profile of dendritic spines

(Grossman, et al., 2006). Huber et al (2002) found that hippocampal neurons from the *FMR1* null mice display alterations in a form of mGluR dependent synaptic plasticity. *FMR1* knockout mice also display smaller intra- and infrapyramidal mossy fiber (IIPMF) terminal fields than their WT counterparts (Mineur, Sluyter, de Wit, Oostra, & Crusio, 2002). These mice also exhibit behavioural deficiencies in spatial memory, consistent with alterations in hippocampal-mediated behaviours in FXS.

1.2.5 Primary hippocampal neuron culture

The growth of rodent hippocampal neurons in culture was optimized in the 1970s by Banker and colleagues (Banker & Cowan, 1977, 1979). Prior to then, rat hippocampal neurons could only be maintained for long periods in culture when they were grown at high densities. The high density of the neurons caused problems with investigations into the neuronal morphologies, because a dense neural network precluded the isolation of individual neurons. Banker therefore defined a hippocampal co-culture procedure, in which neurons were cultured together with glial cells. The glial cells help support the growth of the hippocampal neurons, and permit the growth of low-density cultures for many weeks.

Hippocampal neurons are chosen for the study of neuronal processes due to their well-defined shape. Furthermore, the ease with which a relatively pure population of neurons can be isolated from the late-embryonic hippocampus contributes to their popularity as an *in vitro* tool. When isolating the cells from the hippocampus, tissue from both the hippocampus proper and the dentate gyrus is combined. The combination of tissue becomes less of a problem when isolating cells from embryonic animals. At embryonic day 19 (E19) the majority of cells generated are pyramidal, with the ratio of pyramidal neurons to granule cells as 8:1 (Banker & Cowan, 1979). By comparison, in adult rats, the dentate granule cells out-number pyramidal neurons by 1.3-2.0:1 (Banker & Cowan, 1979). Interneurons are present in the hippocampus, but their frequency is low. In fact, Banker estimated that 80-85% of neurons in the cell population obtained, were pyramidal (Banker & Cowan, 1979). Similar to many cultures of other neuronal cell

types, of the neurons isolated, 20-40% survive *in vitro* and develop processes (Banker & Cowan, 1979).

Banker and others have described four stages of hippocampal neuron growth *in vitro* (Banker & Cowan, 1977, 1979; Dotti, Sullivan, & Banker, 1988). Initially upon dissociation and immediately after plating the isolated neurons are round. Then, the neurons extend 4-5 neurites. Within 24 hours, and via a stochastic process, one neurite extends and becomes the axon. The newly formed axon then inhibits the other neurites from attaining characteristics of axons (Bradke & Dotti, 1997, 2000). The dendrites then acquire their characteristic morphological and structural features. Before the final stage of dendrite differentiation, all neurites have capacity to replace the axon if the axon is lost; however, once the dendrites are finalized, this ability is lost (Dotti & Banker, 1987).

After one week in culture, the neurons develop many of the characteristic features of maturing cells *in vivo*. Their morphologies are very similar, although they exhibit features of a less developed nature, such as: smaller somas, shorter apical dendrites, fewer branches, shorter average length of dendrites, and less dendritic branching (Banker & Cowan, 1979). Banker suggests that this does not necessarily indicate that neurons *in vitro* are retarded in their growth. Instead, he reminds us that when examining the morphology of hippocampal neurons *in vivo*, neurons with a variety of developmental phenotypes are encountered reflecting the range of neurons at various stages of maturation. For examples of neuronal morphologies seen *in vivo* and *in vitro*, see Banker and Cowan, 1979.

Additionally, Banker described the hippocampal neurons in culture as developing a variety of dendritic patterns compared with the pyramidal neurons *in vivo* (Banker & Cowan, 1979); however, it is possible that the population of neurons isolated was not as pure with pyramidal neurons as Banker once thought. Instead, the population of cells isolated may include cells with morphologies reflecting the varied cell populations within the hippocampus proper and dentate gyrus.

Even so, cells with a pyramidal morphology dominate the culture, accounting for 45% of all cells. Another 15% of cells exhibit a single dominant dendrite similar to

pyramidal neurons, but display various divergences from the typical pyramidal form. Approximately 23% of the neurons exhibit two comparable sized dendrites extending from opposite poles and are called bipolar. The least common cells, making up only 2% of the population, were those having a stellate morphology with several similar sized dendrites that ramify from the soma in all directions. The remaining 11% of cells are those not otherwise classified.

1.3 Neurons

The study of brain development is important for the complete understanding of a number of developmental neuropathologies, and central to this knowledge is the study of neuronal architecture. The development of the central nervous system occurs in several stages. The neurons are born and migrate to their final positions in the nervous system. Then, the neurons elaborate axons and dendrites in patterns characteristic of each cell type. The dendrite outgrowth often occurs after the formation of the axon (DeFelipe & Jones, 1988). Finally, the synapses, highly specific connections between neurons, are formed.

Over 100 years ago, Camillo Golgi made the first observations of neuron structure. He recorded that each neuron consisted of a cell body, a long process called the axon and a complex tree-like structure he referred to as the dendritic tree (*dendron* in greek means tree). Ramon y Cajal verified this observation 15 years later, and added that neurons obey "the law of polarization". He postulated that the dendrites constitute the area of the neuron that is involved in obtaining input from all afferent neurons.

Since that time, much research has been completed in this area and we now know that the dendrites are the location at which the input from multiple neurons is collected, and they determine the number and pattern of the synapses received (Hume & Purves, 1981; Purves, Hadley, & Voyvodic, 1986; Purves & Hume, 1981). Therefore, the dendritic tree is crucial for signal integration and firing patterns (Gulledge, Kampa, & Stuart, 2005; Mainen & Sejnowski, 1996; Segev & London, 2000; Vetter, Roth, &

Hausser, 2001). Moreover, brain function is thereby dependent on dendritic shape and the factors that control it.

Most of the foundations for knowledge about the architecture of the dendrites in the cortex is from anatomical studies of the neurons in the visual cortex completed by Gilbert, in 1983. In those experiments the critical relationship between the morphology of cortical neurons and their function was defined. It was once thought that dendrites passively transmit data. It is now known that they are dynamic integrators of synaptic input. The shape of the dendritic tree modulates the transmission of signals by dictating the electrophysiological and integrative properties of a neuron (Koch & Segev, 2000; Rall, et al., 1992). Furthermore, the dendritic arbor morphology determines the population of afferent signals with which the neuron interacts. The specific branching pattern and the distribution of ion channels on dendrites influences how the synaptic signals decay as they propagate towards the soma. Therefore, variations in dendrite morphology in the central nervous system have enormous consequences for neuronal information processing.

1.3.1 Dendrites

The mature shape of a neuron's dendritic arbor is one of the most striking characteristics that varies between neuron cell types. In fact, neurons can be classified in terms of the number of branches and the pattern of branching of their dendritic trees.

The main excitatory neuronal subtypes are the pyramidal cells and the spiny stellate cells (Whitford, Dijkhuizen, Polleux, & Ghosh, 2002). The pyramidal neurons are the dominant cell type in the cortex. The pyramidal neurons have an apical dendrite that branches out into an apical tuft, and several highly branched basal dendrites that emanate from the cell body. The spiny stellate cells have spiny dendrites of similar lengths that radiate in all directions from the cell body (Whitford, et al., 2002). In contrast, the smooth stellate neurons are inhibitory (Houser, Hendry, Jones, & Vaughn, 1983; Prieto, Peterson, & Winer, 1994), and have varying non-pyramidal morphologies.

During early development all excitatory neurons share a common immature

morphology, with a single branched apical dendrite (Banker & Cowan, 1977; Miller & Peters, 1981). Then, over time, the basal dendrites appear, and oblique side branches extend from the apical shaft. Following, as the arborization of the basal and apical dendrites becomes more complex, dendritic spines appear on the dendrites. When the pyramidal neurons reach their mature morphology they have a highly complex dendritic arbor and are covered with spines.

The spiny stellate neurons also start with a pyramidal morphology, and then acquire their stellate morphology by retracting the apical dendrite early in development (Vercelli, Assal, & Innocenti, 1992).

1.3.1.1 Dendrite structure

Ultrastructurally dendrites contain all of the organelles present in the cell body including ribosomes and associated mRNAs. Dendrites are composed of filamentous actin (F-actin) at their exterior, and a microtubule core (Peters, Palay, & Webster, 1991). Microtubules are present throughout the entire trunks of the dendrites, and provide structural integrity.

The most prominent microtubule associated protein (MAP) that is localized specifically to dendrites is MAP2 (Garner, Tucker, & Matus, 1988). MAP2 caps the ends of growing microtubules and imparts stability to the dendrites. MAP2 is a substrate for both cAMP and calcium/calmodulin dependent protein kinases (Mitchison & Kirschner, 1988). The phosphorylation of MAP2 decreases microtubule polymerization and increases dendritic stability. Therefore, MAP2 is crucial for determining the dendritic form by regulating the balance between unstable and stable forms of microtubules (Garner, et al., 1988). Due to the localization of MAP2 specifically to dendrites, it is often used as a dendritic marker, as it was in the experiments included in this dissertation. Importantly, some microtubules are altered by the presence/absence of FMRP. For example, the expression of MAP1B is regulated by FMRP (Wei, et al., 2007). MAP2, on the other hand, is not affected by alterations in the expression of FMRP (Steward,

Bakker, Willems, & Oostra, 1998). Therefore we were able to use MAP2 to enable the visualization of the dendritic arbor of our hippocampal neurons, without concern that the findings were confounded with alterations in its expression.

1.3.1.2 Dendrite differentiation

The process of dendritic arbor elaboration is highly complex, however for simplicity it can be broken down into a series of stages that include: neurite initiation, guided outgrowth, branching, synapse formation and stabilization at predetermined boundaries (Kossel, Williams, Schweizer, & Kater, 1997; Portera-Cailliau, Pan, & Yuste, 2003; Scott & Luo, 2001; Williams & Truman, 2004; Wu, Zou, Rajan, & Cline, 1999).

First, young unpolarized neurons extend neurites that quickly differentiate into an axon and multiple dendrites. The dendrites then go through a stage of extension. Like axons, dendrites must steer towards their targets so that the appropriate neural connections are formed. Also like axons, dendrites are guided to their targets by sources of diffusible ligands (Tessier-Lavigne & Goodman, 1996).

To cover the extent of the dendritic field necessary for correct neural circuitry, neurons must form extensive dendritic branches at defined intervals. Dendritic maturation is a highly dynamic process of branch addition and retraction (Dalva, Ghosh, & Shatz, 1994; Greenough & Chang, 1988; Harris & Woolsey, 1981; McAllister, Lo, & Katz, 1995; Ramoa, Campbell, & Shatz, 1988; Wise, Fleshman, & Jones, 1979). Generally there are two kinds of branching that are observed: interstitial branching (i.e., branching from the dendritic shaft) or tip bifurcation (i.e., splitting of the growth cone) (Acebes & Ferrus, 2000; Mizrahi & Libersat, 2002). Interstitial branching is thought to be the predominant mode of branching *in vivo* (Dailey & Smith, 1996), whereas splitting of the growth cones is more common in certain *in vitro* conditions (Bray, 1973).

In interstitial branching, the branches first appear in the form of a single long thin protrusion called a filopodium. Filopodia are highly motile extensions of dendrites (or axons) that are 2-10μm long and less than 1μm thick (Segal, 2005). Most filopodia quickly retract into the dendritic shaft; however, others develop growth cone structures

that can then develop into stable branches (Dailey & Smith, 1996). The process of dendritic branch stabilization is not fully understood, but can be presumed to occur in a similar manner as that which occurs in axons. In general, local cues cause cytoskeletal destabilization at the prospective branch site. Transient branches, in the form of actin filled filopodia, are extended, and then, with the incorporation of microtubule proteins the branches become stable (Yu, Ahmad, & Baas, 1994).

Next, the dendrites elaborate and many generate small protrusions called dendritic spines (**See Section 1.3.2**). Similar to the formation of dendritic branches (as discussed earlier), dendritic spines emerge as lateral protrusions of membrane and cytoskeleton. Observations of hippocampal neuron dendrite formation revealed that dendritic branching and dendritic spine formation share the same initial stages of development (Dailey & Smith, 1996). In both cases, the structures are first transient filopodia. These transitory structures can then entertain one of three fates: they either retract and disappear, extend to form a branch, or transform into stabile dendritic spines. The determination of whether the filopodium becomes a branch or a spine is in part defined by the cytoskeletal elements that are incorporated: microtubules are required for dendrite stabilization, whereas actin is necessary for dendritic spines. Also, stage of development plays a role in whether the filopodia mature into dendrite branches or dendritic spines; there appears to be a developmental progression from filopodia transitioning into mostly branches or mostly spines (Dailey & Smith, 1996).

Finally, the development of the dendritic arbor is arrested at defined borders. Dendrites appear to know where their territories end, and stop growing if their arbors have covered that territory. The dendritic arbor of neurons covers a pre-determined dendritic field that is critical for the appropriate development of neural circuitry. In fact, the spacing of adjacent dendritic fields is adjusted to optimize the occupation of brain territory. Furthermore, due to space constraints of the skull, the territory of dendrites is dictated by evolution. Signals that regulate the extent of the dendritic arbor include both diffusible factors such as growth factors and signals mediated through direct contact between dendrites (e.g., contact inhibition mediated by adjacent retinal ganglion cells

(Sernagor, Eglen, & Wong, 2001)).

In general, the initial extension of the neurites is quite slow, and then during the period of outgrowth the dendrites lengthen in a very fast manner. For example, in *Xenopus laevis*, the total dendritic length increases from 50μm to 100μm in the first 24 hours. Then, in the following 48 hours, there is a 4-fold increase in the total dendritic length (Wu, et al., 1999). Moreover, the final stage of stabilization occurs over a long period of time (Williams & Truman, 2004; Wu, et al., 1999). The timing of the individual stages described above may vary between species, but this overall sequence is conserved.

Once the maturation of the dendritic arbor is complete, some plasticity is still preserved. However, compared to dendritic arbors during development, mature dendritic trees are much less malleable and have low branch turnover under basal conditions (Wu, et al., 1999). Also, it is important to recognize that while the development of dendritic arbors is presented here as a series of independent stages, in reality, the growth of dendrites occurs as a combination of the above steps in a simultaneous manner.

1.3.1.2.1 Control of dendrite development

Dendritic arbor development is controlled by a complicated interacting network of proteins including those involved in signal transduction, macromolecule synthesis, cytoskeletal rearrangements, and intracellular trafficking of dendritic machinery and components. In turn, these factors are regulated by both intrinsic genetic control and through modification by extracellular signals. Furthermore, this regulation can act either globally (i.e., on the whole cell), or locally (i.e., on specific dendrites or regions of dendrites). The evidence for these mechanisms of developmental control is presented here in this section; and, the generalities of processes involved are presented in the section that follows. However, the detailed molecular mechanisms are beyond the scope of this dissertation and the reader is encouraged to refer to recent reviews by Ethel and Pasquale (2005) and Urbanska and colleagues (2008) for a comprehensive summary of this topic.

The involvement of genetics is evident when we consider the fact that the shape of certain neurons is consistent between species. For example, interneurons look like interneurons, and motorneurons resemble motorneurons, regardless of their species of origin (Consoulas, Duch, Bayline, & Levine, 2000; Consoulas, Restifo, & Levine, 2002; Duch & Levine, 2000, 2002; Mendenhall & Murphey, 1974; Mizrahi, et al., 2000; Scott, Raabe, & Luo, 2002). Pyramidal neurons (and other neuron types) maintain their characteristic appearance regardless of environment (i.e., *in vivo* versus *in vitro*). In fact a number of studies have shown that the dendritic morphology of neurons is so well conserved *in vitro*, that it is possible to identify the type and region of origin of the neurons based on the general shape of their dendritic arbors (Banker & Cowan, 1979; Bartlett & Banker, 1984; Bray, 1973). Additionally, Purkinje cells can develop their fully mature characteristic dendritic arbors and spines, even with very minimal afferent input from granule cells (Altman & Anderson, 1972; Rakic & Sidman, 1973).

However, although the main dendrite organization occurs with little variability, the fine patterning of more distal higher order branches is more variable (Libersat & Duch, 2002; Mizrahi, et al., 2000). Most neurons do not reach the full complexity of their mature *in vivo* form when grown in culture. Therefore it appears that the general shape of the dendritic arbors is controlled by intrinsic genetic factors, whereas the finer details are determined by additional extracellular cues. These factors will be discussed below.

Figure 1.7: Factors that control dendritogenesis

Dendritogenesis is a highly regulated process that is controlled by a number of factors. Aspects of the intrinsic genetic program are modified by extracellular signals. Together these factors cause changes in the cytoskeleton, macromolecule synthesis and membrane turnover. These factors can also act to effect changes to the genetic program. Many of the changes can occur locally or globally on the same dendrite, or neuron.

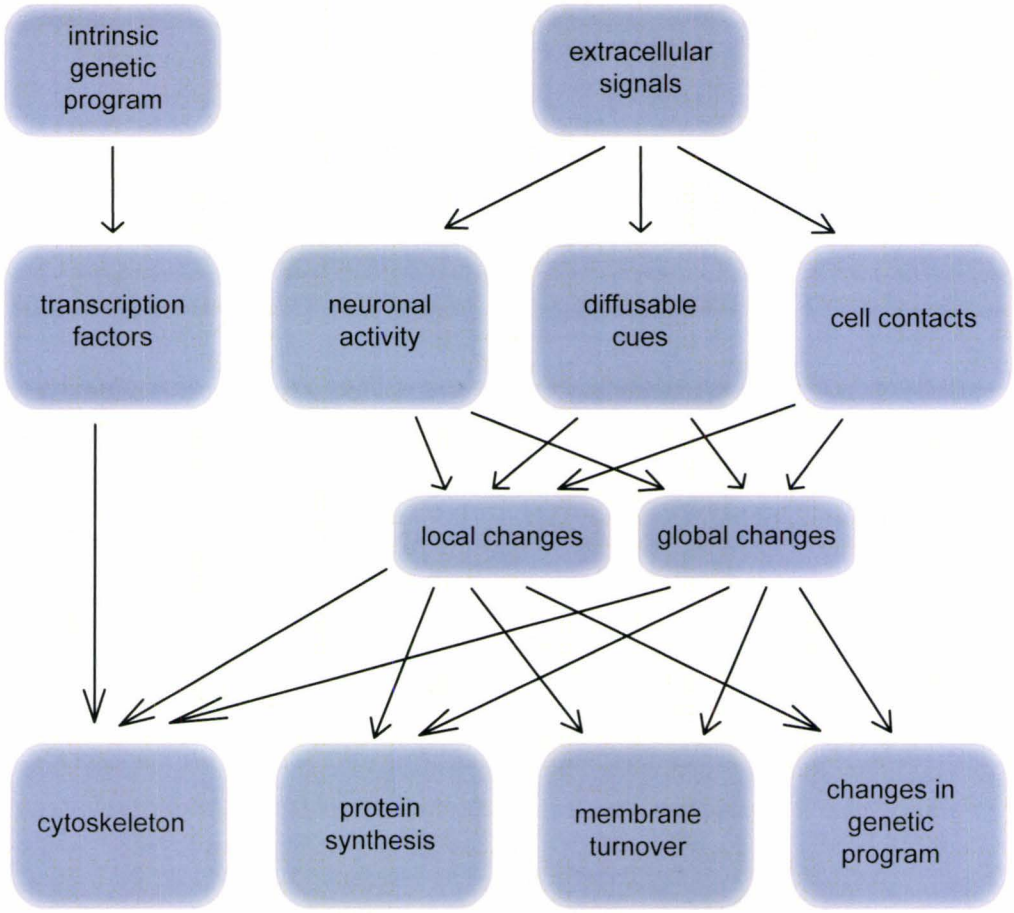
intrinsic genetic program
extracellular signals
transcription factors
neuronal activity
diffusable cues
cell contacts
local changes
global changes
cytoskeleton
protein synthesis
membrane turnover
changes in genetic program

Figure 1.7

1.3.1.2.2 Control of dendrite arbor morphology

As mentioned above, the basic structure of the dendritic arbor is defined by a genetic program and is modified by extrinsic factors (**Figure 1.7**). The genetic program is executed by transcription factors (TF) that can act either as an independent intrinsic program, or can be modified by external factors. Evidence for the independent action of TF comes from studies in *Drosophila*. Specific TF are expressed differentially in the various subtypes of neurons, which enables the generation of the type-specific morphology of each neuron (Moore, Jan, & Jan, 2002). Often, a number of TF work simultaneously to carry out the genetic program. In *Drosophila* neurons multiple TF are involved in the shaping of the dendritic arbor. These TF are expressed in various combinations in the neurons, with different TF expressed at different levels in the individual subtypes of neurons (Parrish, Emoto, Jan, & Jan, 2007; Parrish, Emoto, Kim, & Jan, 2007). Through this differential expression, the characteristic dendritic arbors of the neurons are created. In mammals, less is known about autonomously acting TF in the control of dendrite arbor morphology. One example that defines pyramidal neuron dendrite arborization is the basic helix-loop-helix factor, Neurogenin 2 (Ngn2) (Hand, et al., 2005).

Additionally, the action of TF can be regulated by synaptic activity - both experience dependent and spontaneous. There is convincing evidence for a role of synaptic activity in dendritic arbor maturation. As early as 1969, Morest found that dendrites grow toward sources of input. Twenty years later, Vaughn (1989) found that dendritic branches were formed at points of synaptic contact, and that new dendritic branches were stabilized by synapses. As a result of these findings he proposed the "synaptotropic hypothesis of dendrite growth". In support of this theory, the arrival of afferent contacts is coincident with the stage of dendrite development in many developing systems (Mason, Morrison, Ward, Zhang, & Baird, 1997; Mizrahi & Libersat, 2002; Murphey, Mendenhall, Palka, & Edwards, 1975; Rakic, 1975; Rakic & Sidman, 1973). Additionally, cultured hippocampal neurons were found to only form dendritic branches when they receive afferent innervation (Kossel, et al., 1997). *In vivo*, increased visual

activity driven by exposure to light was found to promote dendrite growth (Sin, Haas, Ruthazer, & Cline, 2002). Furthermore, the theory predicts that branches of dendrites will retract if they are innervated by synapses that are transitory or are weakened. This aspect of the theory has also been proven true. Monocular deprivation results in alteration of the dendritic arbor properties of the lateral geniculate nucleus (LGN) neurons in the cat visual system (Borges & Berry, 1978; Friedlander, Stanford, & Sherman, 1982; Wiesel & Hubel, 1963). Similar alterations to dendrite arborization were observed in *Drosophila* (Barth, Hirsch, Meinertzhagen, & Heisenberg, 1997). However, not all neuron subtypes are equally affected by a lack of synaptic activity. Visual deprivation does not affect the dendrite growth of subpopulations of stellate and pyramidal cells in the visual cortex (Lund, Holbach, & Chung, 1991; Tieman, Zec, & Tieman, 1995). It would therefore appear that afferent activity plays a major role in shaping dendrites of the post-synaptic cell in a variety of systems, but this is not universal for all types of neurons.

Molecular signaling, either by diffusible cues or cell contact, also contributes to defining the shape of neuronal dendritic arbors (**Figure 1.7**). A number of cell-contact factors are known that influence the shape of dendritic arbors by either enhancing or inhibiting dendritic growth and branching, for example: interaction of cell surface proteins like contactin, N-cadherins, seven-pass transmembrane cadherins (Flamingo, Celsr2 and Celsr3), Delta and Notch, ephrinB and EphB, and cell adhesion molecule L1 (as reviewed in Urbanska, et al., 2008). Cell-surface proteins also ensure appropriate dendritic growth by mediating the extent of the dendritic arbor (i.e., contact inhibition) and by inhibiting the crossing of dendrites (e.g., Down's syndrome-related cell adhesion molecule (Dscam) (Hughes, et al., 2007; Matthews, et al., 2007; Soba, et al., 2007; Zhu, et al., 2006). In addition to cell surface proteins that mediate dendritogenesis via interneuronal interactions, communication between neurons and glia also help ensure proper arborization. The details of glia-mediated guidance of dendrite growth will be discussed later (**See Section 1.5.1**).

Diffusible cues are also important factors that shape the development of dendrites and some include: thyroid hormones, steroid hormones and glucocorticoids, agrin,

members of the bone morphogenetic protein family, cpg15, semaphorins, Slits, and neurotrophic factors such as brain-derived neurotrophic factor (BDNF), neural growth factor (NGF), neurotrophins (NT) 3 and 4 (for review see Urbanska, et al., 2008). *In vivo*, NT generally increase the dendrite length and complexity, however, the effect is dependent on the type of NT, the layer in which the neuron resides, and whether the dendrite is apical or basal (Baker, Dijkhuizen, Van Pelt, & Verhaagen, 1998; McAllister, et al., 1995; Niblock, Brunso-Bechtold, & Riddle, 2000).

Depending on the developmental stage the extracellular cues described above are integrated to affect change in the dendritic arbor (Jan & Jan, 2003; McAllister, 2000; Parrish, Kim, Jan, & Jan, 2006; Wong & Ghosh, 2002). The stage of development can also have an effect on the manner of activity dependent morphological changes. In some vertebrate systems there appear to be two types of activity-dependent dendrite growth. The first stage, early in development, is an NMDA receptor (NMDAR) and calcium dependent stage of growth and sprouting (Iwasato, et al., 2000; Rajan & Cline, 1998; Sin, et al., 2002). Later in development, the second stage is an NMDAR-independent but AMPAR-dependent stabilization of dendrites (Rajan & Cline, 1998).

Dendritogenesis is therefore controlled by a complex number of intrinsic factors and extracellular cues that are modified by developmental stage. Given the highly intricate process required for normal dendrite growth, it is not surprising that alterations in the normal functioning of any one of these factors can result in abnormal dendritic arbors, altered neuronal signaling, and disease.

1.3.1.3 Dendrites in disease

Dendritic geometry is important for determining firing patterns of neurons, and the nature of neural circuitry. Alterations in the dendritic organization have a major impact on the processing of afferent information by individual neurons. Even slight alterations in dendritic structure and therefore the organization of many neurons, will lead to significant changes in information processing overall.

Abnormalities in the patterning of dendritic arbors have been found in a number

of neurological diseases including psychiatric disorders such as schizophrenia (Harrison, 1999), and neurodegenerative diseases (Anderton, et al., 1998). Animal studies have also revealed that mild, prolonged stress can induce decreases in the dendritic fields of hippocampal neurons, with regression of dendrites and a loss of dendritic spines (Chen, Dube, Rice, & Baram, 2008; Wood, Young, Reagan, Chen, & McEwen, 2004). Furthermore, animal studies investigating environmental causes of mental retardation such as prenatal alcohol exposure, hypothyroidism, fetal hypoxemia, experimental hyperphenylalaninemia, and protein deprivation, all showed a decrease in dendritic ramification (as reviewed in Dierssen & Ramakers, 2006). In humans, a decrease in dendritic arbor complexity, specifically with a reduced degree of branching, was found in children with mental retardation (Huttenlocher, 1974). Subsequent studies confirmed that dendritic abnormalities were characteristic of diseases of mental retardation, such as Down's, Rett and Fragile X Syndromes (for review see Huttenlocher, 1990; Kaufmann & Moser, 2000).

1.3.1.3.1 Dendrites in Fragile X Syndrome

Unlike some other disorders of mental retardation, the gross alterations of dendrite organization have not been studied extensively in Fragile X syndrome. Studies in *Drosophila* revealed that a loss of *Drosophila FMR1* (*dFMR1*) results in an increase in dendritic branching, whereas over-expression of *dFMR1* causes decreased extension and branching (Pan, et al., 2004). This finding was consistent with the results from a study looking at dendritic development in the in the barrel cortex of the *FMR1* null mouse (Galvez, et al., 2003). Based on their findings of a lack of dendritic rearrangement in the null mouse, the authors suggest that there is some impairment in developmental processes that shapes the dendrites and dendritic spines in Fragile X (Galvez, et al., 2003). In fact, the alterations in dendritic spine morphology are a cardinal feature of FXS, and as such most of the research has focused on this finer detail of dendrite morphology and will be discussed in the following.

1.3.2 Dendritic spines

The final step in the acquisition of mature dendrite morphology is the development of the dendritic spines. Dendritic spines are small protrusions scattered along the dendrites of many neurons, and are approximately 0.5μm in diameter and 0.5-2.0μm in length (Nimchinsky, Sabatini, & Svoboda, 2002) (**Figure 1.8a**). In contrast to the microtubule-based cytoskeleton of the dendrites, dendritic spines are typically composed of a filamentous network of actin and actin-regulating proteins (e.g., calmodulin, myosin, brain spectrin (fodrin) and MAP2). The actin filaments are organized longitudinally in the spine necks, whereas in the spine head they form a lattice, suggesting they form the scaffolding for the elementary structure of the spine

Dendritic spines contain a number of proteins including: the neurotransmitter receptors that mediate the ligand-dependent influx of ions into the post-synaptic neurons, and numerous other proteins that are important for synaptic transmission (**Figure 1.9**). Some cellular organelles are also present in dendritic spines. All spines contain smooth endoplasmic reticulum (SER) in an amount that is proportional to the spine volume and area of the post-synaptic density (PSD), and occupies about 10-20% of the total spine volume (reviewed in Harris & Kater, 1994). Like the sarcoplasm of muscle cells, the SER in neurons is thought to be involved in the sequestration and intracellular release of calcium (Harris & Kater, 1994). In the more complex spines, the SER constitutes a structure known as the spine apparatus (Gray, 1959), and is proposed to carry out functions similar to the Golgi apparatus. Mitochondria are typically not found in dendritic spines, with the exceptions being the very complex and large spines of the cerebral cortex, hippocampal CA3 and olfactory bulb (Harris & Kater, 1994). Significantly, polyribosomes are present in dendritic spines, and their frequency in the spine vicinity increases during synaptogenesis. The localization of polyribosomes, together with associated mRNAs, to the dendritic spines is now known to be important for activity dependent translation of proteins required for synaptic signaling and plasticity.

Figure 1.8: Dendritic spine morphology

(a) Dendrirtic spines are small protrusions extending from the dendrites, which are typically 0.5μm in diameter and 0.5-2.0μm in length.

(Image obtained at http://en.wikivisual.com/index.php/Dendritic_spine)

(b) Dendritic spines are dynamic structures display a wide variety of morphologies. In general, however, spines are one of three general shapes: thin, mushroom, or stubby.

(Image adapted from http://en.wikivisual.com/index.php/Image:Spine-Types.gif)

a

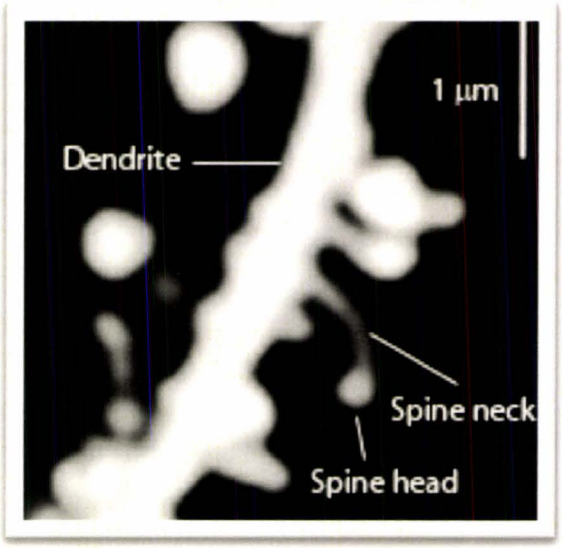
1 µm
Dendrite
Spine neck
Spine head

b

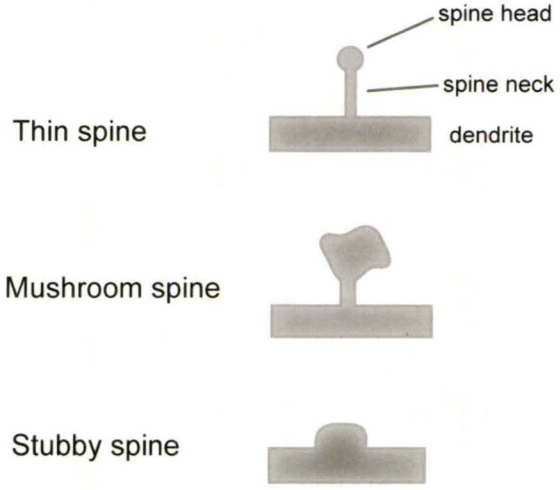
spine head
spine neck
Thin spine
dendrite
Mushroom spine
Stubby spine

Figure 1.8

Figure 1.9: Schematic diagram illustrating some of the components of dendritic spines.

Spines are small membrane protrusions at excitatory synaptic junctions that use the neurotransmitter glutamate, which is released from synaptic vesicles clustered in the pre-synaptic terminal. Across from these glutamate release sites, AMPAR and NMDAR are clustered at the post-synaptic active zone within a dense matrix called the postsynaptic density (PSD; green). Beyond the PSD lie subregions of spine membrane that contain mGluRs and endocytic zones for recycling of membrane proteins. Receptors, in turn, connect to scaffolding molecules, such as PSD-95, which bind to other proteins within the spine. Actin filaments provide the main structural basis for spine shape. Via a network of protein interactions, actin filaments indirectly link up with the neurotransmittter receptors and other transmembrane proteins that regulate spine shape and development, including Eph receptors, cadherins, and neuroligins. Translational regulators (e.g., FMRP) and polyribosomes are also present in the spines to facilitate the activity-dependent protein translation that occurs in response to signaling across the synapse.
(Image adapted from, Figure 1, Calabrese et al., 2006)

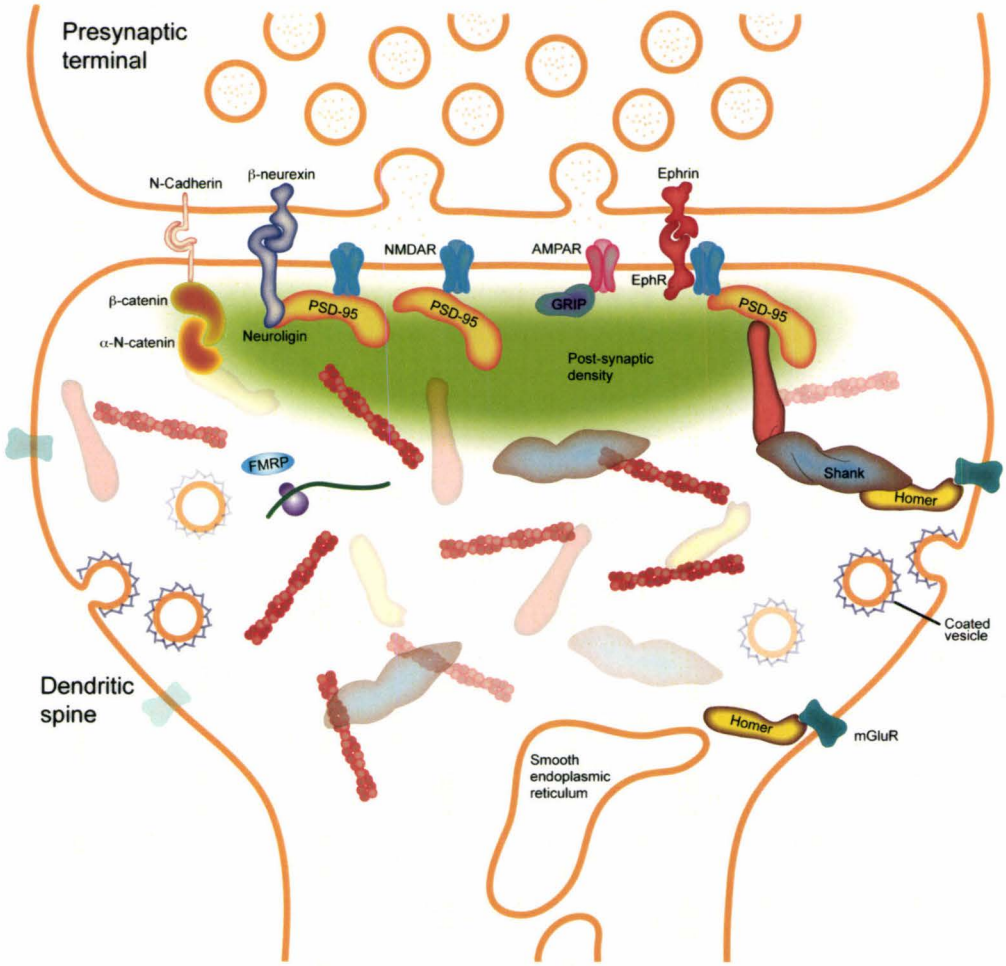
Presynaptic terminal
N-Cadherin
β-neurexin
Ephrin
NMDAR
AMPAR
EphR
β-catenin
α-N-catenin
Neuroligin
PSD-95
PSD-95
GRIP
PSD-95
Post-synaptic density
FMRP
Shank
Homer
Coated vesicle
Dendritic spine
Homer
mGluR
Smooth endoplasmic reticulum

Figure 1.9

Dendritic spines exhibit a wide variety of morphologies (**Figure 1.8b**). Spine necks can be short or long, fat or thin, bent or straight, irregular or cylindrical, with or without branches, or some combination of all of these. The heads of spines can be large or small, and oval, spherical or irregular in shape. In fact, the dimensions of parameters such as the spine length, diameter, volume, area, area of the post-synaptic density, can differ by greater than ten-fold between different spines (Harris & Kater, 1994). Based on these parameters spines can be classified into numerous different types. This classification can become quite complex; however, three basic spine morphologies include: thin spines with thin necks and bulbous heads; mushroom spines that have broader heads; and stubby spines without necks (Vanderklish & Edelman, 2002).

The physical features of spines can differ on each cell type, or even among spines on the same dendrite. In a review by Harris and Kater (1994), the authors suggest that the diversity in spine morphology may be indicative of various changes in the lifetime of one spine, or reflective of varying synaptic efficacies at different synapses along the dendrite at a single point in time. Furthermore, they suggest that the different morphologies could represent successive stages that an individual spine must pass through in its development. Dendritic spines are dynamic structures and the shape of the spine head can change within seconds (Fischer, Kaech, Knutti, & Matus, 1998). The volume of a spine head is proportional to a number of other of its physical features such as: its synaptic area, the number of postsynaptic receptors and pre-synaptic docked vesicles (Harris & Stevens, 1989; Schikorski & Stevens, 1999). The importance of dendritic spine size is due to its relationship with synaptic transmission.

Dendritic spines are the post-synaptic elements of the excitatory synapses in the central nervous system. In fact, the number of spines nearly approximates the number of excitatory synapses. In 1992, Harris and others revealed that the number of dendritic spines on hippocampal pyramidal neurons is approximately equal to the number of excitatory synapses. In 2004, Nimchinsky and coauthors confirmed this finding, establishing the nearly one to one ratio for excitatory synapses and dendritic spines (Nimchinsky, Yasuda, Oertner, & Svoboda, 2004).

1.3.2.1 Development of dendritic spines

The formation of dendritic spines occurs via a developmentally regulated program that is subject to modification by synaptic activity. The specifics of the process of spine formation are not fully understood, however three basic theories have been suggested based on experimental evidence. First, and perhaps most commonly, spines are thought to be formed *de novo*. In this scenario, similar to dendritic branches, dendritic spines are thought to mature from initial protrusions of filopodia from the dendrites. The filopodia are highly dynamic projections that rapidly change their length and shape, and last only a short period of time before they either disappear or become a mature spine (or a dendritic branch; see **Section 1.3.1.2**). These filopodia are thought to sample the surrounding microenvironment for active pre-synaptic partners with which they can form synapses (Dunaevsky & Mason, 2003; Jontes & Smith, 2000; Yuste & Bonhoeffer, 2004; Ziv & Smith, 1996). As neurons mature, the filopodia become less dynamic, and retract into the dendritic shaft just prior to the dendritic spines being formed (Dailey & Smith, 1996; Fiala, Feinberg, Popov, & Harris, 1998).

Interestingly, few filopodia are found in mature neurons, and yet there are large fluctuations in spine density at any point in time (Miller, 1981). Therefore, in mature neurons it is less likely that the new spines being formed are differentiating from new filopodia. Perhaps, then, different mechanisms of spine formation are more prevalent at different stages of development.

Miller (1981) studied the emergence of dendritic spines during development in the pyramidal neurons of the early postnatal rat visual cortex. His work revealed that in the first week post-natally there are relatively few mature spines, and the dendrites are covered with a large number of filopodia-like processes and stubby spines (Miller & Peters, 1981). Then, between post-natal days 6 and 9 (P6-P9), and again at P12-P15, there is a large increase in the number of spines. The spine density then continues to increase over the first post-natal month, and then declines slightly. As the number of mature spines increased, the number of filopodia (and stubby spines) decreased.

Initially the spines are distributed evenly over the dendrites, with the exception of the area adjacent to the cell body. Then, at P15, the spine density increases with distance from the cell body for distances between 0 and 125μm, with a higher density of spines in the more distal dendrites. From there, the density of the spines is fairly stable or decreases slightly. Boothe and colleagues (1979) found a similar pattern of dendritic spine density changes in pyramidal neurons of the visual cortex from the *Macaca nemestrina* monkey (pig-tailed macaques). On the other hand, they revealed that the density of dendritic spines in spiny stellate neurons increased more slowly over development, and were equally distributed along the lengths of the dendrites (Boothe, et al., 1979).

An increased density of spines is associated with an increased complexity of synaptic integration. Jacobs and others (2001) evaluated different Broadman areas and compared the spine density to the complexity of neural processing that occurred in those areas, and found that neurons in those areas with higher order cognitive processing had an increased density of dendritic spines.

It is thought that the variation in spine density is a result of a progressive slow down of spine elimination (Zuo, Lin, Chang, & Gan, 2005). The number of spines present at any given time is a function of the net production of spines formed (i.e., the number of spines formed compared to the number of spines eliminated). The rate of spine formation is relatively constant for most of postnatal life, whereas the rate of spine elimination appears to be developmentally regulated (Holtmaat, et al., 2005; Zuo, et al., 2005). As such, there is a decrease in the rate of elimination with increasing age, and a resulting increase in the net number of spines.

The elimination, or pruning of spines is important for the fine-tuning of mature neural circuitry. Furthermore, given the direct contrast of spine pruning with spine formation, it has been suggested that spine elimination may also be important for synaptic plasticity: if spine formation is associated with long-term potentiation (LTP), it is possible the spine elimination is related to long-term depression (LTD) (Segal, 2005). Segal (2005) cautions that this might be an overly simplistic view, and suggests that while the

evidence for an association between spine formation and LTP is well-established, the proof for a relationship between the elimination of spines and LTD is less than satisfactory.

1.3.2.2 Functions of dendritic spines

1.3.2.2.1 Synaptic Plasticity

Synaptic plasticity was described briefly earlier (**Section 1.1.2.4**), but it warrants a more in depth discussion here. Within the central nervous system, plasticity is considered to be the capacity of experience-generated neural activity to modify neural circuits. Thereby synaptic plasticity shapes future thoughts, feelings and behaviours. Synaptic plasticity refers specifically to the activity-dependent alteration of the efficacy or strength of synaptic signaling at existing synapses. Since the first description by Ramon Y Cajal, synaptic plasticity has been suggested to play a key role in the ability of the brain to form persistent memories from transient experiences. In addition, synaptic plasticity is thought to be central to early neural circuit development.

Synaptic transmission can either be augmented or attenuated by activity, and the changes that result are on the order of milliseconds to hours, days or perhaps even longer. From these characteristics – the effect of activity, and the length of change – a number of types of synaptic plasticity have been described. Short-term plasticity is generally triggered by short bursts of activity that result in transient accumulations of calcium in the pre-synaptic terminal, and the results last only milliseconds to several minutes (for review see Citri & Malenka, 2008). Included among the forms of short-term plasticity are: paired-pulse facilitation and depression, and facilitation and depression following trains of stimuli (Citri & Malenka, 2008). These types of plasticity are thought to play a role in short-term adaptations to sensory inputs, behavioural state changes that are transient, and short-term forms of memory (Citri & Malenka, 2008).

Alternately, long-lasting modifications of synaptic strength caused by experience (i.e., long-term synaptic plasticity) are considered to be the underlying mechanisms of long-term behavioural changes. Over a century ago, Ramon y Cajal first proposed the

idea that the brain encodes events as complex patterns of activity in neural circuits, and that memories are formed (i.e., new information is stored) when the pattern of synaptic weights are altered by activity to generate long-lasting effects. In the 1940s, Donald Hebb further developed this theory and suggested that synapses are strengthened when pre-synaptic activity correlates with post-synaptic firing (Hebb, 1949). The first evidence for the existence of long-term activity dependent alterations in the strength of synapses was first reported 20 years later by Bliss and others (Bliss & Gardner-Medwin, 1973; Bliss & Lomo, 1973). They found that a potentiation of synaptic strength, lasting hours to days, could be induced in hippocampal neurons following the repetitive activation of excitatory synapses (Bliss & Gardner-Medwin, 1973; Bliss & Lomo, 1973). This came to be known as long-term potentiation (LTP).

In addition to being enhanced via LTP, synaptic strength at excitatory synapses can be weakened by activity, in a form of synaptic plasticity called long-term depression (LTD). In contrast to the high frequency stimulation that elicits LTP, LTD is typically triggered by prolonged repetitive low frequency stimulation (Dudek & Bear, 1992; Mulkey & Malenka, 1992). A number of different forms of LTD have been described (reviewed in Citri & Malenka, 2008), the most important in terms of Fragile X research being the mGluR-dependent LTD (**Section 1.1.2.5**).

1.3.2.2.2 Dendritic spines as a cellular basis for learning and memory

Changes in the appearance of dendritic spines are thought to represent a means by which recent synaptic activity leaves a lasting effect on neurons; and this synaptic plasticity is understood to be the physiological correlate of learning and memory. In fact, as early as 1893, Ramon y Cajal and Tanzi suggested that changes in the dendritic spine number and morphology could be a cellular correlate for learning and memory.

A number of studies have found that following tetanic stimulation of hippocampal neurons in slices or in culture there is an increase in dendritic spine volume, providing evidence for a physical alteration in response to activity (reviewed in Segal, 2005). Studies have revealed that mature spine actin dynamics are closely related to both LTP

and LTD. LTP is inhibited by drugs that selectively block actin dynamics (for review see Matus, 2005). Furthermore, these same drugs enhance LTD (Matus, 2005). Also, actin turnover is decreased following the induction of LTD (Matus, 2005).

In addition to the alterations in appearance of the spines, the stabilization of mature spines is thought to require synaptic contact (Marrs, Green, & Dailey, 2001). Dendritic spines in the hippocampus undergo morphological changes in response to activity; synaptic activity results in the enlargement of spines and shortening of spine necks. Evidence for the activity-dependent changes in cortical spines comes from experiments in which deprivation paradigms were employed and followed by examination of the neurons with Golgi staining (Riccio & Matthews, 1985; Valverde, 1967). In these experiments most, but not all, spines were reduced in size with decreased synaptic activity. Furthermore, environmental enrichment results in an increase in spine density (Briones, Klintsova, & Greenough, 2004; Globus, Rosenzweig, Bennett, & Diamond, 1973; Rampon, et al., 2000; Schapiro & Vukovich, 1970). More recently this finding was confirmed in primates whereby environmental enrichment resulted in increases in spine density in pyramidal neurons of hippocampal CA1 (Kozorovitskiy, et al., 2005). The mechanisms through which sensory stimuli elicit increases in spine density are not yet known.

The activity dependent regulation of net spine density may be a result of two different scenarios. First, it is possible that activity may regulate the formation of new synapses. In this model, synaptogenesis is initiated by experience-related neuronal activity that is dependent on signals that arrive at the neuron in a temporally and spatially discrete manner. Second, activity may control the destabilization and/or elimination of synapses after they are formed. In this case, synapse formation occurs in a random, continual manner at a constant rate generating excess synapses. Following their formation the elimination of unnecessary synapses occurs in an activity dependent manner. It is possible that these mechanisms are not mutually exclusive. Different types of neurons may preferentially employ one of the above means of regulating synapse

number. It is also possible that the mechanisms may each be more prominent at specific stages in development; for example, neuronal activity may induce synapse formation early in development, and then may be important for activity dependent elimination of superfluous synapses at later stages.

As mentioned earlier, it has been suggested that while spine formation may be related to LTP, the elimination or pruning of spines may be associated with the contrasting form of synaptic plasticity, LTD. Even though evidence for the latter is lacking, a few studies have demonstrated that LTP is accompanied by increased numbers of enlarged spines, and that following the induction of LTD dendritic spines shrink and/or disappear (for review, see Segal, 2005). However, in some cases, pruning occurs following the intense synaptic stimulation that would normally result in LTP, such as in epilepsy or over-exposure to glutamate (reviewed in Segal, 2005). Therefore, in contrast to the elimination of synapses following stimulation that results in LTD, in certain cases pruning is associated with LTP. Additionally, in cultured hippocampal neurons one form of LTD can be induced by (S)3,5-dihydroxyphenylglycine (DHPG) stimulation of mGluR1 (Huber, Roder, & Bear, 2001), resulting in the elongation rather than the disappearance of spines (Vanderklish & Edelman, 2002). Therefore, it appears that the differentiation between induction of LTP and LTD is within narrow limits, and varies depending on a number of factors.

1.3.2.2.3 Dendritic spines facilitate compartmentalization of the synaptic signal

Dendritic spines are thought to facilitate signaling at synapses by modulating the synaptic response in a compartment that is separate from the dendritic shaft. One hypothesis is that the structure of dendritic spines creates boundaries within which synaptic function can be modulated. It is suggested that the spine neck provides a barrier to the flow of current and diffusion of molecules between the spine head and the dendrite. However, this effect may in fact be minimal, at least for the majority of spines and molecules. On the other hand, calcium diffusion in physiological conditions may be an exception, and the barrier function of the spine neck may prove to be a useful means to

allow the spines to act as independent calcium signaling compartments (for review, see Alvarez & Sabatini, 2007; Harris & Kater, 1994). In fact, mathematical calculations, based on anatomical and functional data have verified these claims.

If the constriction in the spine neck does act as a restrictive barrier, there would be a resulting amplification of the depolarization in the region immediately around the synapse (relative to if the synapse were on the dendritic shaft). Thereby, the narrowing of the spine neck could facilitate LTP induction because it would allow voltage-sensitive channels to open at a lower subsequent depolarizing potential (than on non-spiny dendrites). In fact, there is much evidence to support this hypothesis and is reviewed by Harris and Kater (1994).

The compartmentalization imparted by the constriction of the spine neck therefore allows a localized increase in calcium to reach the threshold level necessary to activate the second messenger systems within the dendritic spine. This increased intracellular calcium concentration could potentially be toxic within the dendrite itself. Notably, the sequestration of the calcium to the spine prevents toxic insults to the dendrite. Furthermore, the small volume of the spine is advantageous because, once the increase in calcium has served its purpose, the SER and cytoplasmic calcium buffers can restore the calcium levels to baseline very quickly.

Additionally, the capacity for a dendritic spine to isolate a synaptic response has the potential to facilitate the specificity of synaptic activation. For example, without the compartmentalization imparted by the dendritic spine neck constriction, the signal transduced at one spine would be able to diffuse and potentially modify adjacent synapses. Therefore, the dendritic spine neck narrowing helps ensure a more specific effect of potentiation.

Figure 1.10: Dendritic spines maximize dendrite surface area

(a) Longitudinal section of a spiny dendrite. The spiny dendrite has access to many axonal boutons.

(b) Longitudinal section through an aspiny dendrite occupying a similar amount of space. For the same area, the aspiny dendrite encounters less axons because there is no interdigitation of processes between spines, as in (a).

(Image adapted from Figure 4, Harris and Kater, 1994)

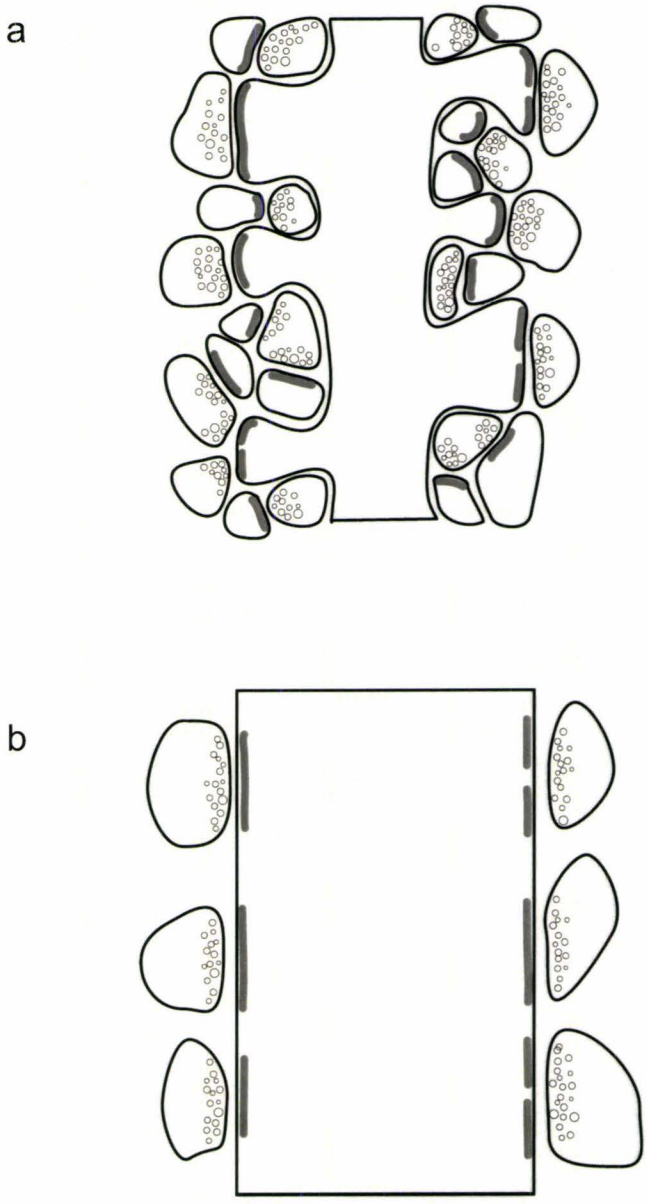

Figure 1.10

1.3.2.2.4 Dendritic spines maximize dendrite surface area

Dendritic spines also increase the surface area of the dendrite on which new synapses can form. Ramon y Cajal proposed this function of the dendritic spine based on the capacity for dendritic spines to allow the dendrite access to multiple axons as they course through the surrounding areas. Furthermore, they permit this increase in potential synaptic contacts within the confines of limited space. For an aspiny dendrite to establish a similar number of contacts, it would have to be greater in radius, and would therefore occupy more space (**Figure 1.10**).

1.3.2.3 Dendritic spines in disease

The proper development of dendritic spines is critical for the development of normal cognitive processes. In fact, dendritic spine abnormalities are found in disorders characterized by mental retardation, such as non-specific X-linked mental retardation, William's syndrome, Rett syndrome, Down's syndrome, Angelman syndrome, autism and FXS (Irwin, Galvez, & Greenough, 2000; Kaufmann & Moser, 2000; Purpura, 1975; Rudelli, et al., 1985). Abnormal dendritic spines are also associated other neurological disorders including schizophrenia and bipolar disorder with psychosis (as reviewed in Ethell & Pasquale, 2005). Additionally, dendritic spines are also altered in individuals with epileptic seizures, and those who have suffered hypoxia, ischemia and stroke (for review see Harris & Kater, 1994). In fact, the health of a neuron is normally reflected in the shape of the dendritic spines. Given the significant role of dendritic spines in the appropriate functioning of excitatory synapses, it is understandable that abnormalities in dendritic spines are associated with the dysfunction of synapses and considerable deficits in cognitive capacity.

1.3.2.3.1 Dendritic spines and Fragile X Syndrome

Both individuals with FXS and *FMR1* null mice exhibit immature spine morphology suggesting that FMRP may play a role in the formation of dendritic spines. Neurons from *FMR1* knockout mice show abnormal dendritic spine length and altered

spine densities (Galvez, et al., 2003; Grossman, et al., 2006; Nimchinsky, et al., 2001). Moreover, stimuli that are known to cause increases in spine density, such as environmental enrichment, promote recovery of both morphological and behavioural alterations in mouse models of FXS (Restivo, et al., 2005). In Fragile X post mortem specimens, investigators found an increase in the density of immature dendritic spines in the cerebral cortex (Hinton, et al., 1991; Irwin, et al., 2001). Hinton and others (1991) studied the brains of three males with Fragile X Syndrome, and found an increase in the number of long thin spines in the adult temporal cortex. Irwin and colleagues (2001) performed a more in depth analysis using the Golgi-Cox method, looking at the length, number and morphology of the dendritic spines of apical dendrites of layer V pyramidal neurons from the visual and temporal cortices. In that study, the authors found that cortices from the individuals with FXS exhibited more immature spines (and fewer mature spines), with a higher density on more distal segments of the apical dendrites. These alterations in spine morphology and density could be indicative of a deficiency in synaptic pruning in FXS.

1.3.2.4 Dendritic spines and FMRP

FMRP is an mRNA binding protein that functions as a translational repressor (Khandjian, 1999; Laggerbauer, et al., 2001; Li, et al., 2001; Zhang, et al., 2001) and a transporter of dendritic mRNAs (Antar, et al., 2004; Jin & Warren, 2003). FMRP and its mRNA are localized to dendritic spines (Todd, Mack, et al., 2003; Weiler & Greenough, 1999; Weiler, et al., 1997). Furthermore, FMRP is proposed to regulate the translation of a number of key postsynaptic molecules in dendritic spines (Brown, et al., 2001; Feng, Gutekunst, et al., 1997; Greenough, et al., 2001; Liao, et al., 2008; Weiler, et al., 1997; Willemsen, et al., 2004; Zalfa & Bagni, 2004; Zou, et al., 2008). Notably, many of these mRNAs are involved in spine development and synaptic plasticity such as: structural proteins (e.g., MAP2, PSD-95), receptor proteins (e.g., glutamate receptor subunits), and translation machinery (e.g., elongation factor 1α).

Dendritic spines are considered to be the cellular correlate for synaptic plasticity,

as mentioned earlier. Alterations in long-term synaptic plasticity of excitatory synapses have been observed in both hippocampal and cortical slices from *FMR1* null mice. The translation of FMRP, and its target mRNAs are both up-regulated in response to stimulation of group 1 mGluRs (Weiler, et al., 1997). Moreover, mice lacking FMRP show alterations in mGluR dependent LTD (Huber, et al., 2002), further supporting a role for FMRP in synaptic plasticity and therefore the physical characteristics of dendritic spines.

1.4 Synapses

Synaptic contacts are highly specialized contact zones across which the signal from the pre-synaptic neuron is transmitted to the post-synaptic neuron. Following their formation as the final step in neuron development, synapses are sculpted and remodeled by neuronal activity to achieve the mature pattern of connectivity of the brain (Katz & Shatz, 1996). It is estimated that the human brain contains approximately 10^{15} synapses (Brose, 1999) that control brain functions from simple motor skills to complex cognitive behaviours such as learning and memory.

1.4.1 The pre-synaptic compartment

The pre-synaptic region of the synapse is the terminal bouton of the afferent neuron's axon, and is the site from which neurotransmitters are released. As such, it contains the synaptic vesicles within which the neurotransmitters are stored, various proteins involved in the on-demand synthesis of neurotransmitters, membrane integrated molecules involved in the re-cycling of neurotransmitters and membrane associated proteins necessary for the docking and exocytosis of the synaptic vesicles. Certain molecular markers are unique to certain pre-synaptic terminals: for example, the enzymes required for neurotransmitter synthesis are only expressed in those neurons utilizing that select neurotransmitter. Other molecules are necessary for the function of all pre-synaptic zones and are therefore expressed ubiquitously and can be used as markers for all pre-synaptic sites. For example, synaptic vesicles and their associated proteins are expressed in all pre-synaptic terminals.

The release of neurotransmitters from synaptic vesicles at the pre-synaptic membrane occurs as a multi-step process: the synaptic vesicle is targets to release sites, docks at the active zone, prepares for fusion with the membrane, undergoes fusion and exocytosis to release the neurotransmitter, and recycles its constituents through endocytosis (Valtorta, Pennuto, Bonanomi, & Benfenati, 2004). At each step, a number of proteins are involved; two such molecules include synaptophysin and synapsin, and they are discussed in the following sections.

1.4.1.1 Synaptophysin

Synaptophysin (Syp/p38) is a 38kDa synaptic vesicle integral membrane protein found in all neurons of the CNS (for review see Valtorta, et al., 2004). It is a glycoprotein with four transmembrane domains, and is the major phosphotyrosine protein of the synaptic vesicles (Valtorta, et al., 2004). *In vitro*, Syp has been shown to interact with various synaptic terminal proteins including synaptobrevin II (VAMP2), the vesicular proton pump V-ATPase, myosin V, dynamin I, and the adaptor protein 1 (AP-1) (Valtorta, et al., 2004). The true function of Syp is not known, but *in vitro* and *in vivo* studies have suggested that it has a role in a number of processes related to the release of neurotransmitters. Some of the potential roles of Syp include: endocytosis/exocytosis of synaptic vesicles, regulation of SNARE assembly, formation of the fusion pore, activation of synaptic vesicle endocytosis, synaptic vesicle biogenesis and synaptic vesicle trafficking (Valtorta, et al., 2004). Since its discovery in 1985, it has become the most frequently used marker for the determination of synaptic density in the CNS.

1.4.1.2 Synapsin

The synapsins are a family of neuron-specific phosphoproteins that play a role in the organization of the pre-synaptic terminals (reviewed in Ferreira & Paganoni, 2002). They are found in the pre-synaptic compartment associated with the synaptic vesicles. The synapsins are encoded by three genes: *synapsin I*, *synapsin II* and *synapsin III*. Increases in synapsin I and synapsin II are associated with the formation of synapses both

in vitro and *in vivo* (Ferreira & Paganoni, 2002). Over-expression of *synapsin II* in a neuroblastoma/glioma cell line resulted in the development of synaptic-like varicosities (Han, Nichols, Rubin, Bahler, & Greengard, 1991). Furthermore, *synapsin I* null mice exhibit a decrease in both the number of synaptic vesicles and the size of the pre-synaptic terminal (Ferreira & Paganoni, 2002). Additionally, cells isolated from these mice display altered synaptogenesis *in vitro* (Ferreira & Paganoni, 2002). Ferreira and Paganoni (2002) reviewed a couple of mechanisms by which the synapsins are suggested to induce the formation of the pre-synaptic terminal. First, by binding to the membranes of synaptic vesicles, the synapsins may play a role in the recruitment of synaptic vesicles to the active zone of the synapse. Second, the synapsins may regulate other synaptic proteins involved in synaptogenesis, such as synaptotagmin, synaptobrevin and synaptophysin. Given the location and role of synapsins in the pre-synaptic terminal, synapsin has also become a widely used marker for the presence of synapses.

1.4.2 The post-synaptic compartment

Lying directly opposite the pre-synaptic neurotransmitter release sites is a specialized region of the post-synaptic membrane. This region is characterized by the presence of clusters of neurotransmitter receptors: glutamate receptors at excitatory synapses, and receptors for GABA or glycine (Gly) at inhibitory synapses. In fact, one of the first events in the differentiation of the post-synaptic compartment is the redistribution of the neurotransmitter receptors. Following that, a number of other related post-synaptic molecules are recruited and help define the nature of the synapse as excitatory or inhibitory.

1.4.3 The synaptic cleft

Between the pre- and post-synaptic compartments is the synaptic cleft, across which synaptic signals are transmitted. It is approximately 10-20nm wide (slightly wider than the usual extracellular space), and is filled with a dense staining material. The membranes of pre- and post-synaptic synaptic cleft are similar to the typical cellular bi-

layer lipid membrane interposed with various proteins. Specific to the synaptic cleft membranes is the presence of cell surface molecules involved in cell-cell adhesion. For example, the synaptic membrane at the site of the synapse is rich in cell adhesion molecules such as: integrin-type adhesion receptors, neural cell adhesion molecules (NCAMs), cadherins, dystroglycans, and the neurexins and neuroligins. These cell adhesion molecules are important for the initial axodendritic contact, and its stabilization (Ferreira & Paganoni, 2002). Also, the adhesion molecules play a role in the signaling pathways of both pre- and post-synaptic terminals during early synaptogenesis (Ferreira & Paganoni, 2002). Notably, the synaptic cell-cell adhesion molecules are expressed differentially throughout the CNS. Various combinations of these molecules are present in different cell types, and may therefore account for the specificity of the synapses in the brain (Brose, 1999). Moreover, some of the synaptic adhesion molecules, such as the neurexins and neuroligins, are present specifically in either the afferent neuron or the receptive terminal (Sudhof, 2008). These cell adhesion molecules and are therefore thought to play a role in the specificity of the pre- or post-synaptic differentiation, via something that is now known as heterotypic transynaptic signaling (Sudhof, 2008).

1.4.4 Inhibitory Synapses

Inhibitory synapses (**Figure 1.11a**) are symmetrical in appearance because their pre- and post-synaptic zones appear to be of almost equal thickness when viewed with electron microscopy (EM). Typically, inhibitory synapse terminal boutons contain both round and flattened synaptic vesicles that enclose the inhibitory neurotransmitters, most commonly GABA. In addition, the pre-synaptic compartments of the inhibitory synapses also contain other molecules that either mediate the effects of GABA, or interact with the post-synaptic cells directly.

The post-synaptic terminal of inhibitory synapses contains the receptors for the inhibitory neurotransmitters, and other molecules required for the transduction of the signal into, and through, the terminal. One molecule specific to inhibitory synapses is gephyrin, an anchoring protein that is vital for the clustering of inhibitory receptor

proteins (O'Sullivan, Hofer, & Betz, 2009).

1.4.5 Excitatory Synapses

The predominant excitatory neurotransmitters in the CNS are glutamate and aspartate. The synaptic vesicles of the pre-synaptic terminal in excitatory synapses are generally round and clear (Peters, et al., 1991). Excitatory synapses (**Figure 1.11b**) typically display an asymmetric appearance with EM due to the increased thickness of the synaptic region apposed to the post-synaptic membrane, the post-synaptic density (when compared to the pre-synaptic terminal).

The post-synaptic density (PSD) is an electron dense area of the membrane of the post-synaptic neuron, located adjacent to the synaptic cleft. The PSD is most commonly spoken of with reference to excitatory synapses, because it is within the excitatory synapses that the PSD is so pronounced. It is about 50 nm thick, and is either disc shaped, or is irregularly shaped and full of perforations. It is present on almost all excitatory synapses, including those that occur on dendritic spines. Notably, the dimensions of the spine are proportional to the total PSD area, and this is true for all brain regions (Harris, et al., 1992). A number of proteins are highly enriched in the PSD of the brain and potentially include proteins such as: receptor proteins, protein kinases, structural and associated proteins, proteins involved in endocytosis, and proteins involved in the glycolytic pathway.

More specifically, the PSD is a region rich in post-synaptic receptors, which in the excitatory synapses include the ionotropic (NMDAR and AMPAR) and metabotropic glutamate receptors (mGluRs). In addition to these receptor proteins, a recent study by Dosemeci and others (2007) presented a large list of proteins that were enriched in this excitatory post-synaptic region including, but not limited to, Homer, Shank1-3, CaMKII, actin, α-tubulin, β-tubulin, BRAG1, SynGAP, post-synaptic density protein 93 (PSD-93) and post-synaptic density protein 95 (PSD-95). In fact, PSD-95 is the major scaffolding protein of this region, with which all of the above proteins are associated (Dosemeci, et al., 2007).

Figure 1.11: Comparison of excitatory and inhibitory synapses

Schematic diagram illustrating the key components of the inhibitory synapse (a) and the excitatory synapse (b). Differences in the synaptic vesicles, post-synaptic receptors and structural proteins of the post-synaptic region are shown. Also, note the identification of the PSD (green) in the excitatory synapse only, reflecting its prominence in these synapses.

(Image modified from Figure 6, Mei & Xiong, 2008)

a

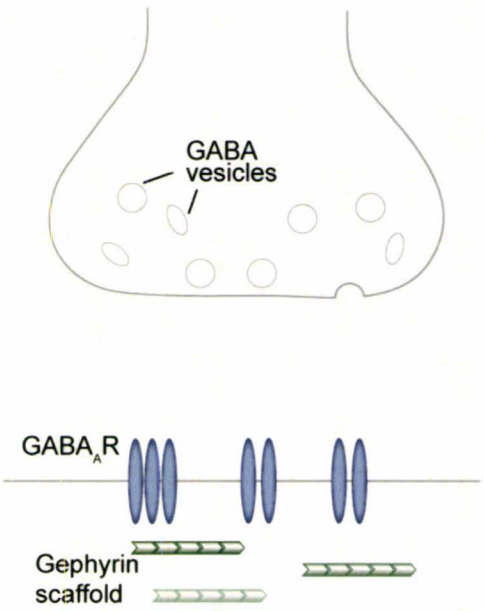

b

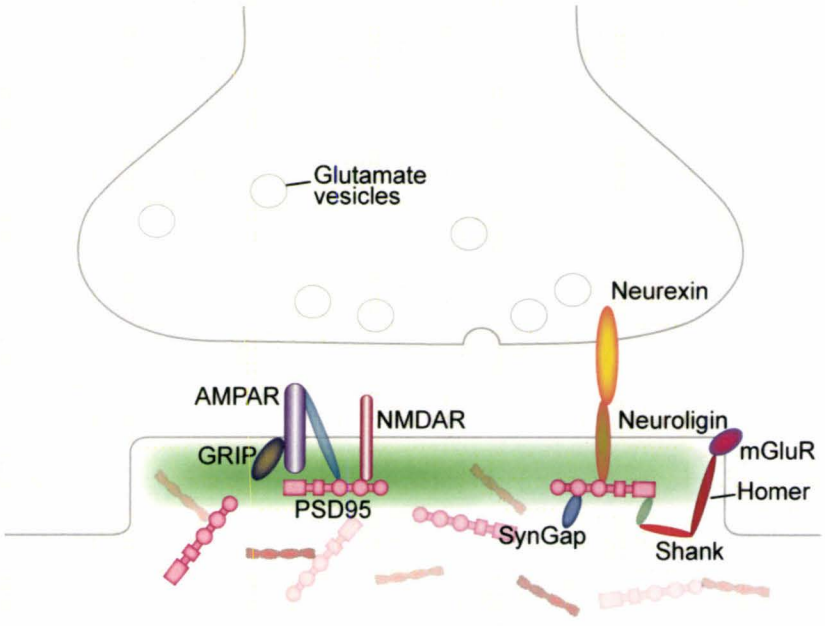

Figure 1.11

1.4.5.1 PSD-95

Post-synaptic density protein–95 (PSD-95/Synapse Associated Protein 90kDa, SAP90) is a PDZ domain containing protein that is localized to the post-synaptic density of asymmetric excitatory synapses (Kornau, Schenker, Kennedy, & Seeburg, 1995; Rao, Kim, Sheng, & Craig, 1998). PSD-95 is a member of the membrane-associated guanylate kinase (MAGUK) family of proteins (Cho, Hunt, & Kennedy, 1992). As mentioned above, PSD-95 helps to anchor synaptic proteins (Kim & Sheng, 2004), and is necessary for the development of excitatory synapses (Rao, et al., 1998). Furthermore, PSD-95 is required for activity driven synapse stabilization (Ehrlich, Klein, Rumpel, & Malinow, 2007). A lack of PSD-95 results in abnormal synaptic plasticity, and the over-expression of PSD-95 increases the size and number of dendritic spines (El-Husseini, Schnell, Chetkovich, Nicoll, & Bredt, 2000).

1.4.6 Synapse maturation

In general, synaptogenesis can be broken down into two stages: first the initial contact is established between pre- and post-synaptic terminals; and second, the differentiation of pre-and post-synaptic compartments is established through the specific recruitment of proteins respective of the synaptic compartment.

One of the first detectable physical characteristics observed in synaptic development, is the formation of the synaptic vesicles within the pre-synaptic region in close proximity to the contact zones (as reviewed in Ferreira & Paganoni, 2002). Following the establishment of the pre-synaptic zone, the differentiation of the post-synaptic zone begins. First, the neurotransmitter receptors are sequestered to the region adjacent to the synaptic cleft. Following that, specific anchoring proteins, such as PSD-95 and gephyrin, are recruited to the post-synaptic zone to limit the lateral movement of the receptors. These molecules also serve as a means to connect the post-synaptic receptors with components of the cytoskeleton, cell adhesion molecules and signal transduction molecules.

Once the synapse is formed, it is a dynamic structure. During early development, newly formed synapses are either strengthened or eliminated (Purves & Lichtman, 1980), as an essential step in the formation of mature, finely tuned neural circuits. As discussed earlier, this process partially depends on external signals and synaptic activity (See **Section 1.3.2.1**). Furthermore, this activity-dependent plasticity of the synapses continues into adulthood where it is important for the processes of learning and memory. As such, synapses are important for the development of neural networks throughout life, and their altered development can have profound pathological results.

1.4.7 Synaptic abnormalities and disease

Abnormalities of the synapse have been implicated as having a role in the pathology associated with a number of diseases including; depression, addiction, dementia, anxiety disorders, autism spectrum disorders and FXS (Luscher & Isaac, 2009).

The proper functioning of neural networks requires a delicate balance between excitatory and inhibitory synaptic inputs. Alterations in the excitatory/inhibitory (E/I) ratio have also been found in a number of disease models of mental impairment including FXS (Eichler & Meier, 2008; Fatemi, Reutiman, Folsom, & Thuras, 2009; Gibson, Bartley, Hays, & Huber, 2008; Kehrer, Maziashvili, Dugladze, & Gloveli, 2008; Majdi, Ribeiro-da-Silva, & Cuello, 2009; Wong, et al., 2006), and therefore have been implicated as a key neurobiological mechanism underlying cognitive impairment.

1.4.7.1 Synaptic abnormalities and Fragile X Syndrome

Because it is known that there is an approximately one to one ratio between the number of excitatory synapses and dendritic spines (Harris, et al., 1992; Nimchinsky, et al., 2004), inferences about the synaptic abnormalities in FXS can be made from the characteristic dendritic spine abnormalities. Both humans and mice lacking FMRP show abnormalities in synapse morphology, including: an increased number of long, thin, immature dendritic spines (Braun & Segal, 2000; Comery, et al., 1997; Grossman, et al.,

2006; Mineur, et al., 2002; Nimchinsky, et al., 2001) as well as an overall increase in spine density (Grossman, et al., 2006; Nimchinsky, et al., 2001). Based on the one-to-one ratio, it is therefore also possible that there is an increase in immature synapses (reflecting the immature spine morphologies), and a decrease in mature synapses in the Fragile X brain.

Some more specific insight into the nature of synaptic abnormalities in FXS has been elucidated recently. In a 2008 study, Gibson and others investigated membrane excitability and circuit activity of excitatory and inhibitory neurons in the Fragile X mouse. They found that the mice exhibited a substantial deficit in the excitatory projections to the layer IV inhibitory neurons in the barrel cortex (Gibson, et al., 2008). Furthermore they found that monosynaptic inhibitory signaling was unaffected (Gibson, et al., 2008). Based on these results the authors suggest that the local feedback inhibition of layer IV is impaired in the *FMR1* null mouse, and that this change results in the hyperexcitabilty of cortical circuits. Furthermore, they posit that this persistent UP state may be involved in the hypersensitivity to sensory stimuli, epilepsy and cognitive impairments seen in individuals with FXS.

A number of studies in the *FMR1* null mouse and Drosophila models of FXS have revealed that there are alterations in the expression of synaptic mRNAs (Zhang, et al., 2001), synaptic plasticity (Huber, et al., 2002; Li, et al., 2002; Nakamoto, et al., 2007; Zhao, et al., 2005), and activity dependent translation of synaptic proteins (Muddashetty, et al., 2007; Weiler, et al., 2004). These studies all support the idea that alterations in synaptic functioning are a key neurobiological mechanism underlying the clinical features of FXS.

1.4.8 Synapses and FMRP

Current evidence suggests that FMRP may be involved in the formation and/or maturation of synapses. mRNP complexes containing FMRP have been found in normal

dendritic spines (Feng et al., 1997; Nimchinsky et al., 2001), making it plausible that FMRP engages in key interactions with synaptic proteins. FMRP is thought to regulate the translation of a number of key postsynaptic molecules (Brown, et al., 2001; Feng, Gutekunst, et al., 1997; Greenough, et al., 2001; Liao, et al., 2008; Weiler, et al., 1997; Willemsen, et al., 2004; Zalfa & Bagni, 2004; Zou, et al., 2008). Notably, many of these mRNAs are involved in synaptic plasticity such as: structural proteins (e.g., MAP2, PSD-95), receptor proteins (e.g., glutamate receptor subunits), and translation machinery (e.g., elongation factor 1α). Additionally, FMRP itself is synthesized in post-synaptic regions (Weiler & Greenough, 1999), further supporting its role in synapse development and maturation.

Therefore a change in local protein synthesis caused by the absence of FMRP may result in a dysregulation of synaptic protein interactions, and therefore abnormal synaptic morphology. In support of this, Pfeiffer and Huber (2007) have shown that FMRP induces synaptic loss via acute postsynaptic regulation of translation. The altered FMRP-dependent protein interaction results in abnormal synapse development and pruning that may also affect synaptic plasticity (Braun & Segal, 2000), and therefore potentially be a contributing factor to mental impairment.

1.5 Astrocytes

Glial cells were first identified around 150 years ago as connective elements of the nervous system that filled the space between neurons or that glued the neurons together. Astrocytes have historically been thought of as secondary cells that have only a passive role in neuron growth, providing structural, metabolic and trophic support to neurons. However, it is now known that astrocytes actively control neuron growth and synapse formation.

Glia occupy approximately 50% of the total brain volume (Peters, et al., 1991), and yet outnumber neurons 10 to 1. Glia are intimately involved with neurons at all stages of development and in adult life. In fact, it is estimated that in the rodent brain, an individual astrocyte may ensheath and interact with as many as 10,000 synapses

(Bushong, Martone, & Ellisman, 2004). However, glia are not uniformly distributed throughout the brain, and the relationship between astrocytes and neurons changes over development.

In EM, astrocytes are identified by the presence of dark glycogen granules and astrocytic fibrils in their cytoplasm. Additionally astrocytes can be identified using a number of protein markers that are specifically expressed in glial cells. For example, glial fibrillary acidic protein (GFAP) is often used to identify astrocytes both *in vivo* and *in vitro*.

1.5.1 Astrocytes and dendrites

Glial cells secrete a number of signals that are known to regulate dendrite growth in both the peripheral and central nervous systems. Without glia, neurons exhibit stunted dendritic arbors with fewer branches (Tropea, Johnson, & Higgins, 1988). Astrocytes may also influence dendrite spine morphology (Murai, Nguyen, Irie, Yamaguchi, & Pasquale, 2003; Seil, Eckenstein, & Reier, 1992; Ventura & Harris, 1999). Astrocytes provide a number of soluble factors that support the appropriate growth of dendrites and dendritic spines such as cholesterol (for review see Ethell & Pasquale, 2005). In addition to signals released by astrocytes, a number of contact-dependent neuron-glia signals are known to provide cues that guide dendrite development and spine maturation. For example, the ephrin (Eph) A4 receptor, expressed on hippocampal pyramidal neurons, interacts with the Eph-A3 ligand that is expressed on the surface of astrocytes, and regulates dendritic spine morphology (Murai, et al., 2003). Furthermore, in 2007, Nishida and Okabe showed that direct astrocyte contacts are important for the stabilization of dendritic protrusions and their development into spines. Most recently, Ballas and others (2009) provided evidence that astrocytes contribute to the abnormal dendrite morphology in Rett syndrome.

1.5.2 Astrocytes and synapses

Astrocytes are found surrounding the synaptic complex forming what is now

known as the tripartite synapse: the presynaptic axonal bouton, the dendritic spine, and the astrocyte (Araque, Parpura, Sanzgiri, & Haydon, 1999). In fact, in the mature hippocampus 57% of synapses are in direct contact with astrocytes (Ventura & Harris, 1999). Astrocytes perform many vital functions for synapses including the regulation of molecules in the extracellular environment such as calcium, and uptake superfluous potassium and glutamate.

Recent evidence suggests an active role for astrocytes in the development and maintenance of synapses (Elmariah, Oh, Hughes, & Balice-Gordon, 2005; Mazzanti & Haydon, 2003; Pascual, et al., 2005). In 2001, Ullian and others revealed that astrocytes are critical for the development of synapses. That same year, astrocytes were also found to be important for synaptogenesis and synapse elimination in cerebellar neurons *in vitro* (Seil, 2001). Furthermore, synapses that are formed *in vitro* in the presence of glial cells rapidly disappear when the astrocytes are removed (Ullian, Christopherson, & Barres, 2004). In fact, astrocytes provide a number of molecules required for the normal development of functional synapses including cholesterol (Mauch, et al., 2001), neurotrophins (Blondel, et al., 2000), tumor necrosis factor-α (Beattie, et al., 2002), and extracellular matrix proteins such as thrombospondin (Christopherson, et al., 2005; Ullian, et al., 2004). In addition to the soluble factors released by astrocytes, the formation of synapses is also mediated by neuron-glia cell-contact mediated factors. For example, direct astrocyte contacts via β1 integrin mediated signals have recently been suggested to have a role in excitatory synaptogenesis of cultured embryonic hippocampal neurons (Hama, Hara, Yamaguchi, & Miyawaki, 2004).

Notably, these effects are not due to indirect effects, such as promoting the survival of the neurons. Early experiments demonstrated that the effects of glial cells on synaptic development were the same in cultures of aged neurons where the survival was more stable (Pfrieger & Barres, 1997). These results supported the notion that the increase in synapse number was not due to an increase in the number of neurons.

Astrocytes are also known to be critical for the proper physiological properties of

synapses, and are known to modulate neuron excitability and synaptic function. Pfrieger and Barres (1997) revealed that synaptic efficacy of retinal ganglion cells was increased by the presence of glial cells in culture. Studies by Nagler and colleagues (2001) confirmed these findings. Experiments by Perea and Araque (2007) demonstrated that astrocytes potentiate transmitter release at hippocampal CA3-CA1 synapses *in vitro*.

Importantly, there is a physiological correlate for these findings. During development, astrocytes appear during the critical period of synaptogenesis (Ullian, et al., 2001). Most neurons innervate their target area approximately one week prior to synapse formation (Pfrieger & Barres, 1996), and it is during this week that the astrocytes are generated. Therefore there is a spatiotemporal correlation between astrocyte appearance and synaptogenesis. Additionally, thrombospondins, extracellular matrix proteins that are secreted by astrocytes, are expressed in the brain during the peak period of synaptogenesis (Christopherson, et al., 2005). These findings suggest that immature astrocytes provide a permissive environment during a critical developmental window in which synapses can form.

1.5.3 Astrocytes and disease

Glial cells are associated with a number of diseases. Perhaps the most widely recognized disease is multiple sclerosis (MS) (reviewed in Jessen, 2004). Glial cells are also involved in the neuropathology of Charcot-Marie-Tooth disease, and a number of malignant brain tumors are derived from glial cells (Jessen, 2004). Additionally, due to the ability of astrocytes to remove cytotoxic elements from the extracellular milieu, astrocytes are likely to be involved in the pathology of stroke and Alzheimer's disease (Jessen, 2004). Recently, Ballas and colleagues (2009) demonstrated that astrocytes play a role in the development of Rett syndrome.

1.5.4 Astrocytes in Fragile X Syndrome

As mentioned above, astrocytes play a role in synaptic pruning and dendritic spine morphology, both processes that are altered in FXS. Therefore, it is plausible that

there is also some role for astrocytes in the development of the neuropathology seen in FXS.

1.5.4.1 Astrocytes and FMRP

Previously, FMRP was thought to be present exclusively in neurons, with negligible expression in other cell types such as mature glia (Bakker, et al., 2000; Devys, et al., 1993). However, Wang and others (2004) revealed that FMRP is present in precursor, but not in mature, oligodendrocytes. Notably, our lab recently confirmed the presence of FMRP in putative astrocytes of the developing brain (Pacey & Doering, 2007). In those experiments, FMRP was expressed in differentiating glial cells *in vitro*, and was co-expressed with GFAP in regions of the fetal and early postnatal mouse brain. Therefore, it is possible that a loss of FMRP, as seen in FXS could result in the altered regulation of signaling in astrocytes, as theorized to occur in neurons. The resulting deregulation of protein interactions could render the astrocytes less capable of effectively promoting the appropriate development of synapses and dendritic spines, and could contribute to the alterations in neuronal development seen in FXS.

CHAPTER 2:
HYPOTHESES & SPECIFIC AIMS

Chapter 2: Hypotheses & Specific Aims

2.1 Hypotheses

The central idea around which the experiments presented in this dissertation were designed can be summarized as:

Astrocytes contribute to the development of
the abnormal neurobiology seen in Fragile X Syndrome.

In an attempt to prove this central theory, a number of specific hypotheses can be proposed. The experiments presented herein focus on the following two specific hypotheses:

1) Fragile X Astrocytes alter the maturation of dendritic arbors of neurons in Fragile X Syndrome.
2) Fragile X Astrocytes contribute to the altered excitatory synapse development of neurons in Fragile X Syndrome.

2.2 Specific aims

In order to prove these hypotheses as true, a number of specific aims were generated as follows:

Specific Aim 1: To show that Fragile X astrocytes alter the morphology of the dendrites of hippocampal neurons in culture.

Specific Aim 2: To show that Fragile X astrocytes change the early excitatory protein expression in hippocampal neurons in culture.

Specific Aim 3: To demonstrate that wild type astrocytes support the growth of normal dendritic arbors in Fragile X neurons in culture.

Specific Aim 4: To demonstrate that wild type astrocytes promote normal excitatory

synaptic protein expression in Fragile X neurons in culture.

Specific Aim 5: To show that the Fragile X astrocytes impart a developmental delay on the maturation of dendritic arbors *in vitro*.

Specific Aim 6: To demonstrate that the Fragile X astrocytes delay the formation of excitatory synapses *in vitro*.

2.3 Summary of manuscripts:

The manuscripts presented in this dissertation each address one or more of these aims, and can be summarized as follows:

Chapter 3: Primary dissociated astrocyte and neuron co-culture

This manuscript describes the co-culture methods used for all experiments in the dissertation. These methods are presented here as a chapter, rather than in the Appendix, as the methods as described were included as a chapter in Protocols for Neural Cell Culture, 4th Ed..

Chapter 4: Astrocytes prevent abnormal neuronal development in the Fragile X mouse

The experiments in this manuscript address specific aims 1 through 4. Morphological measurements of the dendritic arbors of isolated neurons were obtained using Neuronmetrics™, a plug-in for Image J. Quantification of pre- and post- synaptic protein clusters were determined using a custom-written plug-in for Image J, and were assessed independently for isolated neurons. The results show that Fragile X astrocytes contribute to the development of abnormal dendrite and synapse development in hippocampal neurons in culture. Furthermore, the findings demonstrate that normal astrocytes can prevent the abnormal dendrite and synapse development in Fragile X neurons.

Chapter 5: Fragile X astrocytes induce developmental delays in dendrite maturation

and synaptic protein expression

The experiments presented in Chapter 5 address specific aims 5 and 6. Morphological measurements of the dendritic arbors of cells were obtained using Neuronmetrics™, a plug-in for Image J. The formation of excitatory synapses was measured by quantifying the number of co-localized pre- and post-synaptic protein clusters (puncta) along 50μm segments of dendrites. The experiments extended over three time points (7, 14, and 21 days in culture), in order to ascertain whether or not, normal dendritic growth and excitatory synapse maturation would eventually occur even in the presence of Fragile X astrocytes. The findings illustrated that the abnormalities in dendrite morphology and synaptic protein expression induced by Fragile X astrocytes, were only a temporary delay in development; by 21 days in culture, the neurons exhibited characteristics similar to those grown on normal astrocytes.

Chapter 6: Primary mouse hippocampal neurons develop abnormal dendritic arbors in the presence of Fragile X astrocytes

The experiments presented in Chapter 6 address specific aim 5. In these experiments, Sholl analysis was used to ascertain developmental delays in dendrite maturation between neurons grown on normal and Fragile X astrocytes. This analysis of morphological alterations also sought to determine whether the developmental delays were specific to any of the five subtypes of neurons that could be identified in the hippocampal neuron cultures. The findings provided some interesting insight into the nature of the dendritic abnormalities. First, the results illustrated that the increase in dendritic branching seen in the previous study was due to an *increase* in short or inappropriately oriented dendritic branches, and that neurons grown with Fragile X astrocytes exhibited a *decrease* in the longer, and perhaps more mature branches. Second the findings revealed that neurons with a stellate neuron morphology (similar to that of spiny stellate neurons) were more pervasively affected by growth with Fragile X astrocytes.

CHAPTER 3.
PRIMARY DISSOCIATED ASTROCYTE AND NEURON CO-CULTURE

3. Chapter 3

3.1 Preface to Chapter 3

This chapter consists of an author generated version of a methods paper entitled "Primary dissociated astrocyte and neuron co-culture", that was published in Protocols for Neural Cell Culture, 4th Ed, used with kind permission from Humana Press, Springer Science + Business Media. See Appendix II for attached copyright license.

3.1.1 Author's contributions

For this paper I generated the method based on modifications to those existing in the literature, compiling aspects of various culture protocols as necessary. I then optimized the method in practice. I wrote the manuscript, and created the figures and tables within. Dr. Doering edited the manuscript and provided guidance and advice in the generation of the protocol.

3.1.2 Background and rationale

In order to address the central hypothesis stated in the previous chapter, it was necessary to create a co-culture protocol for neurons and astrocytes that could be independently isolated from mice of different genetic backgrounds. Earlier primary neuron-glia culture protocols involved the isolation of both cell types simultaneously from the same animal in a mixed culture (Lester, Quarum, Parker, Weber, & Jahr, 1989). In order for us to investigate the effect of *FMR1* null astrocytes on wild type (WT) neurons (or vice versa), we required the option of isolating the cell types from separate animals. More recently, neuron-glia co-culture procedures are performed in a manner that requires the isolation of the astrocytes and neurons independently (Kaech & Banker, 2006). However, many of the current protocols utilize rat astrocytes, even when culturing mouse neurons. Furthermore, the protocols often suggest that the neurons be grown on pre-treated coverslips that are then inverted over a layer of astrocytes in culture

(Kaech & Banker, 2006). In this way, the neurons are able to benefit from the astrocyte-derived growth and maturation cues, and yet the neurons are separated to permit unobstructed observations of the neuron morphology. However, in addition to astrocyte-secreted signals, there are membrane-delimited signals on glial cells that are important for normal neuron growth (Hama, et al., 2004; Murai, et al., 2003; Nishida & Okabe, 2007). For this reason, and for technical simplicity, we decided to modify the current neuron-astrocyte co-culture protocols to allow the culture of primary mouse neurons directly on top of independently isolated mouse astrocytes. This protocol is included in the following.

3.2 Primary Dissociated Astrocyte and Neuron Co-culture

Shelley Jacobs[1] and Laurie C. Doering[1*]

1. Department of Pathology and Molecular Medicine, McMaster University, 1200 Main Street, West, Hamilton, Ontario L8N 3Z5, Canada

* Corresponding author
doering@mcmaster.ca

3.2.1 Summary

We describe a method to isolate and co-culture dissociated hippocampal neurons and cortical astrocytes from young mice (E17 and newborn, respectively). This protocol is useful to investigate the effects of astrocytes on the developmental biology of neurons. By independently isolating the astrocytes and neurons (with different genetic backgrounds) from different mice, an *in vitro* environment can be created where one cell type is deficient in a gene or protein of interest. For example, this method is well suited to examine the effect of a genetic mutation in astrocytes on the development of neuronal processes and synapses.

Key Words
mouse, astrocyte, neuron, co-culture, development

3.2.2 Introduction

To facilitate the study of interactions between cells of the central nervous system (CNS), *in vitro* preparations are often the method of choice by many neuroscientists. When neurons are isolated from their *in vivo* niche, it becomes possible to manipulate specific aspects of their development, maturation and signaling. *In vitro* cellular preparations can also be used to probe the effects of a genetic mutation (knockout mouse strain) on a specific CNS cell type without the complications and restrictions imposed by the *in vivo* environment.

Hippocampal neurons can be isolated from embryonic or adult tissue. See also the Chapter by Nault and De Koninck (2009). However, the isolation of cells from the embryonic CNS is easier from a technical viewpoint. Neurons and their precursors can be dissociated from late stage embryos (i.e., E17 mouse) with higher viable yields due in part to the immature neural networks. Primary hippocampal neurons grown in vitro develop extensive dendritic arbors studded with characteristic dendritic spines. When seeded in sufficient density, these neurons form networks mediated by synaptic connections (1).

The cellular homogeneity exploited in a number of in vitro paradigms, where neurons are the primary cell type of interest, has prompted a number of laboratories to develop protocols for their isolated growth. However, it appears that unlike their peripheral counterparts, CNS neurons require astroglial support for normal development. This support can come in variety of forms. Some researchers grow neurons in chemically defined media that has been preconditioned by astrocytes, and therefore contains the soluble astrocyte-derived factors required for neuron growth (2,3). Others have developed a protocol where neurons can be grown in a "sandwich" culture, where the neurons are grown on a coverslip, inverted on a monolayer of astrocytes (4). Alternatively, and

perhaps the least complicated, is the use of mixed cultures of neurons and astrocytes from the same tissue source, in which the astrocytes quickly form a monolayer beneath the neurons (3,5).

Given that CNS neurons require glial interactions for growth, it is important to have methods to investigate the molecular interactions between neurons and glial cells. Here we describe a protocol that is relatively simple from a technical point of view, yet provides a means for investigating the effects of non-neuronal cells on neuronal development. Specifically, this protocol examines neuronal maturation and synaptic development when combined with astrocytes carrying a specific genetic mutation. Here, the neurons are isolated from the hippocampus of a late embryonic mouse and co-cultured directly in apposition to cortical astrocytes from a newborn mouse pup. The co-culture is maintained on glass coverslips to facilitate immunocytochemical studies. This protocol therefore provides a key means to investigate the effects of astrocytes on neuronal growth and synapse formation in genetic mouse models of disease.

Our protocol is divided into four steps: cortical astrocyte isolation, preparation of coverslips for co-culture, plating cortical astrocytes for co-culture, and isolating and plating hippocampal neurons for co-culture (Figure 3.1) It is important to note that the steps of this protocol are dependent on the coordinated timing of astrocytes in culture with a timed-pregnant mouse at the appropriate gestational age (E17). Here, E17 is determined with the day of the sperm plug counted as E1. For the purposes of outlining the timing of the protocol the day of neuron isolation will be considered the pivotal step, and the timing of all other steps will be counted from that day.

Table 3.1. Approximate time to perform each step

STEP 1. Isolating cortical astrocytes for co-culture	1.5 - 2 hours
STEP 2. Preparing coverslips for co-culture	DAY 1: 30 min - 1 hour DAY 2: 1 hour
STEP 3. Plating cortical astrocytes for co-culture	1 hour
STEP 4. Isolating and plating hippocampal neurons for co-culture	2 - 3 hours

3.2.3 General Equipment

Biological hood
Water bath (37°C)
Dissecting microscope
Centrifuge
Cell culture incubator, 37°C, 5% CO_2

3.2.4 Solutions

Calcium and Magnesium Free Hanks Buffered Saline Solution (CMF-HBSS)(100 ml)

10 ml 10X HBSS (Invitrogen, Cat No. 14185-052)
1 ml 1M HEPES (Invitrogen, Cat No. 15630-080)
89 ml dH_2O

Filter through 0.22 μm filtration system (Stericup, Cat. No. SCGPU01RE/SCGPU05RE)

Glial Media (GM) (100 ml)

10 ml Horse Serum (Invitrogen, Cat. No. 16050-122)
2 ml 30% (w/v) D-Glucose (filtered through 0.22 μm filter)

(Sigma, Cat. No. G8769)

88 ml Minimal Essential Media with Earl Salts and L-Glutamine (MEM) (Invitrogen, Cat. No. 11095-080)

* Can be stored at 4C for up to a week

Phosphate Buffered Saline (PBS) (500 ml)

50 ml 0.1 M Phosphate buffer

450 ml 0.9% (w/v) NaCl in dH_2O (Sigma, S6191)

Filter through 0.22 μm filtration system (Stericup, Cat. No. SCGPU01RE/SCGPU05RE)

Neural Maintenance Media (NMM) (100 ml)

1 ml N-2 Supplement (100X)(Invitrogen, Cat. No. 17502-048)

1 ml 100 mM Sodium Pyruvate Solution (Invitrogen, Cat. No. 11360-070)

2 ml 30% (w/v) D- Glucose (filtered through 0.22 μm filter, Stericup, Cat. No. SCGPU01RE) (Sigma, Cat. No. G8769)

96 ml MEM (Invitrogen, Cat. No. 11095-080)

* make fresh (can be stored for 24 hours at 4C)

3.2.5 Isolating Cortical Astrocytes for Co-Culture

3.2.5.1 Reagents & Equipment

4 newborn mouse pups (postnatal day 0 or 1)

(4 pups will prepare enough astrocytes for 1 T75 flask)

Dissecting tools sterilized with 95% EtOH : Fine dissecting forceps (2 pair), curved forceps, curved scissors, small scissors

60 mm x 15 mm tissue culture dishes (Falcon, Cat. No. 353002)

15 ml polystyrene falcon tubes (Falcon Cat. No. 352095)

50 ml falcon tubes (Falcon, Cat. No. 352070)

70 μm cell strainer (Falcon, Cat. No. 352350)

T75 culture flask (Sarstedt, Cat. No. 41111066)

5 ml serological pipettes

12 ml serological pipettes

1.5 ml Eppendorf tubes (for tail samples for genotyping if desired) (Eppendorf, Cat. No. 022364120)

No.20 scalpel blades

CMF-HBSS (See Solutions)

DNase I (Roche Applied Science, Cat. No. 10104159)

1 aliquot (1.5 ml) 2.5% (10X) Trypsin (Invitrogen, Ca.t No. 15090-046)

10% Glial Media (GM) (See Solutions)

3.2.5.2 Protocol

Preparation

1. Turn on water bath (37°C) and biological hood
2. Place 1 aliquot 2.5% trypsin in water bath
3. Sterilize dissecting tools and area
4. Prepare DNase I

i) Weigh 15 mg of DNase into 15 ml falcon tube

ii) In hood, add 1.5 ml sterile CMF-HBSS

5. In hood, add 4 ml CMF-HBSS to each 60 mm culture dishes (4 required)
6. In hood, add 8 ml CMF-HBSS to a 50 ml falcon tube

Cell isolation:

7. Isolate brain from pup and place into one dish with CMF-HBSS
8. Repeat with 3 other pups

(optional – clip tail for genotyping, place in 1.5 ml Eppendorf tubes and store at -20°C)

9. Under dissecting microscope, remove hemispheres from hindbrain and midbrain, and

place hemispheres into second 60 mm dish

10. Remove meninges and place into 3rd 60 mm dish

CAUTION: Removal of meninges must be complete. Meninges contain fibroblasts which can overgrow the astrocyte culture.

11. Remove hippocampi and place isolated cortices into final 60 mm dish

12. Mince cortices with No. 20 scalpel blades

13. In biological hood, transfer tissue and CMF-HBSS to 50 ml falcon with 8 mls CMF-HBSS

14. Rinse culture dish with 1.5 ml DNase solution and add to 50 ml falcon tube

15. Rinse culture dish with 1.5 ml 2.5% Trypsin and add to 50 ml falcon tube

16. Swirl tube, and place in 37°C water bath for 5 minutes

17. Triturate with 12 ml serological pipet 10 times, expelling cell suspension against side of tube, and return to 37°C water bath for 5 minutes

18. Triturate with 5 ml serological pipet 10-15 times, and return to water bath for 5 minutes

19. Remove from water bath and add 15 ml of 10% GM, and triturate well.

20. Pass cell suspension through cell strainer into second 50 ml falcon tube

21. Centrifuge for 5 min (150-200g)

22. Re-suspend in 20 mls of 10% GM and plate in T75 flask.

TIP: The cortices of 4 mouse pups should yield on average, 8 x 10^6 cells, which is an appropriate quantity to seed in one T75 flask.

23. Place in incubator 37°C, 5% CO_2

24. Replace with fresh GM after 24 hours.

TIP: do not be alarmed if there appears to be few cells attached to flask. The astrocytes will proliferate quickly. Seeding the astrocytes at too high a density may result in an increased number of microglia in the culture (in high numbers these are toxic to neuron growth).

25. Replace half the GM every 2-3 days.

TIP: while maintaining the culture, never change the media completely; the conditioning

of the media promotes astrocyte growth

TIP: When changing media, slap the flask 5-10 times on the palm of your hand before changing the media. This will help removed any loosely bound cells, and reduce the numbers of microglia in the culture.

TIP: Astrocytes usually reach an appropriate level of confluence to be used for co-culture after 10-14 days in culture.

3.2.6. Preparing Coverslips for Co-Culture

DAY1

Reagents & Equipment

24 well tissue culture plates (Falcon, Cat. No. 353047)

13 mm round glass coverslips (Bellco Glass, Cat. No. 1943-00012)

95% EtOH in a small beaker

Forceps

EtOH burner

Serological pipets

Sterile Pasteur pipets

Sterile filtered dH_2O (filtered with 0.2 μm filter)

Sterile filtered Poly-L-Lysine (PLL)(Sigma, Cat. No. P1399 1mg/ml) (filtered before use with 0.2 μm filter)

3.2.6.1 Protocol Day 1

1. In hood, using forceps, dip coverglass into 95% EtOH and pass through flame of burner.
2. Allow to cool for a few seconds and then place into one well of 24 well plate.
3. Repeat as necessary for the number of wells desired.
4. Rinse each coverslip with 0.5 ml dH_2O.
5. Apply 0.5 ml PLL per well, making sure the coverslip is fully submerged.

TIP: You can use the pipet tip or drop more PLL on the coverslip to ensure full coverage.

6. Cover each 24 well plate with a sheet of paper towel, and place into fridge (4°C) overnight.

DAY 2

Reagents & Equipment

Sterile Filtered dH_2O (filtered with 0.2 μm filter)

Sterile Phosphate Buffered Saline (PBS) (see Solutions)

Natural Mouse Laminin (Invitrogen, Cat. No. 23017-015, aliquoted and stored at –80°C.

3.2.6.2 Protocol Day 2

7. Remove PLL.

TIP: PLL can be re-used. Store at 4°C, and filter before each use.

8. Wash 2 times with dH_2O.

CAUTION: do not allow coverslips to dry out before unbound PLL is completely rinsed. off. This could cause decreased cell survival.

9. Allow plates to air-dry completely in hood. (approximately 30 min)

10. Dilute Laminin in sterile PBS, and add 0.5 ml per well.

(optional - Wrap edges with parafilm)

11. Incubate for at least 4 hours, or more commonly overnight, at room temperature (RT).

TIP: PLL/laminin coating is stable for up to 2 days at RT.

NOTE: before plating cells, the laminin needs to be removed, the wells washed 2 times with MEM, and filled with 10% GM. The plates can then be stored in the cell culture incubator until use. This is done the day of astrocyte plating. ***(STEP 3. Plating Cortical Astrocytes for Co-Culture)***

3.2.7 Plating Cortical Astrocytes for Co-Culture

3.2.7.1 Reagents & Equipment

Previously PLL/Laminin prepared coverslips in 24 well plates

(STEP 2. Preparing Coverslips for Co-Culture)

1 T75 Flask of Astrocytes (isolated approximately 2 weeks prior)

(STEP 1. Isolating Cortical Astrocytes for Co-Culture)

Minimal Essential Media (MEM) (Invitrogen, Cat. No. 11095-080)

10% Glial Medium (GM)

Neural Maintenance Medium (NMM) (See Solutions)

1 aliquot (10 mls) 0.05% Trypsin EDTA (Invitrogen, Cat. No. 25300-062)

15 ml polystyrene Falcon tube (Falcon, Cat. No. 352095)

0.5 ml Eppendorf tube (Eppendorf, Cat. No. 0030124.502)

200 µl yellow tips

Hemacytometer (for counting cells)

Trypan Blue (to determine viability if desired)

3.2.7.2 Protocol

Preparation

1. Wash prepared coverslips 2 times with 0.5 ml MEM.

CAUTION: Be careful not to let the coverslips dry between washes. This is toxic to cells.

2. Replace MEM with 0.5 ml per well 10% GM, and place in incubator 37°C, 5% CO_2 to equilibrate.

3. Remove media from T75 flask.

4. Wash with 5 ml 0.05% Trypsin-EDTA.

5. Add second half of trypsin aliquot, and place into incubator (37°C, 5% CO_2) for 5 minutes (approx). (Check flask to make sure the majority of cells are rounded up and floating)

6. Add 5 ml 10% GM to flask, and rinse 5 times.

7. Move cell suspension into 15 ml falcon tube and centrifuge 150-200g for 5 minutes.

8. Remove supernatant and re-suspend cells in 2 ml 10% GM.

9. Count cells to determine cell density in suspension, and calculate the number of µl needed to result in 9000 cells/well.

e.g. Cell concentration in suspension is 1245 cells/ul. Want 9000 cells/well…9000/1245 is 7ul. Therefore add 7ul of cell suspension to each well of the 24 well plate previously equilibrated in the incubator.

10. Replace half of GM after 3 days.

TIP: Do not replace all of the media. The astrocytes require the conditioned media for optimal growth.

11. At 6 days in culture replace 10% GM with neural maintenance medium (NMM) in preparation for ***STEP 4. Isolation and Plating Hippocampal Neurons for Co-Culture***.

3.2.8. Isolating and Plating Hippocampal Neurons for Co-Culture

3.2.8.1 Reagents & Equipment

Timed Pregnant Dam Mouse: 4 mouse pups at E17 (Day of plug is E1).
(4 pups will prepare enough neurons for 1 experiment)

Previously Plated Astrocytes (With NMM conditioned media i.e., NMM added 24 hours prior to neuron isolation ***(STEP 3. Plating Astrocytes for Co-Culture)***

Dissecting tools sterilized in 95% EtOH: fine dissecting forceps (2 pair), curved forceps, curved scissors, small scissors, 3 pairs of forceps and 3 pairs of scissors (one set for each tissue level of the dissection)

4 100 mm tissue culture dishes (Falcon, Cat. No.353003)
4 60 mm X 15 mm tissue culture dishes (Falcon, Cat. No. 353002)
1 15 ml polystyrene Falcon tube (Falcon, Cat. No. 352095)
5ml serological pipettes
Sterile Pasteur pipettes

Sterile Fire Polished Pasteur pipettes (Polished to remove sharp edges)

Sterile File Polished Pasteur pipette with borehole diameter reduced to half original size – no less

4 1.5 ml Eppendorf tubes (for tail samples for genotyping if desired) (Eppendorf, Cat. No. 022364120)

0.5ml Eppendorf tubes (for counting cells) (Eppendorf, Cat. No. 0030124.502)

Hemacytometer (for counting cells)

Sterile filtered saline (0.9% w/v NaCl in dH_2O) (Sigma, Cat No. S6191)(Filtered through 0.22 μm filter, Stericup Cat. No. SCGPU05RE)

CMF-HBSS (See Table 2.)

1 aliquot (0.5 ml) 2.5% Trypsin (Invitrogen, Cat. No. 15090-046)

NMM (See Solutions)

3.2.8.2 Protocol

Preparation

1. Turn on water bath (37°C) and hood.
2. Place 1 aliquot 2.5% trypsin in water bath.
3. Sterilize dissection tools and dissecting area.
4. In hood, add 4 ml CMF-HBSS to each of 4 60 mm culture dishes.
5. Add 15 ml sterile saline to each of 4 100 mm culture dishes.

Pup isolation:

6. Euthanize preganant dam.
7. Remove uterus and place into one 100 mm culture dish.
8. Rinse blood from uterus and move into second 100 mm culture dish.
9. Remove four pups randomly from uterus and place into third 100 mm dish.

Hippocampal isolation:

10. Using curved scissors decapitate pup, and place in fourth 100 mm dish.
11. Remove brain and place into one dish with CMF-HBSS.

TIP: When dissecting out the brain, it can help to stabilize the skull with forceps placed

through the eye sockets.

12. Repeat with 3 other pups.

(Optional – clip tail for genotyping, place in 1.5 ml Eppendorf tubes and store at -20°C)

13. Under dissecting microscope, remove hemispheres from hindbrain and midbrain, and place hemispheres into second 60 mm dish.

14. Remove meninges and place cleaned cortices into 3rd 60mm dish.

CAUTION: The removal of meninges needs to be complete.

15. Isolate the hippocampi and place into final 60 mm dish

TIP: When isolating the hippocampus handle it as little as possible to avoid damaging the tissue. To minimize damage to the hippocampus, it may help to manipulate the brain by grasping the cortex with a pair of forceps.

Cell isolation:

16. In biological hood, transfer tissue and CMF-HBSS to 15 ml falcon tube and add 0.5 ml CMF-HBSS (to bring volume to 4.5ml)

17. Add 0.5 ml 2.5% Trypsin to 15 ml falcon tube.

18. Swirl tube, and place in 37°C water bath for 15 minutes.

19. Remove supernatant (as much as possible), and add 5 ml CMF-HBSS. Swirl tube and let stand for 5 minutes.

20. Repeat 2 times.

CAUTION: Care must be taken to ensure hippocampal tissue is not removed with the supernatant.

21. Remove supernatant and add 2 ml NMM.

22. Triturate 10-15 times with a fire-polished glass pipette.

23. Switch to a reduced borehole fire-polished pipette and triturate another 10-15 times.

CAUTION: Avoid generating air bubbles. These will reduce the neuron yield. 4 mouse pups should yield ~ 4 x 10^6 cells, with a viability of >85%. Expel suspension against the wall of the tube to minimize the generation of air bubbles.

TIP: When the cells are fully isolated the suspension will appear cloudy, and will contain no visible tissue.

22. Determine cell suspension density, and the number of µl required to yield 20,000 cells per well.
23. Add the appropriate measure of cell suspension to each well of previously plated and conditioned astrocytes.
24. Place in incubator 37°C, 5% CO_2.
25. Replace one third of media with fresh NMM every 7 days in culture, as necessary.

TIP: Do not replace all of the media. The neurons require conditioned media from the astrocytes for optimal growth.

NOTE: Many other neuron-astrocyte co-culture protocols include the addition of a glial inhibitor, such as cytosine arabinoside (AraC), to the medium a few days after the co-culture is established. We prefer not to use inhibitors in consideration that glial inhibitors can alter cell physiology (6,7,8). Instead, we rely on the knowledge that our starting population, E17 mouse hippocampus, consists of a relatively low population of glial cells and the NMM used in this protocol does not promote glial proliferation. Under these conditions we obtain a relatively low level of glial contamination in our neuron population.

3.2.9. Critical Steps

Removal of meninges. This is important to ensure minimal contamination of culture with fibroblasts which do not support neuron growth.

Plating density of the astrocytes. Astrocytes should be seeded at no more than 1 x10^7 cells/T75 flask (~7.5-8 X 10^6 cells/T75 flask is optimal). Increasing the density can result in the increase growth of microglia that, in high numbers, is toxic to neuron growth.

Cooling coverslips. Ensure coverslips are cooled sufficiently. Coverslips that are still warm may stick to the plastic of the 24 well plate.

Rinsing coverslips with dH_2O. The EtOH needs to be rinsed completely. Residual EtOH is toxic to cells.

Applying PLL to coverslip. Check all coverslips - Do not assume coverslips are completely immersed in PLL. Sometimes air bubble can accumulate and lift the coverslip so that some, or all, is exposed beyond the PLL. If the coverslip is not submerged, the astrocytes may not adhere to and cover the entire surface of the coverslip.

Washing after PLL. Do not allow coverslips to dry before all unbound PLL is removed. Residual unbound PLL is toxic to cells.

Air drying of coverslips before laminin. Ensure coverslips are completely dry prior to the addition of laminin. Residual moisture can prevent the laminin from coating the coverslips effectively and can result in poor adherence of the cells.

Washing after laminin. Do not allow coverslips to dry before all unbound laminin is removed. Residual unbound laminin is toxic to cells.

Washing with 0.05% Trypsin EDTA. Rinsing with trypsin by incubation at RT for approximately a minute, and discarding this portion, helps remove any loosely bound cells (i.e., contaminating microglia).

Conditioning NMM. The conditioning of the NMM is essential for optimal neuron growth. The GM on the plated astrocytes should be replaced with NMM at least 24 hours before the addition of the neurons to the culture. If neuron survival is not adequate, increase the conditioning time to 48 hours.

Washing of hippocampi after trypsin. Care needs to be taken when performing this step to ensure that hippocampal tissue is not removed with the supernatant. During the initial washes the tissue may not fully settle into the bottom of the tube. Remove only as much supernatant as possible with each wash. The removal of the supernatant becomes easier with each successive wash. If the supernatant cannot be adequately removed after three washes, wash a fourth time. At this point the tissue should settle more completely into the bottom of the tube. Do not centrifuge to expedite this process; centrifugation will decrease neuron yield.

Trituration of hippocampal tissue. Avoid the generation of air bubbles as this will reduce neuron yield. The expulsion of the suspension against the side of the tube will reduce the generation of air bubbles. The cells will be adequately released from the tissue

when the suspension appears cloudy with no visible pieces of tissue.

3.2.10 Typical Protocol Results

Table 3.2 Typical Cell Yield

Source	Number of cells
Mouse Cortex (newborn: P0-P1) (4 pups)	~ 8 x 10^6 cells
Mouse Cortical Astrocytes (1 flask)	~ 1-1.5 x 10^6 cells
Mouse hippocampus (E17) (4 pups)	~ 4 x 10^6 cells

An example of a neuron-astrocyte co-culture is shown in Figure 3.2. We obtain populations of astrocytes with >95% of cells positive for the astrocyte marker, glial fibrillary acidic protein (GFAP). In part, this could be due to conditions that promote GFAP+ cell growth that are inherent to this protocol (e.g., seeding a low density, plating on laminin, etc.) (9). We suggest that this should be routinely monitored by immunocytochemistry. If a less than an ideal proportion of cells are positive for GFAP, or if a more pure population of astrocytes is desired, there are many options for attaining such a population as outlined in Chapter 11 and also reviewed in reference 9. See Table 1 as a troubleshooting guide.

3.2.11 Acknowledgements

We thank Stephanie Kaech-Petrie for her tireless advice that was instrumental in the development of this protocol. This research is supported by the Natural Sciences and Engineering Research Council of Canada (NSERC) and the Fragile X Research Foundation of Canada.

3.2.12 References & Additional Resources

1. Bartlett WP, Banker GA An electron microscopic study of the development of axons and dendrites by hippocampal neurons in culture II. Synaptic relationships J Neurosci 1984;4:1954-1965.

2. Bi G, Poo M Synaptic modifications in cultured hippocampal neurons: dependences on spike timing, synaptic strength and post-synaptic cell type. J Neurosci 1998;18:10464-10472.

3. Yang Y, Ge W, Chen Y et al. Contribution of astrocytes to hippocampal long term potentiation through release of D-serine. Proc Natl Acad Sci (USA) 2003;11:15194-15195.

4. Kaech S, Banker G Culturing hippocampal neurons. Nat Protocols 2006;1:2406-15.

5. Yoshida M, Saito H, Katsuki H Neurotrophic effects of conditioned media of astrocytes isolated from different brain regions on hippocampal and cortical neurons. Cell Mol Life Sci 1995;51:133-136.

6. Martin DP, Wallace TL,Johnson EM Jr. Cytosine arabinoside kills postmitotic neurons in a fashion resembling trophic factor deprivation: evidence that a deoxycytidine-dependent process may be required for nerve growth factor signal transduction. J Neurosci 1990;10:184-93.

7. Dessi F, Pollard H, Moreau J et al. Cytosine arabinoside induces apoptosis in cerebellar neurons in culture. J Neurochem 1995;64: 1980-1987.

8. Chang JY, Brown S Cytosine arabinoside differentially alters survival and neurite outgrowth of neuronal PC12 cells. *Biochem Biophys Res Commun.* 1996;218:753-8.

9. Saura J. Microglial cells in astroglial cultures: a cautionary note. J Neuroinflammation 2007;4:26.

Table 3.2 Troubleshooting Guide

Problem	**Potential Cause**	**Corrective measures**
Yield normal, but astrocytes die shortly after plating	Failure of astrocytes to adhere to substrate	Ensure coverslips are washed well during coating process
Sticky mass develops while isolating cells from tissue	Triturating too vigorously Pipette tip too small Pipette tip too sharp	Ensure pipette is appropriately firepolished, and work to triturate more steadily. (Trituration takes practice to determine the mechanics for optimal cell yield.)
Neuron yield low	Triturating too vigorously	Triturate at a steady rate, and expel against the wall of the tube
	Borehole of pipette too small	Ensure that the borehole of the reduced borehole pipette is no less than half the original diameter
	Pipette tip too sharp	Ensure that glass pipettes are fully fire polished. The tip of a1ml plastic pipette is too sharp for optimal release of neurons.
Slow initial development of neurons	Insufficient conditioning of NMM	Add NMM to glial cultures at 48 hours prior to plating neurons
	Media exposed too long to air while plating	Ensure plates are out of incubator for minimum time possible. Add cells to plates only 12 wells at a time, and return to incubator between each set.
Sub-optimal neuron survival or maturation	Glial feeder layer has high numbers of microglial (toxic to neurons), or fibroblasts (do not support neuron growth)	Confirm there is a high (>95%) of GFAP positive cells. Discard glial cultures with a high percentage of microglia (small, round, phase bright, loosely attached), or other GFAP-negative cells.

Contamination of culture*	Yeast (10μm diameter with budding structures) - often as a result of breathing or coughing on the culture	Reduce talking while completing isolation, or wear surgical mask.
	Filamentous fungi that form mats	Ensure there is no contamination in incubator. Clean incubator.
	Bacterial (rods/spheres, <1μm diameter) – media will turn yellow.	Improve sterile technique. Determine source of contamination: media, substrate for coverslips, dissection media Replace source of contamination
* We do not recommend the use of antifungal or antibacterial agents. It is better to improve sterile technique than to risk potential development of antibiotic resistance of contaminant or negative effects on the cell physiology.		

Figure 3.1: Co-culture procedure flow diagram

Schematic diagram illustrating the sequential steps for preparing neurons and astrocytes in a co-culture system.

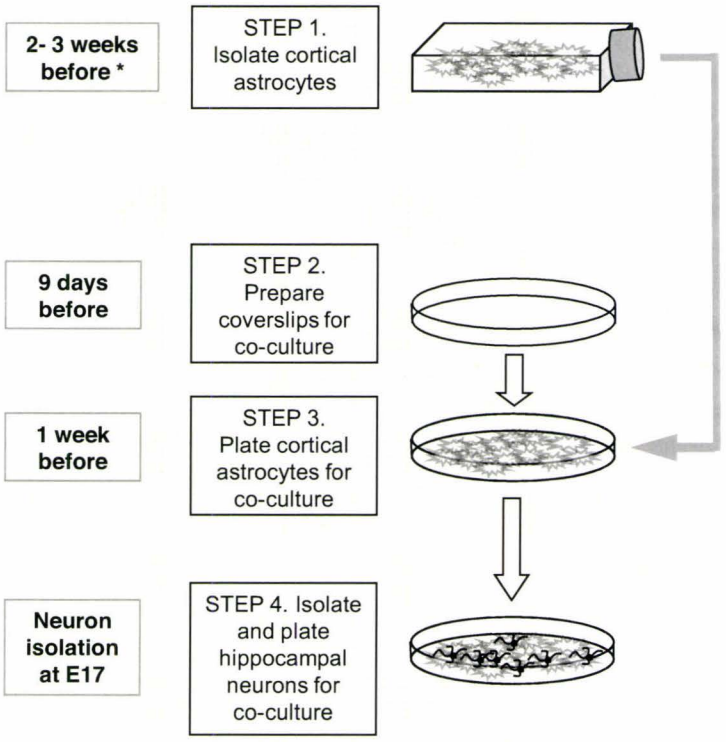
2- 3 weeks before *
STEP 1. Isolate cortical astrocytes
9 days before
STEP 2. Prepare coverslips for co-culture
1 week before
STEP 3. Plate cortical astrocytes for co-culture
Neuron isolation at E17
STEP 4. Isolate and plate hippocampal neurons for co-culture

Figure 3.1

Figure 3.2: Mouse hippocampal neuron – cortical astrocyte co-culture.

Typical appearance of astrocytes identified with an antibody to GFAP (red) and neurons marked with an antibody to MAP2 (green). All cell nuclei counterstained with DAPI (blue). Co-culture photographed after 7 days *in vitro*.

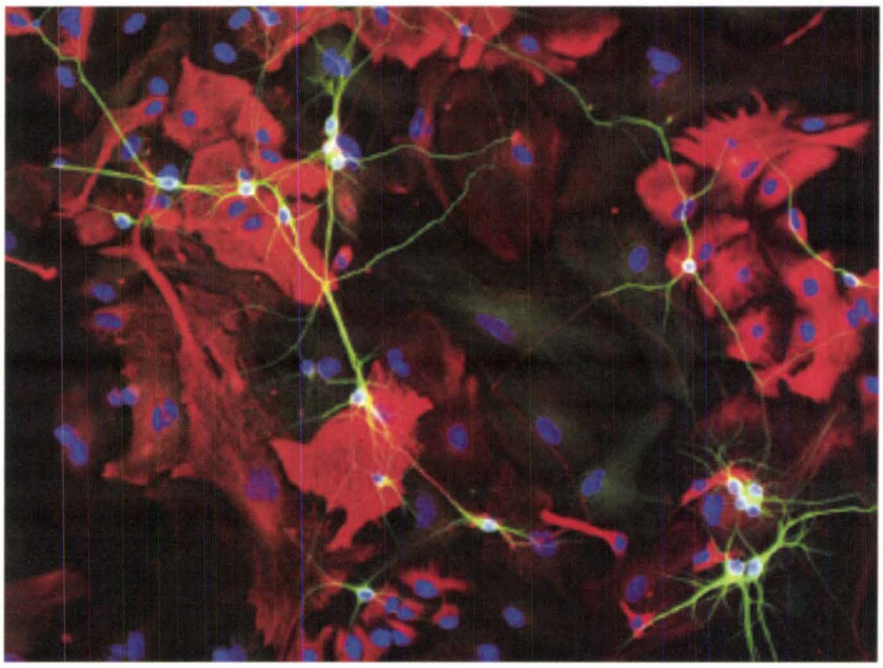

Figure 3.2

CHAPTER 4:
ASRTOCYTES PREVENT ABNORMAL NEURONAL DEVELOPMENT IN THE FRAGILE X MOUSE

4. Chapter 4

4.1 Preface to Chapter 4

This chapter is comprised of an author-generated version of an article prepared for submission to the Journal of Neuroscience. Following the reviewers suggestions the article was revised and resubmitted on the 9th of October; Submission #JN-RM-5027-09.

4.1.1 Author contributions

For this paper, I designed and performed all of the experiments, photographed the images, performed the analyses, carried out the statistical analyses, wrote the manuscript and prepared all figures. Dr. Doering provided guidance in the designing of the experiments and the editing of the manuscript.

4.1.2 Background and rationale

To date, the majority of clinical and basic science research investigating the abnormal neurobiological mechanisms that cause FXS has focused on the abnormalities intrinsic to the neurons as a function of a loss of neuronal FMRP. Neurons in both humans and mice lacking FMRP exhibit abnormal dendrite morphologies (Comery, et al., 1997; Dierssen & Ramakers, 2006; Galvez, et al., 2003; Galvez & Greenough, 2005; Grossman, et al., 2006; Irwin, et al., 2000; Irwin, et al., 2002; Irwin, et al., 2001; Kaufmann & Moser, 2000; Lee, et al., 2003; McKinney, Grossman, Elisseou, & Greenough, 2005; Nimchinsky, et al., 2001; Pan, et al., 2004) and altered synaptic protein expression (Brown, et al., 2001; Liao, et al., 2008; Pfeiffer & Huber, 2007; Weiler, et al., 2004; Zalfa, et al., 2007; Zalfa, et al., 2003; Zhang, et al., 2001), and these atypical neuronal characteristics are thought to result in the clinical features of FXS.

In contrast to the previous belief that FMRP is solely expressed in neurons, more recent studies have revealed the expression of FMRP in cells of the glial lineage (Pacey

& Doering, 2007; Wang, et al., 2004). Our laboratory recently demonstrated that developing astrocytes also express FMRP (Pacey & Doering, 2007). Interestingly, astrocytes are key players in the development of dendrite morphology and synaptic maturation (Ballas, et al., 2009; Christopherson, et al., 2005; Guizzetti, Moore, Giordano, & Costa, 2008; Mauch, et al., 2001; Murai, et al., 2003; Nagler, et al., 2001; Nishida & Okabe, 2007; Pfrieger & Barres, 1997; Ullian, et al., 2001). Given that FMRP is also expressed in astrocytes it is possible that astrocytes in FXS also suffer from a loss of FMRP, and are therefore deficient in their usual role in shaping the neural circuitry of the CNS. As such, it is now important to investigate the potential for a role of astrocytes in the development of the abnormal neurobiology seen in FXS.

We therefore used a co-culture protocol (see **Chapter 3**) in which the neurons and astrocytes were independently isolated from wild type (WT) or *FMR1* null mice. In this manner, we were able to culture the astrocytes and neurons in one of four combinations (WT neurons with WT or *FMR1* null astrocytes, or *FMR1* null neurons with WT or *FMR1* null astrocytes) in order to isolate the effects of the Fragile X astrocytes on neuronal dendrite morphology and synapse maturation.

4.1.3 Specific aims

- To show that Fragile X astrocytes alter the morphology of the dendrites of hippocampal neurons in culture (1).
- To show that Fragile X astrocytes change the early excitatory protein expression in hippocampal neurons in culture (2).
- To demonstrate that wild type astrocytes support the growth of normal dendritic arbors in Fragile X neurons in culture (3).
- To demonstrate that wild type astrocytes promote normal excitatory synaptic protein expression in Fragile X neurons in culture (4).

4.2 Astrocytes prevent abnormal neuronal development in the Fragile X mouse

Shelley Jacobs[*] and Laurie C. Doering[*#]

[*]Department of Pathology and Molecular Medicine
McMaster University, HSC 1R1
1200 Main Street West
Hamilton, Ontario, Canada
L8N 3Z5

[#]Corresponding author:

Laurie C. Doering

E-mail: doering@mcmaster.ca

Tel: 905-525-9140 x22913

Fax: 905-525-7400

Number of text pages: 21

Abbreviations:

FXS	Fragile X Syndrome
FMR-1	Fragile X Mental Retardation 1 gene
FMRP	Fragile X Mental Retardation Protein
DIV	days in vitro
MAP2	microtubule associated protein
GFAP	glial fibrillary acidic protein
WT	wild type
PSD-95	post-synaptic density 95
IR	immunoreactive
MeCP	methyl-CpG-binding protein
BSA	bovine serum albumin

4.2.1 Abstract

Astrocytes are now distinguished as major regulators of neuronal growth and synaptic development. Recently, they have been identified as key players in the progression of a number of developmental disorders; however, in Fragile X Syndrome (FXS), the role of astrocytes is not known. Using a co-culture design, we found that hippocampal neurons exhibited abnormal dendritic morphology and a decreased number of pre- and post-synaptic protein aggregates when they were grown on astrocytes from a Fragile X mouse. Moreover, we found that normal astrocytes could prevent the development of abnormal dendrite morphology and preclude the reduction of pre- and post-synaptic protein clusters in neurons from a Fragile X mouse. These experiments are the first to establish a role for astrocytes in the altered neurobiology of FXS. Our results support the notion that astrocytes contribute to abnormal dendrite morphology and the dysregulated synapse development in FXS.

4.2.2 Introduction

Fragile X syndrome (FXS) is a neurodevelopmental disorder, caused by a mutation in the *Fragile X Mental Retardation 1 (FMR1)* gene (Kremer et al., 1991). Affecting approximately 1/2500 individuals (both male and female with the full mutation) (Hagerman, 2008), FXS is the most common cause of inherited mental retardation. Children with FXS exhibit a wide spectrum of cognitive and behavioural features including: mild to severe cognitive impairment, attention deficit, anxiety, social withdrawal, susceptibility to seizures, motor disorders and autistic behaviours (Beckel-Mitchener and Greenough, 2004). To date, the mutation in the *FMR1* gene is the leading known inherited cause of autism (Reddy, 2005).

FMR1 codes for the Fragile X Mental Retardation Protein (FMRP) (Devys et al., 1993), a regulator of mRNA translation (Brown et al., 2001; Miyashiro et al., 2003; Liao et al., 2008), that plays an important role modulating the translation of a number of mRNAs that are important for dendritic growth (Brown et al., 2001; Lee et al., 2003) and the development of synapses (Greenough et al., 2001; Miyashiro et al., 2003; Liao et al., 2008). In FXS, there is an abnormal number (>200) of CGG repeats in the 5' non-coding region of the *FMR1* gene (Kremer et al., 1991), which results in hypermethylation, transcriptional silencing, and a lack of FMRP. Without FMRP, there is a disturbance of translational regulation and a disruption in the composition of the normal protein milieu.

The *Fmr1* knockout (*Fmr1* KO) mouse is a well-established model of FXS. As in the human, the *Fmr1* KO mouse displays a lack of FMRP (Bakker et al., 1994). This model recapitulates many characteristics of FXS, both behaviourally and at the cellular level, including: learning impairments (Bakker et al., 1994), hyperactivity (Qin et al., 2002), susceptibility to seizures (Chen and Toth, 2001), characteristics associated with attention deficits (Nielsen et al., 2002), predictors of autistic behaviours (Frankland et al., 2004), and abnormal neuronal dendritic spine development (Comery et al., 1997; Nimchinsky et al., 2001). While preclinical and clinical studies have suggested a neuronal pathology in

FXS, there is new evidence that glial-neuronal interactions may be important in FXS. In the past ten years FMRP has also been found in oligodendrocytes and their precursors (Wang et al., 2004; Castren et al., 2005). We recently reported that FMRP is also expressed in developing mouse astrocytes (Pacey and Doering, 2007). In fact it appears that the expression of FMRP is developmentally regulated. Pacey and Doering (2007) found that FMRP was expressed in early development in cells of the glial lineage both *in vitro* and *in vivo*, but not in adult astrocytes. Wang and others (2004) also demonstrated a developmental expression of FMRP in glial cells. In their experiments they found that FMRP was expressed in oligodendrocyte progenitors but not in mature oligodendrocytes (Wang et al., 2004). However, the effect of a lack of FMRP in the glial lineage on neuronal development has not been determined experimentally.

4.2.3 Results

In these experiments we investigated the role of astrocytes in the development of the abnormal dendrite morphology and synaptic aberrations seen in FXS. In order to examine whether astrocytes from an FMRP deficient animal could affect normal neuron growth we employed a co-culture procedure in which neurons are grown at low densities (400cells/ul) in serum free media (Jacobs and Doering, in press). In these cultures the neurons are dependent on a feeder layer of astrocytes for survival (Banker, 1980). Consistent with previously reported findings, hippocampal neurons from both wild type (WT; normal) and *Fmr1* KO (Fragile X) mice grown in the absence of an astrocyte feeder layer, did not survive. Both WT and *Fmr1* KO neurons grown on WT astrocytes, exhibited normal neuronal growth at 7 DIV (Fig. 1a, top row). In stark contrast, when *Fmr1* KO neurons were grown on *Fmr1* KO astrocytes the neurons exhibited a distinct abnormal morphology (Fig. 4.1a, bottom row). The dendritic arbors were more complex and individual processes showed random meandering on the astrocyte surface.

The survival of *Fmr1* KO neurons (grown on either WT or *Fmr1* KO astrocytes) was decreased in comparison to WT neurons ($p=0.004$, Fig. 4.1b). However, survival was not

significantly affected by growth on *Fmr1* KO astrocytes compared to WT, for either WT ($p=0.977$) or *Fmr1* KO neurons ($p=0.382$)(Fig. 4.1b). Therefore, the results that we present are not due to a density effect or selective neuron survival, and the morphological differences seen are a result of some quality of the different astrocyte populations. This difference could not be attributed to a significant variance in the purity of the astrocyte populations because the astrocytes isolated from both WT and *Fmr1* KO mice were 98.7 ± 0.5% GFAP positive. Therefore, the observed alterations in the neuronal phenotype can be concluded to result from the characteristics of the astrocytes imparted by the genotype of their origin animal.

*Fmr1*KO astrocytes alter the morphology of WT neurons

In order to evaluate more precisely how the *Fmr1* KO astrocytes affected the growth of the neurons we performed a detailed morphological analysis of the dendritic arbors. After staining with an antibody targeting the dendrite marker, MAP2, isolated neurons were selected at random from a minimum of two coverslips per experiment, and the morphology of their dendritic arbors was analyzed. WT neurons exhibited altered morphology when grown on astrocytes isolated from an *Fmr1* KO mouse (Fig.4.2a,b). Comparison of the dendritic arbor morphology of WT neurons grown on *Fmr1* KO astrocytes with those grown on WT astrocytes showed: the length of the longest primary dendrite and the extent of the area covered by the dendritic arbor were decreased by 15.5% ($p<0.001$) and 31.8% ($p<0.001$), respectively (Fig. 4.2c,d); the area covered per micrometer of dendrite was decreased by 17.3% ($p<0.001$) (Fig.4.2g); the number of branches per cell was increased by 13.0% ($p=0.046$, Fig.4.2e); and, the branch density (number of dendritic branches per μm^2) was increased by 57.4% ($p<0.001$, Fig.4.2h). These observations indicate that growth on *Fmr1* KO astrocytes appeared to alter the normal dendritic arborization of WT neurons.

WT astrocytes prevent the abnormal dendrite morphology of *Fmr1* KO neurons

Given that *Fmr1* KO astrocytes impacted the dendrite morphology of the cultured WT hippocampal neurons, we next tested whether WT astrocytes are able to prevent the development of the abnormal neuron morphology in *Fmr1* KO hippocampal neurons. We analyzed the morphology of *Fmr1* KO neurons grown on both *Fmr1* KO and WT astrocytes. Notably, *Fmr1* KO neurons grown on WT astrocytes exhibited morphological alterations towards a normal neuronal dendritic phenotype (Fig.4.3a-h). When grown on WT astrocytes, *Fmr1* KO neurons exhibited an increase in the length of the longest dendrite (16.7%, $p<0.001$, Fig.4.3c), the total area covered by the dendritic arbor (36.9%, $p<0.001$, Fig.4.3d), and the area covered per micrometer of dendrite (24.9%, $p<0.001$, Fig.4.3g). Conversely, when grown on WT astrocytes, *Fmr1* KO neurons showed a decrease in the number of branches (Fig.4.3e), number of primary dendrites (Fig.4.3f) and branch density (Fig.4.3h), by 6.9% ($p=0.381$), 13.8% ($p<0.001$) and 33.3% ($p<0.001$), respectively. However, for all parameters, growth on WT astrocytes restored the *Fmr1* KO phenotype closer to the WT neuron morphology. In fact, growth of *Fmr1* KO neurons on WT astrocytes restored the phenotype by as much as 71.7% (Relative difference of *Fmr1* KO neurons grown on WT astrocytes vs. *Fmr1* KO astrocytes compared to WT neurons grown on WT astrocytes, dotted line in Fig.4.3c-h). These observations support the notion that astrocytes from a WT mouse prevent the development of abnormal dendritic morphology of *Fmr1* KO neurons.

Fmr1 KO astrocytes alter the synaptic protein expression in WT neurons

Next, we sought to determine if the initial synaptic protein packaging was altered in the WT neurons grown on *Fmr1* KO astrocytes. Early in neuron development before synaptic formation, pre- and post-synaptic protein complexes are packaged for transport to future synaptic sites. These synaptic protein aggregates can be visualized as puncta (spots of intense staining) with immunocytochemistry. We used antibodies directed at synaptophysin (a pre-synaptic protein that exists as part of the synaptic vesicle

membrane) and PSD-95 (a post-synaptic protein that forms part of the post-synaptic density) to determine if the early packaging of synaptic proteins was altered.

At 7 DIV the clustering of both pre- and post-synaptic proteins was altered in WT neurons grown on *Fmr1* KO astrocytes (Fig. 4.4a,b). We found a 34.8% decrease ($p<0.001$, Fig. 4.4c) in the number of synaptophysin immunoreactive (IR) puncta per cell, and a 13.9% reduction ($p<0.001$, Fig 4.4d) in the number of PSD-95 IR puncta per cell. These results demonstrate that the initial synaptic protein clustering is impaired when WT neurons are grown on *Fmr1* KO astrocytes.

WT astrocytes prevent the alterations of synaptic proteins in *Fmr1* KO neurons

Given that the dendritic morphology of *Fmr1* KO neurons approached normal when grown on WT astrocytes, we examined whether astrocytes from a WT mouse could also influence the synaptic protein distribution of *Fmr1* KO neurons. At 7 DIV the clustering of both pre- and post-synaptic proteins was increased in *Fmr1* KO neurons grown on WT astrocytes (Fig. 4.4e,f). We found a 40.3% ($p=0.003$, Fig. 4.4g) increase in the number of synaptophysin IR puncta in *Fmr1* KO neurons grown on WT astrocytes. This equated to 30.6% of the number seen in WT neurons on WT astrocytes (compared to 22.8% of normal). Similarly, we observed an increase in the number of PSD-95 IR puncta per cell. In fact, there was almost three times ($p<0.001$, Fig. 4.4h) the number of PSD-95 IR puncta per cell, increasing the quantity to 39.0% of normal numbers (compared to 14.7%). Therefore, these results support the concept that WT astrocytes can increase the number of both pre- and post-synaptic protein clusters, contributing to the recovery of the alterations in synaptic protein expression in *Fmr1* KO neurons.

4.2.4 Discussion

These experiments are novel and exciting as they are the first to establish a role for astrocytes in the altered neurobiology of FXS. Our data show that astrocytes are involved in shaping the dendritic arbors of neurons in FXS. During development,

numerous pathways between neurons are made and then the redundant connections are pared back to create a streamlined neural communication network. Glial cells provide guidance cues that aid in the correct extension (Banker, 1980; Powell and Geller, 1999) and elimination of neural processes (Barres, 2008). In FXS, as in other disorders that manifest with cognitive impairment (Kaufmann and Moser, 2000), the fine-tuning is often impaired. It follows that the astrocytes in FXS (and other disorders of cognitive impairment) could be lacking in their capacity to promote appropriate neurite patterning. Consistent with this, our results revealed more complex dendritic arbors with increased branch density in neurons grown with astrocytes from a Fragile X mouse. Furthermore, the abnormal increase in branch density was prevented in Fragile X neurons when cultured with normal astrocytes. These results are consistent with the abnormal pruning associated with FXS. Furthermore, the findings imply that FXS astrocytes are deficient in their capacity to effectively regulate the pruning process that is required for efficient neural communication, and could contribute to the cognitive impairment seen in individuals with FXS.

The current experiments demonstrated that astrocytes are also involved in the early stages of synapse development. Abnormal levels of synaptic proteins have been shown in FXS (Liao et al., 2008), and synaptic inefficiencies have also been described in a number of developmental disorders (Sudhof, 2008). Astrocytes are required for the efficient formation, maturation and maintenance of synapses (Pfrieger and Barres, 1997; Ullian et al., 2001). Therefore, in addition to lacking the full capacity to promote appropriate dendrite elaborations, astrocytes in FXS could also be deficient in their ability to regulate synapse development. In agreement with this, we found that neurons grown with astrocytes from a Fragile X mouse exhibited a decreased number of pre- and post-synaptic protein aggregates. Furthermore, this abnormal decrease was prevented in Fragile X neurons when they were cultured with normal astrocytes. These findings are in concert with the current understanding of synaptic protein dysregulation in FXS. In addition, these experiments suggest that astrocytes contribute to the erroneous synapse

development in FXS, and could therefore be a fundamental factor in the development of the behavioural maladaptations seen in individuals with FXS.

Previous research has shown that glial cells contribute to the development of several neurological disorders (reviewed in (Barres, 2008)) and our results support the concept of astrocytes guiding appropriate neurite and synapse development (Pfrieger and Barres, 1997; Mauch et al., 2001; Ullian et al., 2001; Murai et al., 2003; Christopherson et al., 2005; Nishida and Okabe, 2007; Guizzetti et al., 2008). Most recently, Ballas and colleagues (2009) found that astrocytes lacking the protein responsible for Rett syndrome, methyl-CpG-binding protein 2 (MeCP), could not support normal neuron growth. Similar to Rett syndrome, FXS was previously thought to be a disease resulting from a loss-of-function due to a lack of a specific protein in neurons only. However, it is possible that the abnormal phenotype in FXS, as in Rett syndrome, results from additional non-neuronal deficiencies. For example the astrocytes in individuals with FXS may also be dysfunctional, and this deficit could be caused by an indirect or a direct loss of FMRP. The loss of FMRP in neurons could result, indirectly, in aberrant astrocyte mediated support functions as a result of impaired neuron-to-astrocyte signaling caused by the loss of neuronal FMRP. Alternatively, the astrocytes in an individual with FXS may also be deficient in FMRP, and suffer abnormalities in normal functioning directly due to the loss of FMRP. Recently, our lab documented that FMRP is expressed in cells of the glial lineage, and that FMRP was absent from putative astrocytes in the *Fmr1* KO mouse (Pacey and Doering, 2007). Therefore, it is possible that astrocytes lack FMRP, specifically at a time during development when astrocyte support of neuron growth and synapse formation are vital, and this lack of FMRP could contribute to the abnormal neuron phenotype seen in FXS. Given that FMRP is a key regulator of translation of a number of mRNA targets in neurons (Brown et al., 2001; Miyashiro et al., 2003; Liao et al., 2008), and that the list is not yet complete, it is plausible that FMRP also regulates a subset of mRNAs in astrocytes. In this scenario, the loss of FMRP seen in FXS, would result in aberrant protein translation in astrocytes in addition to that already documented

in neurons. In turn, this could lead to altered astrocyte-neuron signaling and interfere with astrocyte-mediated neuronal growth and synaptic development. While the present study provides strong evidence for a role of astrocytes in the development of the neurobiological abnormalities seen in FXS, the experiments do not identify the molecular basis of the alterations and cannot confirm whether they are a direct or indirect result of a lack of FMRP.

Future studies designed to investigate these possibilities would provide valuable information on the neurobiological processes that are altered in FXS. For example, *in vitro* studies evaluating the effect of FMRP transfection in *Fmr1* KO astrocytes, and the siRNA mediated specific down-regulation of *Fmr1* in WT astrocytes, on WT neurons could provide more direct evidence for a role of astrocyte FMRP in the neurobiology of FXS. Such studies could yield insight into whether there are any astrocyte-secreted factors that are altered consequent to a deficiency of FMRP, and would therefore provide novel avenues for therapeutic intervention. Additionally, *in vivo* studies targeting FMRP expression in astrocytes using the *Fmr1* conditional knockout and *Fmr1* conditional expression mice (Meintjes et al., 2005) would provide an invaluable *in vivo* correlate and offer insight into the functional consequences of alterations in astrocyte FMRP.

4.2.5 Materials and Methods

Animals

All animal experiments were carried out in accordance with the guidelines set out by the Canadian Council on Animal Care and were approved by the McMaster University Animal Research Ethics Board. The FMRP mouse colony was established from breeding pairs of B6.129.FMR1.FvBN mice originally obtained from Dr. Carl Dobkin at the New York State Institute for Basic Research in Developmental Disabilities. The WT and KO B6.129.FMR1.FvBN mice were maintained as individual strains and genotyped regularly. Both male and female mice were used in the experiments. The FMRP knockout mice (B6.129.FMR1.FvBN) were housed and bred at the McMaster University Central Animal

Facility.

Cell Culture

Primary hippocampal neurons with astrocytes were grown in co-culture conditions as detailed previously by our lab (Jacobs & Doering, 2009; in press). Briefly, astrocytes were isolated from either WT or *Fmr1* KO post-natal day (PND) 0-1 pups and grown on Poly-L-Lysine (1mg/ml) and laminin (0.1mg/ml) coated coverslips in MEM (Invitrogen) supplemented with 6% glucose and 10% horse serum (Invitrogen) for one week. Primary hippocampal neurons were then isolated from embryonic day 17 (day of sperm plug counted as E1) animals and seeded on the astrocytes and maintained in MEM supplemented with N2 (Invitrogen), sodium pyruvate (Invitrogen) and 6% glucose, for the duration of the experiments.

Immunocytochemistry

After seven days *in vitro* (DIV) the cells were fixed with ice-cold (-20°C) methanol and processed for immunocytochemistry. Following the appropriate serum block, the cells were incubated with primary antibodies overnight at 4°C. Secondary antibodies were applied for three hours at room temperature. The following antibodies, diluted in 1% bovine serum albumin (BSA), were used: chicken MAP2 (1:20,000, Neuromics), mouse monoclonal synaptophysin (Clone SVP-38, 1:250, SIGMA), mouse monoclonal PSD-95 (Clone 6G6-1C9, 1:200, Chemicon), anti-mouse AlexaFluor 594 (1:1500, Invitrogen) and anti-chicken FITC (1:100, Jackson). Coverslips were mounted with Vectashield fluorescent mounting medium with DAPI.

Image acquisition and Quantification

Images were captured using a Zeiss Axioskop 2 epi-fluorescence and AxioVision Image Acquisition software. The quantification of dendritic arbor morphology and puncta analysis were performed using plug-ins for Image J (http://rsbweb.nih.gov/ij/). Morphological measurements of isolated neurons were obtained using Neuronmetrics™

(http://www.ibridgenetwork.org/arizona/UA07-56-Neuronmetrics)(Narro et al., 2007). Puncta analysis was performed on isolated cells using a custom written plug-in (©2001 Barry Wark. Source code or binaries available upon request to barrywark@mac.com) (Christopherson et al., 2005).

For each experiment, the same culture conditions were established in multiple wells. For analysis, two or three coverslips per experiment were used to obtain the sample of isolated neurons. For the morphometric analyses approximately 100 cells were selected at random from three coverslips, from each of 3 independent experiments (with the exception of the KO/KO condition where only 2 experiments were performed). For the synaptic protein analysis approximately 50 isolated neurons were selected at random per experiment, over 2 coverslips for each of 3 independent experiments (with the exception of the KO/KO condition as above).

Statistical Analyses

For all analyses, the observer was blind to the identity of the sample. Statistic analyses were conducted using SPSS17, with an alpha level set to 0.05. Data are presented as mean ± s.e.m. . For multiple comparisons a one-way ANOVA with post-hoc Tukey's tests were performed. Where data had significantly different variances (as determined by Levene's test for equal variances), and deviated significantly from a normal distribution (as determined by the Shapiro-Wilk test for normality), Mann-Whitney U (two-tailed) tests were used.

Acknowledgments

This work was supported by the Natural Sciences and Engineering Research Council of Canada (NSERC) and the Fragile X Research Foundation of Canada. The authors would like to thank Momal Mazhar for her help in the quantification of the neurons and astrocytes.

4.2.6 References

Bakker C, Verheij C, Willemsen R, van der Helm R, Oerlemans F, Vermey M, Bygrave A, Hoogeveen A, Oostra B, Reyniers E, De Boulle K, D'Hooge R, Cras P, Van Velzen D, Nagels G, Martin J, De Deyn PP, Darby JK, Willems PJ (1994) Fmr1 knockout mice: a model to study fragile X mental retardation. The Dutch-Belgian Fragile X Consortium. Cell 78:23-33.

Ballas N, Lioy DT, Grunseich C, Mandel G (2009) Non-cell autonomous influence of MeCP2-deficient glia on neuronal dendritic morphology. Nat Neurosci 12:311-317.

Banker GA (1980) Trophic interactions between astroglial cells and hippocampal neurons in culture. Science 209:809-810.

Barres BA (2008) The mystery and magic of glia: a perspective on their roles in health and disease. Neuron 60:430-440.

Beckel-Mitchener A, Greenough WT (2004) Correlates across the structural, functional, and molecular phenotypes of fragile X syndrome. Ment Retard Dev Disabil Res Rev 10:53-59.

Brown V, Jin P, Ceman S, Darnell JC, O'Donnell WT, Tenenbaum SA, Jin X, Feng Y, Wilkinson KD, Keene JD, Darnell RB, Warren ST (2001) Microarray identification of FMRP-associated brain mRNAs and altered mRNA translational profiles in fragile X syndrome. Cell 107:477-487.

Castren M, Tervonen T, Karkkainen V, Heinonen S, Castren E, Larsson K, Bakker CE, Oostra BA, Akerman K (2005) Altered differentiation of neural stem cells in fragile X syndrome. Proc Natl Acad Sci U S A 102:17834-17839.

Chen L, Toth M (2001) Fragile X mice develop sensory hyperreactivity to auditory stimuli. Neuroscience 103:1043-1050.

Christopherson KS, Ullian EM, Stokes CC, Mullowney CE, Hell JW, Agah A, Lawler J, Mosher DF, Bornstein P, Barres BA (2005) Thrombospondins are astrocyte-secreted proteins that promote CNS synaptogenesis. Cell 120:421-433.

Comery TA, Harris JB, Willems PJ, Oostra BA, Irwin SA, Weiler IJ, Greenough WT (1997) Abnormal dendritic spines in fragile X knockout mice: maturation and pruning deficits. Proc Natl Acad Sci U S A 94:5401-5404.

Devys D, Lutz Y, Rouyer N, Bellocq JP, Mandel JL (1993) The FMR-1 protein is cytoplasmic, most abundant in neurons and appears normal in carriers of a fragile X premutation. Nat Genet 4:335-340.

Frankland PW, Wang Y, Rosner B, Shimizu T, Balleine BW, Dykens EM, Ornitz EM, Silva AJ (2004) Sensorimotor gating abnormalities in young males with fragile X syndrome and Fmr1-knockout mice. Mol Psychiatry 9:417-425.

Greenough WT, Klintsova AY, Irwin SA, Galvez R, Bates KE, Weiler IJ (2001) Synaptic regulation of protein synthesis and the fragile X protein. Proc Natl Acad Sci U S A 98:7101-7106.

Guizzetti M, Moore NH, Giordano G, Costa LG (2008) Modulation of neuritogenesis by astrocyte muscarinic receptors. J Biol Chem 283:31884-31897.

Hagerman PJ (2008) The fragile X prevalence paradox. J Med Genet 45:498-499.

Kaufmann WE, Moser HW (2000) Dendritic anomalies in disorders associated with

mental retardation. Cereb Cortex 10:981-991.

Kremer EJ, Pritchard M, Lynch M, Yu S, Holman K, Baker E, Warren ST, Schlessinger D, Sutherland GR, Richards RI (1991) Mapping of DNA instability at the fragile X to a trinucleotide repeat sequence p(CCG)n. Science 252:1711-1714.

Lee A, Li W, Xu K, Bogert BA, Su K, Gao FB (2003) Control of dendritic development by the Drosophila fragile X-related gene involves the small GTPase Rac1. Development 130:5543-5552.

Liao L, Park SK, Xu T, Vanderklish P, Yates JR, 3rd (2008) Quantitative proteomic analysis of primary neurons reveals diverse changes in synaptic protein content in fmr1 knockout mice. Proc Natl Acad Sci U S A 105:15281-15286.

Mauch DH, Nagler K, Schumacher S, Goritz C, Muller EC, Otto A, Pfrieger FW (2001) CNS synaptogenesis promoted by glia-derived cholesterol. Science 294:1354-1357.

Miyashiro KY, Beckel-Mitchener A, Purk TP, Becker KG, Barret T, Liu L, Carbonetto S, Weiler IJ, Greenough WT, Eberwine J (2003) RNA cargoes associating with FMRP reveal deficits in cellular functioning in Fmr1 null mice. Neuron 37:417-431.

Murai KK, Nguyen LN, Irie F, Yamaguchi Y, Pasquale EB (2003) Control of hippocampal dendritic spine morphology through ephrin-A3/EphA4 signaling. Nat Neurosci 6:153-160.

Narro ML, Yang F, Kraft R, Wenk C, Efrat A, Restifo LL (2007) NeuronMetrics: software for semi-automated processing of cultured neuron images. Brain Res 1138:57-75.

Nielsen DM, Derber WJ, McClellan DA, Crnic LS (2002) Alterations in the auditory startle response in Fmr1 targeted mutant mouse models of fragile X syndrome. Brain Res 927:8-17.

Nimchinsky EA, Oberlander AM, Svoboda K (2001) Abnormal development of dendritic spines in FMR1 knock-out mice. J Neurosci 21:5139-5146.

Nishida H, Okabe S (2007) Direct astrocytic contacts regulate local maturation of dendritic spines. J Neurosci 27:331-340.

Pacey LK, Doering LC (2007) Developmental expression of FMRP in the astrocyte lineage: implications for fragile X syndrome. Glia 55:1601-1609.

Pfrieger FW, Barres BA (1997) Synaptic efficacy enhanced by glial cells in vitro. Science 277:1684-1687.

Powell EM, Geller HM (1999) Dissection of astrocyte-mediated cues in neuronal guidance and process extension. Glia 26:73-83.

Qin M, Kang J, Smith CB (2002) Increased rates of cerebral glucose metabolism in a mouse model of fragile X mental retardation. Proc Natl Acad Sci U S A 99:15758-15763.

Reddy KS (2005) Cytogenetic abnormalities and fragile-X syndrome in Autism Spectrum Disorder. BMC Med Genet 6:3.

Sudhof TC (2008) Neuroligins and neurexins link synaptic function to cognitive disease. Nature 455:903-911.

Ullian EM, Sapperstein SK, Christopherson KS, Barres BA (2001) Control of synapse

number by glia. Science 291:657-661.

Wang H, Ku L, Osterhout DJ, Li W, Ahmadian A, Liang Z, Feng Y (2004) Developmentally-programmed FMRP expression in oligodendrocytes: a potential role of FMRP in regulating translation in oligodendroglia progenitors. Hum Mol Genet 13:79-89.

Figure 4.1: Effects of astrocytes on the growth of hippocampal neurons in co-culture at 7 DIV.

E17 primary hippocampal neurons were co-cultured with P0-1 primary cortical astrocytes for 7 days *in vitro* (DIV) in each of four co-culture conditions. **a**, Immunofluorescent images of neurons in each of the four culture combinations. Neurons are stained with an antibody directed against the neuronal dendritic marker, MAP2. Scale bar represents 100μm. **b**, Quantification of percent of surviving neurons at 7DIV in each of the four culture conditions. Data shown are mean values ± s.e.m. from two or three independent experiments (10-15 regions of 1.5 mm^2 from 2 coverslips per experiment). Significant differences revealed by post-hoc Tukey's tests are indicated, $p<0.001$.

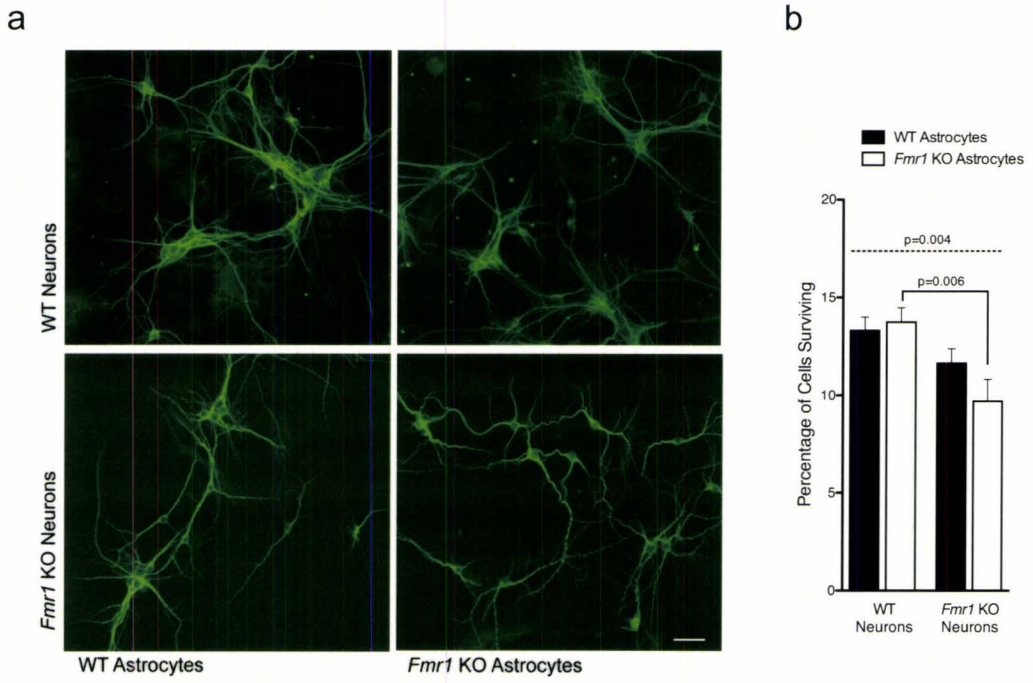
a
b
WT Neurons
Fmr1 KO Neurons
WT Astrocytes
Fmr1 KO Astrocytes
WT Astrocytes
Fmr1 KO Astrocytes
p=0.004
p=0.006
Percentage of Cells Surviving
20
15
10
5
0
WT Neurons
Fmr1 KO Neurons

Figure 4.1

Figure 4.2: Effects of *Fmr1* KO astrocytes on dendritic morphology of WT neurons.

WT E17 primary hippocampal neurons were co-cultured for 7 DIV with primary cortical astrocytes from either WT or *Fmr1* KO mice. **a**, Immunofluorescent images of neurons at 7DIV stained with an antibody directed against the neuronal dendritic marker, MAP2. The left and right images are representative WT neurons cultured on WT and *Fmr1* KO astrocytes, respectively. Scale bar represents 50μm. **b**, Representative dendritic arbor skeletons of WT neurons grown on WT astrocytes (left panel), or *Fmr1* KO astrocytes (right panel). **c-h**, Quantification of dendritic arbor morphology. Data shown are mean values ± s.e.m. of 297 (WT) and 282 (*Fmr1* KO) cells, from three independent experiments. Significant differences revealed by Mann-Whitney U tests (two-tailed) are indicated, * $p<0.05$, *** $p<0.001$.

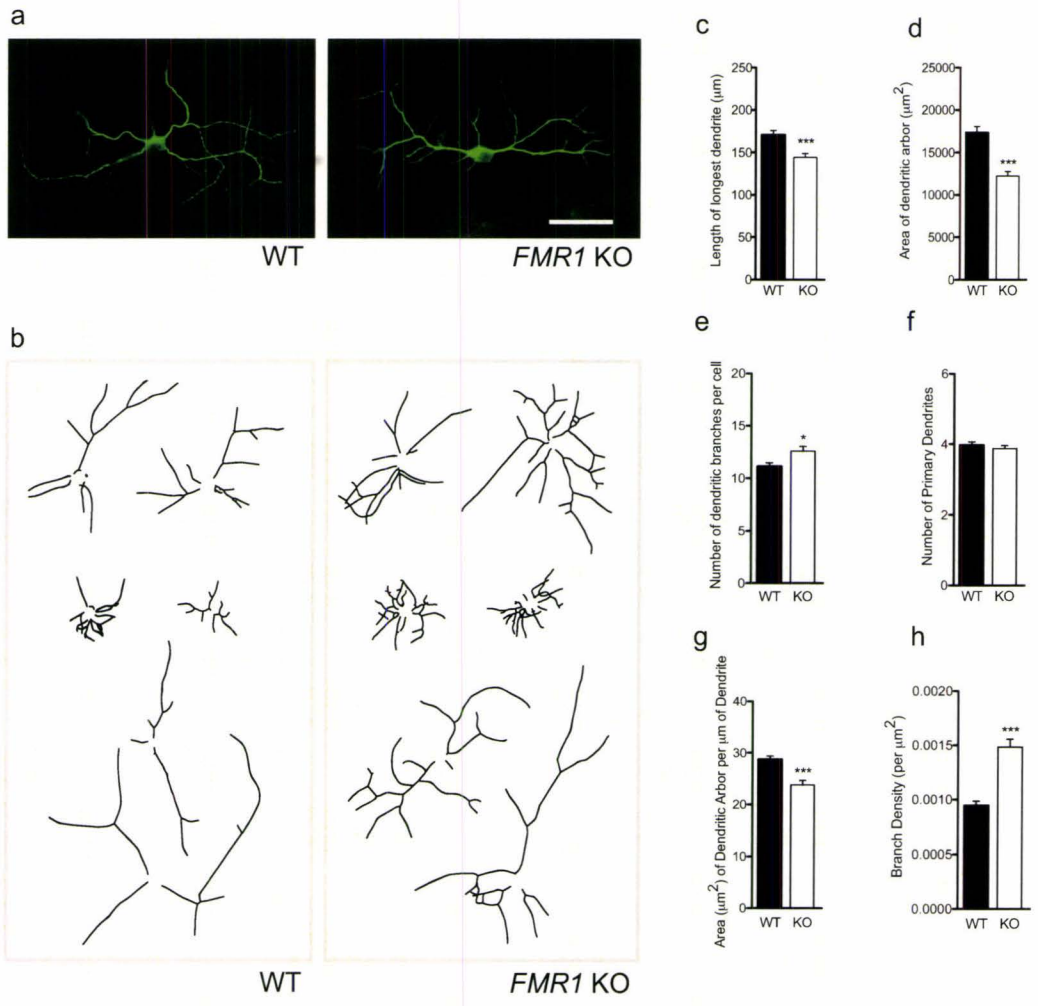
a
WT
FMR1 KO
b
WT
FMR1 KO
c
Length of longest dendrite (μm)
250
200
150
100
50
0
***
WT KO
d
Area of dendritic arbor (μm2)
25000
20000
15000
10000
5000
0
***
WT KO
e
Number of dendritic branches per cell
20
15
10
5
0
*
WT KO
f
Number of Primary Dendrites
6
4
2
0
WT KO
g
Area (μm2) of Dendritic Arbor per μm of Dendrite
40
30
20
10
0
***
WT KO
h
Branch Density (per μm2)
0.0020
0.0015
0.0010
0.0005
0.0000
***
WT KO

Figure 4.2

Figure 4.3: WT astrocytes rescue the dendritic morphology of *Fmr1* KO neurons.

Fmr1 KO E17 primary hippocampal neurons were cultured for 7 DIV with primary cortical astrocytes from either WT or *Fmr1* KO mice. **a**, Neurons stained with an antibody directed against the neuronal dendritic marker, MAP2. The left and right images are representative of *Fmr1* KO neurons cultured on WT or *Fmr1* KO astrocytes, respectively. Scale bar represents 50μm. **b**, Representative dendritic arbor skeletons of *Fmr1* KO neurons grown on WT astrocytes (left panel), or *Fmr1* KO astrocytes (right panel). **c-h**, Quantification of dendritic arbor morphology. Data shown are mean values ± s.e.m. of 318 (WT) and 201 (*Fmr1* KO) cells, from two or three independent experiments. Significant differences revealed by Mann-Whitney U tests (two-tailed) are indicated, *** $p<0.001$. Horizontal dotted line indicates mean value for WT neurons grown on WT astrocytes (from **Fig. 2c-h**).

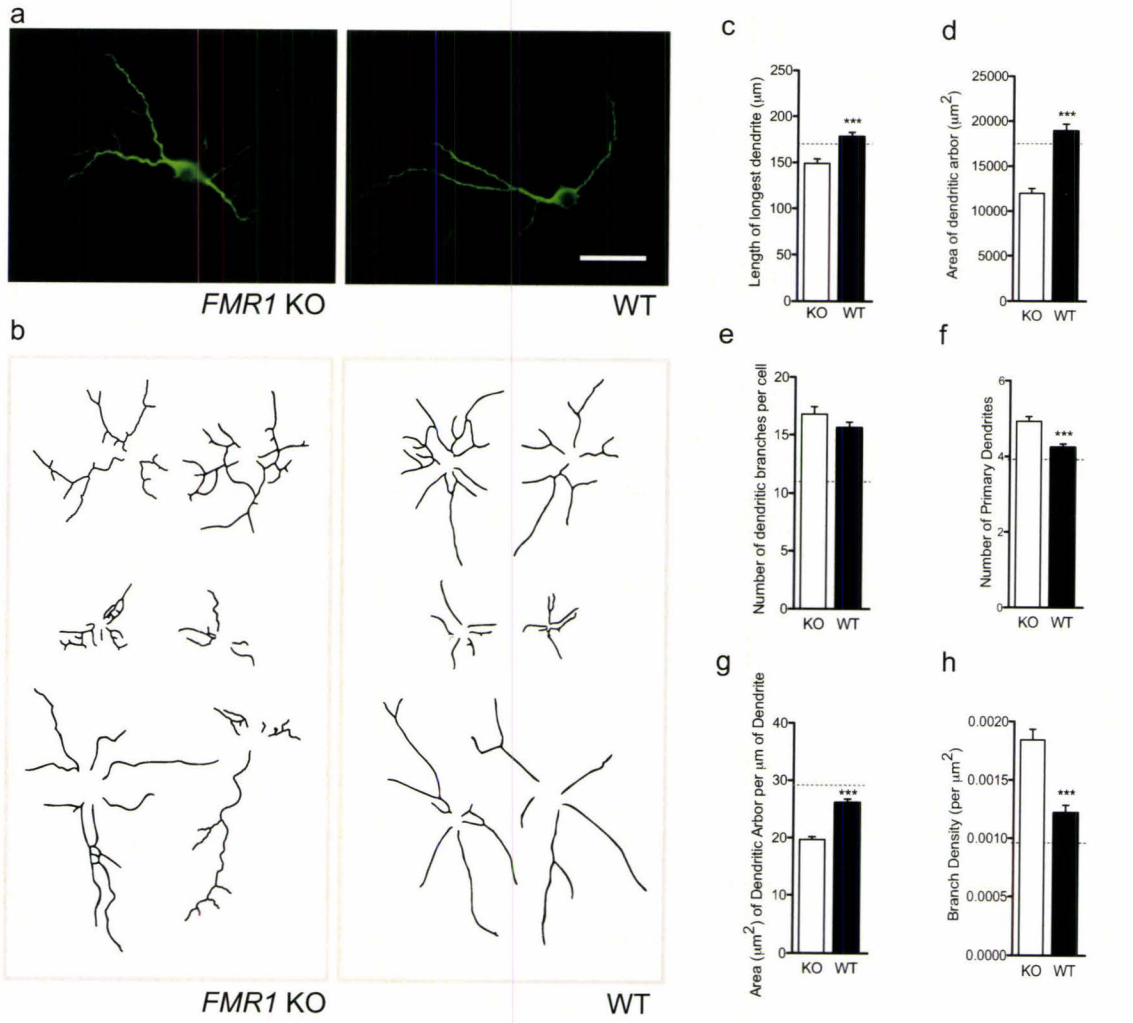
a
FMR1 KO
WT
b
FMR1 KO
WT
c
Length of longest dendrite (µm)
250
200
150
100
50
0
***
KO WT
d
Area of dendritic arbor (µm2)
25000
20000
15000
10000
5000
0
***
KO WT
e
Number of dendritic branches per cell
20
15
10
5
0
KO WT
f
Number of Primary Dendrites
6
4
2
0
***
KO WT
g
Area (µm2) of Dendritic Arbor per µm of Dendrite
40
30
20
10
0
***
KO WT
h
Branch Density (per µm2)
0.0020
0.0015
0.0010
0.0005
0.0000
***
KO WT

Figure 4.3

Figure 4.4: WT astrocytes rescue the synaptic protein aggregation in *Fmr1* KO neurons.

a-d, WT E17 primary hippocampal neurons were cultured for 7 DIV with primary cortical astrocytes from either WT or *Fmr1* KO mice. **a,b**, Immunofluorescent images of WT neurons stained with antibodies directed against Map2 (green) and synaptophysin (**a**) or post-synaptic density protein 95 (PSD-95) (**b**)(red). Nuclei are stained with DAPI (blue). The images on the left and right are representative WT neurons grown on WT astrocytes and *Fmr1* KO astrocytes, respectively. Scale bars represent 50μm. **c,** Quantification of synaptophysin puncta per cell. Data shown are mean values ± s.e.m. of 147 (WT) and 143 (*Fmr1* KO) cells, from three independent experiments. **d,** Quantification of PSD-95 puncta per cell. Data shown are mean values ± s.e.m. of 111 (WT) and 119 (*Fmr1* KO) cells, from three independent experiments. **e-h**, *Fmr1* KO E17 primary hippocampal neurons were cultured for 7 DIV with primary cortical astrocytes from either WT or *Fmr1* KO mice. **e,f,** Immunoflourescent images of neurons stained with antibodies directed against MAP2 (green) and synaptophysin (**e**) or PSD-95 (**f**)(red). Nuclei are stained with DAPI (blue). The images on the left and right are representative *Fmr1* KO neurons grown on WT and *Fmr1* KO astrocytes, respectively. Scale bars represent 50μm. **g**, Quantification of synaptophysin puncta per cell. Data shown are mean values± s.e.m. of 112 (WT) and 94 (*Fmr1* KO) cells, from two or three independent experiments. **h**, Quantification of PSD-95 puncta per cell. Data shown are mean values ± s.e.m. of 143 (WT) and 94 (*Fmr1* KO) cells, from two or three independent experiments. Significant differences revealed by Mann-Whitney U tests (two-tailed) are indicated, $^{**}p<0.05$, $^{***}p<0.001$.

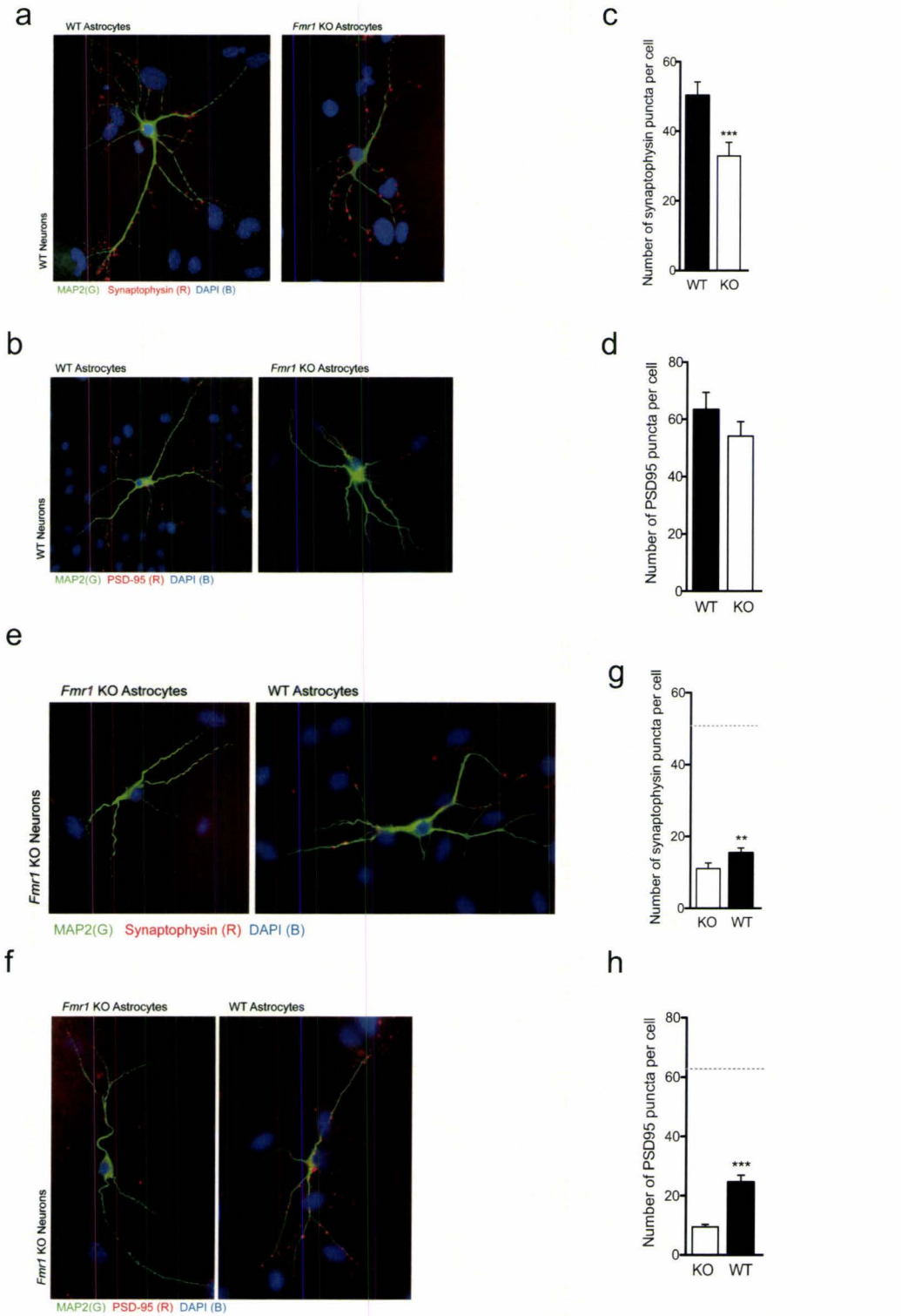
a
WT Astrocytes
Fmr1 KO Astrocytes
WT Neurons
MAP2(G) Synaptophysin (R) DAPI (B)
c
Number of synaptophysin puncta per cell
60
40
20
0
***
WT KO
b
WT Astrocytes
Fmr1 KO Astrocytes
WT Neurons
MAP2(G) PSD-95 (R) DAPI (B)
d
Number of PSD95 puncta per cell
80
60
40
20
0
WT KO
e
Fmr1 KO Astrocytes
WT Astrocytes
Fmr1 KO Neurons
MAP2(G) Synaptophysin (R) DAPI (B)
g
Number of synaptophysin puncta per cell
60
40
20
0
**
KO WT
f
Fmr1 KO Astrocytes
WT Astrocytes
Fmr1 KO Neurons
MAP2(G) PSD-95 (R) DAPI (B)
h
Number of PSD95 puncta per cell
80
60
40
20
0
***
KO WT

Figure 4.4

CHAPTER 5:

FRAGILE X ASTROCYTES INDUCE DEVELOPMENTAL DELAYS IN DENDRITE MATURATION AND SYNAPTIC PROTEIN EXPRESSION

5. Chapter 5

5.1 Preface to Chapter 5

This chapter is comprised of an author-generated version of an article prepared for submission to GLIA, and as presented it is the pre-review version. The manuscript was submitted to GLIA on September 15th, 2009; Submission # GLIA-00303-2009.

As a submitted manuscript the author generated version is reproduced with implicit permission understood from the Wiley-Blackwell Copyright Transfer Agreement:

" Submitted Version. Wiley-Blackwell licenses back the following rights to the Contributor in the version of the Contribution as originally submitted for publication:

…

b. The right to transmit, print and share copies with colleagues."

5.1.1 Author contributions

For this paper, I designed and performed the majority of the experiments*, photographed the images, performed the analyses, carried out the statistical analyses, wrote the manuscript and prepared all figures. Dr. Doering provided guidance in the designing of the experiments and the editing of the manuscript.

* An undergraduate student, Meera Nathwani, conducted the Neuronmetrics™-based morphological analysis on a subset of the neurons from the 14 *DIV* (n(WT)=50, n(KO)=50) and 21 *DIV* (n(KO)=17) time points (data included in her thesis project). For these neurons, MN maintained the tissue culture (with cells I isolated), performed the ICC, and photographed the neurons (after I scanned her cultures to ensure no obvious problems). MN also helped edit the final manuscript.

5.1.2 Background and rationale

In our previous paper (Chapter 4), we found that Fragile X astrocytes alter the dendrite morphology and excitatory synaptic protein expression of normal primary

hippocampal neurons in culture. At 7 *DIV* neurons grown with Fragile X astrocytes exhibited an increase in branching and a decrease in the extension of the dendritic arbors compared to neurons grown on normal astrocytes. Furthermore, the neurons grown with Fragile X astrocytes had fewer pre- and post-synaptic protein clusters than did neurons grown on normal astrocytes.

Fragile X syndrome is a developmental disorder, and evidence suggests that the expression of FMRP is developmentally regulated. Expression peaks in early development (Lu, et al., 2004; Pacey & Doering, 2007; Wang, et al., 2004) and gradually declines with age (Singh, et al., 2007; Singh & Prasad, 2008). Furthermore, FMRP expression is up-regulated in critical periods for learning (Winograd, et al., 2008).
Recent studies indicate that FMRP may also be developmentally regulated in glial cells Wang and colleagues (2004) found that FMRP is expressed in immature, but not mature, oligodendrocytes. Additionally, Pacey and Doering (2007) found that FMRP to be expressed in astrocytes during development. FMRP may therefore be expressed, and exert its regulatory effects, during a specific developmental window.

We therefore wondered if it were possible that the effect of Fragile X astrocytes seen in normal neurons at 7 *DIV* would be minimized if provided a longer period of growth in culture. In other words, was is possible that the Fragile X astrocytes were inducing a delay in the normal development of the dendritic arbors and synapses in the neurons in culture. If this were true, we would expect that the effects of Fragile X astrocytes would be less, and perhaps even no longer, significant at longer time points in culture.

In these experiments we co-cultured neurons with normal or *FMR1* null astrocytes, and evaluated the neuronal dendritic morphology and excitatory protein expression at 7, 14 and 21 *DIV*.

5.1.3 Specific aims

- To show that the Fragile X astrocytes impart a developmental delay on the maturation of dendritic arbors *in vitro* (5).

- To demonstrate that the Fragile X astrocytes delay the formation of excitatory synapses *in vitro* (6).

5.2 Fragile X astrocytes induce developmental delays in dendrite maturation and synaptic protein expression

AUTHORS: Shelley Jacobs[1], Meera Nathwani[1] and Laurie C. Doering[1]

Department of Pathology & Molecular Medicine, McMaster University, 1200 Main Street West, Hamilton, Ontario, Canada, L8N 3Z5

RUNNING TITLE: Astrocytes in Fragile X

CORRESPONDING AUTHOR: Laurie C. Doering
Email: doering@mcmaster.ca
Phone: 905-525-9140 x22913

NUMBER OF FIGURES: 6
NUMBER OF TABLES: 0
NUMBER OF PAGES: 23

NUMBER OF WORDS: Abstract: 239
Introduction: 572
Materials and Methods: 814
Results: 1002
Discussion: 1568

TOTAL NUMBER OF WORDS: 5385

KEYWORDS: Fmr1, hippocampus, dendritic arbor, PSD-95, synapse, neuron

5.2.1 Abstract

The Fragile X mouse was used to study the developmental effects of FMRP null astrocytes on neuronal development. Embryonic hippocampal neurons were seeded on astrocyte monolayers in a co-culture system and allowed to develop for 7, 14 or 21 days. A detailed morphometric analysis was performed on the dendritic arbors of hippocampal neurons defined by a MAP2 antibody. When analyzed at 7 days in culture, we found that the hippocampal neurons grown on FMRP null astrocytes exhibited a significant difference from the neurons grown with normal astrocytes for many parameters including an increase in dendritic branching and area of the cell body. However, after 21 days in culture, the neurons grown on FMRP null astrocytes exhibited morphological characteristics that did not differ significantly from the neurons grown on normal astrocytes. With antibodies to the pre-synaptic protein, synapsin, and to the excitatory post-synaptic protein, PSD-95, we quantified the number of excitatory synapses along 50μm lengths of the dendrites. In addition to the delays in dendritic patterning, the development of excitatory synapses was also delayed in the hippocampal neurons. At 7 days in culture the neurons grown on the Fragile X astrocytes had more than double the number of excitatory synapses when compared to the neurons grown on the normal astrocytes. These experiments are the first to establish a role for astrocytes in the delayed growth characteristics and abnormal morphological features in dendrites and synapses that characterize the Fragile X syndrome.

5.2.2 Introduction

As the central nervous system (CNS) develops numerous events must occur in a highly regulated manner to create the intricate organization of neural networks that control the mature brain. One of the key players recognized in the guidance of neuron development is the astrocyte (Banker 1980; Barres 2008; Pfrieger and Barres 1997; Powell and Geller 1999; Ullian et al. 2001). As such, abnormal or 'diseased' astrocytes are now known to be prominent factors in the neurobiology of a number of developmental diseases of the CNS including Fragile X Syndrome (FXS) (Allen and Barres 2009; Ballas et al. 2009; Barres 2008; Maezawa et al. 2009; Jacobs and Doering, submitted).

FXS is the most common inherited form of mental retardation, affecting approximately 1/2500 children (Hagerman 2008). Children with FXS suffer from a number of behavioural deficiencies including: mild to severe cognitive impairment, hyperactivity, attention deficit, susceptibility to seizures, motor disorders and autistic behaviours (Beckel-Mitchener and Greenough 2004). Underlying neurobiological abnormalities in FXS are recognized in the form of altered dendritic growth, abundant immature dendritic spines and inappropriate synaptic development (Irwin et al. 2000; Irwin et al. 2001; Kaufmann and Moser 2000). The defects in individuals with FXS can be attributed to a mutation in the Fragile X Mental Retardation 1 (*FMR1*) gene causing gene silencing and a lack of the protein product, Fragile X Mental Retardation Protein (FMRP) (Kremer et al. 1991).

The *Fmr1* knockout (KO) mouse model of FXS is well accepted as an appropriate model in which to study the neurobiology of FXS (Bakker et al. 1994). The *Fmr1* KO mouse has been shown to demonstrate behavioural qualities similar to those seen in individuals with FXS, including: susceptibility to seizures, hyperactivity and learning impairments (Bakker et al. 1994; Chen and Toth 2001; Qin et al. 2002). Additionally, the neurons of *Fmr1* KO show similarly abnormal dendritic spine morphology and altered synaptic function (Comery et al. 1997; Nimchinsky et al. 2001), as documented in humans with

FXS (Irwin et al. 2000).

Contrary to the current belief that FMRP is only expressed in neurons, recent work in our lab revealed that FMRP is also expressed in cells of the glial lineage in the *Fmr1* KO mouse (Pacey and Doering 2007). Based on these findings we began our investigation into the role of astrocytes in the development of the abnormal neurobiology of FXS. Previously, we used the *Fmr1* KO mouse model to investigate the role of astrocytes in the development of the abnormal neuronal characteristics seen in FXS (Jacobs & Doering, submitted). In short, we found that Fragile X astrocytes were not able to support normal neuron growth and contributed to the abnormal neuronal phenotype seen in the Fragile X mouse. However, in that series of experiments, we focused on the early development of neurons, solely evaluating the effect of null astrocytes on the neurons after seven days in culture. Given that FXS is a developmental disorder, we wondered if neurons were prevented from normal maturation when exposed to signaling from the Fragile X astrocytes. If so, is it possible that neurons exposed to Fragile X astrocytes could recover from developmental delays? If true, this information would foster insight into the potential for astrocyte-directed therapeutic interventions as a preventative measure against the neuronal abnormalities underlying FXS. Such is the basis for the following experiments in which we investigated the possibility of an astrocyte-mediated a delay in neuron development using detailed morphometric and synaptic protein analyses combined with immunocytochemistry.

5.2.3 Materials and Methods

Animals

The FMRP knockout (KO)(FvBN.129.B6-*Fmr1*)(Bakker et al. 1994) and wild-type (WT) mice used for these experiments were housed and bred at the McMaster University Central Animal Facility. All experiments were completed in accordance with the guidelines set out by the Canadian Council on Animal Care and were approved by the McMaster Animal Research Ethics Board.

Cell Culture

Primary hippocampal neurons with astrocytes were grown in co-culture conditions as detailed previously by our lab (Jacobs and Doering 2009). Briefly, cortical astrocytes were isolated from post-natal day (PND) 0-1 pups and grown on Poly-L-Lysine (1mg/ml, Cat. No. P1399, SIGMA-ALDRICH, Oakville, Canada) and Laminin (0.1mg/ml, Cat. No. 23017-015, Invitrogen, Burlington, Canada) coated coverslips in MEM (Cat No. 11095-080, Invitrogen, Burlington, Canada) supplemented with 6% glucose and 10% horse serum (Cat No. 16050-122, Invitrogen, Burlington, Canada), for one week. Primary hippocampal neurons were then isolated from embryonic day 17 (day of sperm plug counted as PND1) animals and seeded above the astrocytes and maintained in MEM supplemented with N2 (Cat No. 17502-048, Invitrogen, Burlington, Canada), sodium pyruvate (Cat No. 11360-070, Invitrogen, Burlington, Canada) and 6% glucose, for the duration of the experiments. Hippocampal neurons isolated from WT animals were grown with astrocytes, from either WT or *Fmr1* KO mice, in culture for 7, 14 or 21 days. These cultures were grown in culture for 7, 14 or 21 days. A total of three independent cultures per condition (genotype+days *in vitro* (DIV)) were completed.

Immunocytochemistry

Following removal of the media, the cells were fixed with 4% PFA in PBS or ice cold (-20˚C) acetone for 15 or 20 minutes, respectively. After three washes with PBS, and the application of 0.1% Triton X-100 where necessary, non-specific binding was blocked with 1% bovine serum albumin (BSA) for 30 minutes. Primary antibodies were applied to the coverslips and incubated overnight at 4˚C. The second day, following washes with PBS, secondary antibodies were incubated with the cells for 3 hours at room temperature. Following a final set of washes with PBS and distilled water, the coverslips were mounted onto slides with Vectashield fluorescent mounting medium (Vector Labs, Burlington, Canada) containing DAPI to stain the nuclei.

The following antibodies, diluted in 1% BSA, were used: chicken anti-Map2 (Microtubule Associated Protein –2, 1:20,000, Neuromics, Edina, MN), guinea pig anti-synapsin (1:1000, Synaptic Systems, Goettingen, Germany), mouse monoclonal anti-PSD-95 (Post-Synaptic Density protein-95, Clone 6G6-1C9, 1:200, Millipore, Temecula, CA), anti-mouse AlexaFluor 594 (1:1500, Invitrogen, Burlington, Canada), anti-guinea pig FITC (1:200, Jackson ImmunoResearch, West Grove, PA) and anti-chicken FITC (1:100, Jackson ImmunoResearch, West Grove, PA).

Image acquisition

Images were acquired using a Zeiss Axioskop-2 epi-fluorescence microscope and AxioVision (v4.2) image acquisition software.

Dendritic arbor morphology

Morphological measurements were conducted using Neuronmetrics™ (http://www.ibridgenetwork.org/arizona/UA07-56-Neuronmetrics) (Narro et al. 2007), a plug-in for Image J (http://rsbweb.nih.gov/ij/). The following parameters were evaluated: number of dendritic branches, length of the longest primary dendrite, and the area covered by the dendritic arbor. For each independent culture, 50 isolated MAP2(+) neurons were selected and analyzed for morphology. Once each neuron image was converted to a black and white TIFF file, the images were processed through Neuronmetrics™ to generate pixilated skeletons and to obtain the morphological measurements listed above. Examples of representative neurons overlaid with digitized skeletons and area demarcations generated by Neuronmetrics™ are shown in Figure 5.1. Representative skeletons used by Neuronmetrics™ for morphological measurements are shown in Figure 5.2.

Cell body measurements

For each of the above neurons the area of the cell body was also measured, by tracing around the cell body using Image J.

Synaptic puncta analysis

Synapses were identified by the co-localization of the pre- (synapsin) and post-synaptic (PSD-95) puncta, using a custom written plug-in for Image J (©2001 Barry Wark: source code or binaries available upon request to barrywark@mac.com) (Christopherson et al. 2005). After selecting a 50μm segment along the dendrite, the image was processed using the above plug-in. Briefly, low frequency background from each channel (red and green) of the image was removed with the rolling ball background subtraction algorithm. Then, the puncta in each single-channel was 'masked' by thresholding the image so that only puncta remained above threshold. Puncta were then identified in each channel by the "Particle Analyzer" plug-in for Image J. Co-localization of the puncta in each channel was indentified when the distance between the centers of the two puncta was less than the radius of the larger puncta. The number of co-localized puncta was then recorded as synapses. For each independent culture one hundred 50μm-long sections along the dendrites were evaluated for synaptic protein expression.

Statistical Analyses

Statistics were performed using SPSS version 17, with an alpha level set to 0.05. All data are presented as mean ± SEM. Where the data had significantly different variances (as determined by Levene's test for equal variances), and deviated significantly from a normal distribution (as determined by the Shapiro-Wilk test for normality, Mann-Whitney U (two-tailed) tests were used.

5.2.4 Results

Morphological Analysis

In order to visualize the dendritic arbors of the neurons in co-culture, immunofluorescence using an antibody directed against the dendrite marker MAP2 was used (Riederer and Matus 1985). Figure 5.3 provides an example of the hippocampal neuron- astrocyte co-culture at 7 *DIV*, stained with MAP2 (green) to enable the visualization of the dendritic arbors. In the same image the astrocytes are stained with an antibody directed against Glial Fibrillary Acidic Protein (GFAP, red), and the nuclei are stained with DAPI (blue). Upon examination of the cultures, no obvious differences could be seen between clusters of neurons grown on *Fmr1* KO compared to those grown on WT astrocytes. To perform the morphometric analysis, isolated neurons were selected at random from the coverslip (Figure 5.3, inset).

At 7 *DIV*, the number of dendritic branches per cell was significantly ($p=0.045$; Mann Whitney $U=9745.50$; $F=-2.007$) increased in the neurons grown on *Fmr1* KO astrocytes (12.90 ± 0.62) compared to those grown on WT astrocytes (10.93 ± 0.44)(Fig. 5.4a). Branching increased over time in neurons grown on both *Fmr1* KO and WT astrocytes. However, by 14 *DIV* there was no significant difference in the number of dendritic branches between neurons grown on *Fmr1* KO astrocytes versus those grown on WT astrocytes (*Fmr1* KO, 25.62 ± 1.49; WT, 25.69 ± 1.49; $p=0.794$; Mann Whitney $U=11054.00$; $F=-0.261$). This was also true for the cells measured at 21 *DIV* (*Fmr1* KO, 29.13 ± 2.02; WT, 26.27 ± 1.48; $p=0.818$; Mann Whitney $U= 11077.00$; $F=-0.230$).

The length of the longest dendrite was also significantly different at 7 *DIV*. At 7 *DIV,* neurons grown on *Fmr1* KO astrocytes exhibited significantly ($p=0.019$; Mann Whitney $U=9491.00$; $F=-2.342$) lower values (148.93 ± 6.47) of their longest dendrites compared to neurons grown on WT astrocytes (167.40 ± 6.47)(Fig. 5.4b). The length of the longest dendrite increased at 14 *DIV*, and decreased slightly at 21 *DIV*, for neurons grown on

both *Fmr1* KO and WT astrocytes. No significant difference in length of the longest dendrite was observed at 14 *DIV* (*Fmr1* KO, 295.94±16.00; WT, 338.86±21.14; p=0.261; Mann Whitney U= 10335.00; F=-1.124) or 21 *DIV* (*Fmr1* KO, 263.78±12.29; WT, 274.78±11.97; p=0.229, Mann Whitney U=10205.00; F=-1.203).

At 7 *DIV*, but not 14 or 21 *DIV*, the cell body area was significantly (p=0.047; Mann Whitney U=9754.50; F=-1.991) increased in neurons grown on *Fmr1* KO astrocytes (197.10±5.87) compared to those grown on WT astrocytes (179.85±3.95)(Fig. 5.4c). The cell body area was increased in neurons grown on both *Fmr1* KO and WT astrocytes 14 *DIV*, and only slightly so at 21 *DIV*. Once again, there was no significant difference in this morphological parameter between neurons grown on *Fmr1* KO or WT astrocytes at 14 *DIV* (*Fmr1* KO, 242.27±6.45; WT, 246.02±6.66; p=0.840; Mann Whitney U=11098.00; F=-0.202) or 21 *DIV* (*Fmr1* KO, 245.13±9.44; WT, 268.05±11.08; p=0.228; Mann Whitney U=10344.50; F=-1.205).

The area of the dendritic arbor was significantly decreased in neurons grown on *Fmr1* KO astrocytes compared to those grown on WT astrocytes at both 7 *DIV* (*Fmr1* KO, 12373.57±654.79; WT, 17800.08±1038.79; p=0.000; Mann Whitney U=8278.00; F=-3.956) and 14 *DIV* (*Fmr1* KO, 8116.14±1126.15; WT, 23209.23±2153.68; p=0.000; Mann Whitney U=6001.00; F=-6.987) (Fig. 5.4d). The area of the dendritic arbor increased with time in culture for neurons grown on WT astrocytes. At 21 *DIV* the area of the dendritic arbor of neurons grown on *Fmr1* KO astrocytes also increased, and was comparable to that of the neurons grown on WT astrocytes. The difference was not significant at this point (21 *DIV*) in culture (*Fmr1* KO, 30192.00±1995.85; WT, 31900.05±2020.96; p=0.539; Mann Whitney U=10789.00; F=-0.614).

Therefore, by the morphological parameters evaluated in these experiments, it appears that the growth of the neurons early in development (i.e., 7 *DIV*) is altered when grown on *Fmr1* KO astrocytes, but these abnormal characteristics disappear with time. By 14

DIV, three out of four of the morphological characteristics we studied were no longer significantly altered in neurons grown on *Fmr1* KO astrocytes. The last parameter, the area of the dendritic arbor, had also reached levels comparable to values seen in neurons grown with WT astrocytes by 21 *DIV*.

Excitatory Synapse Analysis

Excitatory synapses were visualized using immunofluorescence. An antibody directed at synapsin, a synaptic vesicle protein known to be involved in neurotransmitter release (Greengard et al. 1993), was used to identify pre-synaptic components. Excitatory synapse post-synaptic regions were detected using an antibody directed at the post-synaptic protein, PSD-95, that is known to be part of the post-synaptic density complex found at excitatory synapses (El-Husseini et al. 2000). Double-labeling of these pre- and post-synaptic proteins was followed by the quantification of co-localized pre- and post-synaptic puncta using a plug-in for Image J. Figure 5 provides an example of a network of dendrites in the hippocampal neuron culture double-stained for synapsin (green) and PSD-95 (red). To perform the quantification, segments of dendrites that were 50μm long were isolated and processed for co-localization analysis (Figure 5.5, rectangular region and inset).

The number of synapses per 50μm increased over time in neurons grown on WT astrocytes whereas in neurons grown on *Fmr1* KO astrocytes, there was a slight decrease in the number of synapses over time (Fig. 5.6b). At 7 *DIV* neurons grown on *Fmr1* KO astrocytes had more than double the number of excitatory synapses per 50μm compared to neurons grown on WT astrocytes (*Fmr1* KO, 4.15±0.14; WT, 1.95±0.10; p=0.000; Mann Whitney U=20684.50; F=-11.129)(Fig. 5.6a,b). This significant difference was maintained at 14 *DIV*; neurons grown on *Fmr1* KO astrocytes had 53.8% more synapses per 50μm compared to neurons grown on WT astrocytes (*Fmr1* KO, 3.70±0.17; WT, 2.40±0.14; p=0.000; Mann Whitney U=31908.50; F=-6.229, Fig. 5.6a,b). By 21 *DIV*, however, there was no significant difference between the number of synapses per 50μm

of dendrite for neurons grown on *Fmr1* KO or WT astrocytes (*Fmr1* KO, 3.68±0.18; WT, 4.00±0.21; p=0.577; Mann Whitney U= 43822.50; F=-0.558). The number of synapses per 50μm increased over time in neurons grown on WT astrocytes; whereas in neurons grown on *Fmr1* KO astrocytes, there was a slight decrease in the number of synapses over time (Fig. 5.6b).

Therefore, similar to the morphological characteristics we evaluated, it appears that the abnormal number of synapses found at 7 *DIV* and 14 *DIV* on neurons grown with *Fmr1* KO astrocytes is brought to levels comparable to normal by 21 *DIV*.

5.2.5 Discussion

In this study we used a co-culture procedure in which normal primary hippocampal neurons were co-cultured with normal or *Fmr1* KO astrocytes for up to 21 days *in vitro* in order to investigate the possibility of an astrocyte-mediated delay in hippocampal neuron development. We evaluated the changes in neuron dendritic arbor morphology and excitatory synapse expression at 7, 14 and 21 *DIV*. We found that both the morphological parameters and the synaptic protein expression approached normal levels by 21 *DIV*, with three of four morphological parameters approaching normal at 14 *DIV*. Our results suggest that *Fmr1* KO astrocytes do not completely prevent normal hippocampal neuron growth, but delay it.

The morphological results presented herein are consistent with our previously reported results for the effects of *Fmr1* KO astrocytes on normal primary hippocampal neurons at 7 *DIV* (Jacobs & Doering, submitted). This finding is further supported by the earlier studies done by Lee et al. (2003). Consistent with our results, they described an increase in dendritic branching in neurons from mice lacking the *Drosophila fmr1* gene (Lee et al. 2003). However, the results of the present synaptic protein expression analysis at 7*DIV,* is different from the synaptic protein analysis at 7 *DIV* of that same series of experiments. This difference could be due to the modifications of the experimental design in the

present studies. First, in this study we used synapsin as our pre-synaptic protein antigen. While we would not expect that there would be a difference in the number of pre-synaptic puncta identified by the synapsin antibody versus the previously used synaptophysin antibody, this difference should be noted. Second, in the previous report we evaluated the pre- and post synaptic proteins independently whereas in the present experiments we report the co-localization of the pre-and post-synaptic proteins. It is in fact possible that the number of pre- or post- synaptic protein puncta does not correlate in a positive direction with the number of synapses. In that case there could a decrease in the numbers of pre- and post-synaptic puncta independently, but there could be an increase in the number of co-localized puncta. Third, and most importantly, here we report the synaptic protein expression in segments of dendrites taken from neuron networks, whereas in the previous paper we focused on the absolute numbers of pre- and post-synaptic puncta per isolated neuron. It could be expected that synapse number will vary when comparing neural networks with isolated neurons.

Dendritic arborization is delayed in neurons grown with *Fmr1* KO astrocytes

The results presented here support the idea that hippocampal neurons grown with *Fmr1* KO astrocytes reach normal maturity, but are delayed in the process. At 7 *DIV* the neurons grown on *Fmr1* KO astrocytes had significantly different cell measurements from the neurons grown on WT astrocytes for all of the parameters we measured. However, by 21 *DIV* those neurons had morphological measurements that closely resembled those of neurons grown on normal astrocytes.

During development the growth of dendritic arbors is a highly choreographed dynamic balance between phases of extension and retraction. Cues that regulate the initiation and promote dendritic arbor development are equally as important as those that stop its elaboration (Cline 2001). There is compelling evidence suggesting that dendritic arborization is regulated by both intrinsic and extrinsic signals. Astrocytes are known to provide a number of molecules that have been shown to be involved in the growth and

maturation of dendritic arbors (Banker 1980; Barres 2008; Powell and Geller 1999).

In the early stages of development the neurons grown on *Fmr1* KO astrocytes appear to be in a branching mode of growth, versus a mode dominated by arbor extension. This suggests that the dendritic arborization is altered in a manner that would interfere with the normal appropriate wiring of the hippocampal circuits. In 2001, Cline suggested that mechanisms that enhance dendritic arbor complexity have the potential to affect the integrative properties and firing characteristics of a neuron (Cline 2001). Neurons with more densely branched arbors may receive greater numbers of synaptic input that may affect the manner in which convergent inputs influence the neuron (Cline 2001). Astrocytes are known to provide cues that can alter the development of dendritic arbors (Banker 1980; Barres 2008; Powell et al. 1997). Here we show that astrocytes induce increased branching in the early stages of development of hippocampal neuron dendritic arbors *in vitro*. Thus, there is the possibility that astrocytes induce an increase in branching in the early development of hippocampal neurons in FXS, resulting in the alteration of the signaling properties of the neurons. In tune, this may affect key developmental stages when initial neural networks are being established. As such, these alterations could contribute to the underlying abnormal neurobiology, and therefore the clinical deficiencies observed in FXS.

In addition, it is possible that astrocytes from an *Fmr1* KO animal may be unable to appropriately regulate the establishment of the receptive field margins. Under normal conditions there are "stop" signals that inhibit the expansion of dendrites beyond the normal receptive field of the arbor (Gao 2007). Although poorly understood, some of these cues are known to originate in a contact dependent manner from the dendrites of adjacent neurons, and from contact independent means via secreted molecules (reviewed in (Gao 2007). Astrocytes present a number of signals that mediate other aspects of dendrite growth and elaboration and therefore it is possible that astrocytes may also play a role in dendritic tiling. In FXS, the 'diseased' astrocytes may inhibit the expansion of

the arbor to an abnormal extent, reducing the size of the area of coverage. At later stages in development, other cues could help mediate these adverse effects, and enable the extension of the arbor. However, during that early period of inhibited expansion, irreversible damage may have occurred, thereby preventing the establishment of local circuits in a timely manner necessary for normal neural network maturation. Once again, these alterations that develop early in the dendritic arbor could contribute to the underlying abnormal neurobiology, and result in cognitive impairments.

Excitatory synapse formation is delayed in neurons grown with *Fmr1* KO astrocytes

The findings of this study suggest that the growth of hippocampal neurons with *Fmr1* KO astrocytes impedes the appropriate timing of excitatory synaptic development. At 7 *DIV,* neurons grown on *Fmr1* KO astrocytes had significantly more excitatory synapses than the neurons grown on WT astrocytes. However, by 21 *DIV* the numbers of excitatory synapses in neurons grown on *Fmr1* KO astrocytes were equal to the quantity seen in neurons under normal conditions.

The formation of mature synapses is a dynamic process with a continuous fluctuation between synapses being formed and unwanted synapses being eliminated (Puro et al. 1977). Therefore at any time the number of synapses observed can be considered to be the net result of the number of new synapses formed and those being eliminated. At 7 *DIV* neurons grown on *Fmr1* KO astrocytes have a significantly greater number of synapses than neurons grown on WT astrocytes. Perhaps at 7 *DIV,* growth with *Fmr1* KO astrocytes promotes an increase in the production of synapses or a decrease the degree of pruning. A number of studies have suggested that many developmental disorders are caused by a lack of pruning early in development. Our findings therefore support a lack of appropriate synaptic pruning early in development as a potential contributor to the neurological abnormalities seen in FXS.

We found an abnormally high net number of excitatory synapses being maintained in

neurons grown on *Fmr1* KO astrocytes at 7 *DIV*, when compared to neurons grown on WT astrocytes. Over time, the difference between the net number maintained in the neurons grown on *Fmr1* KO astrocytes and those grown on WT astrocytes decreased, until 21 *DIV* at which point there is no longer a significant difference. The neurons grown on *Fmr1* KO astrocytes have reached a stage of maturity at which their net production of excitatory synapses equals that of neurons grown under normal conditions. Still, there is the potential that the abnormal early stages of development could play a major role in the ability of neurons to later integrate and transmit information effectively. Abnormal synapses may have been formed alongside atypical local neural networks, and these early alterations may negatively affect the neural circuitry of the region in the long run.

However, from the findings of this study we cannot make conclusions about synapse maturity. It is possible that the increase in synapses observed in the neurons grown on *Fmr1* KO astrocytes reflects an increased number of immature synapses. Given that the dendritic spine is the site for the majority of excitatory synapses, this finding would be in agreement with numerous studies that identified neurons in Fragile X with an abnormally high number of immature dendritic spines. The methods used in the current study did not permit the assessment of alterations in dendritic spine morphology.

The development of the CNS is a highly organized process requiring the establishment of correct connectivity with specific target cells. The creation of appropriate neural networks requires an intimate coupling of dendritic arborization and synaptogenesis, perfectly timed to promote the normal circuitry underlying normal neurological function. Individuals with FXS syndrome suffer a diverse range of cognitive impairments. Most research has focused on the effects of a lack of FMRP in neurons, and its implications for the underlying neurobiology of FXS. Knowing that astrocytes contribute to the abnormal neurobiology of the disease, the current results should promote new therapeutic avenues in the treatment of FXS and related autistic disorders.

5.2.6 Acknowledgments

This work was supported by the Natural Sciences and Engineering Research Council of Canada (NSERC) and the Fragile X Research Foundation of Canada.

5.2.7 References

Allen NJ, Barres BA. 2009. Neuroscience: Glia - more than just brain glue. Nature 457(7230):675-7.

Bakker C, Verheij C, Willemsen R, van der Helm R, Oerlemans F, Vermey M, Bygrave A, Hoogeveen A, Oostra B, Reyniers E and others. 1994. Fmr1 knockout mice: a model to study fragile X mental retardation. The Dutch-Belgian Fragile X Consortium. Cell 78(1):23-33.

Ballas N, Lioy DT, Grunseich C, Mandel G. 2009. Non-cell autonomous influence of MeCP2-deficient glia on neuronal dendritic morphology. Nat Neurosci 12(3):311-7.

Banker GA. 1980. Trophic interactions between astroglial cells and hippocampal neurons in culture. Science 209(4458):809-10.

Barres BA. 2008. The mystery and magic of glia: a perspective on their roles in health and disease. Neuron 60(3):430-40.

Beckel-Mitchener A, Greenough WT. 2004. Correlates across the structural, functional, and molecular phenotypes of fragile X syndrome. Ment Retard Dev Disabil Res Rev 10(1):53-9.

Chen L, Toth M. 2001. Fragile X mice develop sensory hyperreactivity to auditory stimuli. Neuroscience 103(4):1043-50.

Christopherson KS, Ullian EM, Stokes CC, Mullowney CE, Hell JW, Agah A, Lawler J, Mosher DF, Bornstein P, Barres BA. 2005. Thrombospondins are astrocyte-secreted proteins that promote CNS synaptogenesis. Cell 120(3):421-33.

Cline HT. 2001. Dendritic arbor development and synaptogenesis. Curr Opin Neurobiol 11(1):118-26.

Comery TA, Harris JB, Willems PJ, Oostra BA, Irwin SA, Weiler IJ, Greenough WT. 1997. Abnormal dendritic spines in fragile X knockout mice: maturation and pruning deficits. Proc Natl Acad Sci U S A 94(10):5401-4.

El-Husseini AE, Schnell E, Chetkovich DM, Nicoll RA, Bredt DS. 2000. PSD-95 involvement in maturation of excitatory synapses. Science 290(5495):1364-8.

Gao FB. 2007. Molecular and cellular mechanisms of dendritic morphogenesis. Curr Opin Neurobiol 17(5):525-32.

Greengard P, Valtorta F, Czernik AJ, Benfenati F. 1993. Synaptic vesicle phosphoproteins and regulation of synaptic function. Science 259(5096):780-5.

Hagerman PJ. 2008. The fragile X prevalence paradox. J Med Genet 45(8):498-9.

Irwin SA, Galvez R, Greenough WT. 2000. Dendritic spine structural anomalies in fragile-X mental retardation syndrome. Cereb Cortex 10(10):1038-44.

Irwin SA, Patel B, Idupulapati M, Harris JB, Crisostomo RA, Larsen BP, Kooy F, Willems PJ, Cras P, Kozlowski PB and others. 2001. Abnormal dendritic spine characteristics in the temporal and visual cortices of patients with fragile-X syndrome: a quantitative examination. Am J Med Genet 98(2):161-7.

Jacobs S, Doering LC. 2009. Primary Dissociated Astrocyte and Neuron Co-Culture. In: Doering LC, editor. Protocos for Neural Cell Culture. New York: Humana Press. p 269-284.

Kaufmann WE, Moser HW. 2000. Dendritic anomalies in disorders associated with mental retardation. Cereb Cortex 10(10):981-91.

Kremer EJ, Pritchard M, Lynch M, Yu S, Holman K, Baker E, Warren ST, Schlessinger D, Sutherland GR, Richards RI. 1991. Mapping of DNA instability at the fragile X to a trinucleotide repeat sequence p(CCG)n. Science 252(5013):1711-4.

Lee A, Li W, Xu K, Bogert BA, Su K, Gao FB. 2003. Control of dendritic development by the Drosophila fragile X-related gene involves the small GTPase Rac1. Development 130(22):5543-52.

Maezawa I, Swanberg S, Harvey D, LaSalle JM, Jin LW. 2009. Rett syndrome astrocytes are abnormal and spread MeCP2 deficiency through gap junctions. J Neurosci 29(16):5051-61.

Narro ML, Yang F, Kraft R, Wenk C, Efrat A, Restifo LL. 2007. NeuronMetrics: software for semi-automated processing of cultured neuron images. Brain Res 1138:57-75.

Nimchinsky EA, Oberlander AM, Svoboda K. 2001. Abnormal development of dendritic spines in FMR1 knock-out mice. J Neurosci 21(14):5139-46.

Pacey LK, Doering LC. 2007. Developmental expression of FMRP in the astrocyte lineage: implications for fragile X syndrome. Glia 55(15):1601-9.

Pfrieger FW, Barres BA. 1997. Synaptic efficacy enhanced by glial cells in vitro. Science 277(5332):1684-7.

Powell EM, Geller HM. 1999. Dissection of astrocyte-mediated cues in neuronal

guidance and process extension. Glia 26(1):73-83.

Powell EM, Meiners S, DiProspero NA, Geller HM. 1997. Mechanisms of astrocyte-directed neurite guidance. Cell Tissue Res 290(2):385-93.

Puro DG, De Mello FG, Nirenberg M. 1977. Synapse turnover: the formation and termination of transient synapses. Proc Natl Acad Sci U S A 74(11):4977-81.

Qin M, Kang J, Smith CB. 2002. Increased rates of cerebral glucose metabolism in a mouse model of fragile X mental retardation. Proc Natl Acad Sci U S A 99(24):15758-63.

Riederer B, Matus A. 1985. Differential expression of distinct microtubule-associated proteins during brain development. Proc Natl Acad Sci U S A 82(17):6006-9.

Ullian EM, Sapperstein SK, Christopherson KS, Barres BA. 2001. Control of synapse number by glia. Science 291(5504):657-61.

Figure 5.1: A selection of representative images of neurons overlaid with skeletons as generated by Neuronmetrics™.

The parameters measured in these experiments are indicated on the left of the images: number of dendritic branches (green), longest dendrite (pink), area of dendritic arbor (bounded by yellow), and cell body area (blue).

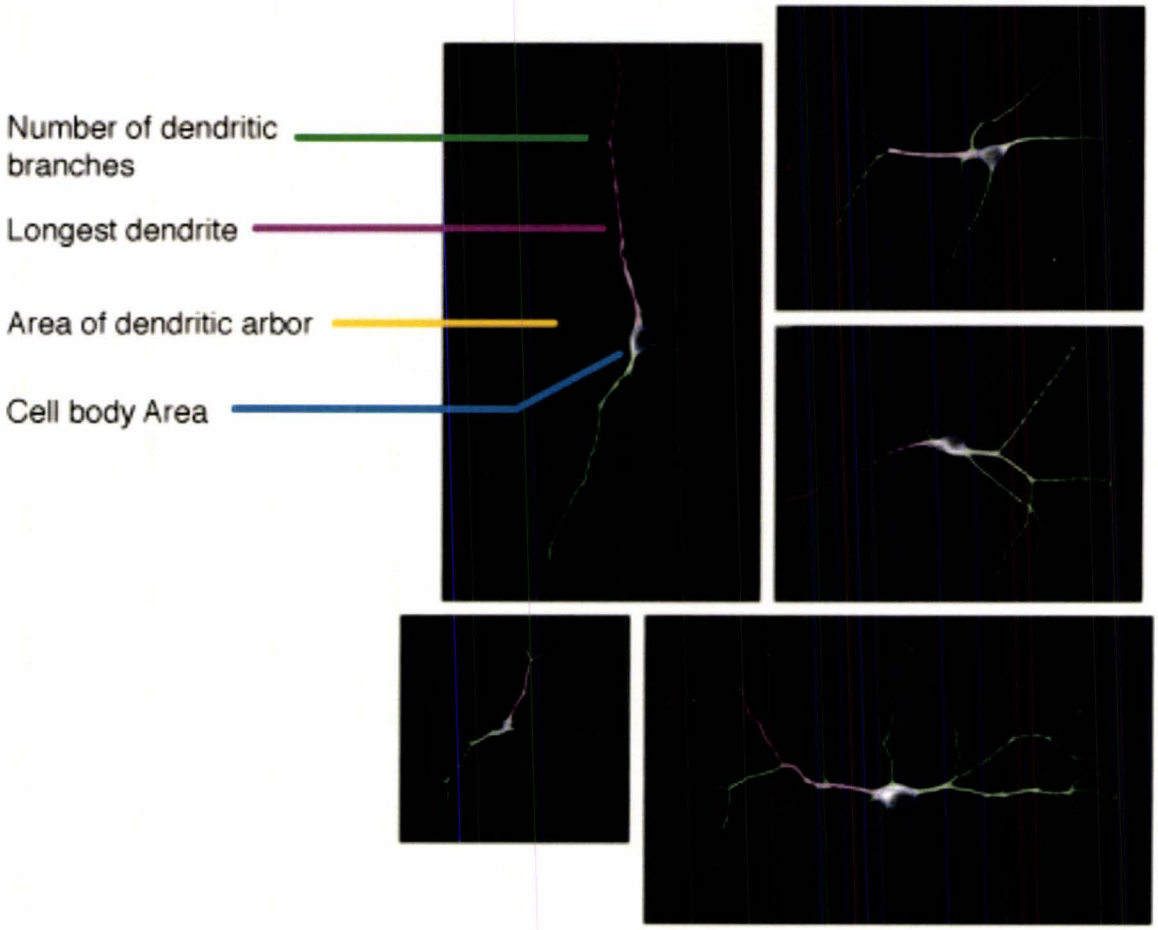
Number of dendritic branches
Longest dendrite
Area of dendritic arbor
Cell body Area

Figure 5.1

Figure 5.2: Neuronmetrics™-generated digitized skeletons

A selection of digitized skeletons, generated by Neuronmetrics™, used to generate the measurements of the dendritic arbors.

Figure 5.2

Figure 5.3: Hippocampal neurons in co-culture.

WT primary embryonic hippocampal neurons (MAP2, green) on top of a monolayer of WT primary cortical astrocytes (GFAP, red). Nuclei are stained with DAPI (blue). Scale bar represents 100μm. Inset is an example of an isolated neuron that would be selected for morphometric analysis.

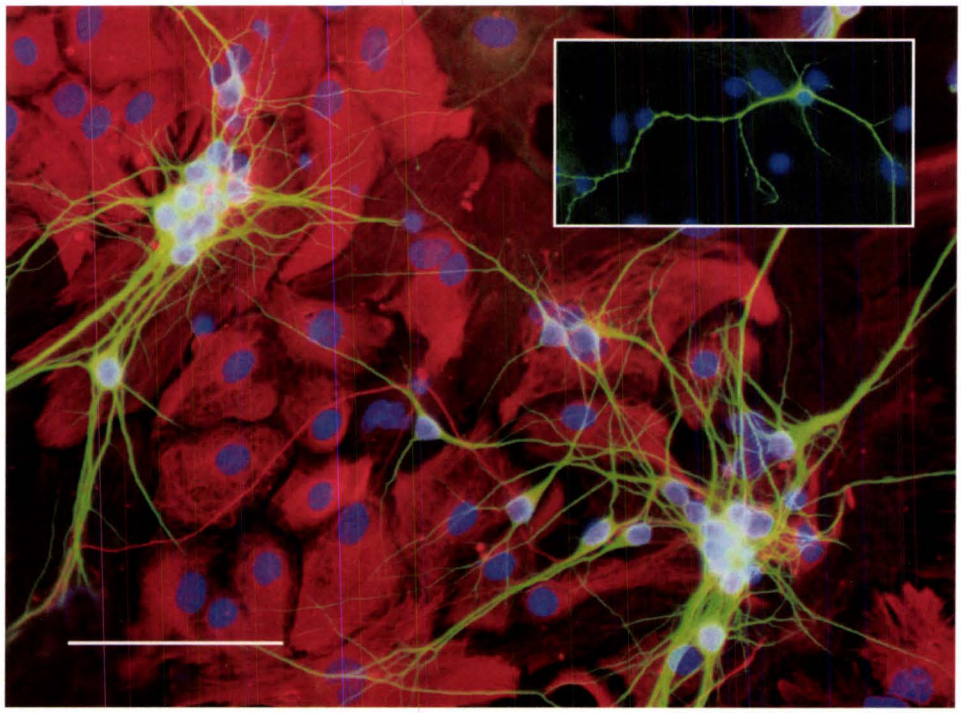

Figure 5.3

Figure 5.4: Analysis of the morphological measurements generated by Neuronmetrics™.

a, number of dendritic branches per cell; **b**, length of the longest dendrite; **c**, cell body are; **d**, area of dendritic arbor. In each graph the number of days *in vitro* (*DIV*) is represented along the x-axis. Data from neurons grown on WT astrocytes are represented by the solid bars, and from neurons grown on *Fmr1* KO astrocytes are represented by the white bars. Data are presented as mean ± s.e.m. of 150 neurons from three independent experiments. *, significantly different at $P<0.05$; ***, significantly different at $P<0.001$; Mann Whitney U Tests (two-tailed).

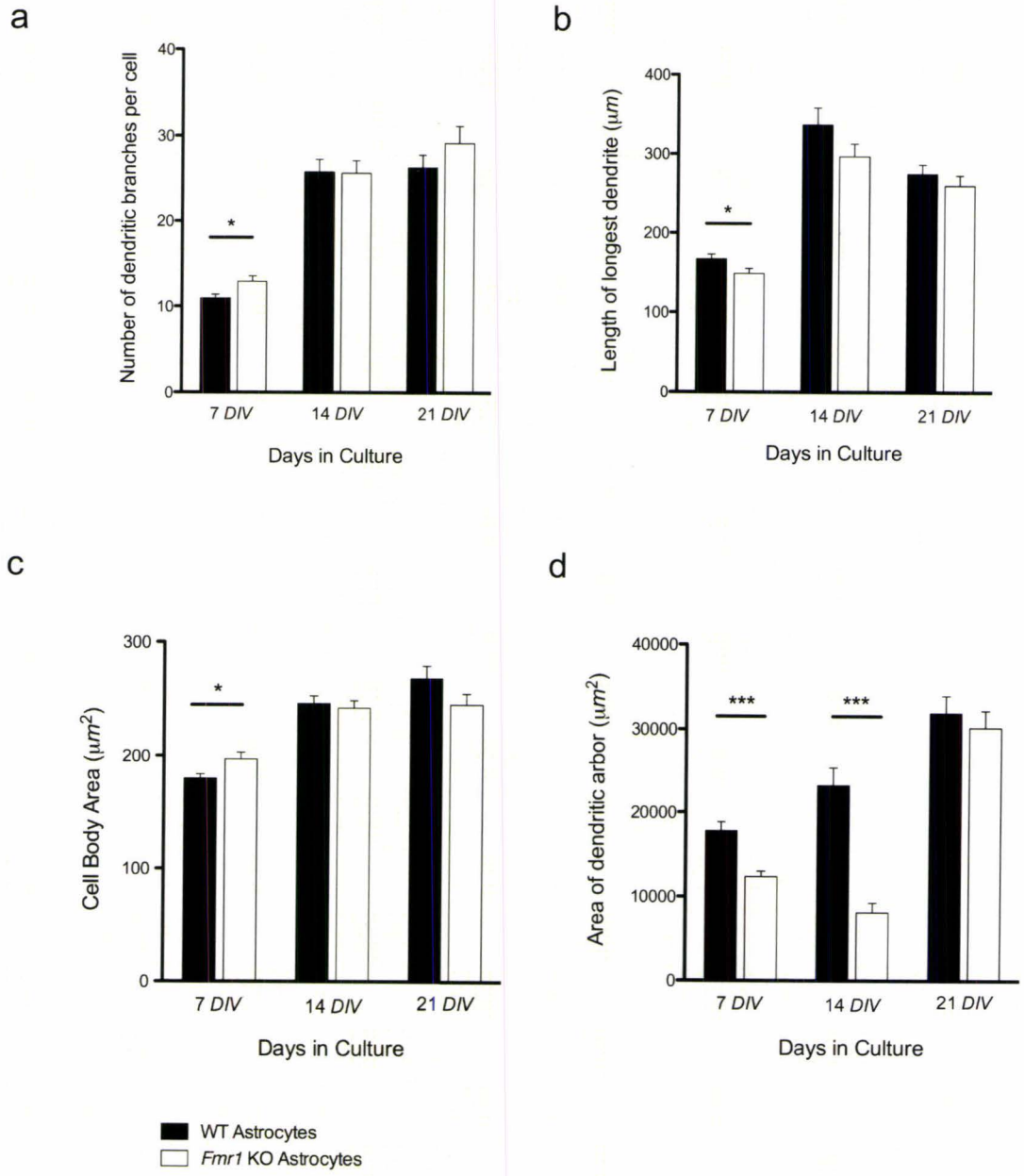
a
Number of dendritic branches per cell
40
30
20
10
0
*
7 DIV
14 DIV
21 DIV
Days in Culture
b
Length of longest dendrite (μm)
400
300
200
100
0
*
7 DIV
14 DIV
21 DIV
Days in Culture
c
Cell Body Area (μm²)
300
200
100
0
*
7 DIV
14 DIV
21 DIV
Days in Culture
d
Area of dendritic arbor (μm²)
40000
30000
20000
10000
0
***
***
7 DIV
14 DIV
21 DIV
Days in Culture
WT Astrocytes
Fmr1 KO Astrocytes

Figure 5.4

Figure 5.5: Excitatory synaptic protein expression in hippocampal neurons in co-culture. Hippocampal neurons are stained with antibodies to the pre-synaptic protein, synapsin (green) and the excitatory post-synaptic protein, PSD-95 (red). Nuclei are stained with DAPI (blue). Scale bar represents 100μm. Inset is an example of a 50μm segment that would be used for excitatory synapse quantification.

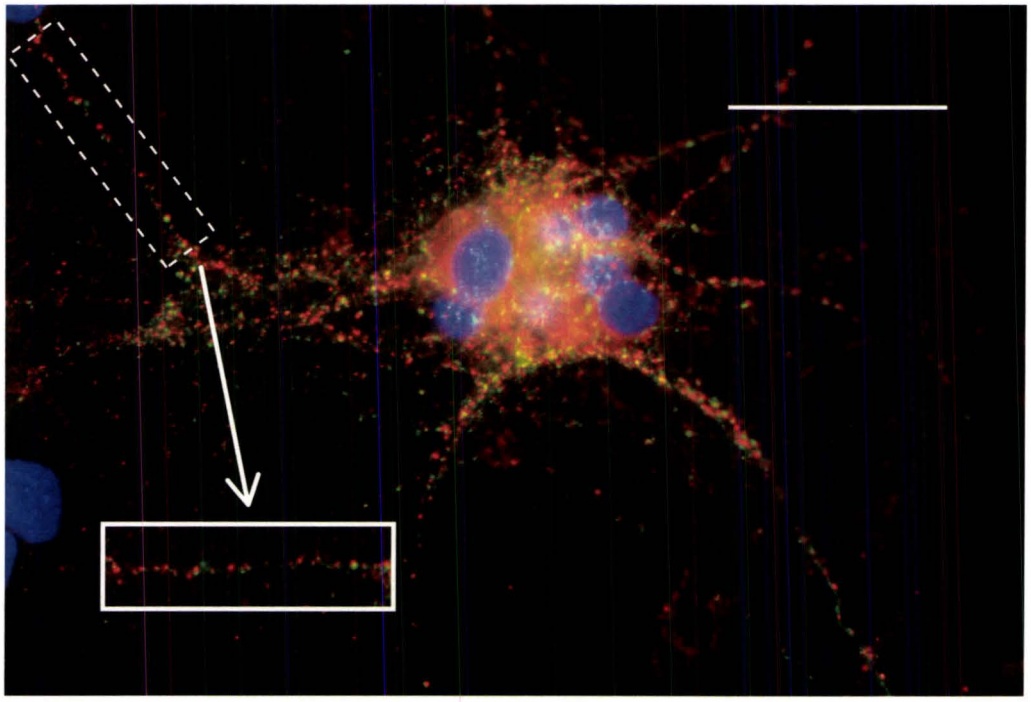

Figure 5.5

Figure 5.6: Excitatory synaptic protein expression

a. Excitatory synaptic protein expression in segments of dendrites from neurons grown for 7, 14 or 21 *DIV* on either WT astrocytes (left panel) and on *Fmr1* KO astrocytes (right panel). Each set of three images represents the same 50μm segment visualized with immunofluorescence directed at pre- and post-synaptic proteins (top), pre-synaptic synapsin (green, middle), and post-synaptic PSD-95 (red, bottom). Closed arrow-heads indicate those instances of co-localization where the pre- and post-synaptic puncta were located in the same space; open arrow-heads indicate those incidences of co=localization where the pre- and post-synaptic puncta were located immediately adjacent to one another. **b.** From similar 50μm segments, the number of synapses (i.e., instances of co-localized puncta as defined above) per 50 μm were quantified. The number of days in culture (*DIV*) are indicated along the x-axis. The solid bars are data from neurons grown on WT astrocytes. The white bars are data from neurons grown on *Fmr1* KO astrocytes. Data are presented as mean ± s.e.m., from 300 segments from three independent experiments. ***, significant at $P<0.001$, Mann Whitney U tests (two-tailed).

a

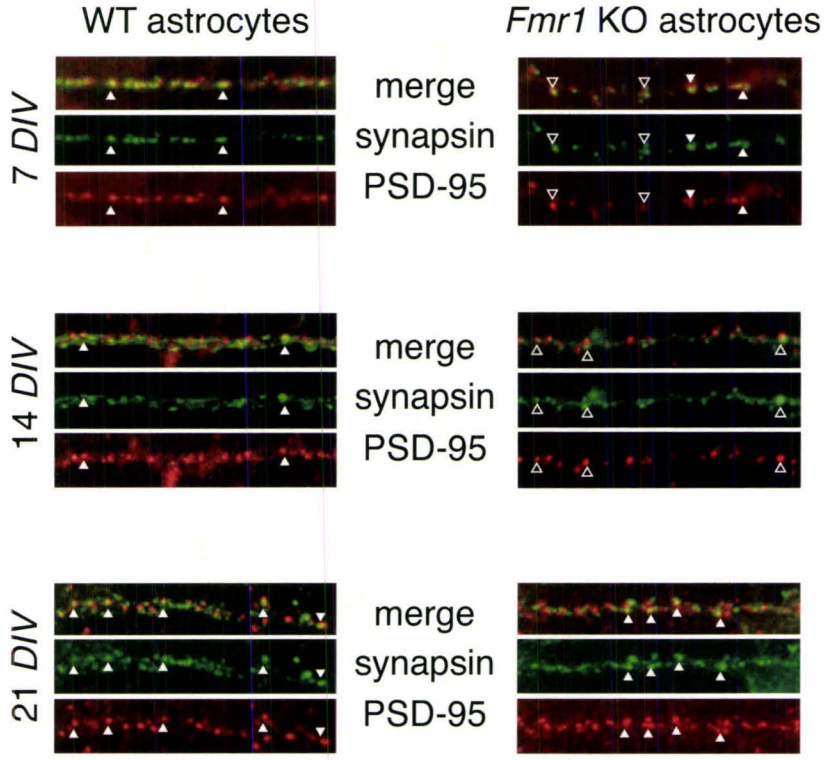
WT astrocytes
Fmr1 KO astrocytes
7 DIV
14 DIV
21 DIV
merge
synapsin
PSD-95

b

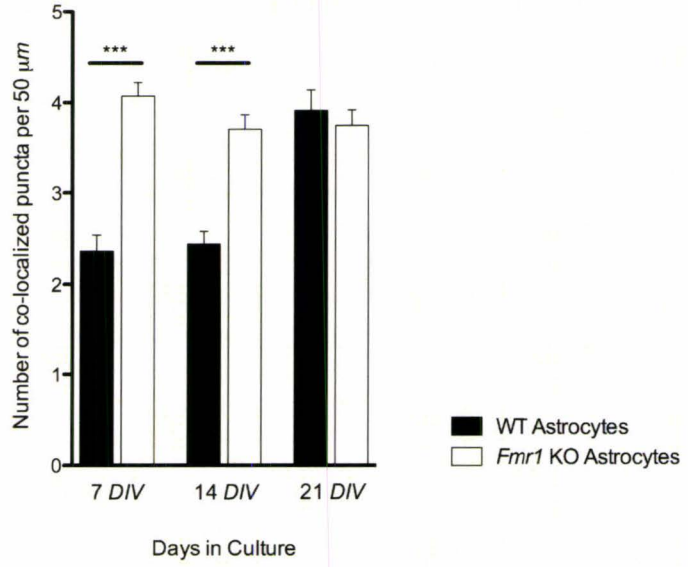
Number of co-localized puncta per 50 µm
***
***
0
1
2
3
4
5
7 DIV
14 DIV
21 DIV
Days in Culture
WT Astrocytes
Fmr1 KO Astrocytes

Figure 5.6

CHAPTER 6:

PRIMARY MOUSE HIPPOCAMPAL NEURONS DEVELOP ABNORMAL DENDRITIC ARBORS IN THE PRESENCE OF FRAGILE X ASTROCYTES

6. Chapter 6

6.1 Preface to Chapter 6

This chapter is comprised of an author-generated version of an article prepared for submission to the Journal of Comparative Neurology, and as presented it is the pre-review version. The manuscript was submitted to the Journal of Comparative Neurology on October 16th, 2009; Submission # JCN-09-0469.

As a submitted manuscript the author generated version is reproduced with implicit permission understood from the Wiley-Blackwell Copyright Transfer Agreement:

" Submitted Version. Wiley-Blackwell licenses back the following rights to the Contributor in the version of the Contribution as originally submitted for publication:

...

b. The right to transmit, print and share copies with colleagues."

6.1.1 Author contributions

For this paper, I designed and performed all of the experiments, photographed the images, performed the analyses, carried out the statistical analyses, wrote the manuscript and prepared all figures. Dr. Doering provided guidance in the designing of the experiments and the editing of the manuscript.

6.1.2 Background and rationale

In our previous paper (Chapter 5), we found that the effect of Fragile X astrocytes on the dendrite morphology of wild type (WT) hippocampal neurons appears to be a result of a developmental delay. At 7 *DIV* the WT neurons grown on *FMR1* null astrocytes exhibited significant alterations in their dendrite morphology compared to neurons grown on WT astrocytes; neurons on *FMR1* null astrocytes exhibited significant increases in branching, and significant deceases in the extension of the dendritic arbors and in the area of the neuron cell bodies. By 21 *DIV*, the WT neurons grown on *FMR1*

null astrocytes no longer displayed significant differences in their dendritic morphology, compared to WT neurons grown on WT astrocytes.

The previous findings indicated that there was an increase in branching, but did not specify the nature of the alterations in dendrite ramification: was the increase in branching uniform along the extent of the arbor or was it localized to specific regions. In this paper we sought to perform a more in depth morphological analysis of the alterations in the dendritic branching patterns of the neurons. Here, we used the traditional methods of linear and semi-log Sholl analyses to evaluate the differences in the dendritic arbor ramification patterns of WT neurons grown on *FMR1* null astrocytes compared to WT neurons grown on WT astrocytes, at each of the time points used previously (i.e., 7, 14 and 21 *DIV*). In this manner we were able to obtain more detailed information regarding how the dendritic arbors of the WT neurons were affected by the Fragile X astrocytes. Furthermore, the measures obtained through Sholl analysis are constant for neurons from specific subpopulations. For example, the value for the Sholl's regression coefficient is unique for neurons with pyramidal morphologies versus neurons with stellate morphologies (Sholl, 1953). The dendritic arbor morphology of a neuron determines its properties as an integrative unit in neural circuitry (Hume & Purves, 1981; Purves, et al., 1986; Purves & Hume, 1981). Additionally, dendritic arbor morphology can be used to identify subpopulations of neurons with varying signaling properties. For example, hippocampal excitatory neurons are typically pyramidal or stellate in appearance, whereas the inhibitory neurons of the hippocampus have multiple morphologies including bipolar and multipolar neurons and do not resemble pyramidal or stellate neurons (Banker & Cowan, 1979; Kriegstein & Dichter, 1983; Spruston & McBain, 2007). In our culture preparation we were able to identify a variety of neuronal subtypes based on the morphologies of their dendritic arbors, as described elsewhere (Kriegstein & Dichter, 1983). We therefore decided to divide our neuron population into five subtypes, and evaluated the effects of the Fragile X astrocytes on each subtype independently. By doing this, we were able to obtain information regarding specific subtypes of neurons that are targeted by the developmental delay induced by the *FMR1* null astrocytes, and gain

important insight into the nature of the abnormalities in neural circuitry underlying the clinical features of FXS.

6.1.3 Specific aims

- To show that the Fragile X astrocytes impart a developmental delay on the maturation of dendritic arbors *in vitro* (5).

6.1.3.1 Specific aim not previously identified

- To investigate whether the developmental delay imparted by the Fragile X astrocytes affects all neuronal subtypes equally

6.2 Primary mouse hippocampal neurons develop abnormal dendritic arbors in the presence of Fragile X astrocytes

AUTHORS: Shelley Jacobs[1] and Laurie C. Doering[1]

Department of Pathology & Molecular Medicine, McMaster University, Hamilton, ON L8N 3Z5, Canada.

RUNNING HEAD: Astrocytes and dendrites

ASSOCIATE EDITOR: Oswald Stewart

KEY WORDS: Co-culture, FMRP, Fragile X, Sholl analysis, astrocyte, neuron, dendrite

CORRESPONDING AUTHOR: Address: McMaster University, HSC1R1
Pathology and Molecular Medicine
1200 Main Street West
Hamilton, Ontario L8N 3Z5

Phone: 905-525-9140

Fax: 905-525-7400

Email: doering@mcmaster.ca

This work was supported by the Natural Sciences and Engineering Research Council of Canada (NSERC) and the Fragile X Research Foundation of Canada.

6.2.1 Abstract

Astrocytes are now recognized as key players in the neurobiology of neurodevelopmental disorders such as Fragile X Syndrome. However, the nature of Fragile X astrocyte – mediated control of dendritic arbor development in subtypes of hippocampal neurons is not yet known. In these experiments we used a co-culture procedure in which normal primary hippocampal neurons were cultured together with astrocytes from either a wild type or Fragile X mouse, for either 7, 14 or 21 days. The neurons were processed for immunocytochemistry using an antibody against the dendritic marker MAP2, classified based on morphological criteria into one of five groups, and subjected to Sholl analyses. Both linear and semi-log methods of Sholl analyses were applied to the neurons in order to provide an in depth analysis of the dendritic arborizations. We found that Fragile X astrocytes affect the development of dendritic arborization of all subtypes of hippocampal neurons. Furthermore, we show that hippocampal neurons with spiny stellate neuron morphology exhibit the most pervasive developmental delays, with significant dendritic arbor alterations persisting at 21 days in culture. The results presented here are the first to provide a detailed examination of the manner through which cell-type specific astrocyte-mediated signaling plays a role in the development of Fragile X Syndrome, and provide important insight into potential targets for novel therapeutic strategies.

6.2.2 Introduction

Fragile X Syndrome (FXS) is the most common inherited cause of mental retardation affecting approximately 1/2500 individuals (Hagerman, 2008). Individuals with FXS are characterized by a set of physical features including: an elongated and narrow face, protruding jaw, hyperextensible joints and macroorchidism (O'Donnell and Warren, 2002). Children with FXS also suffer a number of neurological symptoms including attention deficit, hyperactivity, susceptibility to seizures and varying degrees of cognitive impairment (Beckel-Mitchener and Greenough, 2004). The symptoms of FXS result from a mutation in the Fragile X Mental Retardation (*FMR1*) gene, that causes gene silencing and a lack of the protein product, the Fragile X Mental Retardation Protein (FMRP)(Kremer et al., 1991).

Analysis of the brains of individuals with FXS reveals abnormalities in neuron development (Irwin et al., 2001). Appropriate neuron growth and neural network formation is essential for the effective cell-cell signaling required in a fully mature brain. The dendritic arbors of neurons are specialized to receive and process information in neurons, and as such their proper growth and arborization is crucial for the proper functioning of the nervous system. Due to the space constraints in the brain, the wiring of the neural circuits is optimized in part through the shape of the dendritic arborizations. This optimization is dependent upon precise regulation of dendritic shape and contacts. Therefore, their precise morphologies are indicative of neural connectivity and normal flow of information through neural circuits. Since dendrites are the sites of most synaptic contacts, the shape of the dendritic arbors determines the number and pattern of synapses received by each neuron (Hume and Purves, 1981; Purves and Hume, 1981; Purves et al., 1986). In fact, each type of neuron in the nervous system exhibits its own specific dendritic arbor pattern, and these patterns are maintained in culture (Banker and Cowan, 1979; Threadgill et al., 1997), with unique membrane properties, that determine the computational capability of each cell (Stuart et al., 2008). Given this important functional role of dendrites, the consequence of abnormal arborization is often severe, and is often

found in many CNS disorders associated with mental retardation (Dierssen and Ramakers, 2006; Kaufmann and Moser, 2000; Purpura, 1975).

Until now, the majority of the research on the neurobiology of FXS has focused on the effect of a lack of FMRP in the neuronal population. Recently however, our lab discovered that FMRP was also expressed in cells of the glial lineage (Pacey and Doering, 2007). Astrocytes are recognized as important regulators of neuron growth and maturation, and are documented as key players in the abnormal neurobiology of a number of developmental disorders in addition to FXS (Ballas et al., 2009; Barres, 2008). Under normal conditions, astrocytes are known to provide signals that guide synapse formation and neurite development (Banker, 1980; Barres, 2008; Powell and Geller, 1999). In fact, astrocyte-derived cues help ensure appropriate dendritic arborizations (Yamamoto et al., 2006).

Recently, we provided evidence that establishes astrocytes as key players in the development of abnormal neuron morphology in FXS (Jacobs and Doering, submitted). Given the importance of appropriate dendritic arbor development for normal neural circuitry and cognitive function, we sought to further clarify the nature of the dendrite morphology that is altered by the astrocytes in Fragile X. Here, we used Sholl analysis to determine more precisely if, and how the astrocytes in Fragile X affect the branching pattern of the dendritic arbors of hippocampal neurons in culture. Furthermore, by classifying the morphology of the hippocampal neurons, we were able to analyze if the dendritic arborization of certain subtypes of neurons were preferentially affected.

6.2.3 Methods

Animals

The FMRP mouse colony was established from breeding pairs of B6.129.FMR1.FvBN mice originally obtained from Dr. Carl Dobkin at the New York State Institute for Basic Research in Developmental Disabilities. The WT and KO B6.129.FMR1.FvBN mice were maintained as individual strains, and are genotyped regularly. Both male and female mice were used in the experiments. The *Fmr1* knockout (KO, FvBN.129.B6-*Fmr1*) and wild-type (WT) mice used for these experiments were housed and bred at the McMaster University Central Animal Facility. All experiments complied with the guidelines set out by the Canadian Council on Animal Care and were approved by the McMaster Animal Research Ethics Board.

Cell Culture

Primary hippocampal neurons and astrocytes were grown in co-culture conditions as detailed previously by our lab (Jacobs and Doering, 2009b). Briefly, cortical astrocytes were isolated from post-natal day (PND) 0-1 pups and grown on Poly-L-Lysine (1mg/ml, SIGMA Cat. No. P1399) and Laminin (0.1mg/ml, Invitrogen Cat. No. 23017-015) coated coverslips in MEM (Invitrogen, Cat No. 11095-080) supplemented with 6% glucose and 10% horse serum (Invitrogen, Cat No. 16050-122), for one week. Primary hippocampal neurons were then isolated from embryonic day 17 (E17; day of sperm plug counted as E1) animals and seeded above the astrocytes and maintained in MEM supplemented with N2 (Invitrogen, Cat No. 17502-048), sodium pyruvate (Invitrogen, Cat No. 11360-070) and 6% glucose, for the duration of the experiments. Hippocampal neurons isolated from the WT animals were grown with astrocytes from either WT or *Fmr1* KO mice, and grown for 7, 14 or 21 days. A total of three independent cultures per condition (genotype+days *in vitro* (*DIV*)) were completed.

Immunocytochemistry

Following the removal of the media, the cells were fixed with ice-cold (-20˚C) acetone for 20 minutes. The cells were then washed three times with PBS and treated with 0.1% Triton X-100 for five minutes at room temperature. Non-specific binding was blocked with 1% bovine serum albumin (BSA) for 30 minutes. Chicken MAP2 primary antibody (1:20 000, Neuromics), diluted in 1% BSA, was applied to the cells and incubated overnight at 4˚C. On the second day, after washing three times with PBS, an anti-chicken FITC (1:100, Jackson) secondary antibody was applied to the cells and incubated for 3 hours at room temperature. Following a final set of washes with PBS (twice) and distilled water (twice), the coverslips were mounted onto slides with Vectashield fluorescent mounting medium containing DAPI to stain the nuclei. Controls for the immunocytochemistry were performed with the inclusion of only the primary or secondary antibody.

Image acquisition

Images were acquired using a Zeiss Axioskop-2 epi-fluorescence microscope and AxioVision image acquisition software. At each time point (7 *DIV*, 14 *DIV*, 21 *DIV*), for each independent culture (three on *Fmr1* KO astrocytes, and three on WT astrocytes), 50 isolated neurons were selected at random for analysis.

Neuron Classification

Neurons were classified according to the shape of their cell body and dendritic arbor into one of five groups: bipolar, bitufted, multipolar, stellate and pyramidal (Fig. 6.1), using a modified classification scheme based on one previously defined by Kriegstein and Dichter (1983). Bipolar and bitufted neurons were identified as neurons having a fusiform cell body with dendrites extending from opposing ends. Bitufted neurons had an increased number of branches projecting from each end of the cell body, with a high degree of branching occurring in close proximity to the cell body. Neurons classed as

bipolar had a lesser degree of branching immediately adjacent to the cell body with some branching occurring at increasing distances. Neurons classified as having a multipolar dendritic arbor were characterized by a round or square soma and had more than two primary dendrites (and generally more than three) with multiple branches that increased with distance from the cell body. Neurons classified as multipolar included those neurons that had only three primary dendrites and could not be classified as pyramidal due to the shape of the cell body. These neurons did not comprise a large proportion of the cells classified as multipolar. Those neurons classified as stellate, also had a round cell body and greater than three primary dendrites; however, their dendritic arbors exhibited a high degree of branching along their length. Lastly, those neurons classified as having a pyramidal dendritic arbor had a roughly triangular cell body and three primary dendrites that branched modestly in close proximity to the soma, with increased degrees of branching with increasing distance. In the majority of the cells that were classified as pyramidal, the dendritic arbors formed three clearly distinct regions with two primary dendrites exiting on one side of the soma, and the third exiting on the opposite. At 7 *DIV*, one neuron of the 50 in each condition could not be classified under any of the above types because it had only one dendritic process. These two neurons were excluded from further analysis. There was no difference in the proportion of cell types between the cultures grown on *Fmr1* KO astrocytes when compared to those grown on WT astrocytes (data not shown). The resulting numbers of cells per class in each condition are shown in Table 6.1.

Sholl Analysis

The Sholl analysis is a method of determining the nature of the neuronal dendritic arbor branching (Sholl, 1953). In this analysis, the image of the neuron's dendritic arbor is first simplified into a digital skeleton. Then, a series of equidistant concentric circles, centered on the perikaryon, are overlaid on the image of the skeleton (Sholl, 1953). In this way, the number of dendritic crossings per circle is quantified. This data can then be analyzed by either a linear or a log approach, as described below.

In this study, the Sholl analysis was performed using a plug-in for Image J (http://rsbweb.nih.gov/ij/) obtained from the Ghosh Lab web site (http://www-biology.ucsd.edu/labs/ghosh/software/). Digitized skeletons of each neuron were generated using Neuronmetrics™ (http://www.ibridgenetwork.org/arizona/UA07-56-Neuronmetrics) (Narro et al., 2007), a plug-in for Image J. Neuron skeletons were smoothed (using the smooth function in Image J) and the Sholl analysis (Sholl, 1953) was performed with equidistant concentric circles, in steps of 10μm ranging from 10-300μm from the neuron soma (Fig. 6.2).

Linear Sholl Analysis

In the linear Sholl analysis the frequency data (number of intersections/circle) was plotted as a function of the distance from the cell body (i.e., radius of the circle). The data from 50 neurons per neuron type was averaged and presented in the linear Sholl analysis plots. From this, the pattern of dendrite branch density, from the soma to the extremes, was obtained for each neuron type, in each condition, at each of the three time points. Thereby, three morphometric parameters were attained for each neuron subtype (in each condition, at each time point): the critical value (the radius at which maximal numbers of intersections occurs), the dendritic max (the number of intersections at the critical value) and the Schoenen's ramification index (dendritic max/number of primary dendrites) (Schoenen, 1982).

Semi-log Sholl Analysis

Semi-log Sholl analysis, as it's name suggests, involves taking the log of 'the number of intersections per circle area' and plotting it as a function of the distance from the soma (Sholl, 1953). In this study, the 'number of intersections per circle area' was calculated for each neuron. The log value was calculated, and then the values of the 50 neurons were averaged and plotted on the semi-log Sholl analysis plots. A straight line was then fit to the data using linear regression analysis. From this line, the rate of decrease of the

branch density as a function of the distance from the cell body can be obtained from the slope. Multiplying the slope (m) by negative one yields the Sholl regression coefficient, k. In this study the Sholl regression coefficient was determined for each neuron subtype, in each condition at each of the three time points. The Sholl regression coefficient accurately predicts the type of a given neuron based on the branching pattern as revealed by the Sholl analysis (Sholl, 1953), and therefore is a useful parameter for determining if two cell populations of the same type have different dendritic arborizations.

Statistical Analyses

For all analyses the observer was blind to the experimental condition. Statistics were performed using SPSS version 17, with an alpha level set to 0.05. All data are presented as the mean ± s.e.m. Analyses were performed for each neuron class independently, with a focus on the differences observed between the genotypes (*Fmr1* KO and WT) at each time point (7 *DIV*, 14 *DIV*, 21 *DIV*) and within a genotype over time. Linear Sholl analysis data had significantly different variances (as determined by Levene's test for equal variances), and deviated significantly from a normal distribution (as determined by the Shapiro-Wilk test for normality, and therefore Mann-Whitney U (two-tailed) tests were used. Semi-log Sholl data was analyzed with linear regression.

6.2.4 Results

Bipolar Neurons:

Linear Sholl analysis revealed that *Fmr1* KO astrocytes induced alterations in the dendritic arbors of bipolar neurons. At 7 *DIV*, the arbors of bipolar neurons grown on *Fmr1* KO astrocytes extended to a lesser distance than bipolar neurons on WT astrocytes (280μm vs. 300μm, respectively)(Fig. 6.3a and Table 6.2). The radius at which the bipolar neurons reached maximal branching density was closer to the cell body in those neurons grown on *Fmr1* KO astrocytes (20μm), compared to those grown on WT astrocytes (40μm)(Fig. 6.3a and Table 6.2). This difference was no longer apparent by 14 *DIV* (Fig. 6.3 and Table 6.2). Additionally, bipolar neurons grown on *Fmr1* KO

astrocytes consistently had a similar or lesser degree of branching at all distances from the cell body (Fig. 6.3a-c). At 7 *DIV* bipolar neurons grown on *Fmr1* KO astrocytes exhibited a significantly decreased ($p<0.05$) degree of branching at 160μm, 170μm and 190μm, compared to bipolar neurons grown on WT astrocytes (Fig. 6.3a). Closer to the cell body, the difference was not significant which is similarly indicated by only a 0.01 difference in the Schoenen's coefficient at 7 *DIV* (Table 6.2). However, an overall relative decrease in branching became more pronounced by 21 *DIV*, specifically for the region of the arbor closer to the cell body (Fig. 6.3c). A decrease of 0.22 in the Schoenen's coefficient at 21 *DIV* reflects this difference, as does a 10.9% decrease in the dendritic max (Table 6.3).

Semi-log Sholl analysis with linear regression yielded a Sholl's regression coefficient of 0.013±0.000 (R^2=0.84) for bipolar neurons grown for 7 *DIV* on *Fmr1* KO astrocytes, which was significantly different ($p<0.01$) than the Sholl's regression coefficient of 0.012±0.000 (R^2=0.83) for bipolar neurons grown for 7 *DIV* on WT astrocytes (Fig. 6.4a and Table 6.3). At 14 *DIV* and 21 *DIV* linear regression revealed that there was no difference in the Sholl's coefficient between bipolar neurons grown on *Fmr1* KO or WT astrocytes (Fig. 6.4b,c and Table 6.3).

It therefore appears, that by both linear and semi-log Sholl analysis, that there is a significant difference in the dendritic branching patterns of bipolar neurons when grown on *Fmr1* KO astrocytes compared to WT astrocytes at 7 *DIV* and that this difference is minimized by 14 *DIV* and 21 *DIV*.

Bitufted Neurons:

At 7 *DIV*, bitufted neurons grown on *Fmr1* KO astrocytes exhibited a decreased extension of their dendritic arbors, on average reaching only 240μm, compared to those grown on WT astrocytes reaching 270μm (Fig. 6.5a and Table 6.4). This difference was absent at 14 *DIV* (Fig. 6.5b and Table 6.4). However, at 21 *DIV*, bitufted neurons grown

on *Fmr1* KO astrocytes, once again exhibited a decrease in the extent of their dendritic arbors (200μm vs. 300μm) (Fig. 6.5c and Table 6.4). By a linear Sholl analysis, bitufted neurons exhibited a significantly ($p<0.05$, Fig. 6.5a) decreased degree of branching at distances greater than 180μm when grown on *Fmr1* KO astrocytes compared to those grown on WT astrocytes, at 7 *DIV*. However, at distances closer to the soma there was no significant difference in the degree of branching, which is matched by a lack of a major difference in the Schoenen's ramification indices at 7 *DIV* (0.07, Table 6.4). The difference in ramification of the more distant dendrites was no longer significant at 14 *DIV* or 21 *DIV* (Fig. 6.5b,c). Although, at 21 *DIV* bitufted neurons grown on *Fmr1* KO did not have dendrites extending beyond 210μm, whereas a proportion of bitufted neurons grown on WT astrocytes had dendritic arbors that extended to 300μm. An interesting finding was that, at 14 *DIV* bitufted neurons grown on *Fmr1* KO astrocytes exhibited an increase in branching at distances of less than 90μm and greater than 150μm, although these differences were not significant (Fig. 6.5b). Once again, this difference is reflected in an increase of 1.07 for the Schoenen's ramification index for neurons grown on *Fmr1* KO astrocytes at 14 *DIV* (Table 6.4). In addition, at 14 *DIV* bitufted neurons grown on *Fmr1* KO astrocytes had a dendritic max that was 37.6% greater than neurons grown on WT astrocytes (Table 6.4).

Semi-log Sholl analysis of bitufted neurons indicated a similar pattern of dendritic arbor changes (Fig. 6.6a-c). At 7 *DIV* linear regression revealed that bitufted neurons grown on *Fmr1* KO astrocytes had a significantly higher ($p<0.001$) Sholl's regression coefficient than bitufted neurons grown on WT astrocytes (0.015 ± 0.000, $R^2=0.85$ vs. 0.012 ± 0.000, $R^2=0.90$)(Table 6.5). At 14 *DIV* the Sholl's regression coefficients were not significantly different between bitufted neurons grown on *Fmr1* KO or WT astrocytes (Table 6.5). However, at 21 *DIV* bitufted neurons grown on *Fmr1* KO astrocytes again exhibited a significantly increased ($p<0.05$) Sholl's regression coefficient compared to bitufted neurons grown on WT astrocytes (0.013 ± 0.001, $R^2=0.79$ vs. 0.011 ± 0.000, $R^2=0.80$)(Table 6.5).

Therefore, by both linear and semi-log Sholl analysis there is a significant difference in the dendritic arborization patterns seen at 7 *DIV* between bitufted neurons grown on *Fmr1* KO astrocytes and WT astrocytes, and this is no longer significant at 14 *DIV*. Interestingly, at 21 *DIV* only the semi-log Sholl analysis indicated a significant difference in the branching of the dendritic trees of bitufted neurons grown on *Fmr1* KO versus WT astrocytes.

Pyramidal Neurons:

At 7 *DIV*, pyramidal neurons grown on *Fmr1* KO astrocytes displayed a decrease in the extent of their dendritic arbor, reaching distances of only 240μm compared to the 290μm of those grown on WT astrocytes (Fig. 6.7a and Table 6.6). This difference was no longer apparent by 14 *DIV* when neurons in both conditions exhibited arbors that extended 300μm (Fig. 6.7b,c and Table 6.6). Linear Sholl analysis revealed that when grown on *Fmr1* KO astrocytes, pyramidal neurons exhibited significantly ($p<0.05$, Fig. 6.7a) decreased branching at 7 *DIV* for distances greater than160μm from the cell body. This trend of a lesser degree of ramification continued at 14 *DIV*; however, the difference was no longer significant at this stage in culture (Fig. 6.7b). At 21 *DIV*, pyramidal neurons grown on *Fmr1* KO astrocytes exhibited an increase in the degree of branching from greater than 80μm, which was significant ($p<0.05$) at 100μm and 190μm (Fig. 6.7c). This lack of a significant difference at distances closest to the soma are reflected in Schoenen's coefficients that are similar between pyramidal neurons grown on *Fmr1* KO and WT astrocytes, especially at 7 *DIV* (1.65 and 1.67 for WT and *Fmr1* KO, respectively)(Table 6.6). Furthermore, the inversion that occurs between 14 *DIV* and 21 *DIV* is also evident when noting the Schoenen's ramification indices. At 14 *DIV* pyramidal neurons grown on *Fmr1* KO astrocytes had a Schoenen's ramification index that was 0.12 less than neurons grown on WT astrocytes; however, at 21 *DIV* the Schoenen's ramification index was greater by 0.16 (Table 6.6). In addition, at 21 *DIV* the pyramidal neurons grown on *Fmr1* KO astrocytes had a shift in the value of the radius of

the maximal number of branches compared to the pyramidal neurons grown on WT astrocytes. At 21 *DIV* the pyramidal neurons grown on *Fmr1* KO astrocytes had maximal branching at 90μm compared to 40μm for WT.

When the branching pattern of pyramidal neurons was evaluated with the semi-log Sholl analysis (Fig. 6.8a-c), there was only a significant ($p<0.001$) difference in the ramification pattern of the pyramidal neurons grown on *Fmr1* KO astrocytes compared to WT astrocytes at 7 *DIV* (Table 6.7). The value of Sholl's regression coefficient for pyramidal neurons grown on *Fmr1* KO astrocytes (0.017 ± 0.000, $R^2=0.83$) was significantly higher ($p<0.001$) than the Sholl's regression coefficient for pyramidal neurons grown on WT astrocytes (0.014 ± 0.000, $R^2=0.84$) (Table 6.7). This significant difference was absent at the 14 and 21 *DIV* time points.

Therefore, both linear and semi-log Sholl analyses showed significant alterations in the dendritic arborization patterns of pyramidal neurons at 7 *DIV*. Linear Sholl analysis revealed a potentially important reversal of the degree of branching at 21 *DIV* with pyramidal neurons grown on *Fmr1* KO astrocytes shifting from less branching (compared to those grown on WT astrocytes) at 7 and 14 *DIV* to an increase in branching at 21 *DIV*. However, there was great variability in the dendrite ramification patterns of the pyramidal neurons and the difference was only significant at two locations from the soma. This difference seen at 21 *DIV* was not found to be significant by the semi-log Sholl analysis.

Multipolar Neurons:

At 7 *DIV*, multipolar neurons grown on *Fmr1* KO astrocytes displayed a decrease in the extent of their dendritic arbors compared to those grown on WT astrocytes (250μm vs. 290μm)(Fig.6.9a and Table 6.8). This difference was absent at 14 and 21 *DIV* (Fig.6.9b,c and Table 6.8). When evaluated by linear Sholl analysis, multipolar neurons grown on *Fmr1* KO astrocytes exhibited a decreased degree of branching along their extent, at both 7 *DIV* and 21 *DIV* (Fig. 6.9a,c). At 14 *DIV* multipolar neurons were observed to have a

similar ramification pattern whether grown on *Fmr1* KO or WT astrocytes (Fig. 6.9b). The difference in ramification was significant ($p<0.05$) only when analyzed at greater than 100μm from the soma at 7 *DIV* (Fig. 6.9a), which is reflected in a small shift in the Schoenen's ramification index (Table 6.8). However, at 21 *DIV* multipolar neurons grown on *Fmr1* KO astrocytes exhibited a highly visible decrease in branching from 40μm, which was significant at 120μm ($p<0.01$), 130μm ($p<0.05$) and between 210-260μm ($p<0.05$) (Fig. 6.9c). This corresponded to a decrease of 0.35 in the Schoenen's ramification index and a 9.6% decrease in the dendritic max (Table 6.8).

Semi-log Sholl analysis with linear regression (Fig. 6.10) revealed that multipolar neurons grown on *Fmr1* KO astrocytes had a significantly higher ($p<0.05$) Sholl's regression coefficient in comparison to the multipolar neurons grown on WT astrocytes at 7 *DIV* (0.014 ± 0.001, $R^2=0.90$ vs. 0.010 ± 0.001, $R^2=0.80$)(Table 6.9). The values of the Sholl regression coefficients were not significantly different at 14 or 21 *DIV*.

Therefore, both linear and semi-log Sholl analyses identified a significant difference in the branching patterns of multipolar neuron dendritic arbors when they were grown on *Fmr1* KO astrocytes versus WT astrocytes at 7 *DIV*. By 14 *DIV* the difference in dendrite branching was not found to be significantly different by either method of analysis. However, at 21 *DIV* linear Sholl analysis revealed a significant difference in ramification of the distant dendritic arbors, whereas this difference was not suggested by semi-log Sholl analysis.

Stellate Neurons:

At 7 *DIV*, stellate neurons grown on *Fmr1* KO astrocytes exhibited an increased extent of their dendritic arbor compared to those grown on WT astrocytes (180μm vs. 110μm) (Fig.6.11a and Table 6.10). This difference was absent at 14 *DIV* (Fig. 6.11b and Table 6.10). However, at 21 *DIV*, stellate neurons grown on *Fmr1* KO astrocytes displayed a decrease in the extent of their dendritic arbors (220μm vs. 300μm) (Fig. 6.11c and Table

6.10). Linear Sholl analysis showed that at 7 *DIV,* stellate neurons grown on *Fmr1* KO astrocytes exhibited a decrease in branching at distances less than 50μm from the cell body, and an increase in ramification at greater than 70μm (Fig. 6.11a). By 14 *DIV* this pattern of branching reversed. At 14 *DIV* and 21 *DIV* stellate neurons grown on *Fmr1* KO astrocytes exhibited an increase in the branch density at distances of less than 50μm, and a decrease in branching at greater than 60μm (Fig. 6.11 b, c). By 21 *DIV* the decreased degree of branching beyond 170μm was significantly different from stellate neurons grown on WT astrocytes (Fig. 6.11c). However, the Schoenen's ramification indices of stellate neurons were consistently lower when grown on *Fmr1* KO astrocytes compared to stellate neurons grown on WT astrocytes (less 0.60, 0.52 and 0.67 for 7, 14 and 21 *DIV* respectively, Table 6.10). Growth of stellate neurons on *Fmr1* KO astrocytes also decreased the dendritic max by 17.5%, 3.3% and 4.6%, at 7, 14 and 21 *DIV* respectively (Table 6.10).

Semi-log Sholl analysis of stellate neurons (Fig. 6.12) revealed significant differences in their dendritic arborization patterns at both 7 and 21 *DIV*. At 7 *DIV* stellate neurons grown on *Fmr1* KO astrocytes had a Sholl's regression coefficient of 0.019±0.001 (R^2=0.88); significantly higher ($p<0.0001$) than the value of 0.031±0.001 (R^2=0.96) for stellate neurons grown on WT astrocytes (Table 6.10). There was no significant difference observed at 14 *DIV*. However, at 21 *DIV* stellate neurons grown on *Fmr1* KO astrocytes had a significantly higher ($p<0.001$) Sholl's regression coefficient than stellate neurons grown on WT astrocytes (0.017±0.000, R^2=0.84 vs. 0.012±0.000, R^2=0.83) (Table 6.11).

Therefore, these analyses indicate that stellate neurons exhibited significantly different dendrite ramification when grown on *Fmr1* KO astrocytes at 21 *DIV*. At 7 *DIV*, semi-log Sholl analysis indicated a significant difference between the dendritic arbor branching patterns of stellate neurons grown on *Fmr1* KO astrocytes compared to those grown on WT astrocytes; yet, this significant was not recapitulated by the linear Sholl analysis. At

14 *DIV* no significant difference was noted by either method of analysis.

An overall summary of the analysis for each neuronal subtype is presented in Table 6.12.

6.2.5 Discussion

In this study we provide evidence in support of two major findings. First, we show that the abnormal dendritic arborization pattern induced by *Fmr1* KO astrocytes is exhibited by all subpopulations of neurons found in primary hippocampal neuron cultures. Second, our results suggest that stellate neurons are the subtype of neurons that suffer from significant pervasive alterations in the branching patterns of their dendritic arbors until 21 *DIV*.

Fmr1 KO astrocytes induced significant alterations in dendritic arbors

All classes of neurons that we distinguished (i.e., bipolar, bitufted, pyramidal, stellate and multipolar), exhibited significant differences in their dendritic arbors when grown on *Fmr1* KO astrocytes at 7 *DIV*, when analyzed by linear and semi-log Sholl methods. However, the bitufted and pyramidal neurons appeared to be most affected by the astrocytes early in development. All of the five classes exhibited an overall decrease in branching when grown on *Fmr1* KO astrocytes compared to the growth on normal astrocytes.

In earlier experiments we found that at 7 *DIV*, neurons exposed to *Fmr1* KO astrocytes exhibited significantly increased branching; whereas, here we report a decrease in the extent of dendritic ramification. One important difference needs to be considered. In the previous studies we determined the extent of branching using Neuronmetrics™, which is a computerized system for determining the number of branches in the dendritic arbor of neurons (Narro et al., 2007). The difference between the previous results and the results here sheds light on a very important characteristic of the dendritic branching patterns. In Figure 6.13, two neurons with similar dendritic arbors are represented with overlays of

concentric virtual Sholl circles. The neuron on the right differs from the neuron on the left only by an increase in the number of branches. If evaluated by Neuronmetrics ™, we would find an increased number of branches in the arbor of the neuron on the right. On the other hand, when analyzed by the Sholl analysis, we would find no difference between the two neurons. Looking closely at the neuron on the right, the 'extra' branches (that would have been counted in Neuronmetrics™) branch from the higher order dendrite between two concentric Sholl circles and either a) do not extend long enough to cross the next virtual Sholl circle (closed triangle) or b) extend along the curvature of the circle (open triangle). Either type of branch does not reach the next virtual Sholl circle, and therefore would not be counted using Sholl's analysis.

If a neuron, or population of neurons, is found to have a decreased number of branches on Sholl analysis compared to a method such as Neurometrics™, it is likely that the dendritic arbor has a number of short dendrites, or the dendrites do not extend radially outwards (similar to the example in Fig. 6.13b). Therefore, taking the previous findings together with the results of the present study it appears that hippocampal neurons grown on *Fmr1* KO astrocytes may extend a significant number of short dendritic branches (Jacobs and Doering, submitted; and Jacobs, Nathwani and Doering, submitted), while exhibiting a significant decrease in the highly branched patterns (the current study).

With respect to astrocyte-mediated alterations in the development of dendrite arbors, the alterations we observed in the dendritic branch complexity are consistent with other neurodevelopmental studies (Kaufmann and Moser, 2000) and disorders of cognitive impairment (Dierssen and Ramakers, 2006; Kaufmann and Moser, 2000). Furthermore, our results highlight the involvement of glial cells in neurological diseases (Allen and Barres, 2009; Ballas et al., 2009; Barres, 2008; Blackburn et al., 2009; Salmina, 2009), and illustrate astrocytes as a contributing factor in the cellular mechanisms underlying the impairments in cognitive function (Nair et al., 2008), specifically FXS.

Dendritic branching patterns may reflect developmental delays

In conjunction with a significant decrease in the complexity of the dendritic arbors, we observed an abnormal number of short dendrites in hippocampal neurons cultured with *Fmr1* KO astrocytes. Dendritic arbor development is a dynamic process, during which new dendritic branches are continually extended and retracted, and only a subset of these attain full maturity (Libersat and Duch, 2004; McAllister, 2000; Scott and Luo, 2001). Early in dendrite development immature dendrite precursors, or filopodia, appear as long thin projections branching in an orientation nearly perpendicular to the origin dendrite (Libersat and Duch, 2004; McAllister, 2000; Scott and Luo, 2001). The appearance of the short dendrites seen on the hippocampal neurons grown with *Fmr1* KO astrocytes resembles this description. It is therefore possible that these short dendrites are immature filopodia. If this is true, the neurons grown in the presence of *Fmr1* KO astrocytes are delayed in an early developmental stage of extension and retraction of immature dendrite precursors. This delay in dendritic arbor development would cause deficits in the neural networks formed and could play a role in the underlying neurobiology of FXS.

Interestingly, the increase in the number of immature dendritic branches observed in the hippocampal neurons grown with *Fmr1* KO astrocytes in this study parallels the increase in immature dendritic spines that is documented in FXS. In addition to filopodia being the precursors for dendrite extension, it has been proposed that dendritic spines are also formed through a sequence of events following the extension of filopodia from the dendrites (Dailey and Smith, 1996; Okabe et al., 2001). Moreover, a correlation between the density of dendrite branching and the density of dendritic spines has been found in rat cortical neurons *in vitro* (Kriegstein and Dichter, 1983). Therefore, our finding could indicate that in addition to inducing significant alterations in the dendritic arbor branching patterns of hippocampal neurons, astrocytes may influence the dendritic spine densities of the same neurons in FXS. If true, this would be consistent with the current knowledge of the characteristic dendritic spine abnormalities in FXS (Comery et al., 1997; Irwin et al., 2000; Irwin et al., 2002; Irwin et al., 2001). Future studies directly

investigating the role of astrocytes in dendritic spine development would provide important insight into the neurobiology of FXS.

Second, we proposed that the 'extra' dendrites found in the previous studies could be a result of an altered orientation of the dendritic branches in a manner that prevents them crossing the next Sholl circle. As mentioned early, filopodia often project orthogonally from the parent dendrite. If these perpendicularly projecting early dendrite precursors were to continue their maturation along the same trajectory, this would result in a highly woven dendritic arbor. The normal radial organization of the branching of the dendrites is essential to ensure the most efficient coverage of the receptive field (Urbanska et al., 2008). Molecular signals that prevent the crossing of dendrites have been documented (Parrish et al., 2007). For example, Down's syndrome related cell adhesion molecule (Dscam) has been indicated in dendrite self-avoidance in the mouse retina (Fuerst et al., 2008), and in *Drosophila* dendritic arborization neurons (Hughes et al., 2007; Matthews et al., 2007; Soba et al., 2007). The absence of this molecule has been shown to result in highly disorganized dendritic arbors in *Drosophila* (Hughes et al., 2007; Matthews et al., 2007; Soba et al., 2007). In fact, a number of studies have shown altered organization of the dendritic arbors in diseases of cognitive impairment (reviewed inDierssen and Ramakers, 2006; Kaufmann and Moser, 2000). Based on the above explanation, the hippocampal neurons grown on astrocytes from an *Fmr1* KO animal exhibited altered dendritic arborizations with an increased number of orthogonally oriented dendrites. If this were true, it is possible that organizational cues are also altered in hippocampal neurons through astrocyte mediated mechanisms, and could contribute to the underlying neurobiology of FXS.

Hippocampal neurons with stellate morphologies are most affected

The data presented here suggest that neurons with a stellate morphology were the only subtypes that continued to show significant dendritic alterations at 21 *DIV* when grown on the *Fmr1* KO astrocytes. These stellate neurons exhibited significantly increased branching proximal to the cell body, and significantly reduced dendritic arborization at distances beyond 50μm from the soma. Stellate neurons were the only subtype that was found to have astrocyte-induced alterations that were significant by both linear and semi-log Sholl analyses.

Spiny stellate neurons of the hippocampus are excitatory neurons (Spruston and McBain, 2007). Although we were not able to identify the presence (or absence) of dendritic spines on the hippocampal neurons in culture, our stellate neurons appeared similar to the spiny stellate neurons seen in the hippocampus *in vivo*. In Kriegstein and Dichter's (1983) description of rat cortical neuron morphology, *in vitro* spiny multipolar cells have more complex dendritic arbors than aspiny multipolar cells. Additionally, stellate cells of the hippocampus possess five or more thick primary dendrites that project from the cell body (Spruston and McBain, 2007). In comparison, the cells classified as stellate in our cultures possessed five or more thick primary dendrites, and the dendritic arbors branched extensively. Therefore, based on this description and the morphological characteristics of the neurons in our culture, it is possible that our stellate neurons are the equivalent of the stellate neurons of the hippocampus, and are therefore excitatory in nature.

Role of astrocytes in excitatory synapse development and cognition

The proper functioning of neural networks requires a delicate balance between excitatory and inhibitory synaptic inputs. Alterations in the excitatory/inhibitory (E/I) ratio are found in a number of disease models of mental impairment including FXS (Eichler and Meier, 2008; Fatemi et al., 2008; Gibson et al., 2008; Kehrer et al., 2008; Majdi et al.,

2009; Wong et al., 2006), and therefore have been implicated as a key neurobiological mechanism underlying cognitive impairment. Our results indicate that astrocytes may play a role in mediating this balance of excitatory and inhibitory circuitry by selectively altering the dendritic arborization patterns of excitatory neurons *in vitro*. Previous studies have documented astrocytes as mediators of the patterning of neuronal dendritic arbors *in vitro* (Ballas et al., 2009; Jacobs and Doering, 2009a; Jacobs et al., 2009; Nishida and Okabe, 2007); however, the cell-type selective action of astrocyte-derived cues guiding dendrite arborization has not been studied excessively. In earlier work, Deni-Donini and Estenoz (1988) demonstrated that excitatory efferent neurons and inhibitory interneurons respond differently to glia-derived signals. More recently, Lee and co-workers (2006) found that in response to the same environmental milieu *in vivo*, pyramidal and inhibitory interneurons exhibited contrasting modes of growth. In their study, they showed that the pyramidal neurons remained relatively stable, whereas the inhibitory neurons exhibited numerous extensions and retractions of their dendritic arbors (Lee et al., 2006). That same year, a study by Yamamato and colleagues (2006) revealed that a subset of *Drosophila* dendritic arborization (da) neurons selectively respond to glia-derived signaling. Based on previous studies it is reasonable to conclude that all subtypes of neurons exhibit different growth and maturation responses to common signals; including astrocyte-derived signals with cell-type specific effects. The findings presented here suggest that the potential exists for astrocyte-mediated neuron-class specific pervasive alterations of dendritic arborizations as a contributing factor in the underlying neurobiology of FXS.

In summary, we have shown for the first time that *Fmr1* KO astrocytes affect the dendritic arborization of all subtypes of hippocampal neurons. Furthermore, we have provided evidence that select populations of hippocampal neurons are more effected by this astrocyte-mediated developmental delay. Specifically, the stellate neurons grown on *Fmr1* KO astrocytes exhibit the most pervasive developmental delays. Given that hippocampal neurons with spiny stellate dendritic arbors are often excitatory in nature,

and the influence of astrocytes in dendritic patterning, the role of FMRP deficient astrocytes on neural development in FXS is significant. The results presented here shed light on the specific avenues through which astrocytes exert their effect in FXS, and may provide potential routes in view of astrocyte-directed therapeutics for FXS.

6.2.6 Literature Cited

Allen NJ, Barres BA. 2009. Neuroscience: Glia - more than just brain glue. Nature 457(7230):675-677.

Ballas N, Lioy DT, Grunseich C, Mandel G. 2009. Non-cell autonomous influence of MeCP2-deficient glia on neuronal dendritic morphology. Nat Neurosci 12(3):311-317.

Banker GA. 1980. Trophic interactions between astroglial cells and hippocampal neurons in culture. Science 209(4458):809-810.

Banker GA, Cowan WM. 1979. Further observations on hippocampal neurons in dispersed cell culture. J Comp Neurol 187(3):469-493.

Barres BA. 2008. The mystery and magic of glia: a perspective on their roles in health and disease. Neuron 60(3):430-440.

Beckel-Mitchener A, Greenough WT. 2004. Correlates across the structural, functional, and molecular phenotypes of fragile X syndrome. Ment Retard Dev Disabil Res Rev 10(1):53-59.

Blackburn D, Sargsyan S, Monk PN, Shaw PJ. 2009. Astrocyte function and role in motor neuron disease: A future therapeutic target? Glia.

Comery TA, Harris JB, Willems PJ, Oostra BA, Irwin SA, Weiler IJ, Greenough WT. 1997. Abnormal dendritic spines in fragile X knockout mice: maturation and pruning deficits. Proc Natl Acad Sci U S A 94(10):5401-5404.

Dailey ME, Smith SJ. 1996. The dynamics of dendritic structure in developing hippocampal slices. J Neurosci 16(9):2983-2994.

Denis-Donini S, Estenoz M. 1988. Interneurons versus efferent neurons: heterogeneity in their neurite outgrowth response to glia from several brain regions. Dev Biol 130(1):237-249.

Dierssen M, Ramakers GJ. 2006. Dendritic pathology in mental retardation: from molecular genetics to neurobiology. Genes Brain Behav 5 Suppl 2:48-60.

Eichler SA, Meier JC. 2008. E-I balance and human diseases - from molecules to networking. Front Mol Neurosci 1:2.

Fatemi SH, Folsom TD, Reutiman TJ, Lee S. 2008. Expression of astrocytic markers aquaporin 4 and connexin 43 is altered in brains of subjects with autism. Synapse 62(7):501-507.

Fuerst PG, Koizumi A, Masland RH, Burgess RW. 2008. Neurite arborization and mosaic spacing in the mouse retina require DSCAM. Nature 451(7177):470-474.

Gibson JR, Bartley AF, Hays SA, Huber KM. 2008. Imbalance of neocortical excitation and inhibition and altered UP states reflect network hyperexcitability in the mouse model of fragile X syndrome. J Neurophysiol 100(5):2615-2626.

Hagerman PJ. 2008. The fragile X prevalence paradox. J Med Genet 45(8):498-499.

Hughes ME, Bortnick R, Tsubouchi A, Baumer P, Kondo M, Uemura T, Schmucker D. 2007. Homophilic Dscam interactions control complex dendrite morphogenesis. Neuron 54(3):417-427.

Hume RI, Purves D. 1981. Geometry of neonatal neurones and the regulation of synapse elimination. Nature 293(5832):469-471.

Irwin SA, Galvez R, Greenough WT. 2000. Dendritic spine structural anomalies in fragile-X mental retardation syndrome. Cereb Cortex 10(10):1038-1044.

Irwin SA, Idupulapati M, Gilbert ME, Harris JB, Chakravarti AB, Rogers EJ, Crisostomo RA, Larsen BP, Mehta A, Alcantara CJ, Patel B, Swain RA, Weiler IJ, Oostra BA, Greenough WT. 2002. Dendritic spine and dendritic field characteristics of layer V pyramidal neurons in the visual cortex of fragile-X knockout mice. Am J Med Genet 111(2):140-146.

Irwin SA, Patel B, Idupulapati M, Harris JB, Crisostomo RA, Larsen BP, Kooy F, Willems PJ, Cras P, Kozlowski PB, Swain RA, Weiler IJ, Greenough WT. 2001. Abnormal dendritic spine characteristics in the temporal and visual cortices of patients with fragile-X syndrome: a quantitative examination. Am J Med Genet 98(2):161-167.

Jacobs S, Doering LC. 2009a. Astrocytes prevent abnormal neuronal development in the Fragile X mouse.

Jacobs S, Doering LC. 2009b. Primary Dissociated Astrocyte and Neuron Co-Culture. In: Doering LC, Editor. Protocols for Neural Cell Culture. 4th ed. New York: Humana Press. p 269-284.

Jacobs S, Nathwani M, Doering LC. 2009. Fragile X Astrocytes induce developmental delays in dendrite maturation and synaptic protein expression.

Kaufmann WE, Moser HW. 2000. Dendritic anomalies in disorders associated with mental retardation. Cereb Cortex 10(10):981-991.

Kehrer C, Maziashvili N, Dugladze T, Gloveli T. 2008. Altered Excitatory-Inhibitory

Balance in the NMDA-Hypofunction Model of Schizophrenia. Front Mol Neurosci 1:6.

Kremer EJ, Pritchard M, Lynch M, Yu S, Holman K, Baker E, Warren ST, Schlessinger D, Sutherland GR, Richards RI. 1991. Mapping of DNA instability at the fragile X to a trinucleotide repeat sequence p(CCG)n. Science 252(5013):1711-1714.

Kriegstein AR, Dichter MA. 1983. Morphological classification of rat cortical neurons in cell culture. J Neurosci 3(8):1634-1647.

Lee WC, Huang H, Feng G, Sanes JR, Brown EN, So PT, Nedivi E. 2006. Dynamic remodeling of dendritic arbors in GABAergic interneurons of adult visual cortex. PLoS Biol 4(2):e29.

Libersat F, Duch C. 2004. Mechanisms of dendritic maturation. Mol Neurobiol 29(3):303-320.

Majdi M, Ribeiro-da-Silva A, Cuello AC. 2009. Variations in excitatory and inhibitory postsynaptic protein content in rat cerebral cortex with respect to aging and cognitive status. Neuroscience 159(2):896-907.

Matthews BJ, Kim ME, Flanagan JJ, Hattori D, Clemens JC, Zipursky SL, Grueber WB. 2007. Dendrite self-avoidance is controlled by Dscam. Cell 129(3):593-604.

McAllister AK. 2000. Cellular and molecular mechanisms of dendrite growth. Cereb Cortex 10(10):963-973.

Nair A, Frederick TJ, Miller SD. 2008. Astrocytes in multiple sclerosis: a product of their environment. Cell Mol Life Sci 65(17):2702-2720.

Narro ML, Yang F, Kraft R, Wenk C, Efrat A, Restifo LL. 2007. NeuronMetrics: software for semi-automated processing of cultured neuron images. Brain Res 1138:57-75.

Nishida H, Okabe S. 2007. Direct astrocytic contacts regulate local maturation of dendritic spines. J Neurosci 27(2):331-340.

O'Donnell WT, Warren ST. 2002. A decade of molecular studies of fragile X syndrome. Annu Rev Neurosci 25:315-338.

Okabe S, Miwa A, Okado H. 2001. Spine formation and correlated assembly of presynaptic and postsynaptic molecules. J Neurosci 21(16):6105-6114.

Pacey LK, Doering LC. 2007. Developmental expression of FMRP in the astrocyte lineage: implications for fragile X syndrome. Glia 55(15):1601-1609.

Parrish JZ, Emoto K, Kim MD, Jan YN. 2007. Mechanisms that regulate establishment, maintenance, and remodeling of dendritic fields. Annu Rev Neurosci 30:399-423.

Powell EM, Geller HM. 1999. Dissection of astrocyte-mediated cues in neuronal guidance and process extension. Glia 26(1):73-83.

Purpura DP. 1975. Dendritic differentiation in human cerebral cortex: normal and aberrant developmental patterns. Adv Neurol 12:91-134.

Purves D, Hume RI. 1981. The relation of postsynaptic geometry to the number of presynaptic axons that innervate autonomic ganglion cells. J Neurosci 1(5):441-452.

Purves D, Rubin E, Snider WD, Lichtman J. 1986. Relation of animal size to convergence, divergence, and neuronal number in peripheral sympathetic pathways. J

Neurosci 6(1):158-163.

Salmina AB. 2009. Neuron-glia interactions as therapeutic targets in neurodegeneration. J Alzheimers Dis 16(3):485-502.

Schoenen J. 1982. Dendritic organization of the human spinal cord: the motoneurons. J Comp Neurol 211(3):226-247.

Scott EK, Luo L. 2001. How do dendrites take their shape? Nat Neurosci 4(4):359-365.

Sholl DA. 1953. Dendritic organization in the neurons of the visual and motor cortices of the cat. J Anat 87(4):387-406.

Soba P, Zhu S, Emoto K, Younger S, Yang SJ, Yu HH, Lee T, Jan LY, Jan YN. 2007. Drosophila sensory neurons require Dscam for dendritic self-avoidance and proper dendritic field organization. Neuron 54(3):403-416.

Spruston N, McBain CJ. 2007. Structural and Functional Properties of Hippocampal Neurons. In: Anderson P, Morris R, Amaral D, Bliss T, O'Keefe J, editors. The HIppocampus Book. New York: Oxford University Press. p 133-202.

Stuart G, Spruston N, H©Þusser M. 2008. Dendrites. Oxford ; New York: Oxford University Press. xv, 560 p. p.

Threadgill R, Bobb K, Ghosh A. 1997. Regulation of dendritic growth and remodeling by Rho, Rac, and Cdc42. Neuron 19(3):625-634.

Urbanska M, Blazejczyk M, Jaworski J. 2008. Molecular basis of dendritic arborization. Acta Neurobiol Exp (Wars) 68(2):264-288.

Wong TP, Marchese G, Casu MA, Ribeiro-da-Silva A, Cuello AC, De Koninck Y. 2006. Imbalance towards inhibition as a substrate of aging-associated cognitive impairment. Neurosci Lett 397(1-2):64-68.

Yamamoto M, Ueda R, Takahashi K, Saigo K, Uemura T. 2006. Control of axonal sprouting and dendrite branching by the Nrg-Ank complex at the neuron-glia interface. Curr Biol 16(16):1678-1683.

Table 6.1: Number of neurons in each morphological class per experimental condition.

	7 *DIV*		14 *DIV*		21 *DIV*	
	WT	*Fmr1* KO	WT	*Fmr1* KO	WT	*Fmr1* KO
Bipolar	24	25	27	31	43	45
Bitufted	10	18	6	5	8	5
Pyramidal	41	28	26	16	20	22
Multipolar	69	66	76	86	65	53
Stellate	5	12	15	12	15	25

Table 6.2: Linear Sholl analysis values for bipolar neurons.

Days in culture	7 DIV		14 DIV		21 DIV	
Astrocytes	WT	*Fmr1* KO	WT	*Fmr1* KO	WT	*Fmr1* KO
Schoenen's ramification index[a]	1.71	1.72	1.64	1.63	2.01	1.79
Critical Value (μm)[b]	40	20	70	60	60	75
Dendritic Max[c]	3.42	3.44	3.28	3.23	4.02	3.58

a, dendritic max/number of primary dendrites; b, radius (μm) at maximum number of dendritic crossings; c, maximum number of crossings at critical value.

Table 6.3: Semi-log Sholl analysis linear regression values for bipolar neurons.

	7 DIV		14 DIV		21 DIV	
Astrocytes	WT	*Fmr1* KO	WT	*Fmr1* KO	WT	*Fmr1* KO
k (-m) [a]	0.012 ±0.000	0.013 ±0.000 **	0.011 ±0.000	0.010 ±0.000	0.010 ±0.000	0.010 ±0.000
Intercept [b]	-2.737 ±0.032	-2.678 ±0.032	-2.795 ±0.029	-2.810 ±0.027	-2.748 ±0.023	-2.794 ±0.021
R^{2} [c]	0.83	0.84	0.83	0.83	0.82	0.83

a, Sholl's regression coefficient, k, is equal to the slope multiplied by negative one; b, the intercept of the regression line; c, the goodness of fit of the regression line; ASTS, astrocytes; *, significantly different from WT at $p<0.05$; **, significantly different from WT at $P<0.01$; ***, significantly different from WT at $p<0.001$.

Table 6.4: Linear Sholl analysis values for bitufted neurons.

Days in culture	7 DIV		14 DIV		21 DIV	
Astrocytes	WT	*Fmr1* KO	WT	*Fmr1* KO	WT	*Fmr1* KO
Schoenen's ramification index[a]	2.40	2.33	2.83	3.90	3.81	3.70
Critical Value (μm)[b]	40	40	60	50	40	80
Dendritic Max[c]	4.80	4.66	5.67	7.80	7.63	7.40

a, dendritic max/number of primary dendrites; b, radius (μm) at maximum number of dendritic crossings; c, maximum number of crossings at critical value.

Table 6.5: Semi-log Sholl analysis linear regression values for bitufted neurons.

	7 DIV		14 DIV		21 DIV	
Astrocytes	WT	*Fmr1* KO	WT	*Fmr1* KO	WT	*Fmr1* KO
k (-m) [a]	0.012 ±0.000	0.015 ±0.000 ***	0.011 ±0.000	0.010 ±0.000	0.011 ±0.000	0.013 ±0.001 *
Intercept [b]	-2.596 ±0.040	-2.465 ±0.038	-2.642 ±0.054	-2.605 ±0.066	-2.526 ±0.058	-2.394 ±0.077
R^2 [c]	0.90	0.85	0.88	0.83	0.80	0.79

a, Sholl's regression coefficient, k, is equal to the slope multiplied by negative one; b, the intercept of the regression line; c, the goodness of fit of the regression line; ASTS, astrocytes; *, significantly different from WT at $p<0.05$; **, significantly different from WT at $P<0.01$; ***, significantly different from WT at $p<0.001$.

Table 6.6: Linear Sholl analysis values for pyramidal neurons.

Days in culture	7 DIV		14 DIV		21 DIV	
Astrocytes	WT	*Fmr1* KO	WT	*Fmr1* KO	WT	*Fmr1* KO
Schoenen's ramification index[a]	1.65	1.67	1.68	1.56	1.88	1.94
Critical Value (μm)[b]	40	30	40	55	40	90
Dendritic Max[c]	4.95	5.00	5.04	4.69	5.65	5.82

a, dendritic max/number of primary dendrites; b, radius (μm) at maximum number of dendritic crossings; c, maximum number of crossings at critical value.

Table 6.7: Semi-log Sholl analysis linear regression values for pyramidal neurons.

	7 DIV		14 DIV		21 DIV	
Astrocytes	WT	*Fmr1* KO	WT	*Fmr1* KO	WT	*Fmr1* KO
k (-m) [a]	0.014 ±0.000	0.017 ±0.000 ***	0.011 ±0.000	0.011 ±0.000	0.011 ±0.000	0.011 ±0.000
Intercept [b]	-2.509 ±0.026	-2.343 ±0.036	-2.654 ±0.030	-2.705 ±0.038	-2.620 ±0.035	-2.640 ±0.032
R^2 [c]	0.84	0.83	0.83	0.83	0.82	0.82

a, Sholl's regression coefficient, k, is equal to the slope multiplied by negative one; b, the intercept of the regression line; c, the goodness of fit of the regression line; *, significantly different from WT at $p<0.05$; **, significantly different from WT at $P<0.01$; ***, significantly different from WT at $p<0.001$.

Table 6.8: Linear Sholl analysis values for multipolar neurons.

Days in culture	7 DIV		14 DIV		21 DIV	
Astrocytes	WT	*Fmr1* KO	WT	*Fmr1* KO	WT	*Fmr1* KO
Schoenen's ramification index[a]	1.66	1.55	1.63	1.57	2.08	1.73
Critical Value (μm)[b]	40	30	60	45	50	40
Dendritic Max[c]	4.95	5.00	6.55	6.51	6.95	6.28

a, dendritic max/number of primary dendrites; b, radius (μm) at maximum number of dendritic crossings; c, maximum number of crossings at critical value.

Table 6.9: Semi-log Sholl analysis linear regression values for multipolar neurons.

	7 DIV		14 DIV		21 DIV	
Astrocytes	WT	*Fmr1* KO	WT	*Fmr1* KO	WT	*Fmr1* KO
k (-m) [a]	0.010 ±0.001	0.014 ±0.001 *	0.010 ±0.001	0.010 ±0.001	0.010 ±0.001	0.010 ±0.001
Intercept [b]	-2.840 ±0.164	-2.531 ±0.136	-2.647 ±0.100	-2.651 ±0.100	-2.645 ±0.092	-2.662 ±0.100
R^2 [c]	0.80	0.90	0.92	0.92	0.93	0.92

a, Sholl's regression coefficient, k, is equal to the slope multiplied by negative one; b, the intercept of the regression line; c, the goodness of fit of the regression line; *, significantly different from WT at $p<0.05$; **, significantly different from WT at $P<0.01$; ***, significantly different from WT at $p<0.001$.

Table 6.10: Linear Sholl analysis values for stellate neurons.

Days in culture	7 DIV		14 DIV		21 DIV	
Astrocytes	WT	*Fmr1* KO	WT	*Fmr1* KO	WT	*Fmr1* KO
Schoenen's ramification index[a]	2.17	1.57	2.55	2.03	3.08	2.41
Critical Value (μm)[b]	30	20	60	40	50	40
Dendritic Max[c]	10.00	8.25	12.93	12.50	13.13	12.52

a, dendritic max/number of primary dendrites; b, radius (μm) at maximum number of dendritic crossings; c, maximum number of crossings at critical value.

Table 6.11: Semi-log Sholl analysis linear regression values for stellate neurons.

	7 DIV		14 DIV		21 DIV	
Astrocytes	WT	*Fmr1* KO	WT	*Fmr1* KO	WT	*Fmr1* KO
k (-m) [a]	0.031 ±0.001	0.019 ±0.001 ***	0.012 ±0.000	0.013 ±0.000	0.012 ±0.000	0.017 ±0.000 ***
Intercept [b]	-1.578 ±0.053	-2.059 ±0.056	-2.202 ±0.041	-2.205 ±0.051	-2.230 ±0.043	-1.991 ±0.038
R^{2} [c]	0.96	0.88	0.84	0.83	0.83	0.84

a, Sholl's regression coefficient, k, is equal to the slope multiplied by negative one; b, the intercept of the regression line; c, the goodness of fit of the regression line; *, significantly different from WT at $p<0.05$; **, significantly different from WT at $P<0.01$; ***, significantly different from WT at $p<0.001$.

Table 6.12: Summary of Sholl analyses results

All arrows represent change compared to WT. **Linear Sholl**, values represent distance (μm) from soma with significant differences, * $p<0.05$, ** $p<0.01$, *** $p<0.001$; ***Rext***, radius (μm) at extent of arbor, single arrow indicates a change of 10μm; ***Rmax***, the radius at which there was maximum number of crossings, each arrow represents 10μm; ***Dmax***, the number of crossings at *Rmax*, one arrow is change of >0.1, two arrows are change of >1.0; ***SRI***, Schoenen's Ramification Index, single arrow is change of > 0.1, double arrow is change of >1.0; ***k***, Sholl's coefficient, * $p<0.05$, ** $p<0.01$, *** $p<0.001$.

	7 DIV		14 DIV		21 DIV	
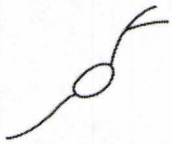	Linear Sholl	---	Linear Sholl	---	Linear Sholl	20*
	Rext	↓	*Rext*	---	*Rext*	---
	Rmax	↓↓	*Rmax*	↓	*Rmax*	↑
	Dmax	---	*Dmax*	---	*Dmax*	↓
	SRI	---	*SRI*	---	*SRI*	↓
	k	↑**	*k*	---	*k*	---
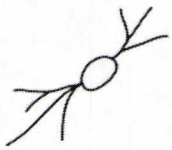	Linear Sholl	190*, 200*, 210*, 220*, 250*	Linear Sholl	10*	Linear Sholl	---
	Rext	↓	*Rext*	---	*Rext*	↓
	Rmax	---	*Rmax*	↓	*Rmax*	↑↑↑↑
	Dmax	↓	*Dmax*	↑↑	*Dmax*	↓
	SRI	↓	*SRI*	↑↑	*SRI*	---
	k	↑***	*k*	---	*k*	↑*
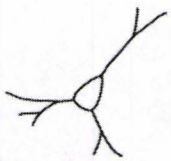	Linear Sholl	120*, 170**, 180**, 190*, 200*, 210**, 220**, 230***, 240***	Linear Sholl	---	Linear Sholl	100*, 190*
	Rext	↓	*Rext*	---	*Rext*	---
	Rmax	↓	*Rmax*	↑	*Rmax*	↑↑↑↑↑
	Dmax	---	*Dmax*	↓	*Dmax*	↑
	SRI	---	*SRI*	↓	*SRI*	---
	k	↑***	*k*	---	*k*	---
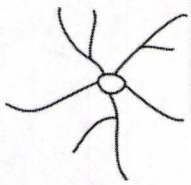	Linear Sholl	100*, 120*, 150**, 180***	Linear Sholl	---	Linear Sholl	120**, 130*, 210*, 230*, 240*, 250**, 260*, 270*, 280*
	Rext	↓	*Rext*	---	*Rext*	---
	Rmax	↓	*Rmax*	↓	*Rmax*	↓
	Dmax	---	*Dmax*	---	*Dmax*	↓
	SRI	↓	*SRI*	---	*SRI*	↓
	k	↑*	*k*	---	*k*	---
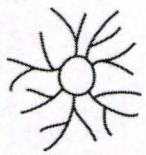	Linear Sholl	---	Linear Sholl	20*	Linear Sholl	20**, 170*, 180*, 190*, 200*, 220*, 230**, 240**, 250**, 260*
	Rext	↑	*Rext*	---	*Rext*	↓
	Rmax	↓	*Rmax*	↓↓	*Rmax*	↓
	Dmax	↓↓	*Dmax*	↓	*Dmax*	↓
	SRI	↓	*SRI*	↓	*SRI*	↓
	k	↓***	*k*	---	*k*	↑***

Figure 6.1: Neuron classification based on dendrite morphology.

Examples of neurons in culture stained with MAP2, representing each of the subtypes of neurons identified in culture, a, bipolar neurons, b, bitufted neurons, c, pyramidal neurons, d, multipolar neurons, e, stellate neurons. Scale bars are 50μm.

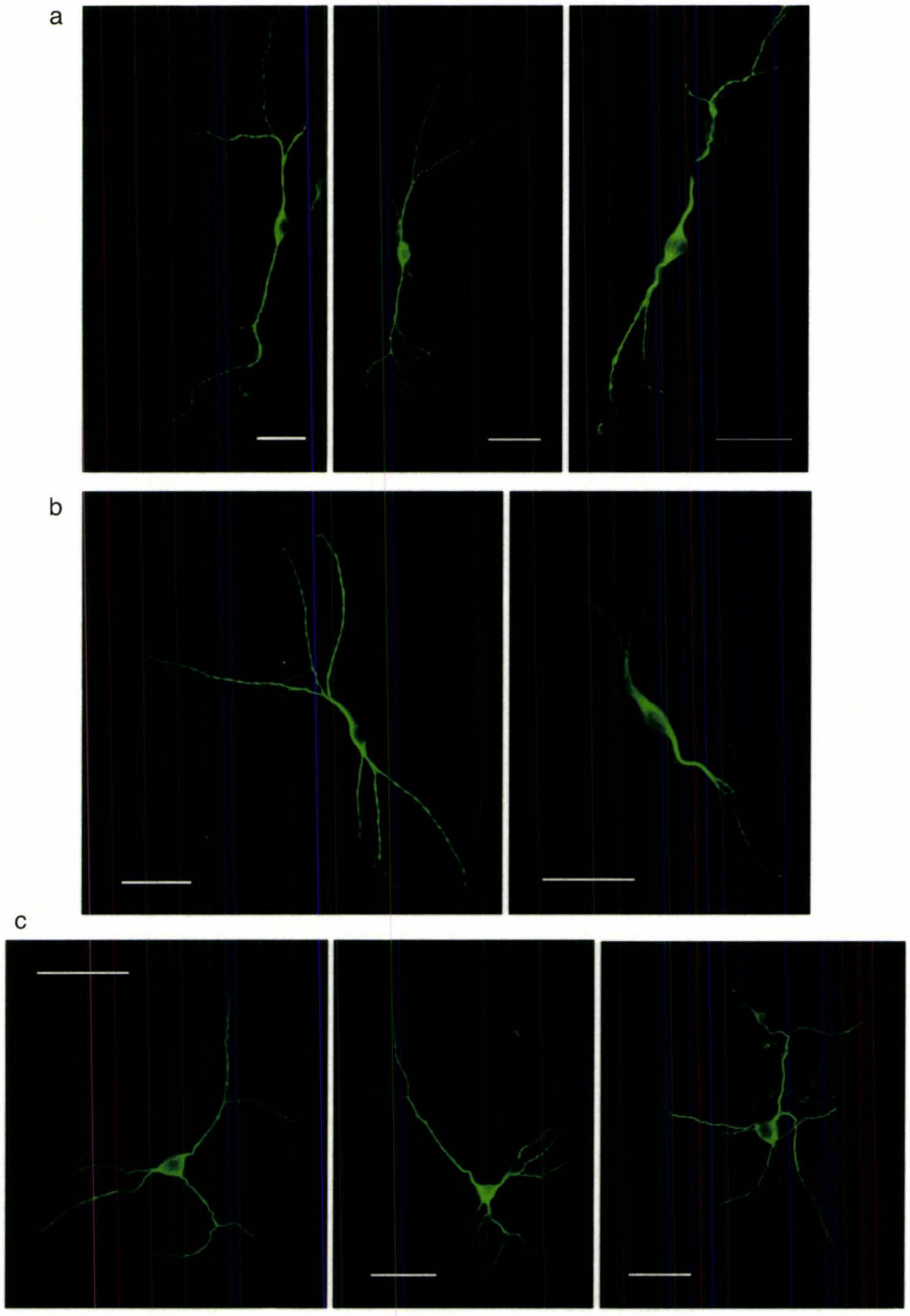

Figure 6.1 (a-c)

d

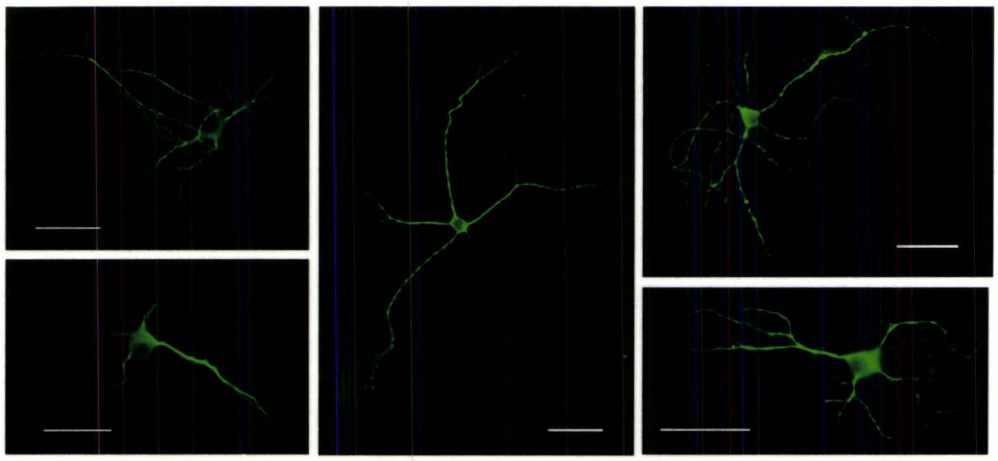

e

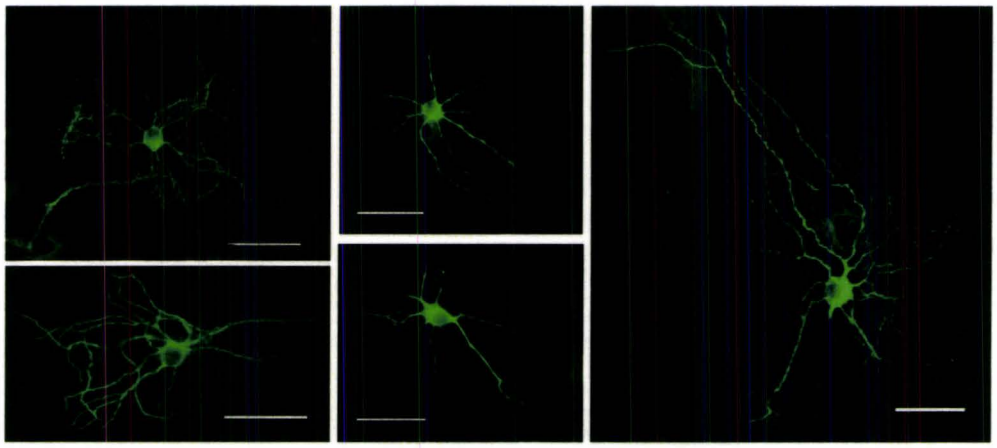

Figure 6.1 (d-e)

Figure 6.2: Sholl analysis schematic.

Example of a representative neuron dendritic arbor skeleton generated by Neuronmetrics™, with a simplified overlay of virtual concentric Sholl circles. In these experiments the Sholl circles began at 10μm and continued every 10μm until 300μm.

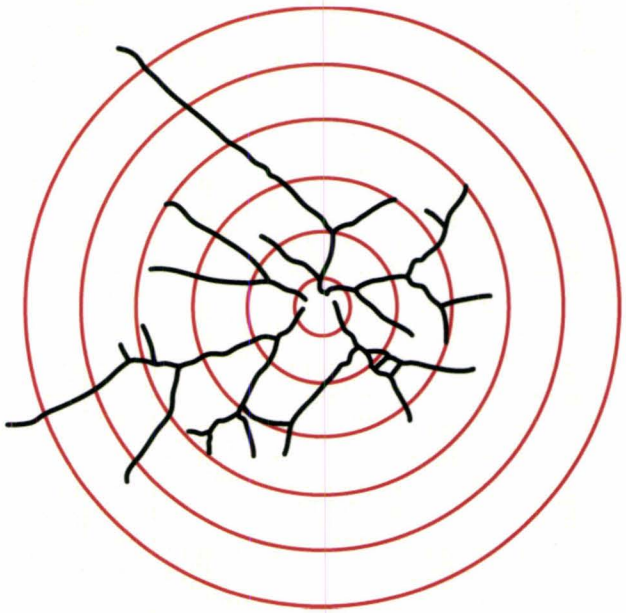

Figure 6.2

Figure 6.3: Linear Sholl analysis of bipolar neurons.

(a) 7 *DIV*, (b) 14 *DIV* and (c) 21 *DIV*. Solid circles are data from neurons grown on WT astrocytes, and open circles are from data of neurons grown on *Fmr1* KO astrocytes. Data are mean ± s.e.m. from three independent experiments, a, n(WT)=24 and n(*Fmr1* KO)=25, b, n(WT)=27 and n(*Fmr1* KO)=31, c, n(WT)=43 and n(*Fmr1* KO)=45. *, significantly different from WT at $p<0.05$, Mann Whitney U tests (two-tailed).

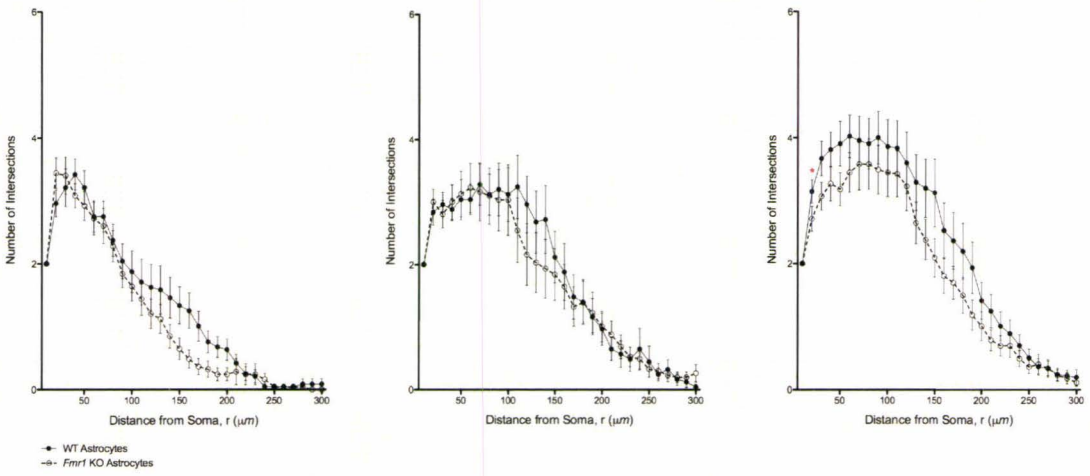
Number of Intersections
Distance from Soma, r (μm)
WT Astrocytes
Fmr1 KO Astrocytes

Figure 6.3

Figure 6.4: Semi-log Sholl analysis of bipolar neurons.

(a) 7 *DIV*, (b) 14 *DIV* and (c) 21 *DIV*. Solid circles are data from neurons grown on WT astrocytes, and open circles are from data of neurons grown on *Fmr1* KO astrocytes. Data are mean ± s.e.m. from three independent experiments, a, n(WT)=24 and n(*Fmr1* KO)=25, b, n(WT)=27 and n(*Fmr1* KO)=31, c, n(WT)=43 and n(*Fmr1* KO)=45. Linear regression lines are shown. Solid line is for data from neurons grown on WT astrocytes, and the dashed line is for data from neurons grown on *Fmr1* KO astrocytes.

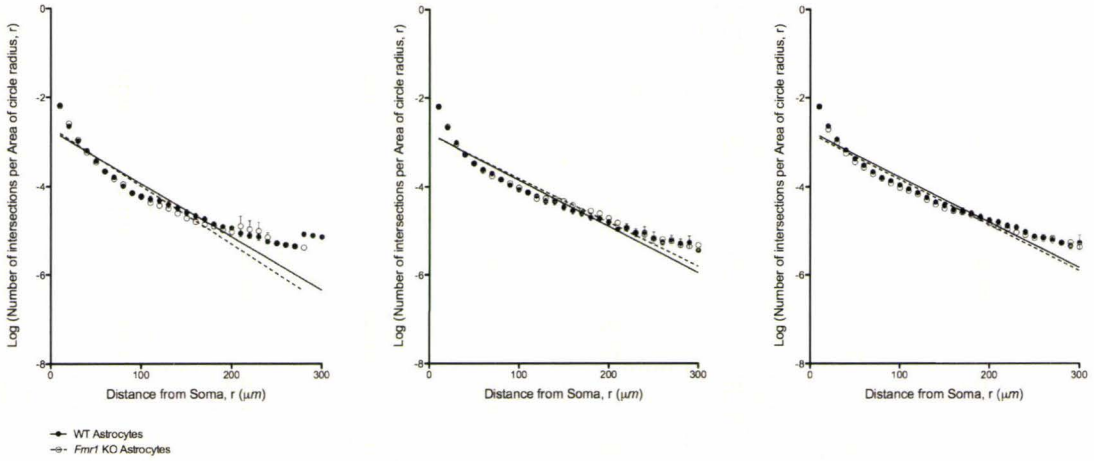
Log (Number of intersections per Area of circle radius, r)
0
-2
-4
-6
-8
0
100
200
300
Distance from Soma, r (μm)
WT Astrocytes
Fmr1 KO Astrocytes

Figure 6.4

Figure 6.5: Linear Sholl analysis of bitufted neurons.

(a) 7 *DIV*, (b) 14 *DIV* and (c) 21 *DIV*. Solid circles are data from neurons grown on WT astrocytes, and open circles are from data of neurons grown on *Fmr1* KO astrocytes. Data are mean ± s.e.m from three independent experiments, a, n(WT)= 10 and n(*Fmr1* KO)=18, b, n(WT)=6 and n(*Fmr1* KO)=5, c, n(WT)=8 and n(*Fmr1* KO)=5. *, significantly different from WT at $p<0.05$, Mann Whitney U tests (two-tailed).

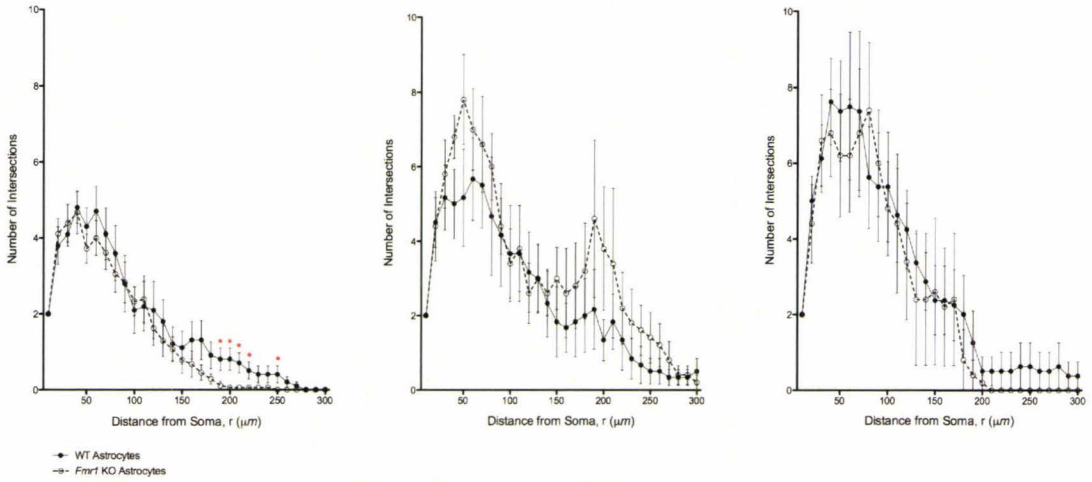
Number of Intersections
Distance from Soma, r (μm)
WT Astrocytes
Fmr1 KO Astrocytes

Figure 6.5

Figure 6.6: Semi-log Sholl analysis of bitufted neurons.

(a) 7 *DIV*, (b) 14 *DIV* and (c) 21 *DIV*. Solid circles are data from neurons grown on WT astrocytes, and open circles are from data of neurons grown on *Fmr1* KO astrocytes. Data are mean ± s.e.m from three independent experiments, a, n(WT)= 10 and n(*Fmr1* KO)=18, b, n(WT)=6 and n(*Fmr1* KO)=5, c, n(WT)=8 and n(*Fmr1* KO)=5. Linear regression lines are shown. Solid line is for data from neurons grown on WT astrocytes, and the dashed line is for data from neurons grown on *Fmr1* KO astrocytes.

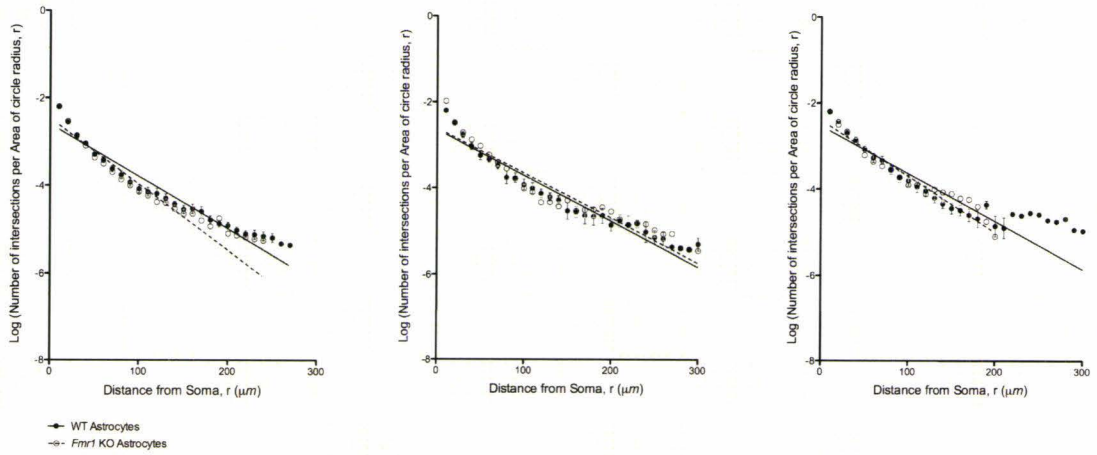
Log (Number of intersections per Area of circle radius, r)
0
-2
-4
-6
-8
0
100
200
300
Distance from Soma, r (μm)
WT Astrocytes
Fmr1 KO Astrocytes

Figure 6.6

Figure 6.7: Linear Sholl analysis of pyramidal neurons.

(a) 7 *DIV*, (b) 14 *DIV* and (c) 21 *DIV*. Solid circles are data from neurons grown on WT astrocytes, and open circles are from data of neurons grown on *Fmr1* KO astrocytes. Data are mean ± s.e.m. from three independent experiments, a, n(WT)=24 and n(*Fmr1* KO)=28, b, n(WT)=26 and n(*Fmr1* KO)=16, c, n(WT)=20 and n(*Fmr1* KO)=22. *, significantly different from WT at $p<0.05$; **, significant at $p<0.01$; ***, significant at $p<0.001$, Mann Whitney U tests (two-tailed).

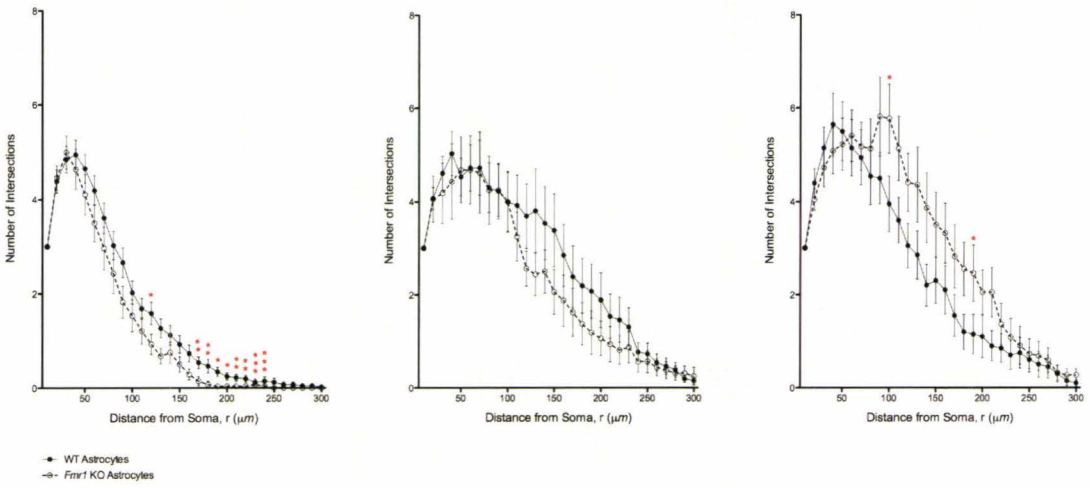
Number of Intersections
Distance from Soma, r (μm)
WT Astrocytes
Fmr1 KO Astrocytes

Figure 6.7

Figure 6.8: Semi-log Sholl analysis of pyramidal neurons.

(a) 7 *DIV*, (b) 14 *DIV* and (c) 21 *DIV*. Solid circles are data from neurons grown on WT astrocytes, and open circles are from data of neurons grown on *Fmr1* KO astrocytes. Data are mean ± s.e.m. from three independent experiments, a, n(WT)=24 and n(*Fmr1* KO)=28, b, n(WT)=26 and n(*Fmr1* KO)=16, c, n(WT)=20 and n(*Fmr1* KO)=22. Linear regression lines are shown. Solid line is for data from neurons grown on WT astrocytes, and the dashed line is for data from neurons grown on *Fmr1* KO astrocytes.

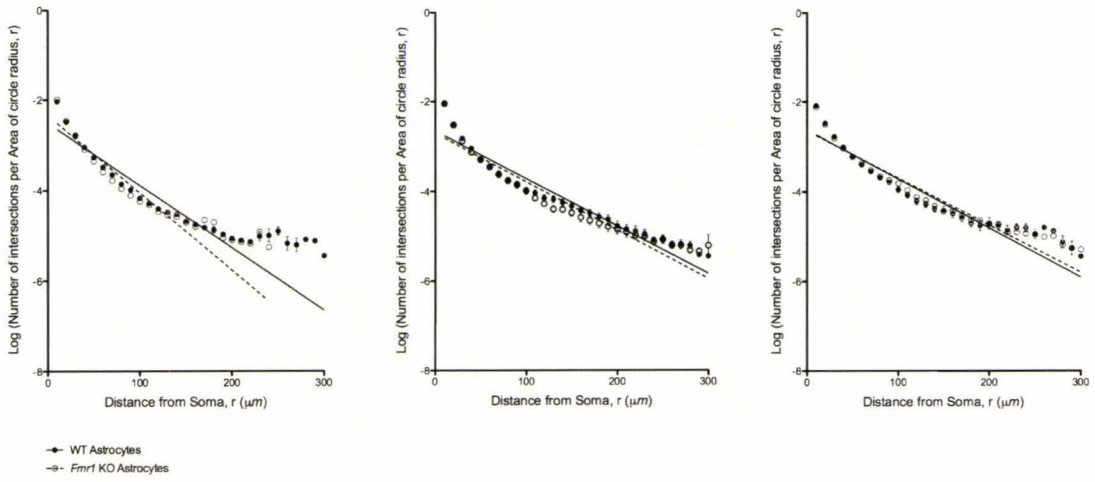
Log (Number of intersections per Area of circle radius, r)
0
-2
-4
-6
-8
0
100
200
300
Distance from Soma, r (μm)
WT Astrocytes
Fmr1 KO Astrocytes

Figure 6.8

Figure 6.9: Linear Sholl analysis of multipolar neurons.

(a) 7 *DIV*, (b) 14 *DIV* and (c) 21 *DIV*. Solid circles are data from neurons grown on WT astrocytes, and open circles are from data of neurons grown on *Fmr1* KO astrocytes. Data are mean ± s.e.m., from three independent experiments, a, n(WT)=69 and n(*Fmr1* KO)=66, b, n(WT)=76 and n(*Fmr1* KO)=86, c, n(WT)=65 and n(*Fmr1* KO)=53. *, significantly different from WT at $p<0.05$; **, significant at $p<0.01$; ***, significant at $p<0.001$, Mann Whitney U tests (two-tailed).

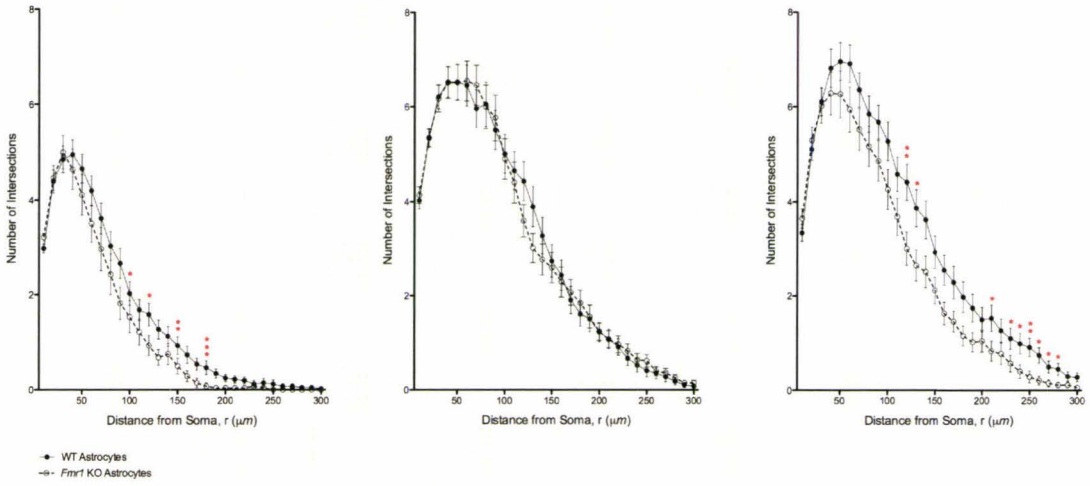
Number of Intersections
Distance from Soma, r (μm)
WT Astrocytes
Fmr1 KO Astrocytes

Figure 6.9

Figure 6.10: Semi-log Sholl analysis of multipolar neurons.

(a) 7 *DIV*, (b) 14 *DIV* and (c) 21 *DIV*. Solid circles are data from neurons grown on WT astrocytes, and open circles are from data of neurons grown on *Fmr1* KO astrocytes. Data are mean ± s.e.m., from three independent experiments, a, n(WT)=69 and n(*Fmr1* KO)=66, b, n(WT)=76 and n(*Fmr1* KO)=86, c, n(WT)=65 and n(*Fmr1* KO)=53. Linear regression lines are shown. Solid line is for data from neurons grown on WT astrocytes, and the dashed line is for data from neurons grown on *Fmr1* KO astrocytes.

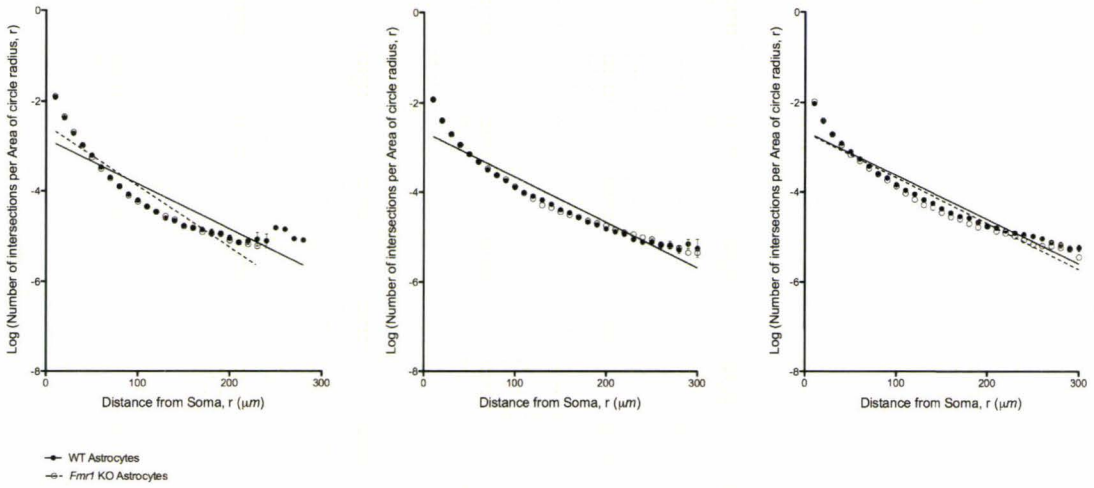
Log (Number of intersections per Area of circle radius, r)
0
-2
-4
-6
-8
0
100
200
300
Distance from Soma, r (μm)
WT Astrocytes
Fmr1 KO Astrocytes

Figure 6.10

Figure 6.11: Linear Sholl analysis of stellate neurons.

(a) 7 *DIV*, (b) 14 *DIV* and (c) 21 *DIV*. Solid circles are data from neurons grown on WT astrocytes, and open circles are from data of neurons grown on *Fmr1* KO astrocytes. Data are mean ± s.e.m., from three independent experiments, a, n(WT)=5 and n(*Fmr1* KO)=12, b, n(WT)=15 and n(*Fmr1* KO)=12, c, n(WT)=15 and n(*Fmr1* KO)=25. *, significantly different from WT at $p<0.05$; **, significant at $p<0.01$, Mann Whitney U tests (two-tailed).

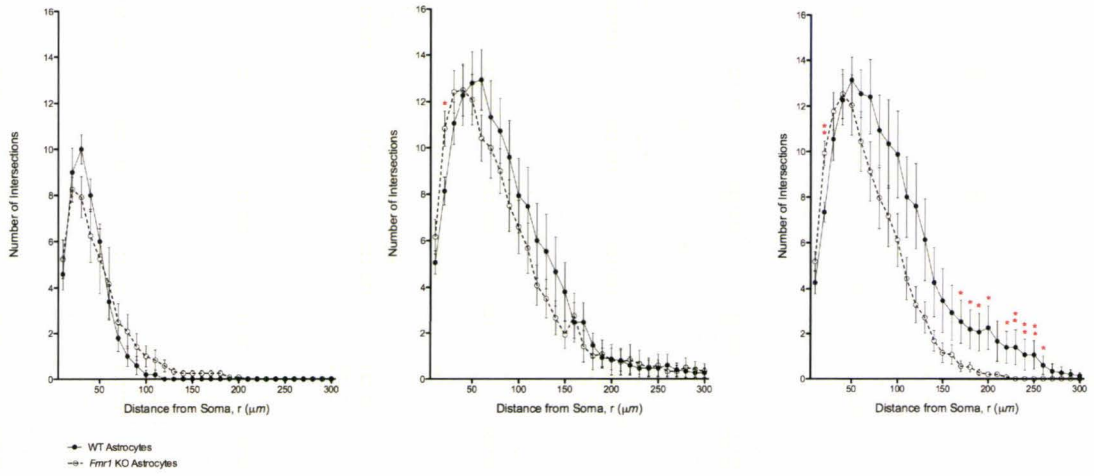
Number of Intersections
Distance from Soma, r (μm)
WT Astrocytes
Fmr1 KO Astrocytes

Figure 6.11

Figure 6.12: Semi-log Sholl analysis of stellate neurons.

(a) 7 *DIV*, (b) 14 *DIV* and (c) 21 *DIV*. Solid circles are data from neurons grown on WT astrocytes, and open circles are from data of neurons grown on *Fmr1* KO astrocytes. Data are mean ± s.e.m., from three independent experiments, a, n(WT)=5 and n(*Fmr1* KO)=12, b, n(WT)=15 and n(*Fmr1* KO)=12, c, n(WT)=15 and n(*Fmr1* KO)=25. Linear regression lines are shown. Solid line is for data from neurons grown on WT astrocytes, and the dashed line is for data from neurons grown on *Fmr1* KO astrocytes.

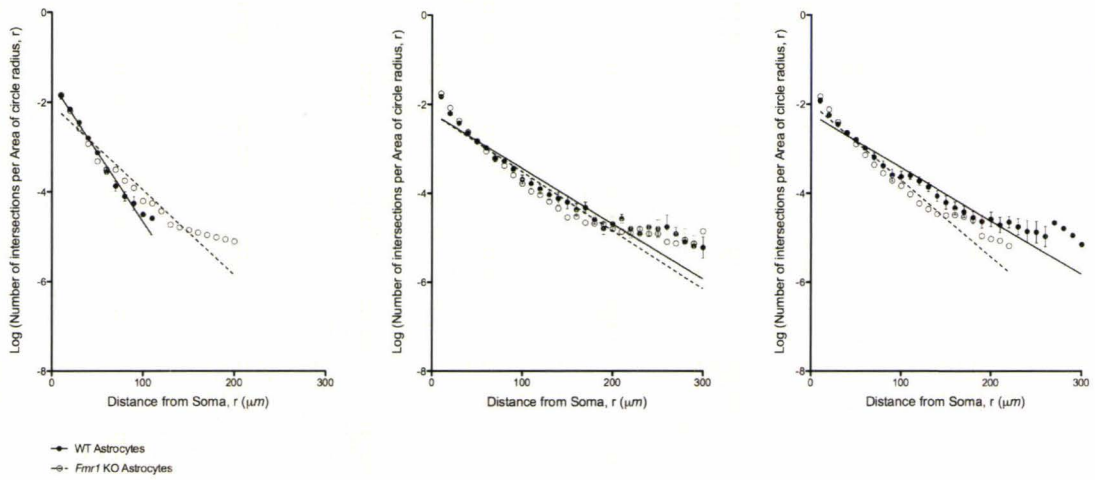
Log (Number of intersections per Area of circle radius, r)
0
-2
-4
-6
-8
0
100
200
300
Distance from Soma, r (μm)
WT Astrocytes
Fmr1 KO Astrocytes

Figure 6.12

Figure 6.13: Dendrite branching and Sholl analysis

Schematic diagram depicting an important concept to remember when interpreting the results from Sholl analysis as an indicator of ramification of dendritic arbors. The neuron on the right has a dendritic arbor that is visibly more densely branched than the neuron on the left. However, due to the nature of the branches – shorter than the space between concentric circles (closed arrow-head), or branches that extend some distance but fall completely within on circle (open arrow-head) – these branches will be overlooked when using Sholl analysis. The end result would be that the two neurons had identical degrees of ramification.

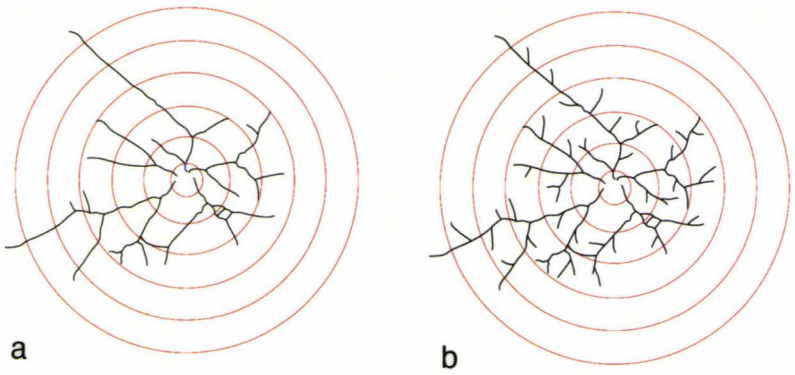

Figure 6.13

CHAPTER 7:
CONCLUSIONS AND FUTURE DIRECTIONS

7. Conclusions & Future directions

7.2 Conclusions

The manuscripts presented in this dissertation were comprised of experiments that were designed to provide evidence for the central hypothesis of this thesis:

Astrocytes contribute to the development of
the abnormal neurobiology seen in Fragile X Syndrome.

From this hypothesis, two specific hypotheses followed:

1) Fragile X Astrocytes alter the maturation of dendritic arbors of neurons in Fragile X Syndrome.
2) Fragile X Astrocytes contribute to the altered excitatory synapse development of neurons in Fragile X Syndrome.

In order to address these hypotheses, the present experiments were based on a set of six Specific Aims (see **Section 2.2**). Each of the manuscripts in Chapters 4 through 6, contain experiments that were designed to address these Specific Aims. The major findings of each paper, and their contribution to the substantiation of the hypotheses are provided below.

7.1.1 Chapter 4.

In this chapter, the experiments were designed to address the Specific Aims 1 through 4. In the first set of experiments, WT hippocampal neurons were cultured with WT or *FMR1* null astrocytes for 7 *DIV*, and the dendritic morphology and excitatory synaptic protein expression were evaluated. The results indicate that *FMR1* KO astrocytes induce significant changes in the morphology of the dendritic arbors of WT neurons. The neurons grown on *FMR1* null astrocytes exhibit a decrease in the extension, and an increase in the branching, of their dendritic arbors, when compared to WT neurons

grown on WT astrocytes. WT neurons grown on *FMR1* null astrocytes also exhibit significantly fewer pre- and post- synaptic proteins, than the WT neurons cultured on WT astrocytes. Therefore the results provide evidence that *FMR1* KO astrocytes induce abnormal dendrite morphology and alterations of excitatory synaptic protein expression in WT neurons in culture (Specific aims 1 and 2).

In the second set of experiments, *FMR1* KO neurons were cultured with WT or *FMR1* KO astrocytes for 7 *DIV*, and the dendrite morphology and excitatory synaptic protein expression were evaluated. The results suggest that WT astrocytes can prevent the development of an abnormal dendritic arbor morphology in *FMR1* null neurons. The *FMR1* KO neurons grown with WT astrocytes exhibit dendritic arbor morphologies that are significantly different from *FMR1* null neurons grown on *FMR1* null astrocytes. Furthermore, the characteristics of the *FMR1* null neurons grown on WT astrocytes are similar to those of WT neurons grown on WT astrocytes. The findings also provide evidence that WT astrocytes prevent significant alterations in excitatory synaptic protein expression in *FMR1* KO neurons. The *FMR1* KO neurons grown on WT astrocytes exhibited significantly more pre-synaptic protein puncta, and an increased number of post-synaptic protein puncta than the *FMR1* null neurons grown on *FMR1* KO astrocytes. Moreover, the *FMR1* null neurons grown on WT astrocytes displayed similar numbers of excitatory protein puncta as seen in the WT neurons cultured with WT astrocytes. These findings demonstrate that WT astrocytes can prevent the abnormal dendrite morphology and altered synaptic protein expression of *FMR1* null neurons in culture (Specific Aims 3 and 4). Together, these results provide support for the hypothesis that *FMR1* KO astrocytes are involved in the development of the abnormal dendritic morphology and excitatory synaptic protein expression of neurons seen in FXS (Specific Hypotheses 1 and 2), and therefore help substantiate the central hypothesis of this thesis: Astrocytes contribute to the development of the abnormal neurobiology seen in Fragile X Syndrome.

7.1.2 Chapter 5.

In this chapter the experiments were designed to address Specific Aims 5 and 6.

In these experiments WT neurons were cultured with WT or *FMR1* null astrocytes for 7, 14 or 21 *DIV*, and the dendrite morphology and excitatory synaptic protein expression were evaluated. The results suggest that the *FMR1* null astrocytes impart a developmental delay on the maturation of the dendritic arbor and the excitatory synapses. At 7 *DIV* WT neurons grown on *FMR1* KO astrocytes exhibited significantly altered dendritic morphologies and excitatory synaptic protein expression, when compared to WT neurons grown on WT astrocytes. This was consistent with the results reported in Chapter 4. However, at 21 *DIV* the WT neurons grown on *FMR1* null astrocytes no longer displayed significant alterations in their dendrite morphologies or in their excitatory synapse expression, compared to WT neurons grown on WT astrocytes. At 21 *DIV*, the WT neurons grown on *FMR1* null astrocytes exhibited dendrite morphologies and excitatory synaptic protein expression similar to that of WT neurons grown on WT astrocytes. These results provide evidence that the abnormalities in the dendritic arbors and excitatory synapse expression of WT neurons that are induced by the *FMR1* null astrocytes, are due to delays in development (Specific Aims 5 and 6). Furthermore, these findings help substantiate the theory that the abnormalities in the dendrites and in the excitatory synaptic protein expression of the neurons in FXS, are partially caused by astrocytes (Specific Hypothesis 1 and 2). Therefore these results further support the central hypothesis of this thesis: Astrocytes contribute to the development of the abnormal neurobiology seen in Fragile X Syndrome.

7.1.3 Chapter 6.

The experiments in Chapter 6 were designed to further address Specific Aim 5. In these experiments WT hippocampal neurons were grown with WT or *FMR1* KO astrocytes, and the morphology of the neuronal dendritic arbors were assessed by Linear and Semi-log Sholl analyses. Importantly, the population of cultured neurons was divided based on dendritic arbor morphology, and the analyses were performed on the five neuronal subtypes independently. The findings suggest that *FMR1* null astrocytes induce significant alterations in the morphology of WT hippocampal neurons at 7 *DIV*,

consistent with previous results. Furthermore, the results indicate that the effect of *FMR1* null astrocytes specifically targets neurons with a spiny stellate morphology. The WT neurons designated as having stellate morphology displayed significant alterations in dendritic arbor morphology, when grown on *FMR1* null astrocytes compared to those grown on WT astrocytes, and this significant change persisted until the 21 *DIV* time point. These results provide evidence that *FMR1* null astrocytes induce alterations in the morphology of the dendritic arbors of WT neurons in culture (Specific Aim 5). Therefore, these finding help substantiate the hypothesis that astrocytes contribute to the altered dendrite morphology of neurons seen in FXS (Specific Hypothesis 1), and further support the central hypothesis of this thesis: Astrocytes contribute to the development of the abnormal neurobiology seen in Fragile X Syndrome.

Therefore, the results presented in the manuscripts included in this dissertation provide convincing evidence for the central hypothesis of this thesis: Astrocytes contribute to the development of the abnormal neurobiology seen in Fragile X Syndrome. These experiments are the first to suggest a role for astrocytes in the development of the abnormal neuronal phenotype seen in FXS. As such, these findings present significant implications for future Fragile X research. They provide a new, and exciting, direction for studies investigating the underlying processes leading to the abnormal neuronal phenotype seen in FXS, with the potential for gaining a greater understanding of the abnormal neurobiological mechanisms causing FXS. Furthermore, and perhaps most importantly, the novel prospect for a role for astrocytes in the development of FXS will create many possibilities for new therapeutic targets and innovative treatment strategies for individuals with FXS.

7.2 Future directions

The author of this dissertation recognizes that these experiments are only the initial stepping stone towards validating the proposed hypothesis, and that a number of other studies are required to further substantiate the hypothesis. A few of the possible

studies are briefly described below.

7.2.1 Investigations in the GFAP-*FMR1* conditional knockout mouse

In vitro methods provide an excellent means for investigating the mechanisms underlying disease. They allow the study of disease processes in an environment isolated from the complexity of that *in vivo*. Additionally, neurons in culture are more accessible for experiments that require the visualization of neurite and synaptic properties, due to a lessening of the intricate networks present *in vivo*.

However, this isolation also has its draw-backs. In the *in vitro* environment the cells are not subject to all aspects of the normal *in situ* environmental milieu. This can pose problems for the interpretation of *in vitro* results. Therefore, while the information obtained from *in vitro* studies is invaluable, investigations in an *in vivo* correlate are often desirable.

The experiments presented in this dissertation were conducted on primary neurons isolated *in vitro*. Therefore, a logical next step would be to investigate whether a similar affect of astrocytes could be observed *in vivo*.

In 2006, Mientjes and co-workers developed an *FMR1* conditional knockout (CKO) mouse, by flanking the promoter and first exon of the *FMR1* gene with *lox* P sites. In contrast to the *FMR1* knockout mouse model used in these experiments the CKO permits the tissue specific targeted expression of FMRP. Mientjes and colleagues demonstrated how, through the breeding with a Purkinje-cell-specific cre-recombinase expresser, mice with FMRP expression in all cells except the Purkinje neurons could be generated (Mientjes, et al., 2006).

In order to determine whether astrocytes have the same effects on the dendrite morphology and synaptic development *in vivo*, as seen in the present experiments *in vitro*, a mouse would need to be created in which the *FMR1* gene was absent in astrocytes. A GFAP-specific cre-recombinase expressing mouse is available through The Jackson Laboratories. Through breeding the *FMR1* CKO and the GFAP-cre mice, offspring would be created that should have normal FMRP expression in all tissues, with

the exception of GFAP expressing cells (i.e., astrocytes).

Once the FMRP expression patterns of the offspring were confirmed, a series of experiments could be performed to address the *in vivo* questions. For example, using the Golgi stain, the dendrite morphologies of neurons in these mice could be studied. Additionally, any alterations in synaptic protein expression could be assessed using western blotting of proteins from synaptoneurosome preparations. These two examples would provide an *in vivo* correlate for the results presented in this dissertation. Moreover, the GFAP-*FMR1*-CKO mice would provide a model in which more in depth investigations of the astrocyte mediated effects in the neuropathology of FXS.

7.2.2 Dendritic spine morphologies

An example of one such study would be the investigation into the effects of astrocytes on dendritic spine morphology in FXS. The most prominent feature of neurons in both humans and mice with Fragile X are the alterations in the dendritic spines (Comery, et al., 1997; Galvez & Greenough, 2005; Grossman, et al., 2006; Irwin, et al., 2000; Irwin, et al., 2002; Irwin, et al., 2001; McKinney, et al., 2005; Nimchinsky, et al., 2001).

In the experiments presented here, we assessed the astrocyte-mediated alterations in neuronal dendrite morphology, however the MAP2-based immunofluorescent technique used was not sensitive enough to visualize the dendritic spines. It has been suggested that the co-localization of pre- and post-synaptic proteins identifies a mature synapse (Ullian, et al., 2001), and that the number of mature synapses exists in an approximately 1:1 ratio with the number of dendritic spines (Harris, et al., 1992; Nimchinsky, et al., 2004). Therefore, from the results presented in this thesis, an approximation of the alterations in the number of dendritic spines can be deduced: since the number of excitatory synapses increased the number of mature dendritic spines was probably also increased when neurons were grown with *FMR1* null astrocytes. However, this supposition needs to be confirmed with methods intended to directly assess astrocyte-mediated alterations on dendritic spines. For example, using carbocynaine fluorescent

lipophilic dyes such as DiI or DiO to label the dendritic spines of fixed neurons (Godement, Vanselow, Thanos, & Bonhoeffer, 1987), or the Golgi staining method in the above-suggested *in vivo* GFAP-*FMR1*-CKO mouse model, could provide information about the numbers of dendritic spines. Furthermore, these methods would also enable evaluations of the morphologies of the dendritic spines when neurons were in the presence (whether *in vitro* or *in vivo*) of astrocytes lacking FMRP.

7.2.3 Astrocyte FMRP

From the experiments presented in this dissertation it is not possible to draw a conclusion regarding the molecular mechanisms of the effects *FMR1* astrocytes. We found that astrocytes isolated from an *FMR1* null mouse exert inhibitory effects on dendrite and synapse maturation. However, this could be due to one of two mechanisms. First, it is possible that the astrocyte-mediated alterations are due to an indirect effect of the loss of FMRP. In other words, the lack of FMRP in the neurons (and in the animal as a whole) creates a 'diseased' environment that fosters the development of abnormal astrocytes that are unable to support normal neuron growth. Neurons are known to signal to astrocytes (Allen & Barres, 2009), and therefore it is possible that *FMR1* null neurons are unable to effectively signal to astrocytes to promote the astrocytes' normal maturation and functioning.

Second, and perhaps more intriguing, is the possibility that it is a direct effect of the loss of FMRP: the functioning of the astrocytes is altered by a lack of their own FMRP. Our lab recently demonstrated that FMRP is expressed in cells of the glial lineage early in development (Pacey & Doering, 2007). The primary cultures of astrocytes used in the experiments for this thesis were also found to express FMRP (personal observation). Therefore it is possible that, similar to the role of FMRP in neurons, FMRP may act as a translational regulator in astrocytes. In fact, there are a number of known FMRP targets that are also found in astrocytes such as the structural proteins, actin (Groschel-Stewart, Unsicker, & Leonhardt, 1977) (Liao, et al., 2008), vimentin (Fedoroff, White, Neal, Subrahmanyan, & Kalnins, 1983; Liao, et al., 2008),

and MAP1B (Lu, et al., 2004; Ulloa, Ibarrola, Avila, & Diez-Guerra, 1994). Dynamic structural changes in astrocytic processes surround synapses have been shown to affect the morphology of dendritic spines (Haber, Zhou, & Murai, 2006). Subunits of the glutamate transporter (GLT1) are also found in astrocytes, and are a known target of FMRP (Guillet, et al., 2002; Kugler & Schleyer, 2004; Liao, et al., 2008). Astrocytes are responsible for the rapid removal of glutamate from the extracellular space, a process that is essential for the normal functioning and survival of neurons (Anderson & Swanson, 2000). Additionally, glutamate uptake and release via the reversal of glutamate transporters, is important for regulating the activity of glutamatergic synapses (Anderson & Swanson, 2000). Therefore a lack of astrocyte FMRP could cause alterations in the expression of these proteins, and thereby potentially impede these vital astrocyte functions. Furthermore, the complete array of FMRP targets is not yet known, and therefore it is possible that there are a number of other proteins that are regulated by astrocyte-FMRP. A lack of astrocyte FMRP would thereby have a direct effect on translation of astrocyte proteins, which could therefore affect the functioning of the astrocyte. In turn, this lack of astrocyte FMRP would result in abnormal astrocytes that cannot support normal neuron growth and development.

The differentiation between these two mechanisms is important for the development of more tailored therapies for FXS. In order to determine if it is astrocyte FMRP that is causing the observed effects, the following *in vitro* experiments could be performed. Using a similar co-culture procedure, WT neurons could be grown with both WT and *FMR1* KO astrocytes with the following modifications. WT astrocytes would be treated with *FMR1* siRNA, and then co-cultured with WT neurons. The morphology of WT neurons grown in this condition would be compared to WT neurons grown with untreated WT astrocytes. Similarly, *FMR1* KO astrocytes could be transfected with FMRP. WT neurons could be grown on both the transfected and non-transfected *FMR1* KO astrocytes, and their morphologies and synaptic protein expression profiles could then be compared. These experiments would help determine if it is the astrocyte FMRP specifically that is a contributing factor to the underlying abnormal neurobiology of FXS.

7.2.4 mGluR-dependent protein translation in astrocytes

The role of group 1 mGluRs in FXS has focused solely on neurons; however, cultured hippocampal astrocytes have also been shown to express mGluR1 and mGluR5 (Aronica, et al., 2003; Cai, Schools, & Kimelberg, 2000; Schools & Kimelberg, 1999; Silva, Theriault, Mills, Pennefather, & Feeney, 1999; Vermeiren, et al., 2006). In preliminary experiments we also found that mGluR1 and mGluR5 were expressed in our primary astrocyte population (personal observation). The role of mGluRs in astrocytes is not well understood, but these receptors have been proposed to play a role in astrocyte proliferation and the modulation of synaptic transmission by regulating glutamate levels at the synapse (Ye & Sontheimer, 1999). mGluR agonists also stimulate the transcription of neurotrophins such as BDNF and NGF, and growth factors such as basic fibroblast growth factor (bFGF), in primary astrocyte cultures suggesting that mGluR signaling may influence neuron growth and development including the formation of fully functional synapses (Pechan, Chowdhury, Gerdes, & Seifert, 1993). Interestingly, astrocytic mGluR5 expression is highest during early postnatal development in the rat (Cai, et al., 2000), which correlates with peak periods of synapse formation. Furthermore, this corresponds to the period in which our laboratory observed the expression of FMRP in astrocytes in the mouse brain (Pacey & Doering, 2007). Our preliminary studies also revealed that FMRP was expressed in primary astrocyte cultures (personal observation). Notably, FMRP was co-expressed with group I mGluRs in our astrocyte population *in vitro* (personal observation). Together, this suggests that both FMRP and mGluRs could be expressed in cells of the astrocyte lineage at a developmental time point in which they could play an integral role in neuronal growth and synapse development.

Given that cells of the astrocyte lineage also express group 1 mGluRs, is it possible that FMRP and mGluR5 interact in astrocytes in a manner similar to that proposed in neurons? In other words, is it possible that a loss of FMRP, as seen in FXS could result in the altered regulation of mGluR signaling in astrocytes, as theorized to occur in neurons. The resulting dysregulation of protein interactions could render the

astrocytes less capable of effectively promoting the appropriate development of synapses and dendrites, and could contribute to the alterations in neuronal development seen in FXS. The interactions between astrocytic mGluR and FMRP on neurons have not been studied in relation to dendrite maturation, and could provide an important target for therapies for FXS.

The following experiments could be used to determine whether any changes in neuron survival and/or development in FXS are mediated through changes in FMRP and/or mGluR5 activity in the astrocyte. The question can be addressed through two independent approaches to examine the affects of astrocyte FMRP and mGluR expression and signaling on neuronal maturation *in vitro*. The first is a pharmacological approach using agonists and antagonists of mGluRs. To gain insight into mGluR signaling, the mGluR selective agonist, DHPG (Stoop, Conquet, & Pralong, 2003) or the mGluR5 specific antagonist, MPEP (Chapman, Nanan, Williams, & Meldrum, 2000), could be added to the culture media of similar co-cultures as presented in this thesis. These experiments will explore the role group 1 mGluR activation with or without astrocyte FMRP on the phenotype of the neurons in the co-cultures. It is important to realize that the receptors on both neurons and astrocytes will be stimulated with the addition of mGluR agonists or antagonists in these cultures. However, this is not unlike the *in vivo* environment, and therefore the results can demonstrate the effect of the presence/absence of astrocyte FMRP on neuronal morphology under these conditions.

The second is a double mouse mutant paradigm. The *FMR1* knockout mouse could be crossed with mice expressing one functional copy (reduced expression) of the *mGluR5* gene (The Jackson Laboratory) to develop a double mutant mouse model that exhibits reduced expression of mGluR5 (heterozygote mice) and does not express FMRP. Co-cultures of astrocytes and neurons would then established as described in Chapter 3, from the two lines of mice to create the following possibilities.

	Astrocytes	**Neurons**
A	WT *mGluR5* +/-	*FMR1* KO
B	*FMR1* KO *mGluR* +/-	*FMR1* KO
C	WT *mGluR5* +/-	WT
D	*FMR1* KO *mGluR* +/-	WT

Then, the dendrite and dendritic spine morphology, and synaptic protein expression can be evaluated (as presented in **Chapters 4-6** and **Section 7.2.2**).

As mentioned above, in the *in vitro* experiments all receptors on both astrocytes and neurons will be affected. On the other hand, for the genetic model, combinations of astrocytes expressing or not expressing FMRP, combined with normal or reduced expression of mGluR5, would permit the investigation into a role for mGluR5 in astrocytes, independent of any action of mGluR5 in neurons (which would all express mGluR5 in this model). Given the cognitive deficits observed in mGluR5 knockout mice, a more biologically relevant result would be expected using mice that under-express mGluR5 (heterozygotes) than those that completely lack expression (full knockout). However, if a large enough difference is not seen with mGluR5 heterozygous mice, mGluR5 knockout mice could be crossed with *FMR1* knockout mice and the same experiments repeated.

In summary, the experiments described in this dissertation are the foundation for the theory that is the central hypothesis of this thesis: Astrocytes contribute to the development of the abnormal neurobiology seen in Fragile X Syndrome. However, as described above, a number of other studies need to be completed to further substantiate this proposal. None-the-less, the experiments presented in this thesis are the first to provide evidence for a role of astrocytes in the development of the abnormal neurobiology seen in FXS. As such they provide exciting new avenues for FXS research and many novel possibilities for investigations into innovative therapeutic targets for the treatment of FXS

References

Acebes, A., & Ferrus, A. (2000). Cellular and molecular features of axon collaterals and dendrites. *Trends Neurosci, 23*(11), 557-565.

Adinolfi, S., Bagni, C., Musco, G., Gibson, T., Mazzarella, L., & Pastore, A. (1999). Dissecting FMR1, the protein responsible for fragile X syndrome, in its structural and functional domains. *RNA, 5*(9), 1248-1258.

Allen, N. J., & Barres, B. A. (2009). Neuroscience: Glia - more than just brain glue. *Nature, 457*(7230), 675-677.

Altman, J., & Anderson, W. J. (1972). Experimental reorganization of the cerebellar cortex. I. Morphological effects of elimination of all microneurons with prolonged x-irradiation started at birth. *J Comp Neurol, 146*(3), 355-406.

Alvarez, V. A., & Sabatini, B. L. (2007). Anatomical and physiological plasticity of dendritic spines. *Annu Rev Neurosci, 30*, 79-97.

Anderson, C. M., & Swanson, R. A. (2000). Astrocyte glutamate transport: review of properties, regulation, and physiological functions. *Glia, 32*(1), 1-14.

Anderton, B. H., Callahan, L., Coleman, P., Davies, P., Flood, D., Jicha, G. A., et al. (1998). Dendritic changes in Alzheimer's disease and factors that may underlie these changes. *Prog Neurobiol, 55*(6), 595-609.

Antar, L. N., Afroz, R., Dictenberg, J. B., Carroll, R. C., & Bassell, G. J. (2004). Metabotropic glutamate receptor activation regulates fragile x mental retardation protein and FMR1 mRNA localization differentially in dendrites and at synapses. *J Neurosci, 24*(11), 2648-2655.

Antar, L. N., Dictenberg, J. B., Plociniak, M., Afroz, R., & Bassell, G. J. (2005). Localization of FMRP-associated mRNA granules and requirement of microtubules for activity-dependent trafficking in hippocampal neurons. *Genes Brain Behav, 4*(6), 350-359.

Antar, L. N., Li, C., Zhang, H., Carroll, R. C., & Bassell, G. J. (2006). Local functions for FMRP in axon growth cone motility and activity-dependent regulation of

filopodia and spine synapses. *Mol Cell Neurosci, 32*(1-2), 37-48.

Araque, A., Parpura, V., Sanzgiri, R. P., & Haydon, P. G. (1999). Tripartite synapses: glia, the unacknowledged partner. *Trends Neurosci, 22*(5), 208-215.

Aronica, E., Gorter, J. A., Ijlst-Keizers, H., Rozemuller, A. J., Yankaya, B., Leenstra, S., et al. (2003). Expression and functional role of mGluR3 and mGluR5 in human astrocytes and glioma cells: opposite regulation of glutamate transporter proteins. *Eur J Neurosci, 17*(10), 2106-2118.

Ashley, C. T., Jr., Wilkinson, K. D., Reines, D., & Warren, S. T. (1993). FMR1 protein: conserved RNP family domains and selective RNA binding. *Science, 262*(5133), 563-566.

Bagni, C. (2008). On BC1 RNA and the fragile X mental retardation protein. *Proc Natl Acad Sci U S A, 105*(17), E19.

Baker, R. E., Dijkhuizen, P. A., Van Pelt, J., & Verhaagen, J. (1998). Growth of pyramidal, but not non-pyramidal, dendrites in long-term organotypic explants of neonatal rat neocortex chronically exposed to neurotrophin-3. *Eur J Neurosci, 10*(3), 1037-1044.

Bakker, C., Verheij, C., Willemsen, R., van der Helm, R., Oerlemans, F., Vermey, M., et al. (1994). Fmr1 knockout mice: a model to study fragile X mental retardation. The Dutch-Belgian Fragile X Consortium. *Cell, 78*(1), 23-33.

Bakker, C. E., de Diego Otero, Y., Bontekoe, C., Raghoe, P., Luteijn, T., Hoogeveen, A. T., et al. (2000). Immunocytochemical and biochemical characterization of FMRP, FXR1P, and FXR2P in the mouse. *Exp Cell Res, 258*(1), 162-170.

Ballas, N., Lioy, D. T., Grunseich, C., & Mandel, G. (2009). Non-cell autonomous influence of MeCP2-deficient glia on neuronal dendritic morphology. *Nat Neurosci, 12*(3), 311-317.

Banker, G. A., & Cowan, W. M. (1977). Rat hippocampal neurons in dispersed cell culture. *Brain Res, 126*(3), 397-342.

Banker, G. A., & Cowan, W. M. (1979). Further observations on hippocampal neurons in dispersed cell culture. *J Comp Neurol, 187*(3), 469-493.

Barth, M., Hirsch, H. V., Meinertzhagen, I. A., & Heisenberg, M. (1997). Experience-dependent developmental plasticity in the optic lobe of Drosophila melanogaster. *J Neurosci, 17*(4), 1493-1504.

Bartlett, W. P., & Banker, G. A. (1984). An electron microscopic study of the development of axons and dendrites by hippocampal neurons in culture. II. Synaptic relationships. *J Neurosci, 4*(8), 1954-1965.

Bassell, G. J., & Gross, C. (2008). Reducing glutamate signaling pays off in fragile X. *Nat Med, 14*(3), 249-250.

Bear, M. F., Huber, K. M., & Warren, S. T. (2004). The mGluR theory of fragile X mental retardation. *Trends Neurosci, 27*(7), 370-377.

Beattie, E. C., Stellwagen, D., Morishita, W., Bresnahan, J. C., Ha, B. K., Von Zastrow, M., et al. (2002). Control of synaptic strength by glial TNFalpha. *Science, 295*(5563), 2282-2285.

Bechara, E. G., Didiot, M. C., Melko, M., Davidovic, L., Bensaid, M., Martin, P., et al. (2009). A novel function for fragile X mental retardation protein in translational activation. *PLoS Biol, 7*(1), e16.

Beckel-Mitchener, A., & Greenough, W. T. (2004). Correlates across the structural, functional, and molecular phenotypes of fragile X syndrome. *Ment Retard Dev Disabil Res Rev, 10*(1), 53-59.

Bertram, E. H. (2009). Temporal lobe epilepsy: where do the seizures really begin? *Epilepsy Behav, 14 Suppl 1*, 32-37.

Bittel, D. C., Kibiryeva, N., & Butler, M. G. (2007). Whole genome microarray analysis of gene expression in subjects with fragile X syndrome. *Genet Med, 9*(7), 464-472.

Bliss, T. V., & Gardner-Medwin, A. R. (1973). Long-lasting potentiation of synaptic transmission in the dentate area of the unanaestetized rabbit following stimulation of the perforant path. *J Physiol, 232*(2), 357-374.

Bliss, T. V., & Lomo, T. (1973). Long-lasting potentiation of synaptic transmission in the dentate area of the anaesthetized rabbit following stimulation of the perforant

path. *J Physiol, 232*(2), 331-356.

Blondel, O., Collin, C., McCarran, W. J., Zhu, S., Zamostiano, R., Gozes, I., et al. (2000). A glia-derived signal regulating neuronal differentiation. *J Neurosci, 20*(21), 8012-8020.

Boothe, R. G., Greenough, W. T., Lund, J. S., & Wrege, K. (1979). A quantitative investigation of spine and dendrite development of neurons in visual cortex (area 17) of Macaca nemestrina monkeys. *J Comp Neurol, 186*(3), 473-489.

Borges, S., & Berry, M. (1978). The effects of dark rearing on the development of the visual cortex of the rat. *J Comp Neurol, 180*(2), 277-300.

Bradke, F., & Dotti, C. G. (1997). Neuronal polarity: vectorial cytoplasmic flow precedes axon formation. *Neuron, 19*(6), 1175-1186.

Bradke, F., & Dotti, C. G. (2000). Differentiated neurons retain the capacity to generate axons from dendrites. *Curr Biol, 10*(22), 1467-1470.

Bramham, C. R., & Wells, D. G. (2007). Dendritic mRNA: transport, translation and function. *Nat Rev Neurosci, 8*(10), 776-789.

Braun, K., & Segal, M. (2000). FMRP involvement in formation of synapses among cultured hippocampal neurons. *Cereb Cortex, 10*(10), 1045-1052.

Bray, D. (1973). Branching patterns of individual sympathetic neurons in culture. *J Cell Biol, 56*(3), 702-712.

Brennan, F. X., Albeck, D. S., & Paylor, R. (2006). Fmr1 knockout mice are impaired in a leverpress escape/avoidance task. *Genes Brain Behav, 5*(6), 467-471.

Briones, T. L., Klintsova, A. Y., & Greenough, W. T. (2004). Stability of synaptic plasticity in the adult rat visual cortex induced by complex environment exposure. *Brain Res, 1018*(1), 130-135.

Brose, N. (1999). Synaptic cell adhesion proteins and synaptogenesis in the mammalian central nervous system. *Naturwissenschaften, 86*(11), 516-524.

Brouwer, J. R., Willemsen, R., & Oostra, B. A. (2008). The FMR1 gene and fragile X-associated tremor/ataxia syndrome. *Am J Med Genet B Neuropsychiatr Genet*.

Brown, V., Jin, P., Ceman, S., Darnell, J. C., O'Donnell, W. T., Tenenbaum, S. A., et al.

(2001). Microarray identification of FMRP-associated brain mRNAs and altered mRNA translational profiles in fragile X syndrome. *Cell, 107*(4), 477-487.

Bureau, I. (2009). The development of cortical columns: role of Fragile X mental retardation protein. *J Physiol, 587*(Pt 9), 1897-1901.

Bureau, I., Shepherd, G. M., & Svoboda, K. (2008). Circuit and plasticity defects in the developing somatosensory cortex of FMR1 knock-out mice. *J Neurosci, 28*(20), 5178-5188.

Bushong, E. A., Martone, M. E., & Ellisman, M. H. (2004). Maturation of astrocyte morphology and the establishment of astrocyte domains during postnatal hippocampal development. *Int J Dev Neurosci, 22*(2), 73-86.

Cai, Z., Schools, G. P., & Kimelberg, H. K. (2000). Metabotropic glutamate receptors in acutely isolated hippocampal astrocytes: developmental changes of mGluR5 mRNA and functional expression. *Glia, 29*(1), 70-80.

Calabrese, B., Wilson, M. S., & Halpain, S. (2006). Development and regulation of dendritic spine synapses. *Physiology (Bethesda), 21*, 38-47.

Castets, M., Schaeffer, C., Bechara, E., Schenck, A., Khandjian, E. W., Luche, S., et al. (2005). FMRP interferes with the Rac1 pathway and controls actin cytoskeleton dynamics in murine fibroblasts. *Hum Mol Genet, 14*(6), 835-844.

Castren, M., Lampinen, K. E., Miettinen, R., Koponen, E., Sipola, I., Bakker, C. E., et al. (2002). BDNF regulates the expression of fragile X mental retardation protein mRNA in the hippocampus. *Neurobiol Dis, 11*(1), 221-229.

Ceman, S., O'Donnell, W. T., Reed, M., Patton, S., Pohl, J., & Warren, S. T. (2003). Phosphorylation influences the translation state of FMRP-associated polyribosomes. *Hum Mol Genet, 12*(24), 3295-3305.

Chapman, A. G., Nanan, K., Williams, M., & Meldrum, B. S. (2000). Anticonvulsant activity of two metabotropic glutamate group I antagonists selective for the mGlu5 receptor: 2-methyl-6-(phenylethynyl)-pyridine (MPEP), and (E)-6-methyl-2-styryl-pyridine (SIB 1893). *Neuropharmacology, 39*(9), 1567-1574.

Chen, L., & Toth, M. (2001). Fragile X mice develop sensory hyperreactivity to auditory

stimuli. *Neuroscience, 103*(4), 1043-1050.

Chen, L., Yun, S. W., Seto, J., Liu, W., & Toth, M. (2003). The fragile X mental retardation protein binds and regulates a novel class of mRNAs containing U rich target sequences. *Neuroscience, 120*(4), 1005-1017.

Chen, Y., Dube, C. M., Rice, C. J., & Baram, T. Z. (2008). Rapid loss of dendritic spines after stress involves derangement of spine dynamics by corticotropin-releasing hormone. *J Neurosci, 28*(11), 2903-2911.

Chiang, P. W., Carpenter, L. E., & Hagerman, P. J. (2001). The 5'-untranslated region of the FMR1 message facilitates translation by internal ribosome entry. *J Biol Chem, 276*(41), 37916-37921.

Cho, K. O., Hunt, C. A., & Kennedy, M. B. (1992). The rat brain postsynaptic density fraction contains a homolog of the Drosophila discs-large tumor suppressor protein. *Neuron, 9*(5), 929-942.

Christopherson, K. S., Ullian, E. M., Stokes, C. C., Mullowney, C. E., Hell, J. W., Agah, A., et al. (2005). Thrombospondins are astrocyte-secreted proteins that promote CNS synaptogenesis. *Cell, 120*(3), 421-433.

Citri, A., & Malenka, R. C. (2008). Synaptic plasticity: multiple forms, functions, and mechanisms. *Neuropsychopharmacology, 33*(1), 18-41.

Comery, T. A., Harris, J. B., Willems, P. J., Oostra, B. A., Irwin, S. A., Weiler, I. J., et al. (1997). Abnormal dendritic spines in fragile X knockout mice: maturation and pruning deficits. *Proc Natl Acad Sci U S A, 94*(10), 5401-5404.

Consoulas, C., Duch, C., Bayline, R. J., & Levine, R. B. (2000). Behavioral transformations during metamorphosis: remodeling of neural and motor systems. *Brain Res Bull, 53*(5), 571-583.

Consoulas, C., Restifo, L. L., & Levine, R. B. (2002). Dendritic remodeling and growth of motoneurons during metamorphosis of Drosophila melanogaster. *J Neurosci, 22*(12), 4906-4917.

Corbin, F., Bouillon, M., Fortin, A., Morin, S., Rousseau, F., & Khandjian, E. W. (1997). The fragile X mental retardation protein is associated with poly(A)+ mRNA in

actively translating polyribosomes. *Hum Mol Genet, 6*(9), 1465-1472.

Dailey, M. E., & Smith, S. J. (1996). The dynamics of dendritic structure in developing hippocampal slices. *J Neurosci, 16*(9), 2983-2994.

Dalva, M. B., Ghosh, A., & Shatz, C. J. (1994). Independent control of dendritic and axonal form in the developing lateral geniculate nucleus. *J Neurosci, 14*(6), 3588-3602.

Dan, Y., & Poo, M. M. (2006). Spike timing-dependent plasticity: from synapse to perception. *Physiol Rev, 86*(3), 1033-1048.

Darnell, J. C., Fraser, C. E., Mostovetsky, O., Stefani, G., Jones, T. A., Eddy, S. R., et al. (2005). Kissing complex RNAs mediate interaction between the Fragile-X mental retardation protein KH2 domain and brain polyribosomes. *Genes Dev, 19*(8), 903-918.

Darnell, J. C., Jensen, K. B., Jin, P., Brown, V., Warren, S. T., & Darnell, R. B. (2001). Fragile X mental retardation protein targets G quartet mRNAs important for neuronal function. *Cell, 107*(4), 489-499.

Darnell, J. C., Mostovetsky, O., & Darnell, R. B. (2005). FMRP RNA targets: identification and validation. *Genes Brain Behav, 4*(6), 341-349.

de Vrij, F. M., Levenga, J., van der Linde, H. C., Koekkoek, S. K., De Zeeuw, C. I., Nelson, D. L., et al. (2008). Rescue of behavioral phenotype and neuronal protrusion morphology in Fmr1 KO mice. *Neurobiol Dis, 31*(1), 127-132.

DeFelipe, J., & Jones, E. G. (1988). A light and electron microscopic study of serotonin-immunoreactive fibers and terminals in the monkey sensory-motor cortex. *Exp Brain Res, 71*(1), 171-182.

Denman, R. B., Dolzhanskaya, N., & Sung, Y. J. (2004). Regulating a translational regulator: mechanisms cells use to control the activity of the fragile X mental retardation protein. *Cell Mol Life Sci, 61*(14), 1714-1728.

deToledo-Morrell, L., Stoub, T. R., & Wang, C. (2007). Hippocampal atrophy and disconnection in incipient and mild Alzheimer's disease. *Prog Brain Res, 163*, 741-753.

Devys, D., Lutz, Y., Rouyer, N., Bellocq, J. P., & Mandel, J. L. (1993). The FMR-1 protein is cytoplasmic, most abundant in neurons and appears normal in carriers of a fragile X premutation. *Nat Genet, 4*(4), 335-340.

Dictenberg, J. B., Swanger, S. A., Antar, L. N., Singer, R. H., & Bassell, G. J. (2008). A direct role for FMRP in activity-dependent dendritic mRNA transport links filopodial-spine morphogenesis to fragile X syndrome. *Dev Cell, 14*(6), 926-939.

Dierssen, M., & Ramakers, G. J. (2006). Dendritic pathology in mental retardation: from molecular genetics to neurobiology. *Genes Brain Behav, 5 Suppl 2*, 48-60.

Dobkin, C., Rabe, A., Dumas, R., El Idrissi, A., Haubenstock, H., & Brown, W. T. (2000). Fmr1 knockout mouse has a distinctive strain-specific learning impairment. *Neuroscience, 100*(2), 423-429.

Dobson, T., Kube, E., Timmerman, S., & Krushel, L. A. (2008). Identifying intrinsic and extrinsic determinants that regulate internal initiation of translation mediated by the FMR1 5' leader. *BMC Mol Biol, 9*, 89.

Dockendorff, T. C., Su, H. S., McBride, S. M., Yang, Z., Choi, C. H., Siwicki, K. K., et al. (2002). Drosophila lacking dfmr1 activity show defects in circadian output and fail to maintain courtship interest. *Neuron, 34*(6), 973-984.

Dolen, G., Osterweil, E., Rao, B. S., Smith, G. B., Auerbach, B. D., Chattarji, S., et al. (2007). Correction of fragile X syndrome in mice. *Neuron, 56*(6), 955-962.

Dosemeci, A., Makusky, A. J., Jankowska-Stephens, E., Yang, X., Slotta, D. J., & Markey, S. P. (2007). Composition of the synaptic PSD-95 complex. *Mol Cell Proteomics, 6*(10), 1749-1760.

Dotti, C. G., & Banker, G. A. (1987). Experimentally induced alteration in the polarity of developing neurons. *Nature, 330*(6145), 254-256.

Dotti, C. G., Sullivan, C. A., & Banker, G. A. (1988). The establishment of polarity by hippocampal neurons in culture. *J Neurosci, 8*(4), 1454-1468.

Duch, C., & Levine, R. B. (2000). Remodeling of membrane properties and dendritic architecture accompanies the postembryonic conversion of a slow into a fast motoneuron. *J Neurosci, 20*(18), 6950-6961.

Duch, C., & Levine, R. B. (2002). Changes in calcium signaling during postembryonic dendritic growth in Manduca sexta. *J Neurophysiol, 87*(3), 1415-1425.

Dudek, S. M., & Bear, M. F. (1992). Homosynaptic long-term depression in area CA1 of hippocampus and effects of N-methyl-D-aspartate receptor blockade. *Proc Natl Acad Sci U S A, 89*(10), 4363-4367.

Dunaevsky, A., & Mason, C. A. (2003). Spine motility: a means towards an end? *Trends Neurosci, 26*(3), 155-160.

Eberhart, D. E., Malter, H. E., Feng, Y., & Warren, S. T. (1996). The fragile X mental retardation protein is a ribonucleoprotein containing both nuclear localization and nuclear export signals. *Hum Mol Genet, 5*(8), 1083-1091.

Ehrlich, I., Klein, M., Rumpel, S., & Malinow, R. (2007). PSD-95 is required for activity-driven synapse stabilization. *Proc Natl Acad Sci U S A, 104*(10), 4176-4181.

Eichenbaum, H. (2004). Hippocampus: cognitive processes and neural representations that underlie declarative memory. *Neuron, 44*(1), 109-120.

Eichler, E. E., Richards, S., Gibbs, R. A., & Nelson, D. L. (1993). Fine structure of the human FMR1 gene. *Hum Mol Genet, 2*(8), 1147-1153.

Eichler, S. A., & Meier, J. C. (2008). E-I balance and human diseases - from molecules to networking. *Front Mol Neurosci, 1*, 2.

El-Husseini, A. E., Schnell, E., Chetkovich, D. M., Nicoll, R. A., & Bredt, D. S. (2000). PSD-95 involvement in maturation of excitatory synapses. *Science, 290*(5495), 1364-1368.

Elmariah, S. B., Oh, E. J., Hughes, E. G., & Balice-Gordon, R. J. (2005). Astrocytes regulate inhibitory synapse formation via Trk-mediated modulation of postsynaptic GABAA receptors. *J Neurosci, 25*(14), 3638-3650.

Ethell, I. M., & Pasquale, E. B. (2005). Molecular mechanisms of dendritic spine development and remodeling. *Prog Neurobiol, 75*(3), 161-205.

Fatemi, S. H., Reutiman, T. J., Folsom, T. D., & Thuras, P. D. (2009). GABA(A) receptor downregulation in brains of subjects with autism. *J Autism Dev Disord, 39*(2), 223-230.

Fedoroff, S., White, R., Neal, J., Subrahmanyan, L., & Kalnins, V. I. (1983). Astrocyte cell lineage. II. Mouse fibrous astrocytes and reactive astrocytes in cultures have vimentin- and GFP-containing intermediate filaments. *Brain Res, 283*(2-3), 303-315.

Feng, Y., Absher, D., Eberhart, D. E., Brown, V., Malter, H. E., & Warren, S. T. (1997). FMRP associates with polyribosomes as an mRNP, and the I304N mutation of severe fragile X syndrome abolishes this association. *Mol Cell, 1*(1), 109-118.

Feng, Y., Gutekunst, C. A., Eberhart, D. E., Yi, H., Warren, S. T., & Hersch, S. M. (1997). Fragile X mental retardation protein: nucleocytoplasmic shuttling and association with somatodendritic ribosomes. *J Neurosci, 17*(5), 1539-1547.

Ferreira, A., & Paganoni, S. (2002). The formation of synapses in the central nervous system. *Mol Neurobiol, 26*(1), 69-79.

Fiala, J. C., Feinberg, M., Popov, V., & Harris, K. M. (1998). Synaptogenesis via dendritic filopodia in developing hippocampal area CA1. *J Neurosci, 18*(21), 8900-8911.

Fischer, M., Kaech, S., Knutti, D., & Matus, A. (1998). Rapid actin-based plasticity in dendritic spines. *Neuron, 20*(5), 847-854.

Frankland, P. W., Wang, Y., Rosner, B., Shimizu, T., Balleine, B. W., Dykens, E. M., et al. (2004). Sensorimotor gating abnormalities in young males with fragile X syndrome and Fmr1-knockout mice. *Mol Psychiatry, 9*(4), 417-425.

Freund, T. F., & Antal, M. (1988). GABA-containing neurons in the septum control inhibitory interneurons in the hippocampus. *Nature, 336*(6195), 170-173.

Friedlander, M. J., Stanford, L. R., & Sherman, S. M. (1982). Effects of monocular deprivation on the structure-function relationship of individual neurons in the cat's lateral geniculate nucleus. *J Neurosci, 2*(3), 321-330.

Gabel, L. A., Won, S., Kawai, H., McKinney, M., Tartakoff, A. M., & Fallon, J. R. (2004). Visual experience regulates transient expression and dendritic localization of fragile X mental retardation protein. *J Neurosci, 24*(47), 10579-10583.

Galvez, R., Gopal, A. R., & Greenough, W. T. (2003). Somatosensory cortical barrel

dendritic abnormalities in a mouse model of the fragile X mental retardation syndrome. *Brain Res, 971*(1), 83-89.

Galvez, R., & Greenough, W. T. (2005). Sequence of abnormal dendritic spine development in primary somatosensory cortex of a mouse model of the fragile X mental retardation syndrome. *Am J Med Genet A, 135*(2), 155-160.

Garner, C. C., Tucker, R. P., & Matus, A. (1988). Selective localization of messenger RNA for cytoskeletal protein MAP2 in dendrites. *Nature, 336*(6200), 674-677.

Gatto, C. L., & Broadie, K. (2008). Temporal requirements of the fragile X mental retardation protein in the regulation of synaptic structure. *Development, 135*(15), 2637-2648.

Gatto, C. L., & Broadie, K. (2009). The fragile x mental retardation protein in circadian rhythmicity and memory consolidation. *Mol Neurobiol, 39*(2), 107-129.

Gibson, J. R., Bartley, A. F., Hays, S. A., & Huber, K. M. (2008). Imbalance of neocortical excitation and inhibition and altered UP states reflect network hyperexcitability in the mouse model of fragile X syndrome. *J Neurophysiol, 100*(5), 2615-2626.

Gilbert, C. D. (1983). Microcircuitry of the visual cortex. *Annu Rev Neurosci, 6*, 217-247.

Globus, A., Rosenzweig, M. R., Bennett, E. L., & Diamond, M. C. (1973). Effects of differential experience on dendritic spine counts in rat cerebral cortex. *J Comp Physiol Psychol, 82*(2), 175-181.

Godement, P., Vanselow, J., Thanos, S., & Bonhoeffer, F. (1987). A study in developing visual systems with a new method of staining neurones and their processes in fixed tissue. *Development, 101*(4), 697-713.

Gray, E. G. (1959). Electron microscopy of synaptic contacts on dendrite spines of the cerebral cortex. *Nature, 183*(4675), 1592-1593.

Greenough, W. T., & Chang, F. L. (1988). Dendritic pattern formation involves both oriented regression and oriented growth in the barrels of mouse somatosensory cortex. *Brain Res, 471*(1), 148-152.

Greenough, W. T., Klintsova, A. Y., Irwin, S. A., Galvez, R., Bates, K. E., & Weiler, I. J.

(2001). Synaptic regulation of protein synthesis and the fragile X protein. *Proc Natl Acad Sci U S A, 98*(13), 7101-7106.

Groschel-Stewart, U., Unsicker, K., & Leonhardt, H. (1977). Immunohistochemical demonstration of contractile proteins in astrocytes, marginal glial and ependymal cells in rat diencephalon. *Cell Tissue Res, 180*(1), 133-137.

Grossman, A. W., Elisseou, N. M., McKinney, B. C., & Greenough, W. T. (2006). Hippocampal pyramidal cells in adult Fmr1 knockout mice exhibit an immature-appearing profile of dendritic spines. *Brain Res, 1084*(1), 158-164.

Guillet, B., Lortet, S., Masmejean, F., Samuel, D., Nieoullon, A., & Pisano, P. (2002). Developmental expression and activity of high affinity glutamate transporters in rat cortical primary cultures. *Neurochem Int, 40*(7), 661-671.

Guizzetti, M., Moore, N. H., Giordano, G., & Costa, L. G. (2008). Modulation of neuritogenesis by astrocyte muscarinic receptors. *J Biol Chem, 283*(46), 31884-31897.

Gulledge, A. T., Kampa, B. M., & Stuart, G. J. (2005). Synaptic integration in dendritic trees. *J Neurobiol, 64*(1), 75-90.

Haas, B. W., Barnea-Goraly, N., Lightbody, A. A., Patnaik, S. S., Hoeft, F., Hazlett, H., et al. (2009). Early white-matter abnormalities of the ventral frontostriatal pathway in fragile X syndrome. *Dev Med Child Neurol.*

Haber, M., Zhou, L., & Murai, K. K. (2006). Cooperative astrocyte and dendritic spine dynamics at hippocampal excitatory synapses. *J Neurosci, 26*(35), 8881-8891.

Hagerman, P. J. (2008). The fragile X prevalence paradox. *J Med Genet, 45*(8), 498-499.

Hagerman, P. J., & Hagerman, R. J. (2004a). Fragile X-associated tremor/ataxia syndrome (FXTAS). *Ment Retard Dev Disabil Res Rev, 10*(1), 25-30.

Hagerman, P. J., & Hagerman, R. J. (2004b). The fragile-X premutation: a maturing perspective. *Am J Hum Genet, 74*(5), 805-816.

Hagerman, R. J., Leehey, M., Heinrichs, W., Tassone, F., Wilson, R., Hills, J., et al. (2001). Intention tremor, parkinsonism, and generalized brain atrophy in male carriers of fragile X. *Neurology, 57*(1), 127-130.

Hama, H., Hara, C., Yamaguchi, K., & Miyawaki, A. (2004). PKC signaling mediates global enhancement of excitatory synaptogenesis in neurons triggered by local contact with astrocytes. *Neuron, 41*(3), 405-415.

Han, H. Q., Nichols, R. A., Rubin, M. R., Bahler, M., & Greengard, P. (1991). Induction of formation of presynaptic terminals in neuroblastoma cells by synapsin IIb. *Nature, 349*(6311), 697-700.

Hand, R., Bortone, D., Mattar, P., Nguyen, L., Heng, J. I., Guerrier, S., et al. (2005). Phosphorylation of Neurogenin2 specifies the migration properties and the dendritic morphology of pyramidal neurons in the neocortex. *Neuron, 48*(1), 45-62.

Harris, K. M., Jensen, F. E., & Tsao, B. (1992). Three-dimensional structure of dendritic spines and synapses in rat hippocampus (CA1) at postnatal day 15 and adult ages: implications for the maturation of synaptic physiology and long-term potentiation. *J Neurosci, 12*(7), 2685-2705.

Harris, K. M., & Kater, S. B. (1994). Dendritic spines: cellular specializations imparting both stability and flexibility to synaptic function. *Annu Rev Neurosci, 17*, 341-371.

Harris, K. M., & Stevens, J. K. (1989). Dendritic spines of CA 1 pyramidal cells in the rat hippocampus: serial electron microscopy with reference to their biophysical characteristics. *J Neurosci, 9*(8), 2982-2997.

Harris, R. M., & Woolsey, T. A. (1981). Dendritic plasticity in mouse barrel cortex following postnatal vibrissa follicle damage. *J Comp Neurol, 196*(3), 357-376.

Harrison, P. J. (1999). The neuropathology of schizophrenia. A critical review of the data and their interpretation. *Brain, 122 (Pt 4)*, 593-624.

Hebb, D. O. (1949). *The organization of behavior; a neuropsychological theory*. New York: Wiley.

Hessl, D., Rivera, S. M., & Reiss, A. L. (2004). The neuroanatomy and neuroendocrinology of fragile X syndrome. *Ment Retard Dev Disabil Res Rev, 10*(1), 17-24.

Hinds, H. L., Ashley, C. T., Sutcliffe, J. S., Nelson, D. L., Warren, S. T., Housman, D. E., et al. (1993). Tissue specific expression of FMR-1 provides evidence for a functional role in fragile X syndrome. *Nat Genet, 3*(1), 36-43.

Hinton, V. J., Brown, W. T., Wisniewski, K., & Rudelli, R. D. (1991). Analysis of neocortex in three males with the fragile X syndrome. *Am J Med Genet, 41*(3), 289-294.

Holtmaat, A. J., Trachtenberg, J. T., Wilbrecht, L., Shepherd, G. M., Zhang, X., Knott, G. W., et al. (2005). Transient and persistent dendritic spines in the neocortex in vivo. *Neuron, 45*(2), 279-291.

Houser, C. R., Hendry, S. H., Jones, E. G., & Vaughn, J. E. (1983). Morphological diversity of immunocytochemically identified GABA neurons in the monkey sensory-motor cortex. *J Neurocytol, 12*(4), 617-638.

Huber, K. M., Gallagher, S. M., Warren, S. T., & Bear, M. F. (2002). Altered synaptic plasticity in a mouse model of fragile X mental retardation. *Proc Natl Acad Sci U S A, 99*(11), 7746-7750.

Huber, K. M., Roder, J. C., & Bear, M. F. (2001). Chemical induction of mGluR5- and protein synthesis--dependent long-term depression in hippocampal area CA1. *J Neurophysiol, 86*(1), 321-325.

Hughes, M. E., Bortnick, R., Tsubouchi, A., Baumer, P., Kondo, M., Uemura, T., et al. (2007). Homophilic Dscam interactions control complex dendrite morphogenesis. *Neuron, 54*(3), 417-427.

Hume, R. I., & Purves, D. (1981). Geometry of neonatal neurones and the regulation of synapse elimination. *Nature, 293*(5832), 469-471.

Huttenlocher, P. R. (1974). Dendritic development in neocortex of children with mental defect and infantile spasms. *Neurology, 24*(3), 203-210.

Huttenlocher, P. R. (1990). Morphometric study of human cerebral cortex development. *Neuropsychologia, 28*(6), 517-527.

Iacoangeli, A., Rozhdestvensky, T. S., Dolzhanskaya, N., Tournier, B., Schutt, J., Brosius, J., et al. (2008a). On BC1 RNA and the fragile X mental retardation protein. *Proc*

Natl Acad Sci U S A, 105(2), 734-739.

Iacoangeli, A., Rozhdestvensky, T. S., Dolzhanskaya, N., Tournier, B., Schutt, J., Brosius, J., et al. (2008b). Reply to Bagni: On BC1 RNA and the fragile X mental retardation protein. *Proc Natl Acad Sci U S A, 105*(22), E29.

Irwin, S. A., Christmon, C. A., Grossman, A. W., Galvez, R., Kim, S. H., DeGrush, B. J., et al. (2005). Fragile X mental retardation protein levels increase following complex environment exposure in rat brain regions undergoing active synaptogenesis. *Neurobiol Learn Mem, 83*(3), 180-187.

Irwin, S. A., Galvez, R., & Greenough, W. T. (2000). Dendritic spine structural anomalies in fragile-X mental retardation syndrome. *Cereb Cortex, 10*(10), 1038-1044.

Irwin, S. A., Idupulapati, M., Gilbert, M. E., Harris, J. B., Chakravarti, A. B., Rogers, E. J., et al. (2002). Dendritic spine and dendritic field characteristics of layer V pyramidal neurons in the visual cortex of fragile-X knockout mice. *Am J Med Genet, 111*(2), 140-146.

Irwin, S. A., Patel, B., Idupulapati, M., Harris, J. B., Crisostomo, R. A., Larsen, B. P., et al. (2001). Abnormal dendritic spine characteristics in the temporal and visual cortices of patients with fragile-X syndrome: a quantitative examination. *Am J Med Genet, 98*(2), 161-167.

Iwasato, T., Datwani, A., Wolf, A. M., Nishiyama, H., Taguchi, Y., Tonegawa, S., et al. (2000). Cortex-restricted disruption of NMDAR1 impairs neuronal patterns in the barrel cortex. *Nature, 406*(6797), 726-731.

Jacobs, B., Schall, M., Prather, M., Kapler, E., Driscoll, L., Baca, S., et al. (2001). Regional dendritic and spine variation in human cerebral cortex: a quantitative golgi study. *Cereb Cortex, 11*(6), 558-571.

Jakala, P., Hanninen, T., Ryynanen, M., Laakso, M., Partanen, K., Mannermaa, A., et al. (1997). Fragile-X: neuropsychological test performance, CGG triplet repeat lengths, and hippocampal volumes. *J Clin Invest, 100*(2), 331-338.

Jan, Y. N., & Jan, L. Y. (2003). The control of dendrite development. *Neuron, 40*(2), 229-242.

Jessen, K. R. (2004). Glial cells. *Int J Biochem Cell Biol, 36*(10), 1861-1867.

Jin, P., Alisch, R. S., & Warren, S. T. (2004). RNA and microRNAs in fragile X mental retardation. *Nat Cell Biol, 6*(11), 1048-1053.

Jin, P., & Warren, S. T. (2003). New insights into fragile X syndrome: from molecules to neurobehaviors. *Trends Biochem Sci, 28*(3), 152-158.

Jontes, J. D., & Smith, S. J. (2000). Filopodia, spines, and the generation of synaptic diversity. *Neuron, 27*(1), 11-14.

Kaech, S., & Banker, G. (2006). Culturing hippocampal neurons. *Nat Protoc, 1*(5), 2406-2415.

Kates, W. R., Abrams, M. T., Kaufmann, W. E., Breiter, S. N., & Reiss, A. L. (1997). Reliability and validity of MRI measurement of the amygdala and hippocampus in children with fragile X syndrome. *Psychiatry Res, 75*(1), 31-48.

Katz, L. C., & Shatz, C. J. (1996). Synaptic activity and the construction of cortical circuits. *Science, 274*(5290), 1133-1138.

Kaufmann, W. E., & Moser, H. W. (2000). Dendritic anomalies in disorders associated with mental retardation. *Cereb Cortex, 10*(10), 981-991.

Kehrer, C., Maziashvili, N., Dugladze, T., & Gloveli, T. (2008). Altered Excitatory-Inhibitory Balance in the NMDA-Hypofunction Model of Schizophrenia. *Front Mol Neurosci, 1*, 6.

Khandjian, E. W. (1999). Biology of the fragile X mental retardation protein, an RNA-binding protein. *Biochem Cell Biol, 77*(4), 331-342.

Khandjian, E. W., Corbin, F., Woerly, S., & Rousseau, F. (1996). The fragile X mental retardation protein is associated with ribosomes. *Nat Genet, 12*(1), 91-93.

Khandjian, E. W., Huot, M. E., Tremblay, S., Davidovic, L., Mazroui, R., & Bardoni, B. (2004). Biochemical evidence for the association of fragile X mental retardation protein with brain polyribosomal ribonucleoparticles. *Proc Natl Acad Sci U S A, 101*(36), 13357-13362.

Kim, E., & Sheng, M. (2004). PDZ domain proteins of synapses. *Nat Rev Neurosci, 5*(10), 771-781.

Kindler, S., Rehbein, M., Classen, B., Richter, D., & Bockers, T. M. (2004). Distinct spatiotemporal expression of SAPAP transcripts in the developing rat brain: a novel dendritically localized mRNA. *Brain Res Mol Brain Res, 126*(1), 14-21.

Koch, C., & Segev, I. (2000). The role of single neurons in information processing. *Nat Neurosci, 3 Suppl*, 1171-1177.

Kornau, H. C., Schenker, L. T., Kennedy, M. B., & Seeburg, P. H. (1995). Domain interaction between NMDA receptor subunits and the postsynaptic density protein PSD-95. *Science, 269*(5231), 1737-1740.

Kossel, A. H., Williams, C. V., Schweizer, M., & Kater, S. B. (1997). Afferent innervation influences the development of dendritic branches and spines via both activity-dependent and non-activity-dependent mechanisms. *J Neurosci, 17*(16), 6314-6324.

Kozorovitskiy, Y., Gross, C. G., Kopil, C., Battaglia, L., McBreen, M., Stranahan, A. M., et al. (2005). Experience induces structural and biochemical changes in the adult primate brain. *Proc Natl Acad Sci U S A, 102*(48), 17478-17482.

Kremer, E. J., Pritchard, M., Lynch, M., Yu, S., Holman, K., Baker, E., et al. (1991). Mapping of DNA instability at the fragile X to a trinucleotide repeat sequence p(CCG)n. *Science, 252*(5013), 1711-1714.

Kriegstein, A. R., & Dichter, M. A. (1983). Morphological classification of rat cortical neurons in cell culture. *J Neurosci, 3*(8), 1634-1647.

Kugler, P., & Schleyer, V. (2004). Developmental expression of glutamate transporters and glutamate dehydrogenase in astrocytes of the postnatal rat hippocampus. *Hippocampus, 14*(8), 975-985.

Laggerbauer, B., Ostareck, D., Keidel, E. M., Ostareck-Lederer, A., & Fischer, U. (2001). Evidence that fragile X mental retardation protein is a negative regulator of translation. *Hum Mol Genet, 10*(4), 329-338.

Lee, A., Li, W., Xu, K., Bogert, B. A., Su, K., & Gao, F. B. (2003). Control of dendritic development by the Drosophila fragile X-related gene involves the small GTPase Rac1. *Development, 130*(22), 5543-5552.

Lee, A. D., Leow, A. D., Lu, A., Reiss, A. L., Hall, S., Chiang, M. C., et al. (2007). 3D pattern of brain abnormalities in Fragile X syndrome visualized using tensor-based morphometry. *Neuroimage, 34*(3), 924-938.

Lester, R. A., Quarum, M. L., Parker, J. D., Weber, E., & Jahr, C. E. (1989). Interaction of 6-cyano-7-nitroquinoxaline-2,3-dione with the N-methyl-D-aspartate receptor-associated glycine binding site. *Mol Pharmacol, 35*(5), 565-570.

Li, J., Pelletier, M. R., Perez Velazquez, J. L., & Carlen, P. L. (2002). Reduced cortical synaptic plasticity and GluR1 expression associated with fragile X mental retardation protein deficiency. *Mol Cell Neurosci, 19*(2), 138-151.

Li, Z., Zhang, Y., Ku, L., Wilkinson, K. D., Warren, S. T., & Feng, Y. (2001). The fragile X mental retardation protein inhibits translation via interacting with mRNA. *Nucleic Acids Res, 29*(11), 2276-2283.

Liao, L., Park, S. K., Xu, T., Vanderklish, P., & Yates, J. R., 3rd (2008). Quantitative proteomic analysis of primary neurons reveals diverse changes in synaptic protein content in fmr1 knockout mice. *Proc Natl Acad Sci U S A, 105*(40), 15281-15286.

Libersat, F., & Duch, C. (2002). Morphometric analysis of dendritic remodeling in an identified motoneuron during postembryonic development. *J Comp Neurol, 450*(2), 153-166.

Lim, J. H., Booker, A. B., & Fallon, J. R. (2005). Regulating fragile X gene transcription in the brain and beyond. *J Cell Physiol, 205*(2), 170-175.

Lisman, J. E., Coyle, J. T., Green, R. W., Javitt, D. C., Benes, F. M., Heckers, S., et al. (2008). Circuit-based framework for understanding neurotransmitter and risk gene interactions in schizophrenia. *Trends Neurosci, 31*(5), 234-242.

Lombroso, P., & Ogren, M. (2009). Learning and memory, part II: molecular mechanisms of synaptic plasticity. *J Am Acad Child Adolesc Psychiatry, 48*(1), 5-9.

Lombroso, P. J., & Ogren, M. P. (2008). Learning and memory, part I: brain regions involved in two types of learning and memory. *J Am Acad Child Adolesc Psychiatry, 47*(11), 1228-1232.

Lu, R., Wang, H., Liang, Z., Ku, L., O'Donnell W, T., Li, W., et al. (2004). The fragile X

protein controls microtubule-associated protein 1B translation and microtubule stability in brain neuron development. *Proc Natl Acad Sci U S A, 101*(42), 15201-15206.

Lund, J. S., Holbach, S. M., & Chung, W. W. (1991). Postnatal development of thalamic recipient neurons in the monkey striate cortex: II. Influence of afferent driving on spine acquisition and dendritic growth of layer 4C spiny stellate neurons. *J Comp Neurol, 309*(1), 129-140.

Luscher, C., & Isaac, J. T. (2009). The synapse: center stage for many brain diseases. *J Physiol, 587*(Pt 4), 727-729.

Mainen, Z. F., & Sejnowski, T. J. (1996). Influence of dendritic structure on firing pattern in model neocortical neurons. *Nature, 382*(6589), 363-366.

Majdi, M., Ribeiro-da-Silva, A., & Cuello, A. C. (2009). Variations in excitatory and inhibitory postsynaptic protein content in rat cerebral cortex with respect to aging and cognitive status. *Neuroscience, 159*(2), 896-907.

Marrs, G. S., Green, S. H., & Dailey, M. E. (2001). Rapid formation and remodeling of postsynaptic densities in developing dendrites. *Nat Neurosci, 4*(10), 1006-1013.

Mason, C. A., Morrison, M. E., Ward, M. S., Zhang, Q., & Baird, D. H. (1997). Axon-target interactions in the developing cerebellum. *Perspect Dev Neurobiol, 5*(1), 69-82.

Matthews, B. J., Kim, M. E., Flanagan, J. J., Hattori, D., Clemens, J. C., Zipursky, S. L., et al. (2007). Dendrite self-avoidance is controlled by Dscam. *Cell, 129*(3), 593-604.

Matus, A. (2005). Growth of dendritic spines: a continuing story. *Curr Opin Neurobiol, 15*(1), 67-72.

Mauch, D. H., Nagler, K., Schumacher, S., Goritz, C., Muller, E. C., Otto, A., et al. (2001). CNS synaptogenesis promoted by glia-derived cholesterol. *Science, 294*(5545), 1354-1357.

Mazzanti, M., & Haydon, P. G. (2003). Astrocytes selectively enhance N-type calcium current in hippocampal neurons. *Glia, 41*(2), 128-136.

McAllister, A. K. (2000). Cellular and molecular mechanisms of dendrite growth. *Cereb Cortex, 10*(10), 963-973.

McAllister, A. K., Lo, D. C., & Katz, L. C. (1995). Neurotrophins regulate dendritic growth in developing visual cortex. *Neuron, 15*(4), 791-803.

McBride, S. M., Choi, C. H., Wang, Y., Liebelt, D., Braunstein, E., Ferreiro, D., et al. (2005). Pharmacological rescue of synaptic plasticity, courtship behavior, and mushroom body defects in a Drosophila model of fragile X syndrome. *Neuron, 45*(5), 753-764.

McKinney, B. C., Grossman, A. W., Elisseou, N. M., & Greenough, W. T. (2005). Dendritic spine abnormalities in the occipital cortex of C57BL/6 Fmr1 knockout mice. *Am J Med Genet B Neuropsychiatr Genet, 136B*(1), 98-102.

McKinnon, M. C., Yucel, K., Nazarov, A., & MacQueen, G. M. (2009). A meta-analysis examining clinical predictors of hippocampal volume in patients with major depressive disorder. *J Psychiatry Neurosci, 34*(1), 41-54.

Mei, L., & Xiong, W. C. (2008). Neuregulin 1 in neural development, synaptic plasticity and schizophrenia. *Nat Rev Neurosci, 9*(6), 437-452.

Mendenhall, B., & Murphey, R. K. (1974). The morphology of cricket giant interneurons. *J Neurobiol, 5*(6), 565-580.

Mientjes, E. J., Nieuwenhuizen, I., Kirkpatrick, L., Zu, T., Hoogeveen-Westerveld, M., Severijnen, L., et al. (2006). The generation of a conditional Fmr1 knock out mouse model to study Fmrp function in vivo. *Neurobiol Dis, 21*(3), 549-555.

Miller, M. (1981). Maturation of rat visual cortex. I. A quantitative study of Golgi-impregnated pyramidal neurons. *J Neurocytol, 10*(5), 859-878.

Miller, M., & Peters, A. (1981). Maturation of rat visual cortex. II. A combined Golgi-electron microscope study of pyramidal neurons. *J Comp Neurol, 203*(4), 555-573.

Mineur, Y. S., Sluyter, F., de Wit, S., Oostra, B. A., & Crusio, W. E. (2002). Behavioral and neuroanatomical characterization of the Fmr1 knockout mouse. *Hippocampus, 12*(1), 39-46.

Mitchison, T., & Kirschner, M. (1988). Cytoskeletal dynamics and nerve growth. *Neuron, 1*(9), 761-772.

Miyashiro, K. Y., Beckel-Mitchener, A., Purk, T. P., Becker, K. G., Barret, T., Liu, L., et al. (2003). RNA cargoes associating with FMRP reveal deficits in cellular functioning in Fmr1 null mice. *Neuron, 37*(3), 417-431.

Mizrahi, A., Ben-Ner, E., Katz, M. J., Kedem, K., Glusman, J. G., & Libersat, F. (2000). Comparative analysis of dendritic architecture of identified neurons using the Hausdorff distance metric. *J Comp Neurol, 422*(3), 415-428.

Mizrahi, A., & Libersat, F. (2002). Afferent input regulates the formation of distal dendritic branches. *J Comp Neurol, 452*(1), 1-10.

Moore, A. W., Jan, L. Y., & Jan, Y. N. (2002). hamlet, a binary genetic switch between single- and multiple- dendrite neuron morphology. *Science, 297*(5585), 1355-1358.

Morest, D. K. (1969). The growth of dendrites in the mammalian brain. *Z Anat Entwicklungsgesch, 128*(4), 290-317.

Mostofsky, S. H., Mazzocco, M. M., Aakalu, G., Warsofsky, I. S., Denckla, M. B., & Reiss, A. L. (1998). Decreased cerebellar posterior vermis size in fragile X syndrome: correlation with neurocognitive performance. *Neurology, 50*(1), 121-130.

Muddashetty, R. S., Kelic, S., Gross, C., Xu, M., & Bassell, G. J. (2007). Dysregulated metabotropic glutamate receptor-dependent translation of AMPA receptor and postsynaptic density-95 mRNAs at synapses in a mouse model of fragile X syndrome. *J Neurosci, 27*(20), 5338-5348.

Mulkey, R. M., & Malenka, R. C. (1992). Mechanisms underlying induction of homosynaptic long-term depression in area CA1 of the hippocampus. *Neuron, 9*(5), 967-975.

Murai, K. K., Nguyen, L. N., Irie, F., Yamaguchi, Y., & Pasquale, E. B. (2003). Control of hippocampal dendritic spine morphology through ephrin-A3/EphA4 signaling. *Nat Neurosci, 6*(2), 153-160.

Murphey, R. K., Mendenhall, B., Palka, J., & Edwards, J. S. (1975). Deafferentation slows the growth of specific dendrites of identified giant interneurons. *J Comp Neurol, 159*(3), 407-418.

Murray, A., Webb, J., Grimley, S., Conway, G., & Jacobs, P. (1998). Studies of FRAXA and FRAXE in women with premature ovarian failure. *J Med Genet, 35*(8), 637-640.

Musumeci, S. A., Calabrese, G., Bonaccorso, C. M., D'Antoni, S., Brouwer, J. R., Bakker, C. E., et al. (2007). Audiogenic seizure susceptibility is reduced in fragile X knockout mice after introduction of FMR1 transgenes. *Exp Neurol, 203*(1), 233-240.

Nagler, K., Mauch, D. H., & Pfrieger, F. W. (2001). Glia-derived signals induce synapse formation in neurones of the rat central nervous system. *J Physiol, 533*(Pt 3), 665-679.

Nakamoto, M., Nalavadi, V., Epstein, M. P., Narayanan, U., Bassell, G. J., & Warren, S. T. (2007). Fragile X mental retardation protein deficiency leads to excessive mGluR5-dependent internalization of AMPA receptors. *Proc Natl Acad Sci U S A, 104*(39), 15537-15542.

Narro, M. L., Yang, F., Kraft, R., Wenk, C., Efrat, A., & Restifo, L. L. (2007). NeuronMetrics: software for semi-automated processing of cultured neuron images. *Brain Res, 1138*, 57-75.

Nault, F., & DoKonick, P. (2009). Dissociated hippocampal cultures. In L. C. Doering (Ed.), *Protocols for Neural Cell Culture* (4th ed., pp. 137-160). New York: Humana Press.

Niblock, M. M., Brunso-Bechtold, J. K., & Riddle, D. R. (2000). Insulin-like growth factor I stimulates dendritic growth in primary somatosensory cortex. *J Neurosci, 20*(11), 4165-4176.

Nielsen, D. M., Derber, W. J., McClellan, D. A., & Crnic, L. S. (2002). Alterations in the auditory startle response in Fmr1 targeted mutant mouse models of fragile X syndrome. *Brain Res, 927*(1), 8-17.

Nimchinsky, E. A., Oberlander, A. M., & Svoboda, K. (2001). Abnormal development of dendritic spines in FMR1 knock-out mice. *J Neurosci, 21*(14), 5139-5146.

Nimchinsky, E. A., Sabatini, B. L., & Svoboda, K. (2002). Structure and function of dendritic spines. *Annu Rev Physiol, 64*, 313-353.

Nimchinsky, E. A., Yasuda, R., Oertner, T. G., & Svoboda, K. (2004). The number of glutamate receptors opened by synaptic stimulation in single hippocampal spines. *J Neurosci, 24*(8), 2054-2064.

Nishida, H., & Okabe, S. (2007). Direct astrocytic contacts regulate local maturation of dendritic spines. *J Neurosci, 27*(2), 331-340.

O'Donnell, W. T., & Warren, S. T. (2002). A decade of molecular studies of fragile X syndrome. *Annu Rev Neurosci, 25*, 315-338.

O'Sullivan, G. A., Hofer, W., & Betz, H. (2009). Inhibitory postsynaptic membrane specializations are formed in gephyrin-deficient mice. *Neurosci Lett, 458*(3), 106-110.

Oostra, B. A., & Chiurazzi, P. (2001). The fragile X gene and its function. *Clin Genet, 60*(6), 399-408.

Oostra, B. A., & Willemsen, R. (2009). FMR1: A gene with three faces. *Biochim Biophys Acta*.

Pacey, L. K., & Doering, L. C. (2007). Developmental expression of FMRP in the astrocyte lineage: implications for fragile X syndrome. *Glia, 55*(15), 1601-1609.

Pan, L., Zhang, Y. Q., Woodruff, E., & Broadie, K. (2004). The Drosophila fragile X gene negatively regulates neuronal elaboration and synaptic differentiation. *Curr Biol, 14*(20), 1863-1870.

Parrish, J. Z., Emoto, K., Jan, L. Y., & Jan, Y. N. (2007). Polycomb genes interact with the tumor suppressor genes hippo and warts in the maintenance of Drosophila sensory neuron dendrites. *Genes Dev, 21*(8), 956-972.

Parrish, J. Z., Emoto, K., Kim, M. D., & Jan, Y. N. (2007). Mechanisms that regulate establishment, maintenance, and remodeling of dendritic fields. *Annu Rev Neurosci, 30*, 399-423.

Parrish, J. Z., Kim, M. D., Jan, L. Y., & Jan, Y. N. (2006). Genome-wide analyses identify transcription factors required for proper morphogenesis of Drosophila sensory neuron dendrites. *Genes Dev, 20*(7), 820-835.

Pascual, O., Casper, K. B., Kubera, C., Zhang, J., Revilla-Sanchez, R., Sul, J. Y., et al. (2005). Astrocytic purinergic signaling coordinates synaptic networks. *Science, 310*(5745), 113-116.

Paxinos, G., & Watson, C. (2007). *The rat brain in stereotaxic coordinates* (6th ed.). Amsterdam ; Boston ;: Academic Press/Elsevier.

Pechan, P. A., Chowdhury, K., Gerdes, W., & Seifert, W. (1993). Glutamate induces the growth factors NGF, bFGF, the receptor FGF-R1 and c-fos mRNA expression in rat astrocyte culture. *Neurosci Lett, 153*(1), 111-114.

Perea, G., & Araque, A. (2007). Astrocytes potentiate transmitter release at single hippocampal synapses. *Science, 317*(5841), 1083-1086.

Peters, A., Palay, S. L., & Webster, H. d. (1991). *The fine structure of the nervous system : neurons and their supporting cells* (3rd ed.). New York: Oxford University Press.

Pfeiffer, B. E., & Huber, K. M. (2007). Fragile X mental retardation protein induces synapse loss through acute postsynaptic translational regulation. *J Neurosci, 27*(12), 3120-3130.

Pfrieger, F. W., & Barres, B. A. (1996). New views on synapse-glia interactions. *Curr Opin Neurobiol, 6*(5), 615-621.

Pfrieger, F. W., & Barres, B. A. (1997). Synaptic efficacy enhanced by glial cells in vitro. *Science, 277*(5332), 1684-1687.

Portera-Cailliau, C., Pan, D. T., & Yuste, R. (2003). Activity-regulated dynamic behavior of early dendritic protrusions: evidence for different types of dendritic filopodia. *J Neurosci, 23*(18), 7129-7142.

Prieto, J. J., Peterson, B. A., & Winer, J. A. (1994). Morphology and spatial distribution of GABAergic neurons in cat primary auditory cortex (AI). *J Comp Neurol, 344*(3), 349-382.

Pulsifer, M. B. (1996). The neuropsychology of mental retardation. *J Int Neuropsychol Soc, 2*(2), 159-176.

Purpura, D. P. (1975). Dendritic differentiation in human cerebral cortex: normal and aberrant developmental patterns. *Adv Neurol, 12*, 91-134.

Purves, D., Hadley, R. D., & Voyvodic, J. T. (1986). Dynamic changes in the dendritic geometry of individual neurons visualized over periods of up to three months in the superior cervical ganglion of living mice. *J Neurosci, 6*(4), 1051-1060.

Purves, D., & Hume, R. I. (1981). The relation of postsynaptic geometry to the number of presynaptic axons that innervate autonomic ganglion cells. *J Neurosci, 1*(5), 441-452.

Purves, D., & Lichtman, J. W. (1980). Elimination of synapses in the developing nervous system. *Science, 210*(4466), 153-157.

Qin, M., Kang, J., & Smith, C. B. (2002). Increased rates of cerebral glucose metabolism in a mouse model of fragile X mental retardation. *Proc Natl Acad Sci U S A, 99*(24), 15758-15763.

Raffa, B. (2009). Fragile X Syndrome Mechanism discovered. *The journal of young investigators, 19*(16). Retrieved from www.jyi.org/news/nb.php?id=1364

Rajan, I., & Cline, H. T. (1998). Glutamate receptor activity is required for normal development of tectal cell dendrites in vivo. *J Neurosci, 18*(19), 7836-7846.

Rakic, P. (1975). Role of cell interaction in development of dendritic patterns. *Adv Neurol, 12*, 117-134.

Rakic, P., & Sidman, R. L. (1973). Organization of cerebellar cortex secondary to deficit of granule cells in weaver mutant mice. *J Comp Neurol, 152*(2), 133-161.

Rall, W., Burke, R. E., Holmes, W. R., Jack, J. J., Redman, S. J., & Segev, I. (1992). Matching dendritic neuron models to experimental data. *Physiol Rev, 72*(4 Suppl), S159-186.

Ramoa, A. S., Campbell, G., & Shatz, C. J. (1988). Dendritic growth and remodeling of cat retinal ganglion cells during fetal and postnatal development. *J Neurosci, 8*(11), 4239-4261.

Ramon Y Cajal, S. (1983). Neue darstellung vom histologischen Bau des Centralnerevensystem. *Arch Anat Physiol*, 319-428.

Rampon, C., Tang, Y. P., Goodhouse, J., Shimizu, E., Kyin, M., & Tsien, J. Z. (2000). Enrichment induces structural changes and recovery from nonspatial memory deficits in CA1 NMDAR1-knockout mice. *Nat Neurosci, 3*(3), 238-244.

Rao, A., Kim, E., Sheng, M., & Craig, A. M. (1998). Heterogeneity in the molecular composition of excitatory postsynaptic sites during development of hippocampal neurons in culture. *J Neurosci, 18*(4), 1217-1229.

Reeve, S. P., Bassetto, L., Genova, G. K., Kleyner, Y., Leyssen, M., Jackson, F. R., et al. (2005). The Drosophila fragile X mental retardation protein controls actin dynamics by directly regulating profilin in the brain. *Curr Biol, 15*(12), 1156-1163.

Reiss, A. L., Abrams, M. T., Greenlaw, R., Freund, L., & Denckla, M. B. (1995). Neurodevelopmental effects of the FMR-1 full mutation in humans. *Nat Med, 1*(2), 159-167.

Reiss, A. L., Freund, L. S., Baumgardner, T. L., Abrams, M. T., & Denckla, M. B. (1995). Contribution of the FMR1 gene mutation to human intellectual dysfunction. *Nat Genet, 11*(3), 331-334.

Reiss, A. L., Lee, J., & Freund, L. (1994). Neuroanatomy of fragile X syndrome: the temporal lobe. *Neurology, 44*(7), 1317-1324.

Restivo, L., Ferrari, F., Passino, E., Sgobio, C., Bock, J., Oostra, B. A., et al. (2005). Enriched environment promotes behavioral and morphological recovery in a mouse model for the fragile X syndrome. *Proc Natl Acad Sci U S A, 102*(32), 11557-11562.

Ribak, C. E., & Seress, L. (1983). Five types of basket cell in the hippocampal dentate gyrus: a combined Golgi and electron microscopic study. *J Neurocytol, 12*(4), 577-597.

Ribak, C. E., Seress, L., & Amaral, D. G. (1985). The development, ultrastructure and synaptic connections of the mossy cells of the dentate gyrus. *J Neurocytol, 14*(5),

835-857.

Ribak, C. E., Seress, L., Peterson, G. M., Seroogy, K. B., Fallon, J. H., & Schmued, L. C. (1986). A GABAergic inhibitory component within the hippocampal commissural pathway. *J Neurosci, 6*(12), 3492-3498.

Riccio, R. V., & Matthews, M. A. (1985). Effects of intraocular tetrodotoxin on dendritic spines in the developing rat visual cortex: a Golgi analysis. *Brain Res, 351*(2), 173-182.

Rudelli, R. D., Brown, W. T., Wisniewski, K., Jenkins, E. C., Laure-Kamionowska, M., Connell, F., et al. (1985). Adult fragile X syndrome. Clinico-neuropathologic findings. *Acta Neuropathol, 67*(3-4), 289-295.

Schaeffer, C., Bardoni, B., Mandel, J. L., Ehresmann, B., Ehresmann, C., & Moine, H. (2001). The fragile X mental retardation protein binds specifically to its mRNA via a purine quartet motif. *EMBO J, 20*(17), 4803-4813.

Schaeffer, C., Beaulande, M., Ehresmann, C., Ehresmann, B., & Moine, H. (2003). The RNA binding protein FMRP: new connections and missing links. *Biol Cell, 95*(3-4), 221-228.

Schapiro, S., & Vukovich, K. R. (1970). Early experience effects upon cortical dendrites: a proposed model for development. *Science, 167*(916), 292-294.

Schikorski, T., & Stevens, C. F. (1999). Quantitative fine-structural analysis of olfactory cortical synapses. *Proc Natl Acad Sci U S A, 96*(7), 4107-4112.

Schools, G. P., & Kimelberg, H. K. (1999). mGluR3 and mGluR5 are the predominant metabotropic glutamate receptor mRNAs expressed in hippocampal astrocytes acutely isolated from young rats. *J Neurosci Res, 58*(4), 533-543.

Schuett, J., Falley, K., Richter, D., Kreienkamp, H. J., & Kindler, S. (2009). Fragile X mental retardation protein regulates the levels of scaffold proteins and glutamate receptors in postsynaptic densities. *J Biol Chem*.

Scott, E. K., & Luo, L. (2001). How do dendrites take their shape? *Nat Neurosci, 4*(4), 359-365.

Scott, E. K., Raabe, T., & Luo, L. (2002). Structure of the vertical and horizontal system

neurons of the lobula plate in Drosophila. *J Comp Neurol, 454*(4), 470-481.

Segal, M. (2005). Dendritic spines and long-term plasticity. *Nat Rev Neurosci, 6*(4), 277-284.

Segal, M., Kreher, U., Greenberger, V., & Braun, K. (2003). Is fragile X mental retardation protein involved in activity-induced plasticity of dendritic spines? *Brain Res, 972*(1-2), 9-15.

Segev, I., & London, M. (2000). Untangling dendrites with quantitative models. *Science, 290*(5492), 744-750.

Seil, F. J. (2001). Interactions between cerebellar Purkinje cells and their associated astrocytes. *Histol Histopathol, 16*(3), 955-968.

Seil, F. J., Eckenstein, F. P., & Reier, P. J. (1992). Induction of dendritic spine proliferation by an astrocyte secreted factor. *Exp Neurol, 117*(1), 85-89.

Seress, L., & Ribak, C. E. (1990). The synaptic connections of basket cell axons in the developing rat hippocampal formation. *Exp Brain Res, 81*(3), 500-508.

Sernagor, E., Eglen, S. J., & Wong, R. O. (2001). Development of retinal ganglion cell structure and function. *Prog Retin Eye Res, 20*(2), 139-174.

Sholl, D. A. (1953). Dendritic organization in the neurons of the visual and motor cortices of the cat. *J Anat, 87*(4), 387-406.

Silva, G. A., Theriault, E., Mills, L. R., Pennefather, P. S., & Feeney, C. J. (1999). Group I and II metabotropic glutamate receptor expression in cultured rat spinal cord astrocytes. *Neurosci Lett, 263*(2-3), 117-120.

Sin, W. C., Haas, K., Ruthazer, E. S., & Cline, H. T. (2002). Dendrite growth increased by visual activity requires NMDA receptor and Rho GTPases. *Nature, 419*(6906), 475-480.

Singh, K., Gaur, P., & Prasad, S. (2007). Fragile x mental retardation (Fmr-1) gene expression is down regulated in brain of mice during aging. *Mol Biol Rep, 34*(3), 173-181.

Singh, K., & Prasad, S. (2008). Differential expression of Fmr-1 mRNA and FMRP in female mice brain during aging. *Mol Biol Rep, 35*(4), 677-684.

Smit, A. E., van der Geest, J. N., Vellema, M., Koekkoek, S. K., Willemsen, R., Govaerts, L. C., et al. (2008). Savings and extinction of conditioned eyeblink responses in fragile X syndrome. *Genes Brain Behav, 7*(7), 770-777.

Snyder, E. M., Philpot, B. D., Huber, K. M., Dong, X., Fallon, J. R., & Bear, M. F. (2001). Internalization of ionotropic glutamate receptors in response to mGluR activation. *Nat Neurosci, 4*(11), 1079-1085.

Soba, P., Zhu, S., Emoto, K., Younger, S., Yang, S. J., Yu, H. H., et al. (2007). Drosophila sensory neurons require Dscam for dendritic self-avoidance and proper dendritic field organization. *Neuron, 54*(3), 403-416.

Sobesky, W. E., Taylor, A. K., Pennington, B. F., Bennetto, L., Porter, D., Riddle, J., et al. (1996). Molecular/clinical correlations in females with fragile X. *Am J Med Genet, 64*(2), 340-345.

Somogyi, P., Nunzi, M. G., Gorio, A., & Smith, A. D. (1983). A new type of specific interneuron in the monkey hippocampus forming synapses exclusively with the axon initial segments of pyramidal cells. *Brain Res, 259*(1), 137-142.

Spencer, C. M., Alekseyenko, O., Serysheva, E., Yuva-Paylor, L. A., & Paylor, R. (2005). Altered anxiety-related and social behaviors in the Fmr1 knockout mouse model of fragile X syndrome. *Genes Brain Behav, 4*(7), 420-430.

Spencer, C. M., Graham, D. F., Yuva-Paylor, L. A., Nelson, D. L., & Paylor, R. (2008). Social behavior in Fmr1 knockout mice carrying a human FMR1 transgene. *Behav Neurosci, 122*(3), 710-715.

Spruston, N., & McBain, C. J. (2007). Structural and Functional Properties of Hippocampal Neurons. In P. Anderson, R. Morris, D. Amaral, T. Bliss & J. O'Keefe (Eds.), *The HIppocampus Book* (pp. 133-202). New York: Oxford University Press.

Stefani, G., Fraser, C. E., Darnell, J. C., & Darnell, R. B. (2004). Fragile X mental retardation protein is associated with translating polyribosomes in neuronal cells. *J Neurosci, 24*(33), 7272-7276.

Steward, O., Bakker, C. E., Willems, P. J., & Oostra, B. A. (1998). No evidence for

disruption of normal patterns of mRNA localization in dendrites or dendritic transport of recently synthesized mRNA in FMR1 knockout mice, a model for human fragile-X mental retardation syndrome. *Neuroreport, 9*(3), 477-481.

Stoop, R., Conquet, F., & Pralong, E. (2003). Determination of group I metabotropic glutamate receptor subtypes involved in the frequency of epileptiform activity in vitro using mGluR1 and mGluR5 mutant mice. *Neuropharmacology, 44*(2), 157-162.

Sudhof, T. C. (2008). Neuroligins and neurexins link synaptic function to cognitive disease. *Nature, 455*(7215), 903-911.

Sung, Y. J., Conti, J., Currie, J. R., Brown, W. T., & Denman, R. B. (2000). RNAs that interact with the fragile X syndrome RNA binding protein FMRP. *Biochem Biophys Res Commun, 275*(3), 973-980.

Sung, Y. J., Dolzhanskaya, N., Nolin, S. L., Brown, T., Currie, J. R., & Denman, R. B. (2003). The fragile X mental retardation protein FMRP binds elongation factor 1A mRNA and negatively regulates its translation in vivo. *J Biol Chem, 278*(18), 15669-15678.

Sutcliffe, J. S., Nelson, D. L., Zhang, F., Pieretti, M., Caskey, C. T., Saxe, D., et al. (1992). DNA methylation represses FMR-1 transcription in fragile X syndrome. *Hum Mol Genet, 1*(6), 397-400.

Tanzi, E. (1893). I fatti le induzione nell'odierna istologia del sisterna nervoso. *Riv Sperim Freniatr Med Leg, 19*, 419-472.

Tessier, C. R., & Broadie, K. (2008). Drosophila fragile X mental retardation protein developmentally regulates activity-dependent axon pruning. *Development, 135*(8), 1547-1557.

Tessier-Lavigne, M., & Goodman, C. S. (1996). The molecular biology of axon guidance. *Science, 274*(5290), 1123-1133.

Tieman, S. B., Zec, N., & Tieman, D. G. (1995). Dark-rearing fails to affect the basal dendritic fields of layer 3 pyramidal cells in the kitten's visual cortex. *Brain Res Dev Brain Res, 84*(1), 39-45.

Todd, P. K., Mack, K. J., & Malter, J. S. (2003). The fragile X mental retardation protein is required for type-I metabotropic glutamate receptor-dependent translation of PSD-95. *Proc Natl Acad Sci U S A, 100*(24), 14374-14378.

Todd, P. K., Malter, J. S., & Mack, K. J. (2003). Whisker stimulation-dependent translation of FMRP in the barrel cortex requires activation of type I metabotropic glutamate receptors. *Brain Res Mol Brain Res, 110*(2), 267-278.

Traub, R. D., & Miles, R. (1991). The hippocampus in context *Neuronal Networks of the Hippocampus* (pp. 1-33). Cambridge: Cambridge University Press.

Tropea, M., Johnson, M. I., & Higgins, D. (1988). Glial cells promote dendritic development in rat sympathetic neurons in vitro. *Glia, 1*(6), 380-392.

Ullian, E. M., Christopherson, K. S., & Barres, B. A. (2004). Role for glia in synaptogenesis. *Glia, 47*(3), 209-216.

Ullian, E. M., Sapperstein, S. K., Christopherson, K. S., & Barres, B. A. (2001). Control of synapse number by glia. *Science, 291*(5504), 657-661.

Ulloa, L., Ibarrola, N., Avila, J., & Diez-Guerra, F. J. (1994). Microtubule-associated protein 1B (MAP1B) is present in glial cells phosphorylated different than in neurones. *Glia, 10*(4), 266-275.

Urbanska, M., Blazejczyk, M., & Jaworski, J. (2008). Molecular basis of dendritic arborization. *Acta Neurobiol Exp (Wars), 68*(2), 264-288.

Valtorta, F., Pennuto, M., Bonanomi, D., & Benfenati, F. (2004). Synaptophysin: leading actor or walk-on role in synaptic vesicle exocytosis? *Bioessays, 26*(4), 445-453.

Valverde, F. (1967). Apical dendritic spines of the visual cortex and light deprivation in the mouse. *Exp Brain Res, 3*(4), 337-352.

Vanderklish, P. W., & Edelman, G. M. (2002). Dendritic spines elongate after stimulation of group 1 metabotropic glutamate receptors in cultured hippocampal neurons. *Proc Natl Acad Sci U S A, 99*(3), 1639-1644.

Vaughn, J. E. (1989). Fine structure of synaptogenesis in the vertebrate central nervous system. *Synapse, 3*(3), 255-285.

Ventura, R., & Harris, K. M. (1999). Three-dimensional relationships between

hippocampal synapses and astrocytes. *J Neurosci, 19*(16), 6897-6906.

Vercelli, A., Assal, F., & Innocenti, G. M. (1992). Emergence of callosally projecting neurons with stellate morphology in the visual cortex of the kitten. *Exp Brain Res, 90*(2), 346-358.

Verkerk, A. J., Pieretti, M., Sutcliffe, J. S., Fu, Y. H., Kuhl, D. P., Pizzuti, A., et al. (1991). Identification of a gene (FMR-1) containing a CGG repeat coincident with a breakpoint cluster region exhibiting length variation in fragile X syndrome. *Cell, 65*(5), 905-914.

Vermeiren, C., Hemptinne, I., Vanhoutte, N., Tilleux, S., Maloteaux, J. M., & Hermans, E. (2006). Loss of metabotropic glutamate receptor-mediated regulation of glutamate transport in chemically activated astrocytes in a rat model of amyotrophic lateral sclerosis. *J Neurochem, 96*(3), 719-731.

Vetter, P., Roth, A., & Hausser, M. (2001). Propagation of action potentials in dendrites depends on dendritic morphology. *J Neurophysiol, 85*(2), 926-937.

Wang, H., Ku, L., Osterhout, D. J., Li, W., Ahmadian, A., Liang, Z., et al. (2004). Developmentally-programmed FMRP expression in oligodendrocytes: a potential role of FMRP in regulating translation in oligodendroglia progenitors. *Hum Mol Genet, 13*(1), 79-89.

Wei, Z. X., Yi, Y. H., Sun, W. W., Wang, R., Su, T., Bai, Y. J., et al. (2007). Expression changes of microtubule associated protein 1B in the brain of Fmr1 knockout mice. *Neurosci Bull, 23*(4), 203-208.

Weiler, I. J., & Greenough, W. T. (1999). Synaptic synthesis of the Fragile X protein: possible involvement in synapse maturation and elimination. *Am J Med Genet, 83*(4), 248-252.

Weiler, I. J., Irwin, S. A., Klintsova, A. Y., Spencer, C. M., Brazelton, A. D., Miyashiro, K., et al. (1997). Fragile X mental retardation protein is translated near synapses in response to neurotransmitter activation. *Proc Natl Acad Sci U S A, 94*(10), 5395-5400.

Weiler, I. J., Spangler, C. C., Klintsova, A. Y., Grossman, A. W., Kim, S. H., Bertaina-

Anglade, V., et al. (2004). Fragile X mental retardation protein is necessary for neurotransmitter-activated protein translation at synapses. *Proc Natl Acad Sci U S A, 101*(50), 17504-17509.

Whitford, K. L., Dijkhuizen, P., Polleux, F., & Ghosh, A. (2002). Molecular control of cortical dendrite development. *Annu Rev Neurosci, 25*, 127-149.

Wiesel, T. N., & Hubel, D. H. (1963). Effects of Visual Deprivation on Morphology and Physiology of Cells in the Cats Lateral Geniculate Body. *J Neurophysiol, 26*, 978-993.

Willemsen, R., Oostra, B. A., Bassell, G. J., & Dictenberg, J. (2004). The fragile X syndrome: from molecular genetics to neurobiology. *Ment Retard Dev Disabil Res Rev, 10*(1), 60-67.

Williams, D. W., & Truman, J. W. (2004). Mechanisms of dendritic elaboration of sensory neurons in Drosophila: insights from in vivo time lapse. *J Neurosci, 24*(7), 1541-1550.

Winograd, C., Clayton, D., & Ceman, S. (2008). Expression of fragile X mental retardation protein within the vocal control system of developing and adult male zebra finches. *Neuroscience, 157*(1), 132-142.

Wise, S. P., Fleshman, J. W., Jr., & Jones, E. G. (1979). Maturation of pyramidal cell form in relation to developing afferent and efferent connections of rat somatic sensory cortex. *Neuroscience, 4*(9), 1275-1297.

Wong, R. O., & Ghosh, A. (2002). Activity-dependent regulation of dendritic growth and patterning. *Nat Rev Neurosci, 3*(10), 803-812.

Wong, T. P., Marchese, G., Casu, M. A., Ribeiro-da-Silva, A., Cuello, A. C., & De Koninck, Y. (2006). Imbalance towards inhibition as a substrate of aging-associated cognitive impairment. *Neurosci Lett, 397*(1-2), 64-68.

Wood, G. E., Young, L. T., Reagan, L. P., Chen, B., & McEwen, B. S. (2004). Stress-induced structural remodeling in hippocampus: prevention by lithium treatment. *Proc Natl Acad Sci U S A, 101*(11), 3973-3978.

Wu, G. Y., Zou, D. J., Rajan, I., & Cline, H. (1999). Dendritic dynamics in vivo change

during neuronal maturation. *J Neurosci, 19*(11), 4472-4483.

Yan, Q. J., Rammal, M., Tranfaglia, M., & Bauchwitz, R. P. (2005). Suppression of two major Fragile X Syndrome mouse model phenotypes by the mGluR5 antagonist MPEP. *Neuropharmacology, 49*(7), 1053-1066.

Ye, Z. C., & Sontheimer, H. (1999). Metabotropic glutamate receptor agonists reduce glutamate release from cultured astrocytes. *Glia, 25*(3), 270-281.

Yu, W., Ahmad, F. J., & Baas, P. W. (1994). Microtubule fragmentation and partitioning in the axon during collateral branch formation. *J Neurosci, 14*(10), 5872-5884.

Yuste, R., & Bonhoeffer, T. (2004). Genesis of dendritic spines: insights from ultrastructural and imaging studies. *Nat Rev Neurosci, 5*(1), 24-34.

Zalfa, F., & Bagni, C. (2004). Molecular insights into mental retardation: multiple functions for the Fragile X mental retardation protein? *Curr Issues Mol Biol, 6*(2), 73-88.

Zalfa, F., Eleuteri, B., Dickson, K. S., Mercaldo, V., De Rubeis, S., di Penta, A., et al. (2007). A new function for the fragile X mental retardation protein in regulation of PSD-95 mRNA stability. *Nat Neurosci, 10*(5), 578-587.

Zalfa, F., Giorgi, M., Primerano, B., Moro, A., Di Penta, A., Reis, S., et al. (2003). The fragile X syndrome protein FMRP associates with BC1 RNA and regulates the translation of specific mRNAs at synapses. *Cell, 112*(3), 317-327.

Zhang, J., Fang, Z., Jud, C., Vansteensel, M. J., Kaasik, K., Lee, C. C., et al. (2008). Fragile X-related proteins regulate mammalian circadian behavioral rhythms. *Am J Hum Genet, 83*(1), 43-52.

Zhang, Y. Q., Bailey, A. M., Matthies, H. J., Renden, R. B., Smith, M. A., Speese, S. D., et al. (2001). Drosophila fragile X-related gene regulates the MAP1B homolog Futsch to control synaptic structure and function. *Cell, 107*(5), 591-603.

Zhao, M. G., Toyoda, H., Ko, S. W., Ding, H. K., Wu, L. J., & Zhuo, M. (2005). Deficits in trace fear memory and long-term potentiation in a mouse model for fragile X syndrome. *J Neurosci, 25*(32), 7385-7392.

Zhu, H., Hummel, T., Clemens, J. C., Berdnik, D., Zipursky, S. L., & Luo, L. (2006).

Dendritic patterning by Dscam and synaptic partner matching in the Drosophila antennal lobe. *Nat Neurosci, 9*(3), 349-355.

Ziv, N. E., & Smith, S. J. (1996). Evidence for a role of dendritic filopodia in synaptogenesis and spine formation. *Neuron, 17*(1), 91-102.

Zou, K., Liu, J., Zhu, N., Lin, J., Liang, Q., Brown, W. T., et al. (2008). Identification of FMRP-associated mRNAs using yeast three-hybrid system. *Am J Med Genet B Neuropsychiatr Genet, 147B*(6), 769-777.

Zuo, Y., Lin, A., Chang, P., & Gan, W. B. (2005). Development of long-term dendritic spine stability in diverse regions of cerebral cortex. *Neuron, 46*(2), 181-189.

APPENDIX I:
GENERAL METHODS

Appendix I: General Methods

I.I ICC (IF) on primary neurons in co-culture

Acetone fixation

(MAP2, synapsin, synaptophysin, PSD-95)

DAY1:

Materials:

Ice cold Acetone – acetone in flammables cabinet, aliquot into beaker and cool 20min

PBS filtered for Immuno

0.1% Triton-X 100 in PBS (Immuno station)

1% BSA in PBS (make fresh)

Primary Antibody: MAP2, Neuromics, 1:20000

Methods:

1. Cool Acetone in -20C for 20min

2. Rinse wells with PBS (filtered for immuno)

3. Apply 0.5ml ice cold Acetone per well, and place at -20C for 10 minutes

4. Wash 3X 5 min PBS (0.5ml per well)

5. 0.1% Triton-X 100 in PBS, 5 min RT (0.5ml per well)

6. 1% BSA block: 0.5ml of 1% BSA in PBS per well, RT for 30min

(optional 1:20 or 1:5 Normal goat serum, NGS, in 1% BSA)

7. Apply Primary Antibody (MAP2, 1:20000, Neuromics – P35 on antibody file)

I usually make it up as follows:

a) 0.5ul Ab in 1000ul 1%BSA (with or without 1:20 NGS)

b) Dilute 10 fold with 1% BSA for amount needed

(ie., 250ul per well)

NOTE: for double labeling, both primary antibodies can be applied at same time (if using the above antibodies). However, antibodies need to be made at double the concentration (e.g., MAP2 at 1:10000), and half as much applied per well (e.g., 125ul)

Leave overnight, 4C

DAY2:

Materials:

PBS filtered for immuno

Secondary Antibody: anti-chicken FITC, Jackson (S25)

Methods:

8. Wash 3X5 min PBS (0.5mls per well)

9. Secondary Ab, anti-chicken (S25), 1:100, 3hrs, RT

(250ul per well)

NOTE: for double labeling, both secondaries can be applied at the same time (similar to primary Abs) – see above.

10. Wash 2X 5 min PBS (0.5mls per well)

11. Wash 2 X 5 min dH2O

12. Mount with Fluorescent mounting medium, Vectashield mounting medium with DAPI (top shelf fridge – black box)

Store in fridge

I.II Neuronmetrics™.

Image J v1.36b

Java v.1.5.0_03

Neurometrics™ (with replacement files: Feature J.jar, imagescience.jar)

NOTE: A manual is provided with Neuronmetrics ™ files. Read, and install the program as instructed.

IMPORTANT: Be certain that the version of Image J is the one listed (you will need to obtain this from the archive on the Image J website).

IMPORTANT: Be certain that the version of Java is the one listed. And if there is more that one version of Java on the computer, makes sure that the files for the required Java version are loaded into the Neuronmetrics™ folder, or that the correct file path is chosen when Image J is loading.

1) Take pictures of isolated neurons using AxioVision software.
2) Export files as black & white JPEGs
   a JPEG (default)
   b No compression (change from default 5%, to 0%)
   c Select channel of MAP2 only
   d De-select 'project folder'
   e Select grayscale
3) Process images for use in Neuronmetrics™ (optimize brightness/contrast)
4) Open in windows media viewer or equivalent and alter brightness and contrast to ensure all fine processes are visible and to decrease background.
5) 'Batch convert' all images in folder to TIFF
   a In Image J, use Batch Converter plug-in (available at: http://rsbweb.nih.gov/ij/plugins/batch-converter.html)

b Make certain to name destination folder ending in a number (this is necessary for appropriate processing in Neuronmetrics™, see manual)

6) In Image J, begin Neuronmetrics™

7) Set-up
   - Choose folder
   - Use "non-uniform" neuron signal
   - Leave other defaults under "advanced" (The settings should work, but you can change them if necessary as per Neurometrics™ manual)
   - Scale: 1.95 for 20X images, and 3.92 for 40X images (see step 6, below)
   - Select "optional features": noise ROIs, length correction, polarity index, territory
   - Select "output images" (don't really need faces)

8) Scale (if you need to check the scale, and set it yourself, follow the manual)

9) Neuron & Cell body (with noise correction) * note: if you receive an error message here that says "runs in batch mode", go to file, and select 'close', and then try again (for some reason the program is registering that you have a window open, so continue to close 'windows' until it runs. This should only take once or twice).

a Follow directions prompted in Image J
   - Trace around neuron of interest (try to trace as closely to neuron as possible as this will increase the robustness of the skeleton generated). Press space-bar to save
   - Indicate cell body. Press space bar to save,
   - Trace within all spaces between dendrites (noise). Press space bar after each to save.

10) Run Cell body ROI manually. This is found under NM Tools.

a Trace around the neuron cell body. Press space bar to save.

11) Skeletonize and Improve (this is an automated step).

12) Length Correction.

a Trace along lengths of dendrite where the dendrites fasiculate (Neuronmetrics™

will often read multiple parallel dendrites as one) and enter the number of times that length should be counted.

13) Longest neurite (in our case longest 'dendrite')
   a Click 'indicate neurite'
   b Click on cell dendrites where you estimate is longest dendrite.
   c Trim the dendrite until it has no branches. (click view skeleton in between, and undo indicate neurite, and repeat until all possible selections are made.)
14) Measure skeleton (this is an automated step).
15) Check skeleton overlays to ensure accuracy. And repeat if necessary.
16) Copy and paste all data from data files into excel.

IMPORTANT READING:

(Narro, et al., 2007)

Neuronmetrics™ User Manual (available when downloading Neuronmetrics™),

I.II Sholl Analysis

Sholl plug-in obtained from Ghosh lab (http://www-biology.ucsd.edu/labs/ghosh/software/) - need both shollanalysis.class and shollanalysis.java

Image J (http://rsbweb.nih.gov/ij/)

Digital skeletons of neurons (can be generated using Neuronmetrics™, as described previously – use 'final skeleton' files)

1) Open Image J.
2) Set scale:
   a Open any neuron skeleton file
   b "analyze", "set scale"
   c Enter: 1.95 for images at 20X, 3.92 for images at 40X
   d Select 'global'
3) Close file
4) Open skeleton file of neuron to be analyzed
5) Smooth image – select 'smooth' from 'process' drop down menu
6) Repeat smooth three times
7) Adjust canvas size so that the longest dendrite of the neuron skeleton fits within the boundaries of the window.
   a Select 'canvas size' from 'Image', 'Adjust' drop down menu
   b Check longest dendrite again, to make certain it fits
   c Record the length of the longest dendrite (this will serve as a guide for which values of the Sholl analysis to obtain)
8) Using crosshair pointer click on center of cell body (or where cell body would be)
9) Select Sholl Analysis from "plugins" drop down menu.
   a "starting radius" 10μm
   b "radius step size" 10μm

c "ending radius" 300μm

d Leave all other parameters as default

10) List values

11) Copy and paste values up to the further radius that would contain the last crossing of the longest dendrite into excel sheet.

a Ex. If you measured the longest dendrite to be 213μm, record Sholl values up to and including 210μm (you would not include the measurements at 220μm or beyond, because the skeleton did not exist at those distances**)

12) Close all windows

13) Repeat Steps 4-12 for each neuron to be analyzed

IMPORTANT.

* by selecting global, the scale will stay the same for each neuron image opened, until the scale is changed. Remember to change the scale when switching from processing images at 20X versus those at 40X.

** for some reason (I can not figure it out) the Sholl analysis plug-in counts the number of times the Sholl circles cross the edge of the window as branches (or, at least it seems to be counting that – again I can not figure it out). If you make certain to extend the canvas size so that the longest dendrite is shorter than the shortest distance to the edge of the window (Step 7), and then record only those values up to the maximum of the longest dendrite (Step 11), you will avoid any problems.

I.IV Puncta Analysis

Image J v1.2 (http://rsb.info.nih.gov/ij/download/win32/)
Particle analyzer plug-in (puncta analyzer.zip, on CD)
RBG files of neurons

I.IV.I For Puncta analysis on whole cells

(this is not what the program was written for, but it can be used in this manner – it will not process co-localization because there is only a single channel)

You will need separate red and green channel images of the neuron stained for MAP2 and a synaptic marker. Ex. MAP2 (red), synaptic protein (green)

1) Open Image J
2) Open MAP2 file for neuron to be analyzed
3) Using free hand trace tool, trace around the neuron
4) Open the file for the corresponding synaptic protein
5) Select 'restore selection' from the 'edit' drop down menu
   a this will select the corresponding region of the neuron's dendritic arbor, on the image of the synaptic proteins. In this way you will only be counting the number of puncta around the cell, not in the window as a whole.
6) Select 'Puncta Analyzer' from 'Plugins' drop down menu
   a leave 'condition' blank
   b select channel that puncta are in (red or green), and select appropriate "subtract background" (read left to right, across each row: first one is for red channel, second is for green channel etc).
   c leave "save results" empty (you will manually be copying results into spread sheet)

7) rolling ball radius – leave at default, but deselect "white background" (you want black)
8) You will be prompted to 'threshold' the image
   a Change the top sider until only the puncta remain visible in the "channel image window" (you can compare back to the original to see)
9) Analyze Particles
   a Minimum size: set to 5 pixels
   b Maximum size: set to 20 pixels
   c Leave all other defaults
10) Copy and paste the total number of puncta (ignoring the colour channel in which there was no puncta, and ignoring the co-localization data)*, **
11) Close all windows.
12) Repeat for each neuron (Steps 2-11)

IMPORTANT:

* this plug-in also provides detailed data about the location, size, intensity of the puncta in a list. I believe this data was for all puncta in the window, and therefore I did not use this data, and cannot comment on how it should be used.

**the plug-in also provides information on the average intensity and size of the puncta within the selected region. I did not use either of these measurements for the following reasons: I did not process all cultures on the same day with ICC, and did not take all the pictures on the same day, therefore I was not confident that this would not confound the results; I had already restricted the size of the puncta in the processing, and therefore did not feel that the size measurements were as valid.

I.IV.II For analysis of 50µm sections

RBG images of neurons stained for pre- and post-synaptic proteins. In this analysis you will need the merged image. Ex. Single image with pre-synaptic (red) and post-synaptic (green)

1) Open Image J for Puncta (v1.2)
2) Open file of dendrites to be analyzed
3) Using 'polygon drawing' tool, draw a rectangle enclosing a 50µm section of a dendrite
4) Select "Particle Analyzer" plug-in
5) See "Puncta Analysis for Whole Cells" (6-9).
6) You will be prompted to 'threshold' each channel independently. Move the top slider until only the puncta in that channel are visible (use the original image as a guide).
7) Copy and paste the data*.
8) Repeat for all segments within the window**
9) Close the file
10) Repeat Steps 2-10 for each file to be analyzed.

IMPORTANT:

* the plug-in will return, data for puncta in each channel (i.e., red and green), as well as co-localized puncta.

** make certain you are not choosing overlapping dendrite segments. Once the plug-in has run for a region, it creates a 'hole' where co-localized puncta are found. If it is really necessary to measure two dendrites with overlapping aspects, close and re-open the image.

APPENDIX II:
PERMISSIONS

Appendix II : Permissions

McMaster University
HEALTH SCIENCES

Department of Pathology and Molecular Medicine
Hamilton, Ontario, Canada

1200 Main Street West
Health Sciences Centre – 1R1
L8N 3Z5

Phone 905.525.9140
ext. 22030
Fax 905.525.7400

September 10, 2009

Shelley Jacobs
Pathology and Molecular Medicine
McMaster University
1200 Main Street West, HSC-1R1
Hamilton, ON L8N 3Z5

I am completing a Ph.D. thesis at McMaster University entitled *"Astrocytes in the Neurobiology of Fragile X Syndrome"*. I would like your permission to reprint the photos from following article in my thesis.

> Jacobs S and Doering LC. Primary dissociated astrocyte and neuron co-culture. In: Protocols for Neural Cell Culture, Fourth Edition, 2009 (In press).

Please note that I am a co-author of this work.

I am also requesting that you grant irrevocable, nonexclusive licence to McMaster University (and to the National Library of Canada) to reproduce this material as part of the thesis. Proper acknowledgement of your copyright of the reprinted material will be given in the thesis.

If these arrangements meet with your approval, please sign where indicated below and return this letter to me in the enclosed envelope. Thank you very much.

Sincerely,

Shelley Jacobs

PERMISSION GRANTED FOR THE USE REQUESTED ABOVE

HUMANA PRESS 2009

Authorized By: David C. Cuzzup

Title: Asst. Editor

Date: 9/10/2009

Signature: David C. Cuzzup